# CELLULOSE & LIGNIN IN ADDITIVE MANUFACTURING

Alexsander Alberts Coelho

# Cellulose & Lignin in Additive Manufacturing

Potential and challenges in the fabrication of structural nodes for free-form building envelope structures

MSc Graduation Thesis Report

June 2022

**Alexsander Alberts Coelho**

### Mentors

Dr. Michela Turrin

Architectural Engineering + Technology | *Design Informatics*

Prof. Dr.-Ing. Ulrich Knaack

Architectural Engineering + Technology | *Facade & Product Design*

### Special Advisor

Dr. Serdar Asut

Architectural Engineering + Technology | *Facade & Product Design*

### External Advisor

Dr. Richard J. A. Gosselink

Wageningen University

**TU**Delft Delft University of Technology

# Abstract

The building stock and the construction industry combined are responsible for a large share of greenhouse gases emissions. At the same time, every year tons of wood, paper and agricultural residues are wasted instead of recycled and upcycled into the production chain. In the fabrication field, the relevance of additive manufacturing processes is constantly growing, allowing for maximum customisation and optimisation of material and energy usage.

Lignocellulosic polymers are the most abundant in nature, although meanwhile cellulose is seen as a valuable raw material, lignin is treated as a by-product to be burned and generate energy. Based on the increasing use of both as fibre reinforcements and fillers in feedstocks for additive manufacturing, there is a potential to be explored.

The combination of the development of a novel material for an innovative fabrication process such as liquid deposition modelling, is the scope of work presented in this research.

Cellulose and lignin were studied, analysed and manipulated before mixing them with a vast selection of binding agents and additives. The outcome was evaluated according to a pre-established criteria set and documented, and a comparison drawn to define the best and most promising material mixes for additional investigation. From a universe of twelve mixes and numerous iterations for each recipe, four alternatives were picked for further characterisation and determination of their mechanical properties.

In parallel, the printability of the material considered as the most promising mix was explored through the extrusion of a sequence of simple geometries and shapes designed to understand and define the most adequate printing parameters. Limitations and challenges were observed and general directions and guidelines were documented.

With a complete dataset and overview of this novel bio-based and wood-based material for additive manufacturing, a simple structural node was designed. The fabrication of a prototype was used to further enhance the material properties and to clarify its potential and limitations for applications in the construction industry.

From the initial material exploration to the final prototyping phase, an extensive documentation was prepared to validate the potential and limitations of this novel material and indicate the directions for further research works.

# Acknowledgments

# Index

# 0. Introduction

## 0.1. Presentation

Architecture has been quickly developing in the past few years. Ten years ago, a façade composed of pre-fabricated panels was innovative enough to grant a spot on any website or magazine dedicated to the field. For decades, the construction field focused on strengthening concrete and steel structures to grow in height and reduce in size, adapting and resisting to geological and weather challenges such as earthquakes and inclement storms. Now, propelled by advances in software and computational design, the scenario is changing dramatically. Simulations made with Rhino, Grasshopper and their plugins – combined with lines of code from Python – are making the design process smarter and more comprehensive, pushing for higher levels of customization and optimization also on the fabrication side.

On one hand, renewable materials are necessary for the construction field to move towards a sustainable future where the human carbon footprint and environmental impact must be constantly reminded and reduced. On the other, a revolution on the fabrication processes has already started, with several authors linking it to the concept of the Industry 4.0 (Gibson et al., 2021), with additive manufacturing allowing for ultimate customization and optimization in terms of design and material usage.

This is the scenario where this research project is inserted. Throughout the next chapters, a review on materials and fabrication processes will lead to practical explorations in the material science, prototyping searching for innovations and a bridge between natural materials, innovative manufacturing and the construction sector.

## 0.2. Problem Statement

As the construction field moves towards sustainability, there is a crescent demand for natural and renewable materials to reduce the carbon footprint of human beings and their buildings. In this context, wood is generally the first option, however it has a limited application in complex geometries, due to its anisotropic properties and the potentially elevated waste through subtractive fabrication methods. Unlike other processed materials like steel, aluminium, concrete or thermoplastics, it is also not possible to modify and enhance wood properties to fulfil specific applications.

Additive manufacturing is one of the answers to handle complex geometries and reduce materials to a minimum, if not eliminate them. Natural materials, however, are still not a common available feedstock, especially wood-based ones. There are wood-composite filaments, also advertised as "3d printable wood", but these are usually biodegradable polymer matrices such as PLA with no more than 20-25 wt.% of lignocellulosic fibres or wood powder in its composition (Gauss et al., 2021). A more promising option is a wood paste, which combines almost 90 wt.% wood flour with synthetic adhesives based on formaldehydes (Kariž et al., 2016; Rosenthal et al., 2018). There are researches seeking natural binders to replace toxic components (Petit-Conil et al., 2011), but there is still no commercial alternative for a natural 3D printing material.

Meanwhile, every year tons of wood, paper and agricultural residue go to waste. These are rich in lignocellulosic fibres which, after mechanical and/or chemical processing could be a recycled source of cellulose, the most abundant polymer in nature and bearer of valuable mechanical properties for polymer reinforcements. Following the same line, most of the residual lignin from the paper industry is sub-utilized and burned to generate energy instead of being separated and upcycled into raw material for more valuable applications.

As learned from previous studies, the potential of cellulose and lignin in the building industry as raw material for additive manufacturing is clear (Liebrand, 2018). A working and printable material mix exists, however, there is a lack of information regarding its mechanical properties. Appearance and chemical composition – it includes acetone – need improvement. And no exploration has been pursued towards natural additives and binders to enhance material properties and replace chemical substances.

Lastly, in the design and construction of free-form structures made entirely of renewable materials, customised connection nodes made of timber would demand a lengthy preparation and production through processes such as CNC and laminated object manufacturing (LOM) (Gibson et al., 2021). Resulting in vast amounts of wasted material due to the subtraction fabrication technique, these would be an obstacle to a full design optimization and a sustainable construction. More adequate fabrication processes already exist, based on material extrusion (Gardner et al., 2019), which allow for better control on material usage and direct reproduction from a digital model. Potentially viable materials have already been researched, such as the cellulose and lignin mixture, with acetone as a binding agent, presented in "3D printed
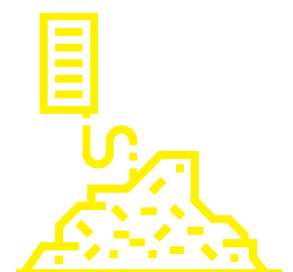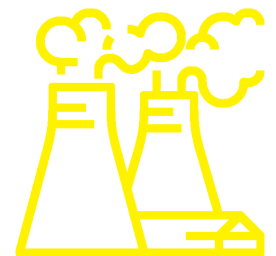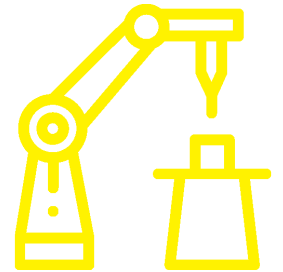
fibre reinforced lignin" (Liebrand, 2018), which offers a viable opportunity for architectural applications. But there are a few gaps between material and use, such as mechanical properties, appearance, composition not being full natural and harmless – acetone is not ideal –, potential to produce façade structural elements and material and fabrication, hot or cold extrusion and the influence of additives and binders, which require further research.

These gaps are the focus of this research project.

## 0.3. Design Vision

This research aims to create a bridge between waste natural material and the construction industry by means of investigating the potential of new feedstock and innovative fabrication processes, catering to the growing challenges posed by complex geometries and design.

Aligned with the climate goals originally established in the Paris Agreement (UNFCCC, 2015) and reindorsed by the European Green Deal (EuropeanComission, 2019), the continent moves towards zero net emissions of greenhouse gases by 2050. As the building stock and construction sector account for 36% of global energy consumption, with greenhouse gas emissions still on the rise at 39% of the worldwide total (GlobalABC, 2019), the incorporation of recycled and natural materials is a necessity towards reducing the carbon footprint of construction sites.

Wood is already commonly used as the base material on small scale pre-fabricated buildings and for interior applications such as walls, floors and ceilings. On larger scale, it can be timidly seen on curtain wall façades and free-form structures. But there are limitations in terms of design and production, rendering it more adequate to simple geometries.

However, if the concept of timber as a solid component is abstracted by taking the elementary blocks which compose wood – a lignin filler and cellulose fibres – and combining them with natural additives into a paste-like substance, a new natural material can be created. And unlike other wood composites that already exist in the market, a thermoplastic matrix can be supressed. Such material is already a possibility, and its potential for use in architectural applications has been attested in previous research. Although it requires further work and improvements, it will be the starting point of this study.

It unlocks the use of additive manufacturing processes to overcome the design challenges aforementioned and broadens the use of 3D printing and natural materials in the construction field. The waste of resources can be reduced, fabrication optimised, and energy can be efficiently used. Architecture does not have to be limited in order to respect the environment and comply with climate goals. These must be the motivation to move technology forward and break paradigms of the industry. The current moment is ideal to investigate
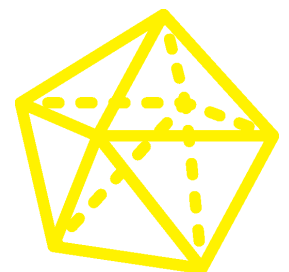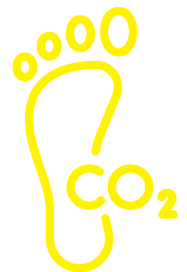
how this material behaves, how can it be improved and, more importantly, its potential uses. And these are the goals of this research.

## 0.4. Research Question

The concept is solid – a wood-like natural feedstock from recycled sources, man-made and tailored to high-tech production methods in line to the challenges imposed by an ever-evolving design panorama. But what is the potential of using it on façade elements? More specifically, what is the potential of using it for structural applications? To attest it, which properties are relevant and how does it perform?

With these uncertainties in mind, the objective of this research is to dive into material sciences and prototyping to answer the following:

What are the **potential** and **challenges** of a material made of **cellulose** and **lignin** as feedstock for additive manufacturing processes in the fabrication of **structural nodes** for free-form structures?

The outcome of this research will be an analysis on whether the material described above is viable as an alternative for the fabrication of structural components for the building envelope. This conclusion will be drawn based on experiments and mechanical testing, which will be summarised in a comprehensive dataset.
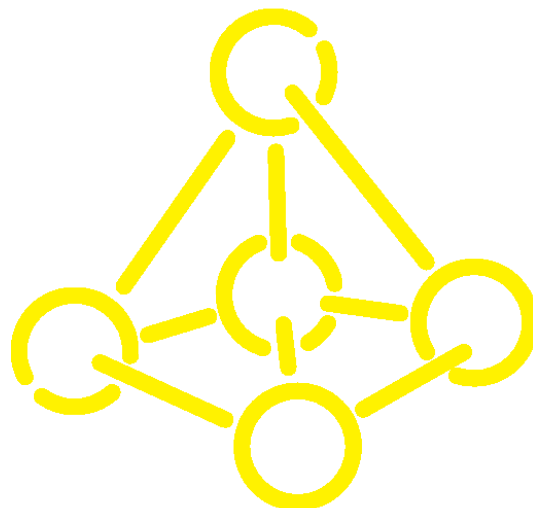
# 0.5. Research Sub-Questions

To answer the main research question, several aspects of the material composition and fabrication processes must be investigated. Experiments will be executed, mechanical testing performed, and conclusions drawn. A set of sub-questions can be defined to direct the research work towards the main goal and to obtain an answer to the main research question.

In terms of material research, the relevant question is the following:

– Is there a natural material which could replace acetone as binding agent in the mix of cellulose and lignin presented in "3D printed fibre reinforced lignin" (Liebrand, 2018) without compromising the observed viscosity, homogeneity and printability characteristics of the mixture?

– What is the potential of enhancing viscosity, homogeneity and printability of cellulose and lignin by incorporating natural additives to the mixture?

In terms of fabrication, the relevant questions is the following:

– What is the most adequate additive manufacturing process for a material mixing cellulose & lignin?

In terms of mechanical properties, the relevant questions are the following:

– What are the most relevant material properties of a 3D printing feedstock for structural applications?

– What is the potential of enhancing the relevant material properties of a material for structural applications by using synthetic and natural additives?

In terms of design and prototyping, the relevant questions are the following:

– Can the model layering/slicing of the 3D printing process impose a challenge to the prototype geometry and structural performance?

– What are the limitations of the printing angle in terms of material and object geometry?

Additional sub-questions might arise during the exploration phase and induce to further developments and research.
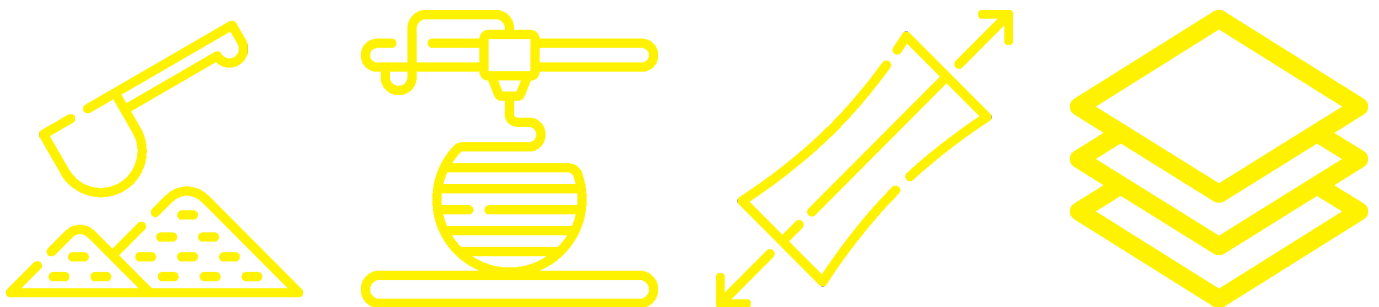
# 0.6. Process & Methodology

The "Wood Without Trees" is an ongoing research line from the Design Informatics chair in collaboration with the Façade & Product Design department, and an external partnership with Wageningen University, where researchers have been studying the valorisation of lignin for more than 15 years. The master thesis entitled "3D printed fibre reinforced lignin", published by Thomas Liebrand as his graduation project in the Building Technology track from this faculty, presented a feedstock for additive manufacturing combining lignin and a reinforcement of cellulosic fibres, attesting its printability and potential for architectural applications.

This mix is the exploratory starting point of this research.

This study was conducted in partnership with another student from the same Building Technology track, Christopher Bierach, and part of the exploratory phases were jointly executed. The research questions are unique and independent, although the external networking and part of the literature studies were developed in collaboration.

With the context above in sight, this research was divided into five main phases, combining a theoretical and a practical framework, plus a preparatory period and a final conclusions & findings summary step:

- – 0. Preparation
- – 1. Literature Review
- – 2. Material Exploration
- – 3. Printability Exploration
- – 4. Mechanical Testing
- – 5. Design & Prototyping
- – 6. Conclusions
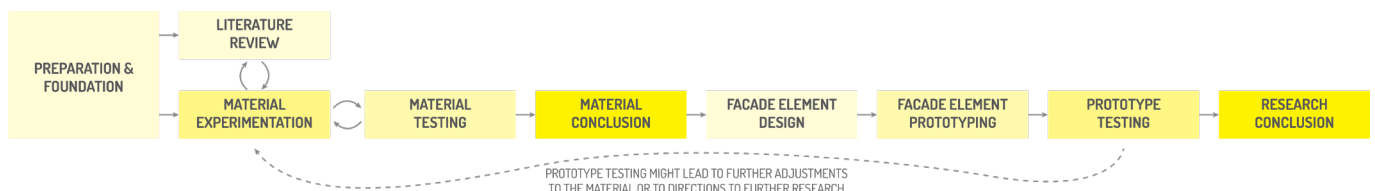


Fig 1 - Thesis general organisation & workflow

Preparation corresponds to the initial weeks and started prior to the thesis commencement. Meetings with both mentors were arranged, the topic was presented and background information was gathered and researched to elaborate a general overview of the topic. An external network was also established, in collaboration with Christopher, for advice and support in terms of material studies and fabrication processes, with companies such as Urban Reef, Strong by Form and WASP and researchers from TU Darmstadt, Saxion University, University of Stuttgart, ETH and RISE. Online meetings, interviews, email exchange and visits were organized and contributed to form a base knowledge to proceed into the theoretical stage of the research.
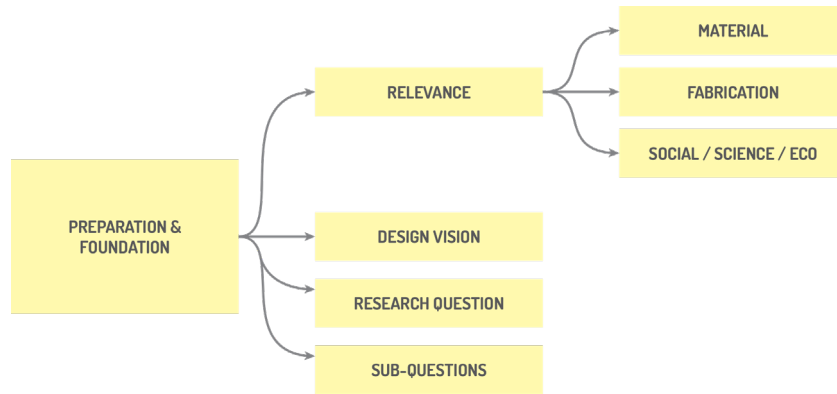
Fig 2 - Preparation Phase Structure

The first main phase of the research was the literature review, executed through offline searches in the library of the Faculty of Architecture and Built Environment from TU Delft; and online, through search engines such as Google Scholar, Scopus, ResearchGate and SpringerLink. From the first one, books on additive manufacturing and wood were consulted to compose the foundation knowledge on material and fabrication. From the second one, scientific papers, articles, reports, and proceedings from conferences revealing the most recent developments on the topic were collected. The contemporary and innovative nature of the topic imply the latter composed most of the bibliography studied.

The literature review covered a board spectrum from the material components, sourcing, mixing and finalised with the fabrication process. It was divided according to the following categories:

– Wood – overview, sourcing, panorama

– Cellulose – overview, properties, sourcing, use in AM, pros & cons

– Lignin – overview, properties, sourcing, use in AM, pros & cons

– Additive Manufacturing – overview, use of bio-based materials, use of wood, use of cellulose & lignin

– Additive Manufacturing Mix – current research status, binders, alternative binders, additives
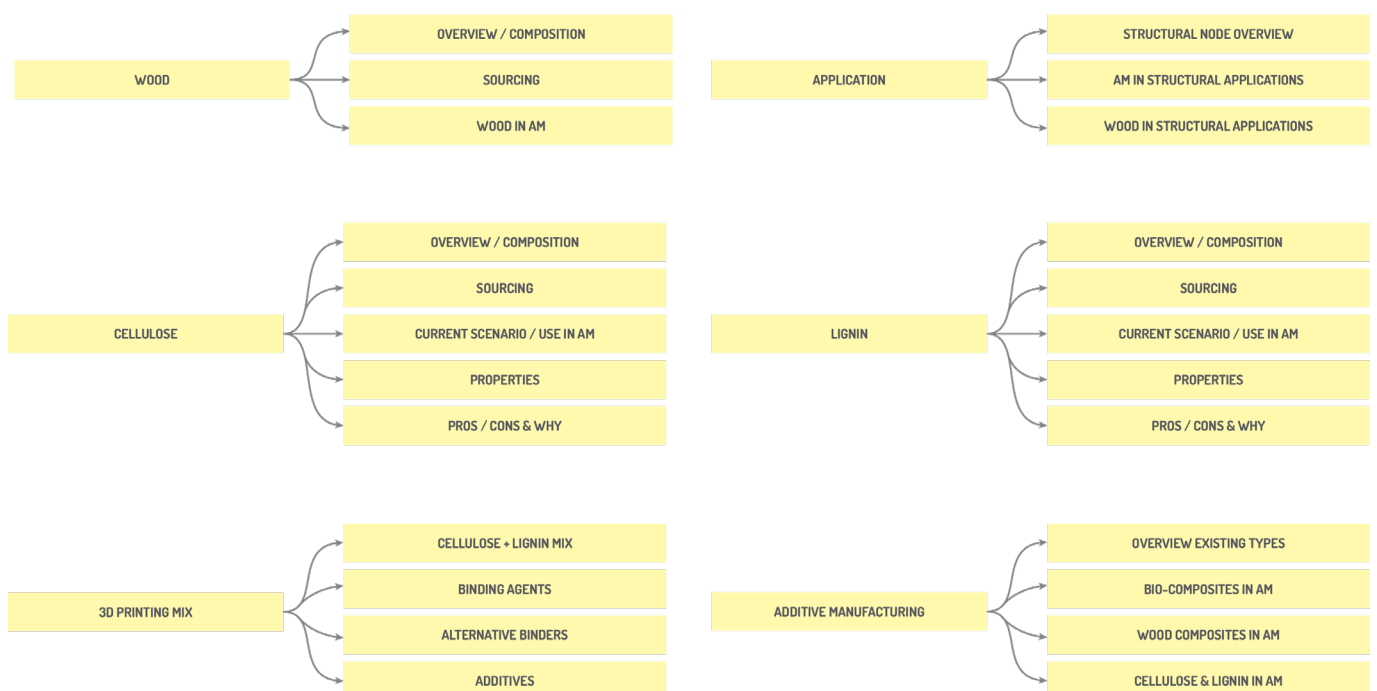


Fig 3 - Literature Review structure

As the exploratory steps evolved, additional literature was necessary to fill in gaps uncovered throughout the process, especially regarding natural additives and replacements to synthetic components. Pertinent references were added, and the background research was updated accordingly.

The practical framework was conducted in partnership with Christopher and followed with the material exploration & testing phase. It started from the findings presented in (Liebrand, 2018), with the reproduction in laboratory of the mix described as the one with the highest potential for use in the additive manufacturing fabrication of architectural elements. This was the base for the material investigation, focused on components proportions, additives and potential replacements to hazardous chemicals towards a bio-based alternative mix.

All the material mixes developed had their viscosity and homogeneity manually tested. In the sequence, their printability was also manually tested with the help of a syringe at room temperature. All results were documented for analysis and grading, allowing for conclusions to be drawn and for the most promising ones to be selected for the following phase.

With the materials defined, the printability exploration could proceed by print-testing samples with a common and simple design. Four mixes were selected as the most promising ones, however, only the one which showed the highest potential and a full bio-based composition was used for the test prints using the robotic arm and extruders available at the Laboratory for Additive Manufacturing in Architecture – LAMA. Such work resulted in further understanding and refinements to the material mix, especially regarding the water content, handling and extrusion preparation.
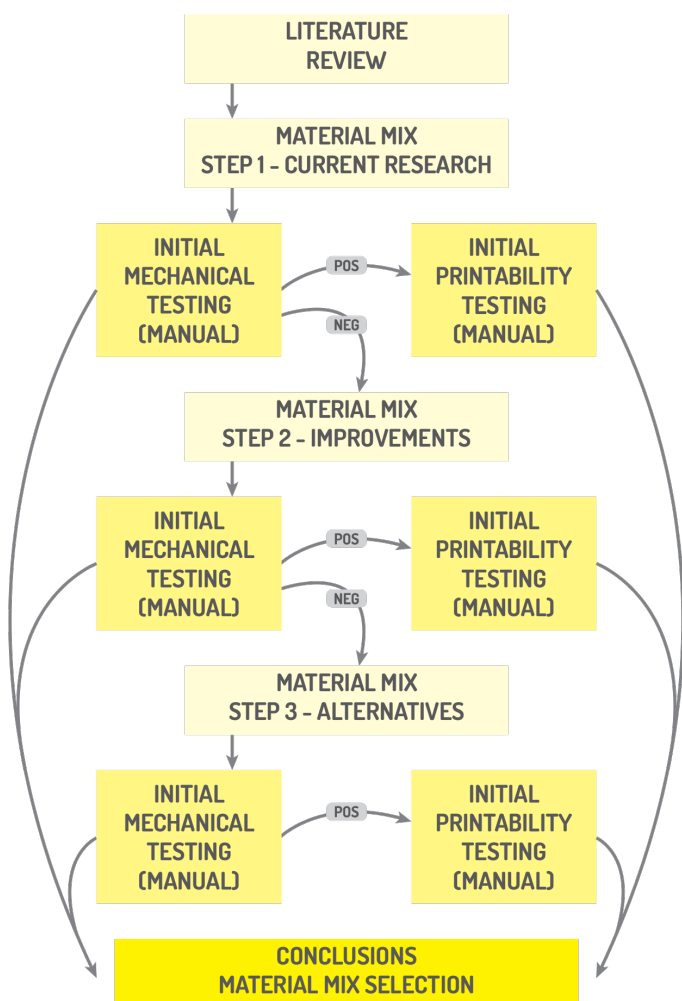


Fig 4 - Material Exploration phase flowchart
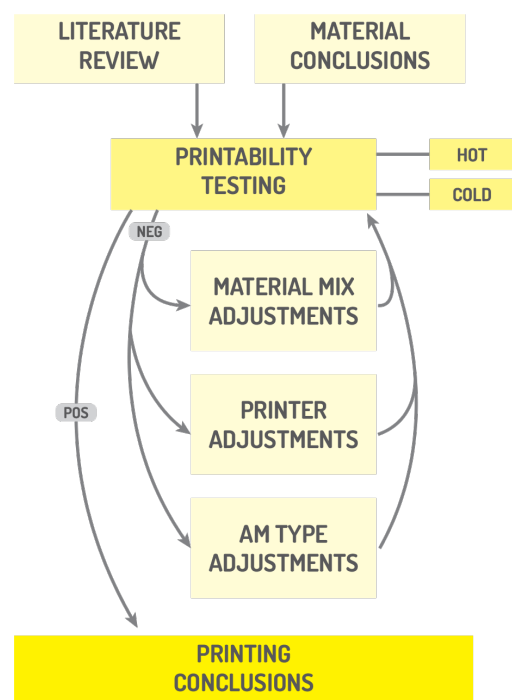
Fig 5 - Printability Expoloration phase flowchart

The mechanical testing phase proceeded in parallel to the printability to document the properties of the four promising material mixes identified at the conclusion of the exploration phase. The aim was to identify the potential for structural applications and to create a benchmark in terms of mechanical properties of wood-based materials for additive manufacturing. Samples were fabricated through moulding and extrusion processes and tested with the collaboration of Prof. Dr. Ir. Christian Louter at the StevinLab, from the Faculty of Civil Engineering and Geosciences of TU Delft.

Since this practical work was developed by two students which are exploring different applications for the same material, a more comprehensive study was made possible. Four different tests were executed: tensile modulus and strength, flexural modulus and strength, water absorption and shrinkage. A summary with the complete data was included in this research and all results were considered to answer the research question and sub-questions.

The last practical step was the design & prototyping, presenting a case study of a structural node for a free-form structure. Such element was fabricated using the material and process explored in the previous phases, but the challenges encountered throughout the process had to be addressed. Mixture composition and printing process were refined in order to obtain relevant input from the prototyping phase to draw the final conclusions of this research.

With the practical works concluded, the final step of this research was the compilation of all work executed during the 7-month timeframe and the final answer to the research question.

Therefore, the outcome of this report is a material mix with the corresponding mechanical properties dataset and an evaluation of its potential and challenges in the fabrication of a façade structural node, setting a direction for further research work.
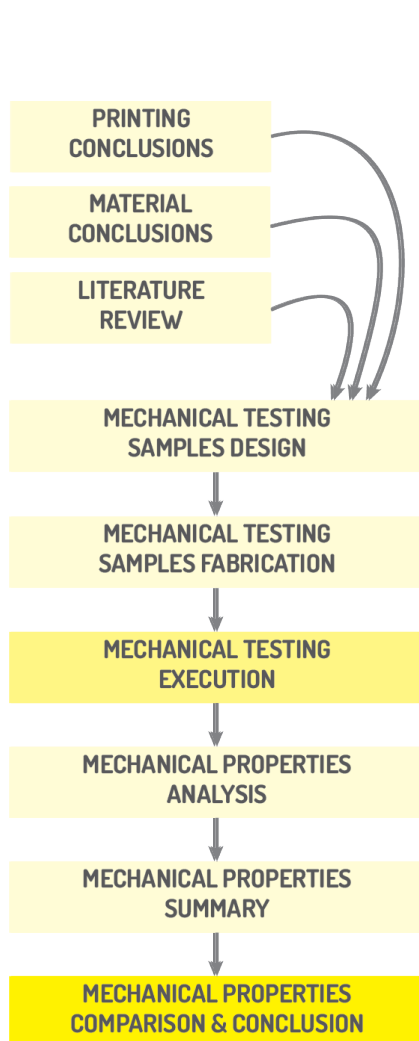


Fig 6 - Material Properties Expoloration phase flowchart
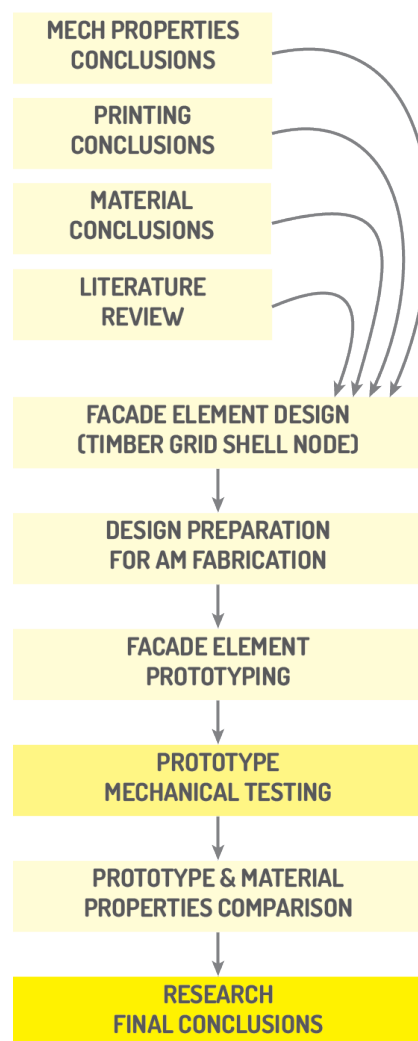
Fig 7 - Design & Prototyping phase flowchart

# 0.7. Framework & Time Plan

The research framework combined theoretical and practical phases spread throughout a timeframe of seven months. The introductory literature review provided the required background knowledge to develop the experimentation phase in material science and fabrication, the core of this work. The key milestone was the P3 presentation, scheduled mid-way the thesis length, around the week 3.8. By that date, the explorations in terms of material mix were finished and the results presented, setting the start of the properties and printability explorations.

**TASKS** — **WEEKS**

Columns: P2 (2.01 2.02 2.03 2.04 2.05 2.06 2.07 2.08 2.09 2.10) | P3 (3.01 3.02 3.03 3.04 3.05 3.06 3.07 3.08 3.09 3.10 4.01 4.02 4.03 4.04 4.05) | P4 (4.06 4.07 4.08 4.09) | P5 (4.10 5.01)

**Preparation**
- General Research
- Reference Projects & Research
- Gathering Information
- Thesis Plan Drafting

**Sourcing**
- Neworking & Connections
- Literature Compilation

**Litearture Review**
- Study & Analysis - Background
- Study & Analysis - Material
- Study & Analysis - Fabrication
- Study & Analysis - Application / Design
- Summary of Findings

**Experiments**
- Experiment Design - Material
- Experiment Design - Fabrication
- Material Sourcing
- Fabrication Sourcing
- Experiment Preparation - Material
- Experiment Preparation - Fabrication
- Experiment Execution - Material
- Experiment Execution - Fabrication
- Summary of Findings

**Material Testing**
- Testing Definition & Clarification
- Testing Design
- Testing Preparation
- Testing Execution
- Summary of Findings

**Design**
- Application Overview
- Final Material Overview
- Final Fabrication Overview
- Design Briefing & Requirements
- Concept Design
- Concept Validation
- Basic Design
- Design Validation
- Design for Prototyping
- Prototyping
- Summary of Findings

**Conclusion**
- Work Review
- Findings Review
- Research Conclusion & Final Findings
- Introduction / Conclusion
- Reflection

**Final**
- Proof Reading
- Text Review
- Text & Images Compilation
- Report Preparation
- Presentation Preparation

Fig 8 - Research Time Plan

# 0.8. Relevance

**Social**

The building stock and construction sector are responsible for a considerable share of greenhouse gas emissions. To limit these, as determined by the European Green Deal (EuropeanComission, 2019), the sector must undergo a series of transformations to become less pollutant and more efficient in terms of energy and material use. Buildings should be responsive and adapted to climate changes and the design smarter to lead the way towards zero-energy or even positive-energy constructions.

A fundamental part in reducing the carbon footprint is the material options and selection. Renewable alternatives, recycled and reused elements should replace synthetic and high-energy demanding ones. Natural materials have the potential to be as durable, strong and versatile as the rest, but experimentation, testing and prototyping are required to validate it. The Exploded View Beyond Building, created by Biobased Creations and exhibited at the Dutch Design Week 2021, was a great showcase of the potential that bio-based materials have in the construction industry and how they can be integrated to it.

Wood is the first option when natural materials are mentioned, and the one that society identifies the most. However, complex geometries, excessive waste from conventional subtractive fabrication processes, mechanical properties and deforestation obfuscate its use. Instead of limiting, these challenges are an extra motivation towards research and development. A wood-like material, natural, with potential for structural applications and viable as feedstocks for additive manufacturing processes would be greatly welcome and could collaborate into popularizing natural options in the construction environment.

**Professional & Economical**

The development of a new material, the study of its properties and the usability with the most innovative manufacturing methods currently available will break paradigms in the construction field. Attesting the potential of using a natural wood-like material for structural applications on the building envelope will allow more freedom of design and fabrication using natural materials and contributing to the environmental goals set for the sector.

Additive manufacturing can be a highly efficient and quick fabrication method. By reducing the material waste to practically zero and eliminating extensive preparations for production of complex geometries, it is an economical process for small batches and complex geometries. It allows for the highest level of customisation and constant adjustments if necessary.

**Scientific**

As mentioned above, the construction sector is one of the greatest contributors to the emissions of greenhouse gases. This research will investigate and contribute towards the development of a new material to be employed in the construction industry. A natural alternative which could replace conventional ones.

Not only the feasibility of a new material will be analysed, but its mechanical properties will also be documented, as well as possible ways of enhancing them. Such procedures will be fully scientifically based and could pave the way for further investigations into other material options and advances in the material science field.

Natural materials are the future of construction, and by studying ways of how to reproduce, alter and improve their characteristics, potential applications will be unlocked. Smarter and more optimal fabrication processes will be presented, with clear pathways to replace traditional materials being suggested.

# 1.  Literature Review

# 1.1. Wood & Derivatives in Additive Manufacturing

### 1.1.1. Cellulose & Lignin Feedstock Research Background

Cellulose and lignin, separately, have been constantly exploited as reinforcement fibres or fillers respectively (Zarna et al., 2021). As one combined compound, however, there are not many references available and the state-of-art research in the field was published in "3D printed fibre reinforced lignin" by Liebrand (2018). It focused on investigating wood as a natural alternative feedstock for additive manufacturing and its potential for architectural applications by experimenting with different proportions of the two elements.

The experiments were based on kraft lignin and bleached kraft cellulose sheets as raw material, pulped and mixed with demineralized water and acetone at different ratios to create a printable paste. The recipes were evaluated in terms of homogeneity, viscosity, bonding and water absorption through manual and visual tests, graded and compared, indicating the most promising materials to be further explored. From the 20 recipes initially explored, four were considered adequate and further tested on a cold extrusion process with plastic syringes, simulating a liquid deposition modelling AM process.

Print settings are intrinsically related to the material properties and can affect greatly the feasibility and quality of the prototype to be fabricated. Layer height and width, printing speed and flow were altered and different shapes – circles and triangles – produced to test the influence of the shape on the material and printing settings and vice-verse.

The conclusion of this study confirmed that the building blocks of wood can be used as feedstock for additive manufacturing, and, through further research, it can be used for architectural applications. Further studies and improvements are still necessary and a direction towards complex geometries which can profit from the benefits of 3D printing is encouraged.

| | type of lignin | amount of water (gr) | amount of acetone (gr) | amount of lignin (gr) | amount of cellulose (gr) |
|---|---|---|---|---|---|
| test 1 | kraft | 16 | 64 | 20 | 5 |
| test 2 | kraft | 15 | 60 | 5 | 7,5 |
| test 3 | kraft | 15 | 60 | 10 | 2,5 |
| test 4 | kraft | 15 | 60 | 7,5 | 5 |
| test 5 | kraft | 15 | 60 | 11 | 1 |
| test 6 | kraft | 0 | 10 | 10 | 0 |
| test 7 | kraft | 40 | 20 | 40 | 1 |
| test 8 | kraft | 40 | 20 | 40 | 3 |
| test 9 | kraft | 26 | 16 | 40 | 4 |
| test 10 | kraft | 20 | 26 | 40 | 5 |
| test 11 | kraft | 45 | 30 | 40 | 10 |
| test 12 | kraft | 5 | 10 | 10 | 2,5 |
| test 13 | kraft | 1,5 | 5 | 10 | 2 |
| test 14 | kraft | 6 | 13 | 8 | 4 |
| test 15 | kraft | 6 | 15 | 10 | 4 |
| test 16 | kraft | 40 | 46 | 160 | 12,5 |
| test 17 | kraft | 5 | 22 | 40 | 5 |
| test 18 | kraft | 10 | 26 | 40 | 5 |
| test 19 | kraft | 10 | 22 | 40 | 5 |
| test 20 | kraft | 10 | 28 | 60 | 5 |

Fig 9 - Material Recipes (Liebrand, 2018)

| percentage of cellulose | lignin / aceton % | cellulose/ lignin % | acetone % | water % | % fluid | homogeneity | viscosity | bonding | notes |
|---|---|---|---|---|---|---|---|---|---|
| 4,76% | 31,25% | 20,00% | 80,00% | 20,00% | 76,19% | -- | low | - | too much liquid |
| 8,57% | 8,33% | 60,00% | 80,00% | 20,00% | 85,71% | -- | high | -- | too much cellulose for printing |
| 2,86% | 16,67% | 20,00% | 80,00% | 20,00% | 85,71% | -- | low | - | too much liquid resulting in shrinkage |
| 5,71% | 12,50% | 40,00% | 80,00% | 20,00% | 85,71% | -- | high | -- | too much cellulose for printing |
| 1,15% | 18,33% | 8,33% | 80,00% | 20,00% | 86,21% | -- | low | - | too much shrinkage |
| 0,00% | 100,00% | 0,00% | 100,00% | 0,00% | 50,00% | + | low | + | too much shrinkage |
| 0,99% | 200,00% | 2,44% | 33,33% | 66,67% | 59,41% | -+ | medium | - | too much liquid resulting in shrinkage |
| 2,91% | 200,00% | 6,98% | 33,33% | 66,67% | 58,25% | -+ | medium | + | too much shrinkage |
| 4,65% | 250,00% | 9,09% | 38,10% | 61,90% | 48,84% | ++ | medium | ++ | printable material |
| 5,49% | 153,85% | 11,11% | 56,52% | 43,48% | 50,55% | ++ | medium | ++ | printable material |
| 8,00% | 133,33% | 20,00% | 40,00% | 60,00% | 60,00% | + | medium | ++ | printable material |
| 9,09% | 100,00% | 20,00% | 66,67% | 33,33% | 54,55% | ++ | high | ++ | printable material cant be extruded by hand |
| 10,81% | 200,00% | 16,67% | 76,92% | 23,08% | 35,14% | ++ | high | + | printable material cant be extruded by hand |
| 12,90% | 61,54% | 33,33% | 68,42% | 31,58% | 61,29% | ++ | high | + | cellulose seems to be too large to print |
| 11,43% | 66,67% | 28,57% | 71,43% | 28,57% | 60,00% | ++ | high | + | cellulose seems to be too large to print |
| 4,84% | 347,83% | 7,25% | 53,49% | 46,51% | 33,27% | ++ | medium | ++ | printable material |
| 6,94% | 181,82% | 11,11% | 81,48% | 18,52% | 37,50% | ++ | high | ++ | printable material cant be extruded by hand |
| 6,17% | 153,85% | 11,11% | 72,22% | 27,78% | 44,44% | ++ | high | ++ | not perfect, printing might be able |
| 6,49% | 181,82% | 11,11% | 68,75% | 31,25% | 41,56% | ++ | medium | ++ | not perfect, printing might be able |
| 4,85% | 214,29% | 7,69% | 73,68% | 26,32% | 36,89% | ++ | medium | ++ | printable material |

Fig 10 - Material Properties (Liebrand, 2018)



Fig 11 - Final Print Sample (Liebrand, 2018)



Fig 12 - Final Print Sample (Liebrand, 2018)



Fig 13 - Final Print Sample (Liebrand, 2018)

### 1.1.2. Wood Powder

Wood has been studied as an alternative feedstock for additive manufacturing for at least ten years, through experiments with sawdust and synthetic resins (Open3DP, 2011) and wood plastic composites made from wood powder and HDPE (Zhao et al., 2011).

Wood powder is imprecisely defined by Reineke (1966) as finely milled wood into grains similar in size and appearance to cereal flours. More accurate, it can be described as small timber particles which can be filtered with a 0.85mm-sieve (Clemons & Caulfield, 2005). Several studies further explored and clarified this concept, nevertheless, not relevant for this research. Overall, in additive manufacturing processes the powders commonly used contain particles with sizes between 0.014 and 2mm, depending on matrix and binder (Das et al., 2021). They are used either as additives for a polymer matrix, such as PLA and other thermoplastics, to produce filaments for FDM processes, or mixed with a binding agent and used for powder bed processes, as the powder mixture, or for LDM processes, as the paste feedstock (Das et al., 2021).

A ground-breaking mark in the use of wood powder in additive manufacturing processes was the vase fabricated at Umea School of Architecture in 2018, considered the largest wooden object 3D printed at the time – 60x45cm (Peeters et al., 2019). The material was based on 85% of wood powder mixed with methylcellulose, which act as glue, and bentonite, the binding agent. The large quantity of water to produce a fluid paste was a challenge to the material weight and to the drying process, directly affecting the geometrical and structural stability and demanding recipe and process adjustments throughout the project (Peeters et al., 2019).



Fig 14 - 3D Printed Wood Vase (Peeters et al., 2019)



Fig 15 - Wood Extrusion (Peeters et al., 2019)

In the research developed by Kariz et. al (2016), a thin wood powder with particles smaller than 0.237mm was mixed with commercially available adhesives based on polyvinyl acetate (PVAc) and urea-formaldehyde (UF) and used as feedstock for a self-made extruder. A range between 12.5-25% of wood powder content was explored and the results indicated that the paste viscosity and the pressure required for extrusion are directly proportional to the timber percentage. However, in terms of mechanical properties the modulus of rupture (MOR) and elasticity (MOE) are highly dependent of the adhesive type and strength, with the UF mixtures performing significantly better than the PVAc-based pastes – MOR = 18-19MPa vs. 3-5MPa and MOE = 1930-2002MPa vs. 13-45MPa respectively.

In the work of Rosenthal et al. (2018) a thicker wood powder with a maximum particle size of 0.4mm was mixed with a gel-like solution of methylcellulose, a derivative from cellulose, creating a paste for a self-made extruder. The material created behaves like a liquid when force is applied and like a solid when the pressure is removed, and maximises the timber content to a range between 84.5-89% of the dry weight. The mechanical properties identified are directly proportional to the material viscosity and binder concentration, improving with the decrease in wood content and particle size. The MOR values stayed in a range between 2.3 and 7.4 MPa and the MOE values between 284.8 and 733.1 MPa.

On the top end of the particle dimensional range, spruce wooden chips between 0.8 and 2mm were mixed with different binding agents - gypsum, methylcellulose, sodium silicate and cement - and tested in a powder bed fusion process (Henke & Treml, 2013). The powder mixture was layered on a movable platform and water sprayed on top, activating the binder and fabricating the designed geometry - a truncated cone. In the mechanical properties assessment, cement presented the best results, reaching values of bending strength between 0.5-0.95 MPa, nevertheless not sufficient for structural applications.
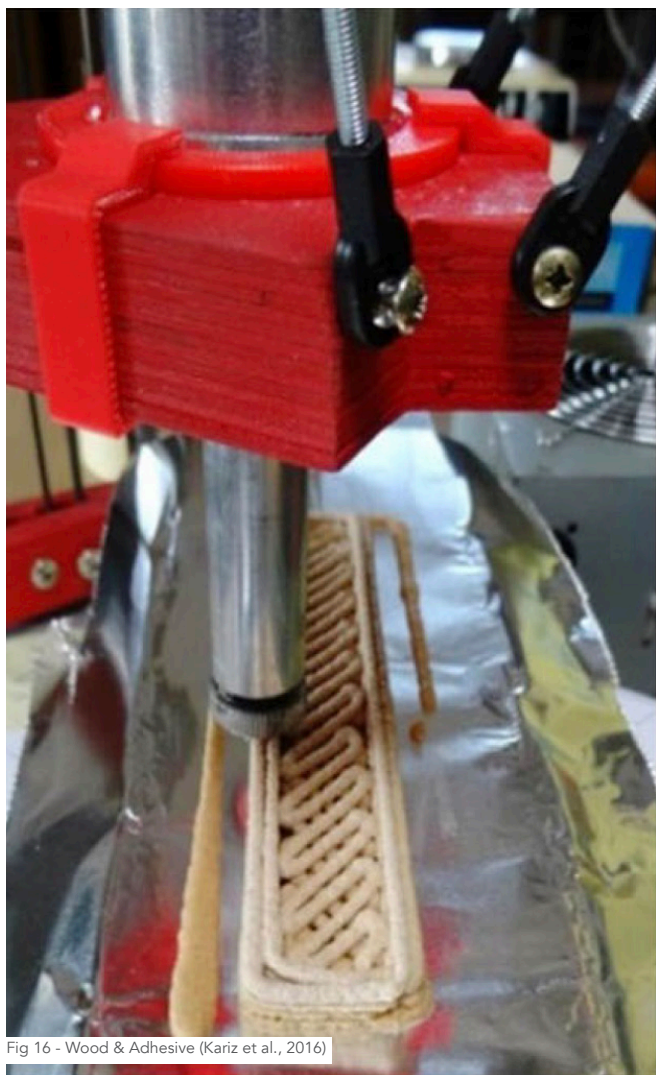

Fig 16 - Wood & Adhesive (Kariz et al., 2016)


Fig 17 - Wood & Methylcellulose (Rosenthal et al., 2018)


Fig 18 - Wood & Methylcellulose (Rosenthal et al., 2018)
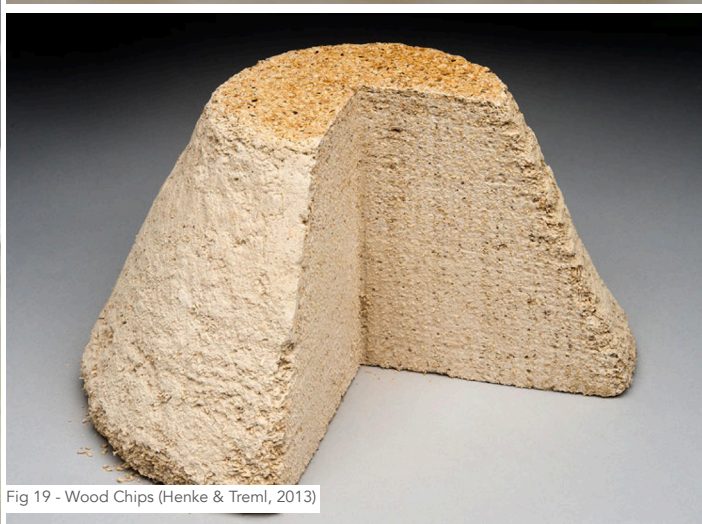

Fig 19 - Wood Chips (Henke & Treml, 2013)

Wood powder is also a popular raw material for bio-composites (Tao et al., 2017). There are a few commercially available filaments, manufactured with a PLA matrix and a wood powder filler content varying from 15% - Woodfill from ColorFab - to 40% - Laywood from CC Products (Duigou et al., 2016). Moreover, these filaments are also easily produced directly from PLA pellets melted and mixed with finely grinded wood powder, incorporating a timber content ranging from 5 wt% (Tao et al., 2017) to 50 wt% (Ayrilmis, Kariž, & Kitek Kuzman, 2019).

In small quantities up to 20 wt%, the wood content improves the mechanical properties and increases the modulus of elasticity of the material (Kariž, Šernek, Obućina, et al., 2018). However, in larger amounts it proved to negatively affect the filament properties with particles not fully encapsulated by the polymer matrix. The powder then acts only as a filler, increasing the layer porosity and clogging the extruder nozzle depending on the grain size (Kariž, Šernek, & Kuzman, 2018).

Adding wood powder to a PLA filament reduces the smoothness of the surface due to the timber micro particles, which do not melt during extrusion and present a higher porosity when compared to the polymer. Its hydrophilic properties also reduce the polymer tolerance to water (Ayrilmis, Kariž, Kwon, et al., 2019).

Wood-based PLA filaments were also used to produce large scale objects, typically respecting a maximum ratio of 20 wt% of wood content to maximise the mechanical properties of the material and the smoothness of the extrusion. A mixture of 20 wt% of wood powder with 1 wt% cellulose nanofibres in a PLA matrix was used to produce the roof of a boat (Gardner et al., 2018). Similar recipe, without the cellulose content, was also used with poplar wood to fabricate the base of a podium (Zhao et al., 2019).


Fig 20 - Sample (Tao et al., 2017)


Fig 21 - Filament (Tao et al., 2017)


Fig 22 - Specimens (Ayrilmis, Kariž, & Kitek Kuzman, 2019)


Fig 23 - Boat Roof (Gardner et al., 2018)

### 1.1.3. Cellulose

Cellulose fibres have a series of advantages that potentialize their use in additive manufacturing. High aspect ratio, availability in nature, ease to process, sustainability (element from renewable sources despite the energy and intense processing involved in its generation) and the suitability to chemical modifications make it a versatile alternative to be employed in the production of bio-composite materials.

Cellulose and nanocellulose have already been introduced in the most varied fields, such as sustainable packaging, water treatment, $CO_2$ capture, electronics (sensors, electrodes, supercapacitors) and biomedical (Gauss et al., 2021). It is a prominent feedstock for hydrogels and aerogels in the tissue engineering and bio-printing areas with the development of drug delivery systems and prothesis to be implanted in the human body (Yang et al., 2020). Overall, the main interest around cellulose regards its mechanical properties and high reinforcement potential to polymeric matrices.



Fig 24 - Cellulose-based Bio-print (Gauss et al., 2021)
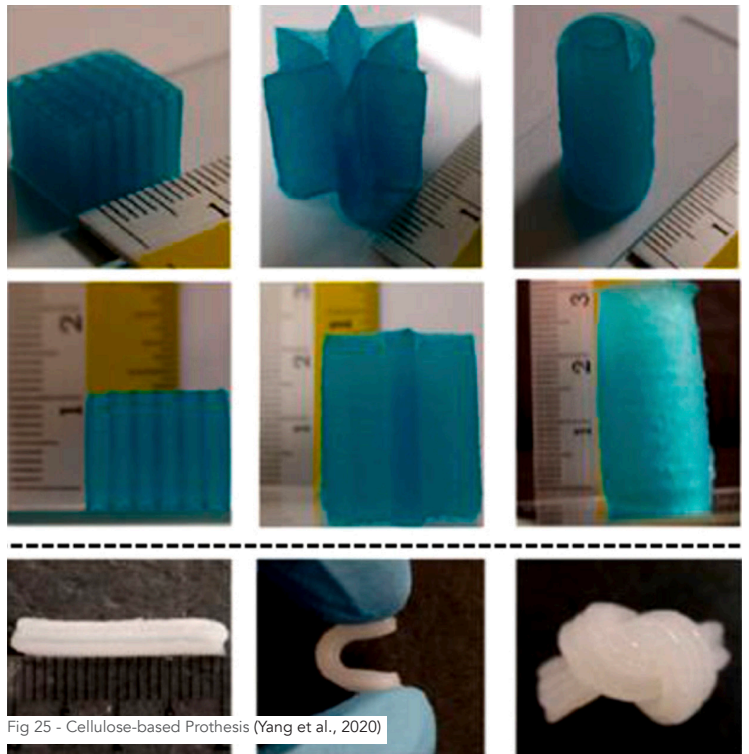
Fig 25 - Cellulose-based Prothesis (Yang et al., 2020)

Arantes et al. (2020) suggests the use of cellulose has been greatly diversified during the course of the last few decades and subdivided into five distinct generations. It started at the micrometre level in textile applications, with cellulose as a textile fibre sourced from cotton. Following up to the second generation, the micrometre scale remained but chemical processes were introduced, and the paper industry became prominent with the exploration of cellulose from wood. The next evolutionary step changed the scale to the molecular level with the development of derivatives and the expansion to other industries such as pharmaceuticals and food. The fourth generation marks the transition to innovative technologies and the focus shift towards sustainability, with biofuels and the recycling of agricultural waste. Finally the current fifth generation introduces the use of cellulose at nanoscale and expands its applications to even more industries from construction to automotive and electronics. More important, it also marks the start of cellulose as feedstock for additive manufacturing processes.

The most promising results regarding the use of cellulose towards the additive manufacture of structural components relate to all-cellulose composites (ACC). By combining a matrix made of regenerated cellulose with cellulose reinforcement fibres, it is possible to reach mechanical properties similar to the theoretical values of pure cellulose (Gauss et al., 2021).

Typically, cellulose is used in composite materials as the natural fibre reinforcement in a plastic matrix or derived into sub-products through complex and polluting processes. A full bio-based alternative was presented by Sanandiya et al. (2018), called FLAM - fungal-like additive material. Inspired on the walls of the oomycetes, it mixes chitin (modified with acetic acid into chitosan) with cellulose at the optimal ratio of 1:8. The extrudable paste resulting presents mechanical properties similar to low-density woods and a modulus of elasticity of 0.26 GPa. Such material can be post-processed and finished with woodworking techniques, and was used to successfully fabricate parts of a wind turbine and a sample column.


Fig 26 - Wind turbine component - FLAM structure (Sanandiya et al., 2018)
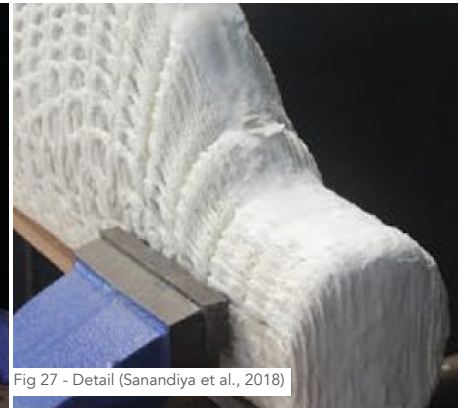

Fig 27 - Detail (Sanandiya et al., 2018)


Fig 28 - Wind turbine component - FLAM finished part (Sanandiya et al., 2018)

In parallel, students from the master's studio Material & Detail, in Architecture and Civil Engineering at Chalmers University, Sweden, designed and fabricated a structural wall using a paste based on cellulose and resin (Runberger & Lundberg, 2019). The installation was produced and assembled in modules, totalling 2 x 2 x 0.5m, and showcased organically shaped geometries for the openings and spatial truss structure. The research was supported by the Research Institutes of Sweden – RISE – within the project WouldWood, aimed at investigating new wood-based sustainable materials (WouldWood, 2018).


Fig 29 - Cellulose wall (Runberger & Lundberg, 2019)


Fig 30 - Cellulose wall (Runberger & Lundberg, 2019)


Fig 31 - Cellulose wall - detail (Runberger & Lundberg, 2019)

### 1.1.4. Lignin

Unlike cellulose, lignin is poorly valorised and not employed in the high technology industry. The gross of the material is still used as biomass for energy generation, although it has less energy content than coal and its market value as energy source is limited to a tenth of the value it would have as raw material for other applications (Tanase-Opedal et al., 2019). Bio-based composites with lignocellulosic fibres and content have attracted particular attention in the past five years, propelled by the abundance of its components in nature and the sustainability potential incorporated. Additive manufacturing is a promising way of valorising lignin and escape from the image of low-value residue burned to generate energy.

According to the ASTM/ISO classifications, there are currently seven categories of additive manufacturing processes (Gibson et al., 2021). Out of these, lignin has been used solely on extrusion-based and vat photopolymerization processes (Ebers et al., 2021). The use of lignin in additive manufacturing has been restricted to combinations with thermoplastics in inks or filaments for FDM fabrication, with less than 70% of content (Grigsby et al., 2020). In Tanase-Opedal et al. (2019), a filament containing 40 wt.% of lignin was produced and used to fabricate a cell phone case. Adding complexity to process, each type of lignin has its own structure and properties and would be adequate for specific fabrication methods.

Filaments are frequently too brittle and difficult to handle. However, when chemically modified and combined with an acrylonitrile butadiene styrene (ABS) matrix, lignin creates a strong composition with excellent printability. Nylon12 is also a suitable matrix and the outcome is a relatively soft but tough polymer. When mixed with fibres, such as carbon fibres, stiffness and strength are enhanced and printability improved by reducing the filament buckling. Replacing carbon with natural fibres such as cellulose on this composite has a good potential towards creating a natural feedstock (Ebers et al., 2021).

With direct ink writing, a wide range of feedstock in the shape of pellets or paste can be used, allowing room temperature processing, well-suited for lignin. However, the examples of use are scarce and restrict to polymer blends to form gels and pastes for use in the bio-printing industry. Although applied in small fractions, lignin does increase the shape fidelity and antioxidant properties of the printed parts (Ebers et al., 2021).

In photopolymerization processes, such as stereolithography (SLA), the use of unmodified lignin mixed with the resin matrix has proved not advantageous, with timid improvements to the parts and loss in curing speed. Although the incorporation of chemically modified organosolv lignin resulted in higher tensile strength (Ebers et al., 2021).

The most promising use of lignin in additive manufacturing so far is described by Nguyen et al. (2018) in two case studies with ABS and nylon12. For both cases, organosolv hardwood lignin and kraft softwood lignin were tested and the former one selected as the most adequate due to its thermal properties and lower viscosity. The blended mix with nylon12 presented a promising compound to be used as feedstock. Experiments were carried with lignin concentrations of 40 wt.% and 60 wt.%, with and without carbon fibre reinforcements, to further enhance the strength. The results identify an increase in the stiffness and a reduction in melt-viscosity at room temperature, favourable for the printing process. Mechanical properties were enhanced in all samples with an increase on tensile strength and modulus, validating the mix as a feasible and promising feedstock to be further developed. As an extra advantage of the use of nylon12 in this case study, there are researches pointing towards the development of a 100% natural version of the raw material.

# 1.2. Raw Materials

### 1.2.1. Cellulose

### 1.2.1.1. Overview, Composition & Structure

Cellulose is the most abundant polymer in nature and one of the building blocks of wood, combined with hemicellulose and lignin. Softwood samples usually contain between 33-42% cellulose meanwhile hardwood ones reach 38-51% of its composition (Sjöström, 1993). It had been used by the human beings for thousands of years in the most varied fields, from energy generation to clothing and paper production, before officially discovered and classified as a plant cell wall sugar by Anseme Payen in 1838 (Gauss et al., 2021). Currently, it sums up to an annual production of 1.5 trillion tons of biomass (Gauss et al., 2021).

The wood cell wall is a highly regular structure composed by cellulose microfibrils organized in crystalline and amorphous regions (Gauss et al., 2021). These are formed by the long string-like molecules of cellulose, which present high tensile strength. These are inserted in a brittle material matrix, lignin, and linked to each other with the help of the smaller molecules of hemicellulose (USDA Forest Service, 2010).

Cellulose is a structural component in plants, embedded in a polymeric matrix of lignin and complex sugars. It appears to be a hierarchical composition of molecules forming elementary fibril structures. These are formed by nanofibers composed of highly ordered nanocrystals and amorphous chains (Zarna et al., 2021).

According to Gauss et al. (2021), cellulose fibres can be classified in six types regarding their structure and morphology:

– Cellulose Microfibre (MF) – also known as cellulose pulp, with average length between 0.7-25mm.

– Microcrystalline Cellulose (MC) – microscopic porous particles with size between 10-50um, originated from chemically treated microfibres (MF).

– Cellulose Nanocrystal (CNC) – also obtained from chemically treated microfibres, presents high crystallinity and maximum dimensions between 77-503nm.

– Nanofibrillated Cellulose (NFC) – 100% of cellulose mechanically refined from microfibres, with amorphous and crystalline portions and a high aspect ratio reaching 500-2000nm long by 4-20nm wide.

– Bacterial Cellulose (BC) – microfibres with high aspect ratio, surpassing 50.

– Regenerated Cellulose (RC) – Microfibrils chemically treated from the original ones for use in the textile industry mostly.

### 1.2.1.2. Properties

Cellulose is a structural component in plants, reinforcing the cellular walls in a lignin matrix (Zarna et al., 2021). All plants contain cellulose and are designed to support their own weight and resist to inclement weather and environmental conditions, such as wind and rain (Gauss et al., 2021).

The cellulose fibres are good at tensile strength and give the wood the flexibility for which it is known. They also make timber be an anisotropic material, meaning its mechanical properties vary according to the fibre direction – higher strength and performance on the fibre direction (Gauss et al., 2021).

The hydroxyl groups which compose cellulose make it be a hygroscopic element, rendering a great affinity to water for the cell walls. On the other hand, such characteristic is counteracted by the hydrophobic lignin, which bonds the cells together, and limits the water intake. (USDA Forest Service, 2010).

The working temperature is relatively low. Wood begins to break at temperatures above 100°C. From 200°C, hemicellulose starts to degrade meanwhile lignin resists until 225°C. Between 300°C and 350°C, a significant depolymerisation of cellulose starts (USDA Forest Service, 2010).

### 1.2.1.3. Sourcing

Cellulose accounts for approximately 1.5 trillion tons of total annual biomass production. It is mainly sourced from wood, plants, agricultural residues, tunicate, algae and bacteria. Pulp production and the paper industry are the primary consumers, although a growing demand has also been documented for the fabrication of inorganic and polymeric composites, nanocomposites, hydrogels and even electronics (Gauss et al., 2021).

Most of the cellulose consumed in the planet is extracted from pulping soft and hardwood though the kraft process. Alternative non-wood biomass sources poorly exploited nowadays include cotton, sugarcane, sisal, hemp and flax, which might include a cellulose content of up to 95% of its total.

According to Gauss et al. (2021) extraction process depends on the structure and amount of lignin and hemicellulose in the material composition. Conventionally, it is through either the kraft process (based on sodium hydroxide and sulphide) or organosolv (based on ethanol and water). Elevated temperature and pressure are necessary to remove the by-products. After passing by the biomass digestion phase and isolated, cellulose can be directed to a sequence of bleaching steps based on the remaining lignin residues.

A less chemical and polluting sourcing is through bacteria cultures. Through specific culturing methods, it is feasible to grow highly pure cellulose without any by-products. Once the product is mature, it can be washed out resulting in a hydrogel with a water content of up to 99%.

Independently from the source, once cellulose microfibres have been isolated, mechanical and chemical treatments are employed to further refine the material into the classification described above. The smaller and purer cellulose is, the more steps and chemical reactions will be necessary.

### 1.2.1.4. Alternative Sourcing

Cellulose and lignin are natural elements, although the conventional extraction and sourcing of cellulose, from the paper industry, results in a considerable impact to the environment and involves intense chemical modification to the wood fibres to break its lignocellulosic structures. Even with reforestation, alternative sources for cellulose, specially from recycled and wasted material are welcome.

Fiberboards such as MDF and HDF are a large source of wood waste due to an unclear recycling path, a short lifespan of 7-18 years (Couret et al., 2017) and a growing annual production of 110 million m3 (FAOSTAT, 2020). In the study presented in Couret et al. (2017), wood powder from milled residual boards is chemically treated in consecutive steps to separate the lignocellulosic content from adhesives and contaminants and subsequently isolate the cellulose nanocrystals. The resulting CNC presented similar physical characteristics and quality to the one extracted from pure virgin wooden fibres.

Agricultural waste is also a vast source of cellulose and, recently, the focus of several studies specifically on alternative sourcing of cellulose nanostructures (Rajinipriya et al., 2018). Pineapple, banana and sisal are some of the biomass sources being investigated (Rajinipriya et al., 2018), together with sugarcane bagasse (Rana et al., 2021) and rice husk (Senthilkumar et al., 2021). Overall, the extraction process is similar for all the agricultural waste sources, and involves two phases – purification and extraction – as described by Rajinipriya et al. (2018). Biomass is first soaked in an alkaline solution then bleached to separate the cellulose content from hemicellulose and lignin. Once purified, depending on the sought outcome – nanofibrils, nanocrystals – the cellulosic mass is treated chemically, mechanically or enzymatically to isolate the nanostructures.

Such processes can also be adapted to another large source of cellulose – paper waste. As described in the research of Sridhar & Park (2020), it is possible to extract microfibrillar cellulose from shredded paper treated with an aqueous solution of sodium hydroxide and urethane. The resulting fibres presented excellent quality and high levels of crystallinity, comparable to the ones obtained directly from wooden fibres.
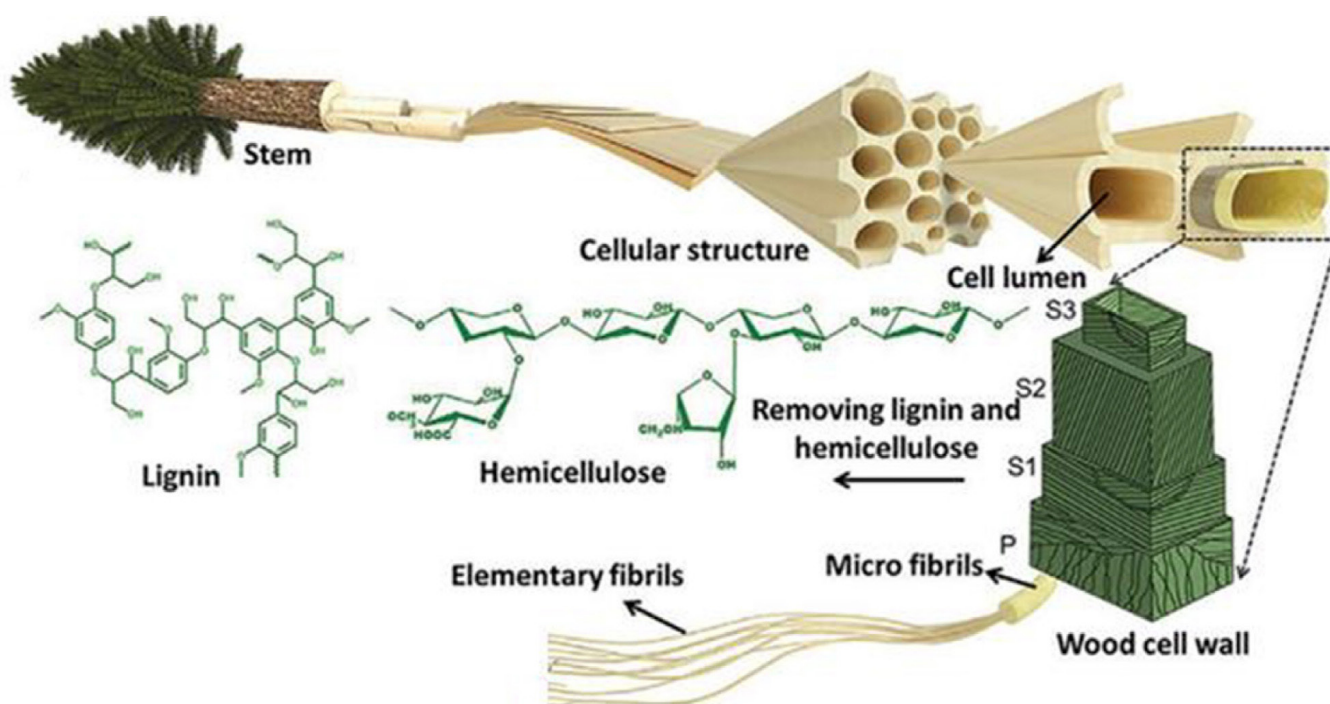


Fig 32 - Wood cell structure - cellulose (Gauss et al., 2021)
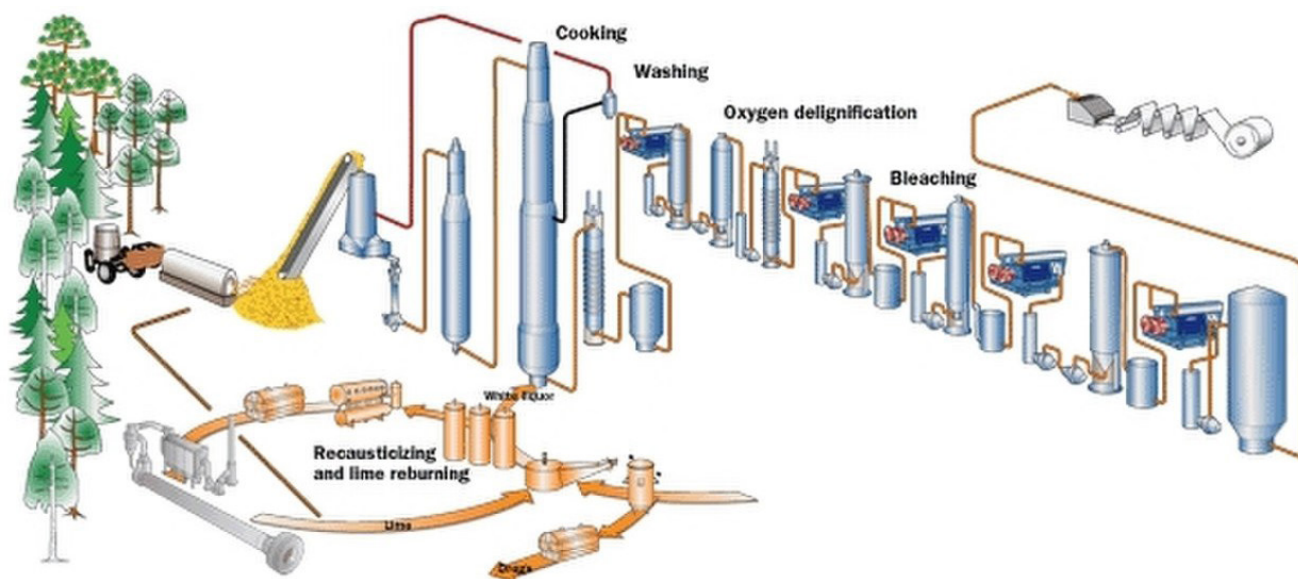


Fig 33 - Cellulose production - Kraft process (Wetterlund et al., 2013)

### 1.2.2. Lignin

#### 1.2.2.1. Overview, Composition, Structure

Just after cellulose, lignin is the second most abundant polymer in nature and another building block of wood, providing its characteristic brown colour. Softwood samples contain between 27-32% of lignin, similar to the values encountered in hardwood, a range between 21-31% (Sjöström, 1993). Lignin is a hydrophobic macromolecule which compose the brittle polymer matrix of wood, responsible for linking cellulose and hemicellulose to form the wall cells and for bonding the cells together (USDA Forest Service, 2010).

Two categories of lignin are derived from the wood/cellulose pulping process, the lignosulfonates, accounting for approx. 88% of the total lignin produced, and kraft, accounting for approx. 9% of the total. The remaining production of approx. 2% corresponds to the organosolv or biorefinery lignin, a growing field and expected to become more popular (Ebers et al., 2021).

This is a vast and inexpensive feedstock with an elevated potential to replace synthetic polymers such as polyethylene (PE) as the matrix or filler in bio-based composites. Its price range is between 20-50% lower than the average for PE (Ebers et al., 2021). It is a biodegradable, antioxidant and antibacterial element, properties which shall be inherited by its compounds.

Lignin is an important structural component of woody plants. It is responsible for providing physical strength and forming the capillary network for water distribution throughout the whole plant. The polymer is composed by three basic blocks – called monomers – which concentrations vary according to the source – hardwood or softwood (Chung & Washburn, 2016). The different chemical composition explains the different behaviours and why one type of lignin might be better suited for a specific use than another.

Lignin is a versatile element which has a valorisation potential into the bio-based materials industry and even compete with commodity polymers. It can be modified and designed to improve affinity with thermoplastics or just incorporated as an additive for UV light stabilisation, anti-oxidant, flame retardant, plasticiser or flow enhancer in the fabrication process (Tanase-Opedal et al., 2019). More than that, it can be combined with natural fibres as a natural coupling agent to combine hydrophilic fibres and hydrophobic matrices and collaborate in the development of bio-composite materials.

#### 1.2.2.2. Properties

Type and source of lignin also define some of its characteristics and properties. Kraft lignin, for example, is not soluble in water or common solvents due to its chemical structure, meanwhile the opposite is true for lignosulfonates, soda and organosolv lignin. Also, the different monomer concentration between softwoods and hardwoods leads to a lower softening temperature for the latter and facilitates the thermal viscous flow, an advantage for 3D printing processes with lower working temperature and energy consumption. However, the degradation temperature is also reduced and should be observed (Ebers et al., 2021).

If exposed to UV radiation, lignin starts to degrade within hours although it might take decades to demonstrate physical effects and erosion. It affects the fibre bond, leaving cellulose loosely attached to the material surface (USDA Forest Service, 2010).

In general, lignin is a polymer which has not been engineered by humans, but sourced in nature, with an amorphous morphology which affects its processability. It does not melt or crystallize on its own, usually requiring it to be blended with other elements or derivatized (Ebers et al., 2021).

Working temperature is relatively low, as wood begins to break at temperatures above 100°C. Lignocellulosic material usually does not melt, except for a few fractions from softwood and hardwood samples which present melt stability. Under intense heat lignin degrades and forms ash and a rigid char. The degradation peaks between 225°C and 450°C, requiring its processing to be executed below this threshold to avoid accelerated thermal degradation (Nguyen et al., 2018) (USDA Forest Service, 2010).

Reinforcing the difference between lignin origins, the glass transition temperature of hardwood lignin, when the element starts transitioning into a viscous state, lays around 87°C, almost 100°C lower than the 181°C characteristic from kraft lignin from softwood (Nguyen et al., 2018).

The very low molar mass of lignin gives it melt-processabilty but also causes brittleness. As a polymeric material alone, the applications are limited. It cannot form a free-standing structure. However by combining it with plasticisers and additives it can modify materials and create new types of bio-composite polymers (Nguyen et al., 2018).

A comprehensive analysis on the properties and differences between hardwood and softwood lignin is offered by Nguyen et al. (2018). Hardwood lignin has a less rigid chemical structure with an increased free volume for the molecules which increase its mobility and explains the reduced melt-viscosity and glass transition temperature by allowing more degrees of freedom for rotating and bending molecules. Softwood lignin has a substantial higher amount of stiff elements.

Hardwood lignin presents also a much longer elastic response – 10% strain versus 1% strain from softwoods.

Softwoods have much higher viscosity. A very high stiffness in molten stage and very high resistance to flow make it not suitable for melting. Hardwood, at room temperature, has extraordinary brittleness and stiffness but at processing temperature it presents a very good flow behaviour and lower viscosity than the former. These properties make hardwood lignin more suitable for bio-based polymer production and 3D printing.

### 1.2.2.3. Sourcing

Annually, 100 million dry-tons are generated from the paper industry (Ebers et al., 2021), to be combined with 50 million dry-tons from biorefineries (Tanase-Opedal et al., 2019). Out of these amounts, 98% of the biomass is burned to generate energy for the industrial plants, and the remaining 2% are used in the production of dispersants and adhesives.

Lignin is largely obtained as a by-product from the cellulose extraction process from wood in the paper industry and as a by-product from biorefineries from agricultural and wood waste. According to Chung & Washburn (2016), commercially-graded lignin can be commonly sourced through six different methods – kraft pulping, sulfite pulping, soda process, organosolv, steam explosion and dilute acid.

Most commonly, it is obtained from the black liquor resulting from the wood pulping processes. Cellulose fibres used in the paper industry are removed from the lignocellulosic structures through a chemical degradation process. In a biomass digestor, wood is cooked in an aqueous solution containing sodium hydroxide and sodium sulphide under elevated temperature and pressure. Approximately half of the initial wood content degrades and dissolves into the liquid, creating the black liquor, a by-product from the process which is then removed and treated to separate the remaining biomass, from the chemicals, which can be reused (Alén, 2018).

Alternatively, lignin can also be obtained through biorefinery processing lignocellulosic biomass for the production of second generation biofuels, green chemicals and biopolymers. The non-digested fraction of this process is rich in lignin and could be removed through biochemical methods before the production of the biofuels and upcycled into other industrial processes (Gosselink, 2011).

The soda lignin is extracted through a process using an alkali substance, such as sodium hydroxide, to depolymerise the lignin and remove it from the biomass matrix. It decomposes the lignocellulosic structure by breaking the chemical bonds between the lignin macromolecules and the hemicellulose fibres. The soda cooking liquor has a reduced content of low-weight wood degradation products which would go to wastewater, reducing the environmental impact. It is also sulphur-free and consequently odour-free. The final product is a composition close to pure lignin (Tanase-Opedal et al., 2019).

Together with the development of new isolation technologies, the possibility of creating technical lignin is also being studied, improving properties for specific applications and compositions (Ebers et al., 2021).
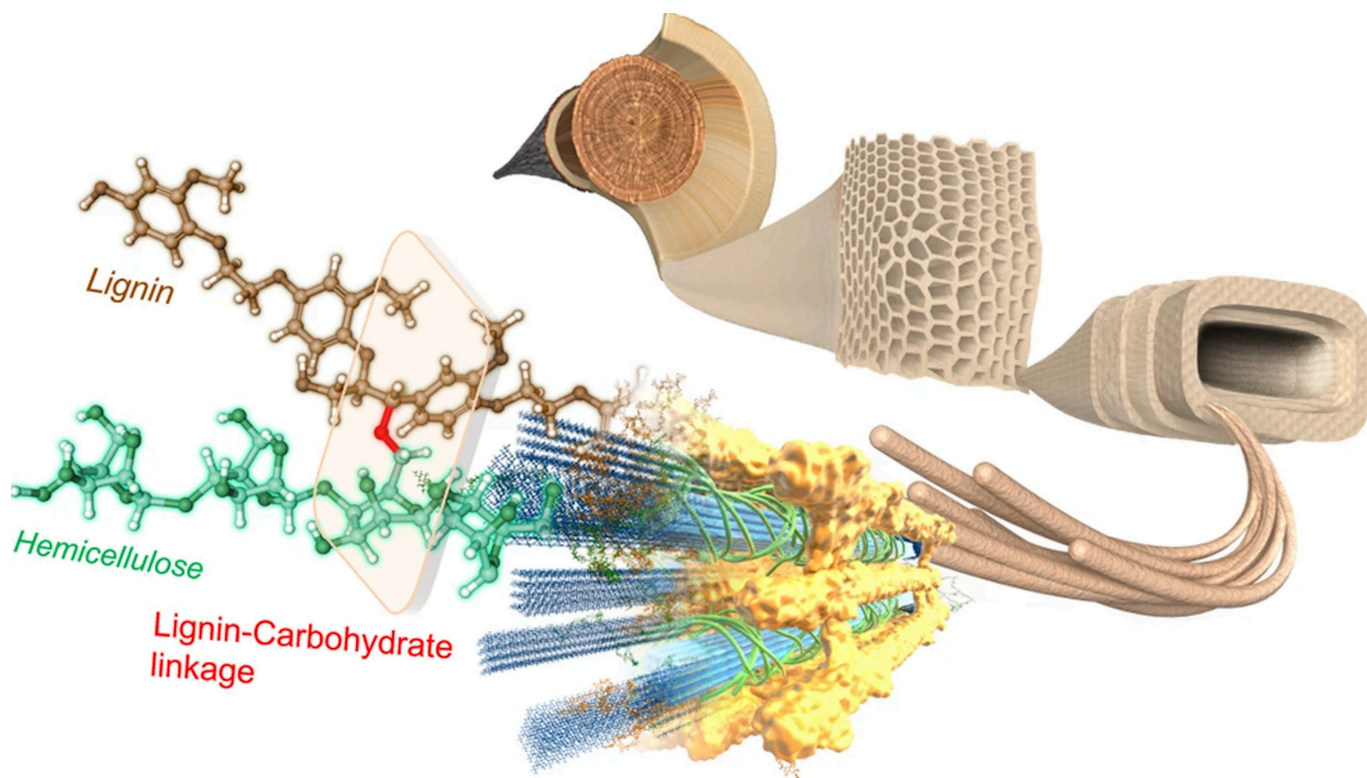


Fig 34 - Wood cell structure - lignin (Nishimura et al., 2018)

### 1.2.3. Binders

### 1.2.3.1. Xanthan Gum

Xanthan gum is a natural polysaccharide obtained from the fermentation of fructose and glucose by the Xanthomonas campestris bacteria (Raschip et al., 2007). It is a biocompatible and stable thickening agent, soluble in water (Ingtipi et al., 2022), capable of forming viscous solutions, steady at high temperatures and cheap to manufacture in large quantities (Raschip et al., 2007). Xanthan is commonly used on a wide range of applications, from gelling agents in the food industry to hydrogel matrices in the pharmaceutical industry.

In Ingtipi et al. (2022), xanthan gum is mixed with lignin in the production of nanocomposite hydrogels, focused mostly as drug delivery/carrier for biomedical applications.

In additive manufacturing, most applications of xanthan gum are specific to the food industry. In Liu et al. (2019), it was combined with carrageenan and starch to create a gel for a 3D food printer. In Gholamipour-Shirazi et al. (2020), several applications showcasing the use of xanthan on food-related extrusions were presented, including a mix based on cellulose powder to be used in a binder jetting process.

### 1.2.3.2. Methylcellulose

Methylcellulose is a derivative from cellulose, typically obtained from the pulped polymer extracted from cotton and wood and chemically processed with sodium hydroxide and methyl chloride (Grover, 1993). Traditionally, it has been used as an additive in the production of adhesives, cement and mortar in the building industry. It increases the viscosity and improves the workability, cohesion, homogeneity and stability of the mixtures (Grover, 1993; Vieira et al., 2009).

The common ratio methylcellulose to water is between 1:20 to 1:33.3, according to the expected viscosity (Vieira et al., 2009), and it is mixed with heated water at 80C, above its gelation point, to enhance the solubility. Continuously stirring until cooling down results in a homogeneous solution and a smooth paste. Repetitive cycles of heating and cooling modify the material consistency although do not affect its overall gel-forming capacity (Grover, 1993). The resulting material typically presents a load-dependent behaviour

As a binder for additive manufacturing materials, methylcellulose has been explored in numerous and diverse bio-based composites. In the biomedical field, it was used to enhance the viscosity of alginate-based hydrogels (Li et al., 2017). In Rosenthal et al. (2018), it was mixed with wood powder from beech in a binder to filler ratio of 15.5:84.5, 14.5:85.5 and 11:89 of the dry weight, resulting on a smooth paste used to extrude test samples. In Peeters et al. (2019) a similar content of timber – 85% of the dry weight – was mixed with methylcellulose and bentonite and successfully used to fabricate a vase, considered the largest 3D printed wood object at the time.

Overall, methylcellulose mixed with lignocellulosic material results on a load-dependent material. It flows like a viscous paste under stress and behaves as a solid once the force is removed. After cured, the material solidifies and becomes independent to the stress applied, until water is added returning the material to its original viscous state (Rosenthal et al., 2018).

### 1.2.3.3. Dimethylsulfoxide (DMSO)

The potential of dimethyl sulfoxide (DMSO) as a binding agent for cellulose and lignin was raised by

Dunia Agha, a researcher from the Institute of Structural Mechanics and Design from TU Darmstadt and an external consultant to this research. According to the information provided, the solvent would be a less harmful alternative to acetone and with a slower evaporative action.

DMSO is a naturally occurring substance, obtained as a by-product from the kraft processing of wood (Dimethyl Sulfoxide, 2022). It is commonly used in the pharmaceutical and cosmetic industries and as a solvent, available in both medical and industrial grades (Aronson & Dukes, 2006). At room temperature it is in liquid state although it solidifies below 18C. (Dimethyl Sulfoxide, 2022).

In Hu et al. (2020) an aqueous solution of DMSO combined with another chemical - tetrabutylammonium hydroxide - was used as a solvent for cellulose in the fabrication of hydrogels for 3D printing. The great results obtained validated the use of DMSO as a solvent in the production of cellulose-based materials. Moreover, in Gunasekera et al. (2016) the solvent was used in ionic liquid solutions of cellulose to reduce and control the material viscosity, preparing it for ink-jet 3D printing.

### 1.2.3.4. Glycerine

In additive manufacturing the use of glycerine has been explored mostly with cellulose nanoproducts – crystals and fibres – in biomedical engineering. In Gauss et al. (2021), cellulose nanocrystals in a glycerol matrix were used to develop an ink for a direct ink writing printing process for bio-applications. In Mohan et al. (2020), the polyol is applied as a plasticiser to control the viscosity of a cellulose-based gel and optimise its extrusion definition and printability for wound-healing applications. The same study also highlights the use of the polyol mixed with nanofibers and used as a coating on woven fabrics. The mechanical properties are retained and the amounts of fabric pigment optimised (Mohan et al., 2020).

### 1.2.3.5. Corn Starch

The potential use of starch as an additive for lignocellulosic materials has been raised by its potential use in the formulation of green adhesives for the wood industry (Norström et al., 2017). No direct use in 3D printing processes has been identified, however as a green adhesive it could replace animal and synthetic glues already experimented.

Starch is a natural polymer commonly used in the food industry and in the formulation of bio-adhesives (Ferdosian et al., 2017). It has been used as a natural binder since ancient times (Onusseit, 1992) and presents a harmless alternative to the toxic formaldehydes normally employed in the wood and building industries (Ferdosian et al., 2017).

Accessibility in nature, easy processing, low cost, good adhesion and non-toxicity are promising characteristics that lead starch as a potential raw material for green adhesives. However, it still requires chemical transformations to enhance its bonding strength and reduce its affinity to water (Ferdosian et al., 2017).

### 1.2.3.6. Alginate

Alginate is a common polysaccharide in nature, which can be found in marine brown algae and soil bacteria, assuming a structural behaviour on the first one. It has stabilizing properties and when absorbing water, it forms gels and viscous solutions, being popularly used in the food and pharmaceutical industries as a hydrogel matrix (Hecht & Srebnik, 2016).

The printability and biocompatibility of alginate makes it a suitable additive in hydrogel inks used in

additive manufacturing (Podstawczyk et al., 2020). It presents a remarkable shape fidelity and bonding, ideal for multi-layered structures, (Li et al., 2017), although its mechanical properties impose limitations in terms of size and complexity of the geometries (Podstawczyk et al., 2020).

In Sauerwein et al. (2020), alginate is showcased as a binding agent for a wide selection of bio-based fillers sourced from waste material – eggshells, walnut shells, cacao shells, olive pomace, pine and maple sawdust. To enhance the mix smoothness and viscosity, methylcellulose was also added to all different recipes. Starting with ground mussel shells, a paste material was developed and used to fabricate a demonstrator – a hairclip – and samples for mechanical testing and material characterization. The maximum value obtained for modulus of elasticity was 2.1 GPa, and for flexural strength, 9.8 MPa, similar to the results achieved by lignin-based PLA filaments (Tanase-Opedal et al., 2019).

### 1.2.3.7. Beeswax

Beeswax is a harmless and biodegradable material, with great ductility and a relatively low melting point at 61-67C (Pavon et al., 2020). Combined with lignin and cellulose derivatives, it shows good anti-oxidant properties and it has been studied and validated as a protective coating on paper packaging (Rumpf et al., 2020).

As an additive for 3D printing materials, it has been used to produce polycaprolactone (PCL) filaments for FDM fabrication processes, either alone or combined with gum rosin (Pavon et al., 2020). The beeswax concentration reached a maximum of 10%, and resulted on a decrease on the tensile and flexural properties of PCL, although increasing its flexibility and workability (Pavon et al., 2020).

### 1.2.3.8. Bone Glue

The relevance of glues from animal origins has been documented since the 1950s (Konnerth et al., 2009). Bone glue is traditionally produced from waste from the food industry, based on animal tissue and bones (Christ et al., 2019) and conventionally used as an adhesive in woodwork. It is presented in dry beads which must be soaked in water for a few hours and heated up in order to produce a viscous adhesive (Konnerth et al., 2009). As most natural adhesives, it demands a longer pressing and curing time, affecting its applicability, although the results presented in Konnerth et al. (2009) validate its use as a replacement to formaldehyde-based adhesives in the fabrication of particleboards.

In additive manufacturing, adhesives in general have already been successfully used mixed with wood-derived material (Kariž et al., 2016). In Christ et al. (2019), bone glue was mixed with mineral aggregate to produce a biopolymer concrete for the building industry. The results showed similarities to conventional cement-based concrete and strong mechanical properties, attesting its feasibility for structural applications with a flexural strength of 8MPa and compressive strength of 21MPa.

### 1.2.3.9. Wood Glue

The conventional wood adhesives used in the building industry and in the wood production are based on polyvinyl acetate (PVAc) and urea-formaldehyde (UF) (Kariž et al., 2016). However, the health hazards from formaldehydes (Sain et al., 2007) have already raised concerns and provided incentive to the research into natural alternatives. Studies identified promising directions with lignin, tannin and starch among others, although further improvements in water resistance, strength and formulation stability are necessary for industrial applications (Norström et al., 2017).

In the additive manufacturing field, both PVAc and UF adhesives have already been explored, mixed with

wood powder in different ratios - between 12.5% and 25% - and used to successfully print test samples (Kariž et al., 2016). The results indicate that the strength and stiffness of the binding agent directly affect the material, and the larger the difference between the mechanical properties of binders and fillers, the less impact the wood content has on the overall performance of the element (Kariž et al., 2016).

### 1.2.3.10.  Sunflower Oil & Baking Soda

These additives were included in the list of raw materials for the material exploration phase by suggestion from the external advisor of this research, Dr. Richard Gosselink, from Wageningen University, to improve the solubility of the lignin and to either replace or reduce the amount of water in the recipes.

According to Evstigneev (2011), lignin is insoluble in water but soluble in alkaline aqueous solutions, depending on the polymer type and on the concentration of sodium hydroxide or another alkali substance, such as sodium bicarbonate (baking soda). The higher the concentration of a base element in the mixture, the higher the solubility of lignin (Evstigneev, 2011).

Vegetable oils from soybeans, linseed and sunflower, can be used as harmless bio-based plasticisers – additives to improve the flexibility and workability of plastics and elastomers (Samarth & Mahanwar, 2015). Composites mixing an acrylate-modified soybean oil matrix and natural fibres such as flax and hemp, present good mechanical properties and have already attracted the interest of different markets, specially in the automotive industry (Samarth & Mahanwar, 2015).

In the additive manufacturing field, chemically modified vegetable oils can also be used as a high quality replacement resin for SLA and DLP processes (Vazquez-Martel et al., 2021). Both virgin and waste cooking oils from houses and restaurants have been tested and produced great results when chemically modified with photoinitiators to formulate 3D printing resins (Wu et al., 2019).

XANTHAN GUM

METHYLCELLULOSE

DMSO

GLYCERINE

CORN STARCH

ALGINATE

BEESWAX

BONE GLUE

WOOD GLUE

BAKING SODA

SUNFLOWER OIL

Fig 35 - Binders overview

# 1.3. Fabrication

### 1.3.1. Additive Manufacturing Overview

Additive manufacturing (AM), popularly known as 3D printing, used to be called as rapid prototyping, a hint to its original purpose as a faster tool in the product research and design environment. It is the process of quickly creating a physical mock-up directly from a digital model, typically used for studying, experimenting, testing and prototyping. Nowadays, it has been increasingly applied to create unique solutions in the fields of product and construction design. Several components and inserts are now created entirely through AM.

Traditional fabrication processes, such as injection moulding and casting, require intense pre-production planning. Geometry must be studied, subdivided into parts in the most logical and effective way for production, assembly and operation, without losing its functionality. Parts must manufactured in a specific ordered to follow the assembly process, connections must be developed. For high production demand and simple products, all this planning is worth it and economical at long-term.

Additive manufacturing on the other side, as presented by Gibson et al. (2021), is based on a digital model elaborated with a CAD software and derived from the model used for the product design, eliminating the planning and offering the possibility of fabrication in one single step without combining different manufacturing processes and phases. Design changes and project updates can be incorporated by updating a digital model only, instead of triggering a re-planning and the production of new moulds and tools. It does require knowledge of the fabrication process to prepare the model respecting the machine and printing process limitations, but simplifies or totally removes the assembly needs and allows for more complexity in geometry and design.

All additive manufacturing machinery currently work with layers. The thinner the layer, the higher the product definition and the closer to the digital model the physical one will be. The difference between 3D printing types and machines are the feedstock and the process of how the layers are created and bonded to each other. These are the basic elements which will determine the fabrication accuracy, precision and speed and the mechanical properties and definition of the printed part.

In a general way, Gibson et al. (2021) describes the fabrication process through additive manufacturing in the following steps:

– CAD – development of the digital model;

– STL – conversion of the digital model into an STL fie, the industry standard which is accepted by almost all devices. It describes the external closed surfaces and will be used to calculate and create the slices which will be printed layer by layer.

– Transfer to AM and File Manipulation – transfer the STL file to the machine and adjust the size, position and orientation of the print;

– Machine Setup – preparation of the machine for fabrication. Settings relate to the material constraints and properties, energy source, layer thickness, model geometry and printing time.

– Build – automated process, but superficial monitoring is required to ensure no errors will happen, such as material or power outages, glitches or setup mistakes.

– Removal – once the part is ready to be removed from the machine – might require

interaction with safety locks and temperature cooling.

– Post-processing – additional cleaning and removal of all residual material and support structure – depends on the print quality and result to be achieved, adding work and cost to the process.

– Application – part is ready to use or assembled to other parts or electronics.

Several technologies and types of additive manufacturing are available nowadays, and grouping them into one classification system is challenging. It is possible to divide them by feedstock material state, such as liquid, solid or powder, by printing technology, such as laser, jetting or extrusion, or even by feedstock or energy source. The issue encountered would be the combination of completely different types of printing into the same category.

The most consistent classification, presented by Gibson et al. (2021), follows the ASTM/ISO standards and divides them into seven categories:

## Vat Photopolymerization (VPP)

This process utilises a photopolymer liquid contained in a vat as the base material. It solidifies by radiation (typically UV) selectively delivered, layer by layer, to specific parts of the surface, curing the resin to build the designed part. VPP was the first AM technology to be developed, and stereolithography (SLA) was the first process commercially available in the 1980s.

## Powder Bed Fusion

This process utilises a container filled with a layer of powder (typically metallic or plastic) as the base material. It reacts to an energy source (typically a laser or electron beam) selectively applied and solidifies. The working platform then moves, a new layer of powder is deposited and the process repeats, building the designed model layer by layer. PBF was also one of the first AM processes to become commercially available.

## Material Extrusion (MEX)

By far this is the most popular and one of the most versatile processes. It is based on the simple principle of continuously extruding a material (commonly solid and melted for processing on demand) through a nozzle layer by layer. Temperature of extrusion will depend on the feedstock (typically polymer filaments and pellets).
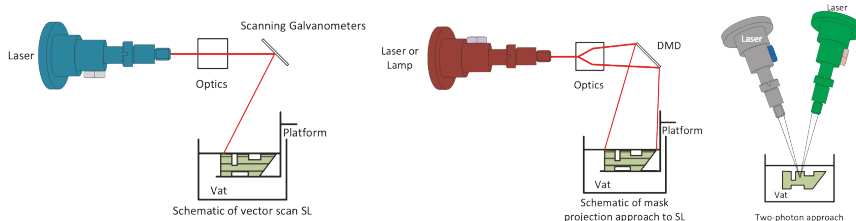


Fig 36 - Vat Photopolymerization (Gibson et al., 2021)
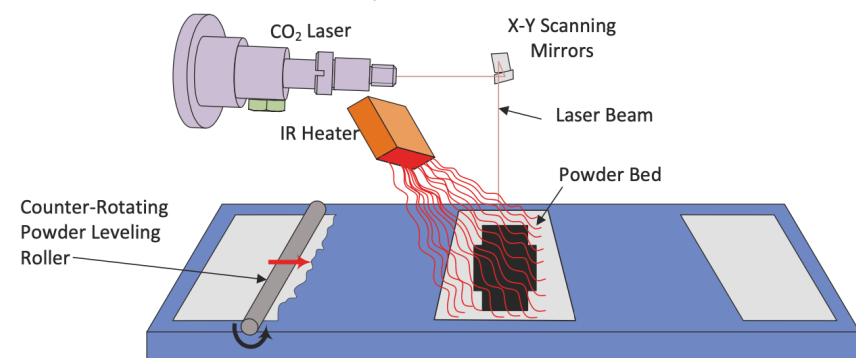


Fig 37 - Powder Bed Fusion (Gibson et al., 2021)
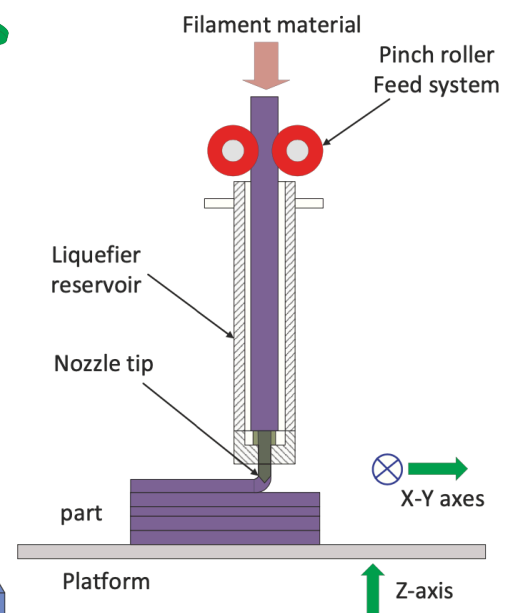
Fig 38 - Material Extrusion (Gibson et al., 2021)

## Material Jetting (MJT)

This processes originated from the conventional 2D printing methods. It is based on the selective deposition of material droplets from a printing head, layer by layer, building the designed model.

## Binder Jetting (BJT)

Similarly to PBF, this processes utilises a powder bed onto which a liquid bonding agent is selectively applied, solidifying the material. Platform then moves, another powder layer is rolled and the process repeats, building the designed model layer by layer.

## Sheet Lamination (SHL)

Sheets of material are placed on a platform, cut and bonded (not necessarily in this order) to build the designed model. Unlike in the other methods, material leftovers are difficult to reuse and typically end up discarded.

## Directed Energy Deposition (DED)

In this process, the energy necessary to melt and cure the base material (typically as a metallic powder or wire) is delivered simultaneously to the material deposition though a single device.

Additive manufacturing has a large potential to be implemented in the construction industry by reducing labour, costs and material waste. As presented by Delgado Camacho et al. (2018), several examples of cement, clay, polymer and metal based parts and even whole structures are already in use in the industry. Around the world, companies are already using 3D printing technology to fabricate entire buildings out of concrete and natural materials such as earth and sand, small parts and connectors out of polymers and structural nodes, columns and bridges out of metal (Delgado Camacho et al., 2018).
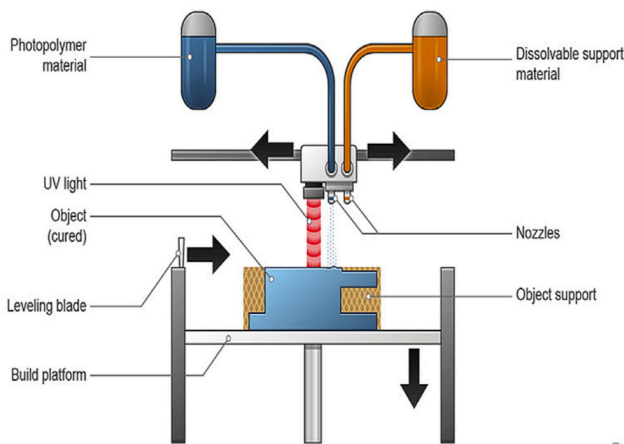


Fig 39 - Material Jetting (Gibson et al., 2021)
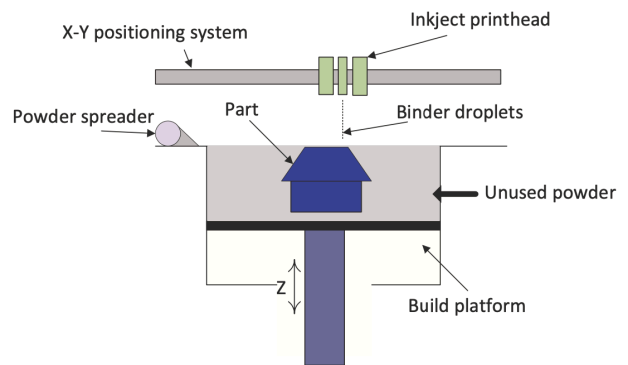


Fig 40 - Binder Jetting (Gibson et al., 2021)
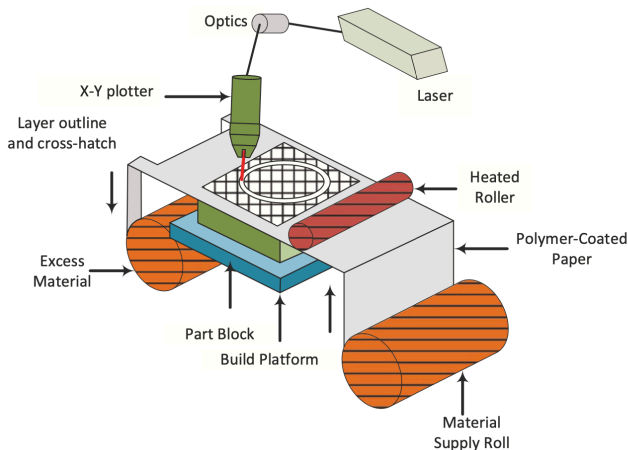


Fig 41 - Sheet Lamination (Gibson et al., 2021)
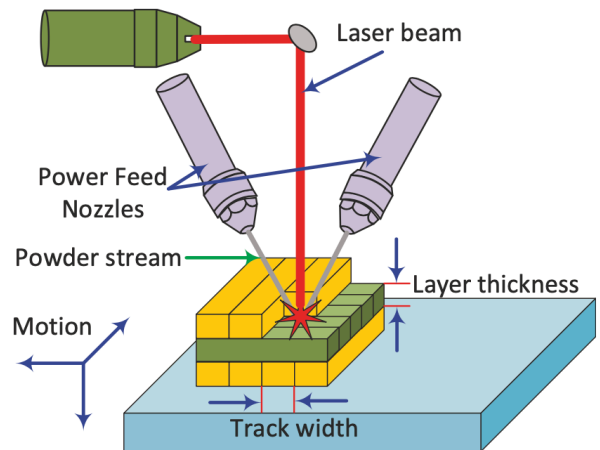


Fig 42 - Direct Energy Deposition (Gibson et al., 2021)

## 1.3.2. Additive Manufacturing with Bio-based Materials

Additive manufacturing processes are classified into seven different categories (Gibson et al., 2021). Out of these, five of them have already been researched or are currently being used with bio-based composite as feedstock - material extrusion, powder bed fusion, photopolymerization, binder jetting and sheet lamination. Applications, material composition and properties should be considered to determine the method to be employed on the fabrication of each element. From the five categories, material extrusion is the most commonly used in this field with the fused deposition modelling (FDM) and direct ink writing (DIW), also known as liquid deposition modelling (Gauss et al., 2021).

FDM uses a filament as feedstock, conventionally made of a thermoplastic, which has been often replaced by a biodegradable polymer, such as PLA (Gauss et al., 2021). Bio-based composite filaments can be produced from the combination of PLA pellets with natural fibres, such as cellulose, hemp, coconut, flax and others. Due to its mechanical properties, the use of cellulose fibres in the filament has been growing recently. Several researches have also highlighted the growing interest in lignin as a filler and reinforcement to enhance the strength of the PLA matrix typically used in FDM processes.

DIW uses a viscous substance as feedstock such as gels/hydrogels and pastes (Gauss et al., 2021). It is frequently used to extrude clay in the artistic and building industry, but also highly developed for biomedical applications in tissue engineering, protheses and implants with cellulose-based gels (Gauss et al., 2021).

In more complex applications, photopolymerization has been used for biomedical purposes with cellulose-based feedstock to improve its mechanical properties and thermal stability. In the same field, stereolithography (SLA) and digital light processing (DLP) have been using cellulose-based biomedical photosensitive resins as an alternative to methacrylate-based resins (Gauss et al., 2021).

There are two possibilities for the incorporation of wood in the feedstock – directly or through lignocellulosic compounds. It can be combined directly with adhesives in the form of sawdust, powder or chips to create a printable paste to be extruded, as explored by Rosenthal et al. (2018) reaching a content of 89% of wood in a material mixture. It can also be combined with PLA and other thermoplastic polymers to fabricate filaments and pellets to be used in FDM processes, with wood content usually lower than 30%.

As separated blocks, cellulose and lignin have also been experimented and incorporated mostly to the fabrication of reinforced filaments for use in FDM processes. Cellulose has also been combined with other biodegradable polymers in aqueous suspensions to produce hydrogels for tissue engineering, drug delivery systems and other biomedical applications. Lignin has been used mostly as a filler and to improve mechanical properties of bio-based filaments and pellets.
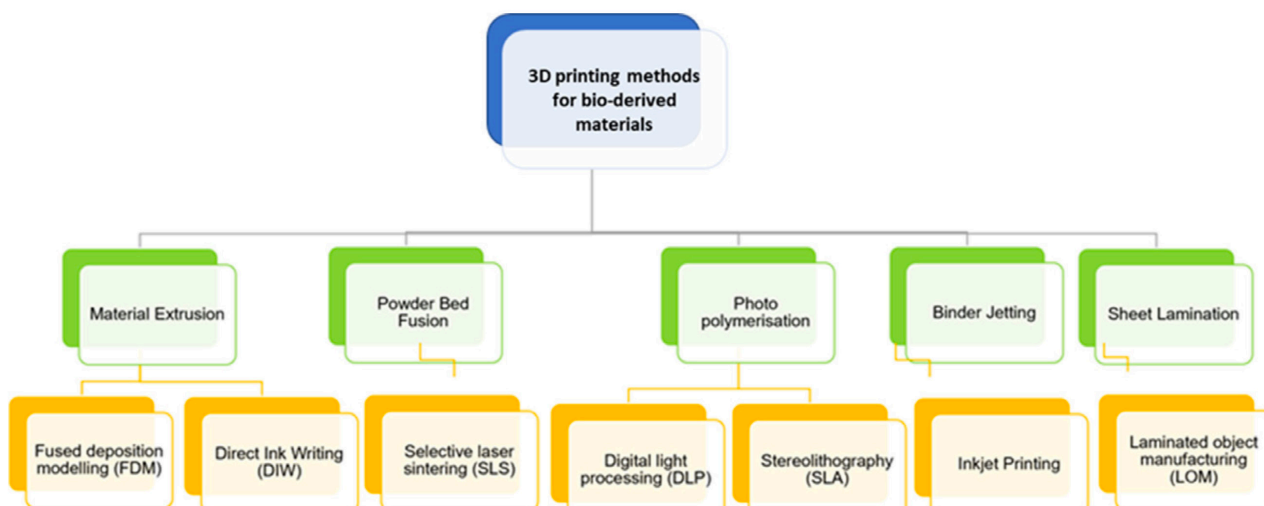


Fig 43 - Additive manufacturing processes for bio-based materials (Gauss et al., 2021)

### 1.3.3. Liquid Deposition Modelling (LDM) Fabrication

Liquid deposition modelling (LDM) is included in the "Material Extrusion" category identified by Gibson et al. (2021). A feedstock with semisolid consistency is stored in a container, which feeds an extruder, and pushed through a nozzle to produce multilayered structures. Pressure, flow and speed are dependent of the material viscosity, and interlayer bonding and overall curing of the parts are fundamental for the feasibility of the part (Gibson et al., 2021).

In material extrusion processes, the feedstock is commonly presented in the shape of filaments or pellets. In LDM processes although, the material is typically used in a paste state, solid when no external forces are applied, and viscous under pressure. It is kept in a container attached to the extruder and connected to an air compressor which will keep a constant and uniform pressure on the feedstock throughout the printing process.

The extrusion is controlled by a stepper motor attached to the piston and body of the device. It is performed through an interchangeable nozzle with a constant diameter during printing. The layer width, height and smoothness will depend on the pressure applied on the material, the speed of the extrusion and the travelling speed of the extruder, commonly controlled by a robotic arm.

Once the material has been extruded, it assumes a solid state either instantaneously, like PLA, or it demands a curing period to achieve maximum strength and stiffness, like clay. Either way, deformations usually occur, varying according to the water content of the paste. The better the adhesion of the material is, the stronger the interlayer bonding. Overhangs, steep and inclined walls and tall parts require strong bonding between the slices of a model.

The model for extrusion is usually prepared with a CAD software like Rhino or AutoCAD and converted into an STL file, which will be sliced with a proprietary software from a printer. As an alternative, RoboDK and Grasshopper can also be used for both the generation of the tool path for the device and its control throughout the printing process.

Overall, the full control of the extrusion process is a trade-off between several different parameters and varies widely according to the material. Input pressure affects the flow rate and depends on the paste consistency and nozzle diameter. Temperature of the material affects its consistency and the post-printing solidification. Nozzle diameter relates to the flow rate, pressure and printing definition. Gravity affects the pressure and flow rate. All parameters must be explored and defined for each type of material and variations (Gibson et al., 2021).



Fig 44 - LDM Extruder WASP

# 1.4. Structural Application

### 1.4.1. AM for Structural Applications

Additive manufacturing has already a wide range of structural applications in the construction sector. Specially by using steel as the primary material. As presented in Lange et al. (2020), there are researches on printing connecting parts directly on steel beams by using arc welding and robotic arms. Structural nodes for spatial structures and free-form curtain walls (Tramontini, 2018) have already been studied and prototyped. Even larger structures such as columns and bridges have already been successfully produced.
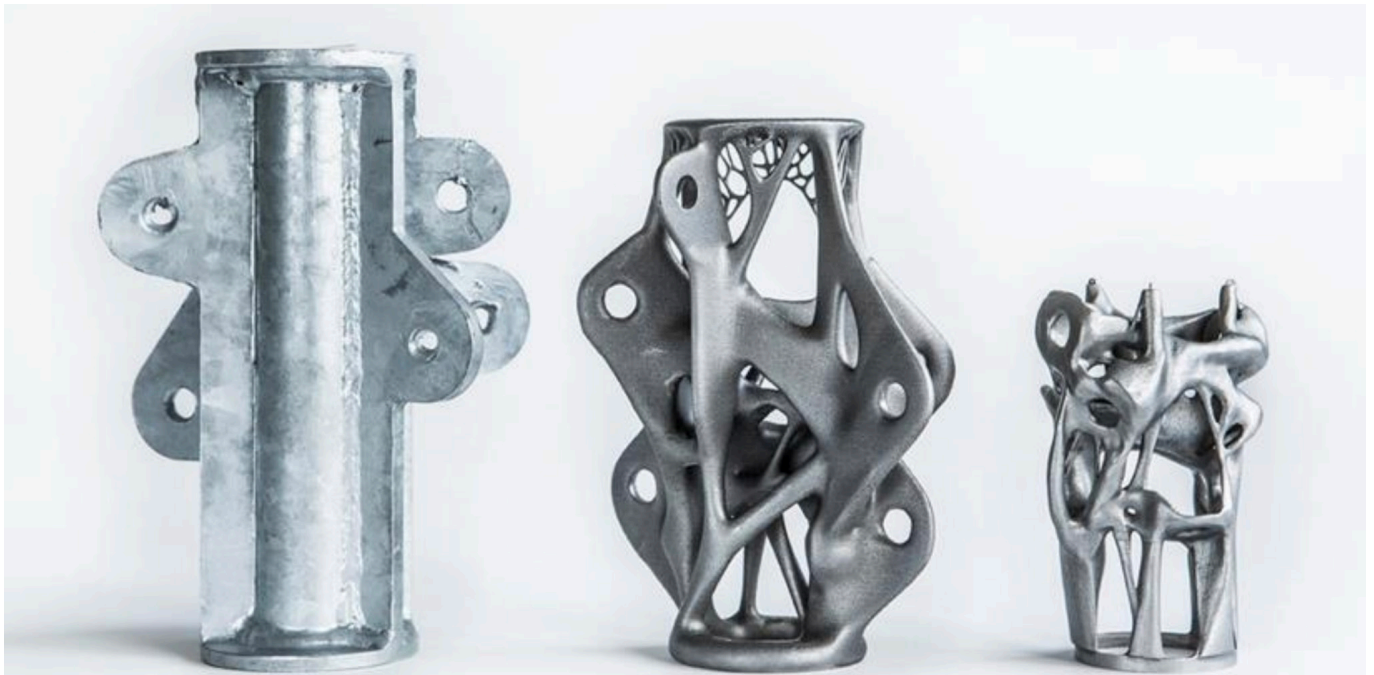


Fig 45 - Progressive steps of steel node optimisation (Galjaard, 2015)
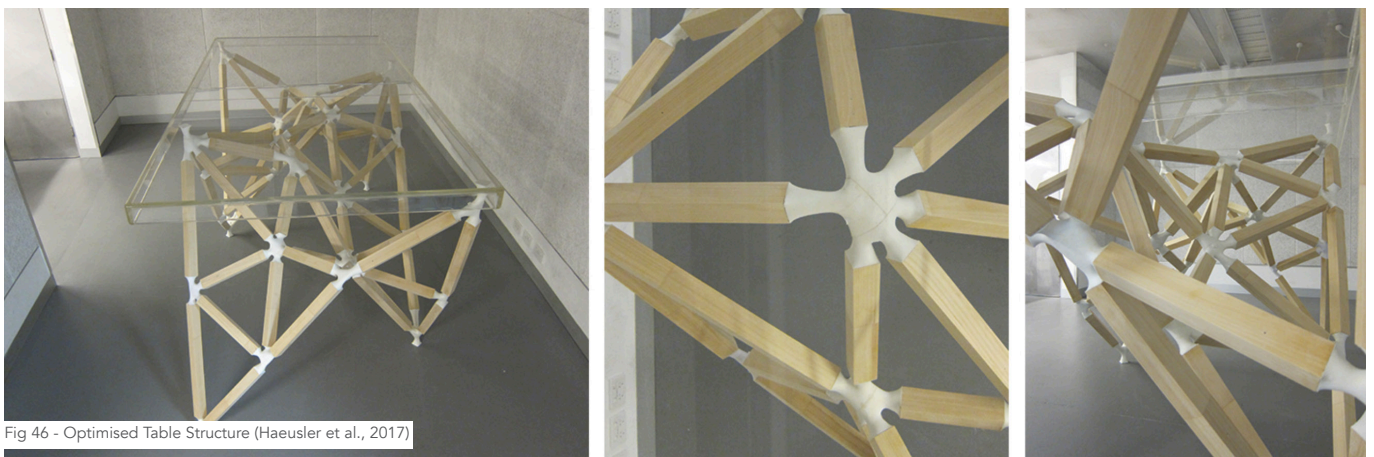


Fig 46 - Optimised Table Structure (Haeusler et al., 2017)

### 1.4.2. Structural Nodes for Timber Structures

Due to the novel nature of the material being developed and applied in this research, structural properties are not expected, therefore the research in terms of application and node design focus mostly on the different geometries. Conventional nodes can be divided into splice connectors and end face connectors (Seifi, 2019) as illustrated below.

Regardign the unconventional ones, the additive manufacturing fabrication processes are the greates source of examples. Through topological and geometrical optimisations, design becomes more efficient and the use of material reduced, filling the areas required for the transfer of stresses and eliminating areas of which are not relevant for the overall stability (Galjaard, 2015).

Not only in the building industry, optmised 3D printed nodes can also be seen in the furniture design field, as showcased by Haeusler et al. (2017) and illustrated above.
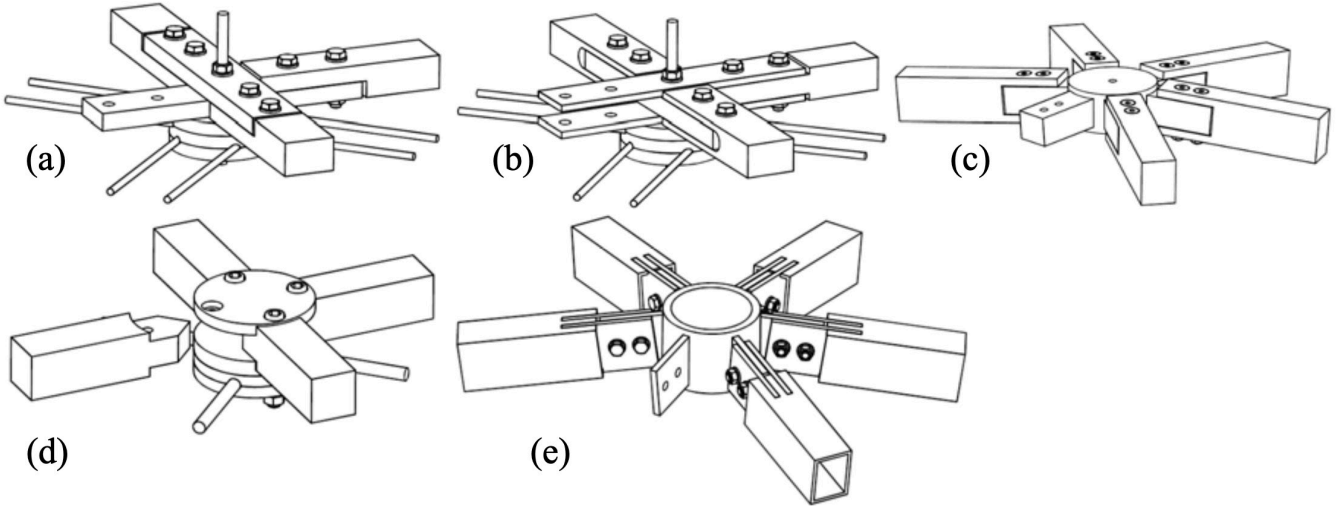


Fig 47 - Splice Connectors (Seifi, 2019)
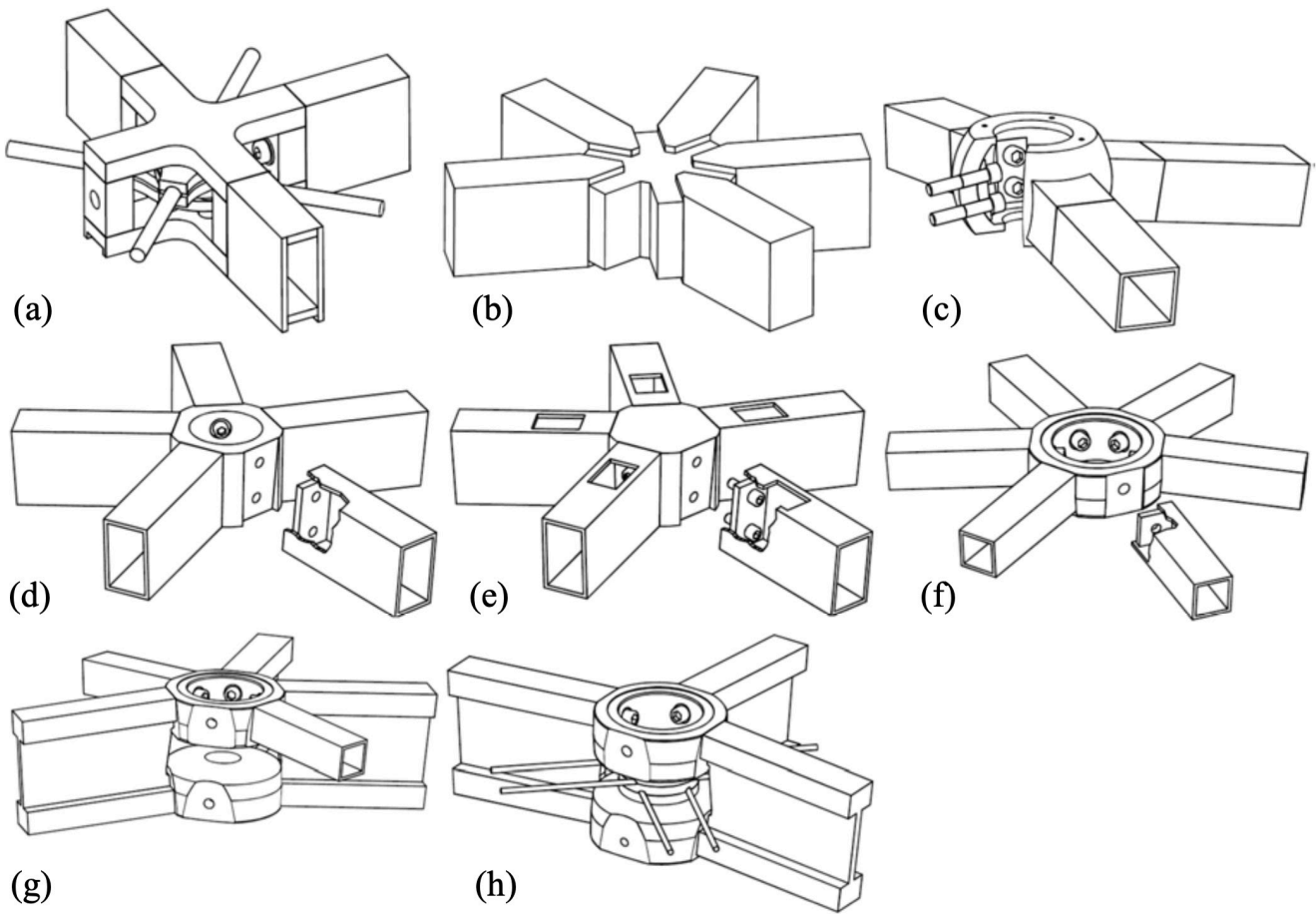


Fig 48 - End Face Connectors (Seifi, 2019)

# 2. Material Exploration

## 2.1. Overview

The material exploration phase commenced with the reproduction of an already existing recipe for an additive manufacturing feedstock based on lignocellulosic polymers and moved towards an improvement process. The result was a wide range of alternative mixes which were evaluated and the most promising ones selected for further assessment regarding their printability and mechanical properties. The state-of-the-art recipe in terms of cellulose & lignin based 3D printing materials was presented in Liebrand (2018) and specified acetone as the binding agent to create a viscous and extrudable paste. Based on the findings from the literature review and with the aim of replacing hazardous chemicals and developing a bio-based recipe, alternative binders were studied during this first step of the practical research. A sequence of material experiments was designed to understand the behaviour of the different elements separately and mixed at different proportions and temperatures. A criteria set, based on eye-sight analysis and manual testing, was defined and applied to evaluate the different outcomes, drawing a comparison between different raw materials and establishing the most promising binding agents and recipes for further investigation in terms of mechanical properties and printability with a robotic arm and a clay extruder.

**CELLULOSE + LIGNIN MIXTURE**

START POINT – MATERIAL MIX PRESENTED IN LIEBRAND (2018):
10g WATER + 26g ACETONE + 40g LIGNIN + 5g CELLULOSE

**MATERIAL INITIAL ANALYSIS**

OBSERVE, EXPERIMENT AND DOCUMENT MATERIAL PROPERTIES:
HOMOGENEITY, VISCOSITY, BONDING

**HOT EXTRUSION WITH SYRINGE**

MATERIAL TO BE MIXED AND PRINTED AT TEMPERATURES BETWEEN 110C AND 180C MANUALLY WITH A MEDICAL SYRINGE

**COLD EXTRUSION WITH SYRINGE**

MATERIAL TO BE MIXED AND PRINTED AT ROOM TEMPERATURE MANUALLY WITH A MEDICAL SYRINGE

SAMPLE SIZE = 80mm x 9mm x 9mm
LAYER THICKNESS / DIAMETER = 3mm

**COMPARE & DOCUMENT SAMPLES & PRINTABILITY**

COMPARE THE RESULTS FROM BOTH EXTRUSION PROCESSES, IDENTIFY DIFFERENCES AND HIGHLIGHT THE MOST ADEQUATE ONE IF RELEVANT

Fig 49 - Material Exploration phase optimal workflow

## 2.2. Planning & Preparation

### 2.2.1. Experiment Design

The target of the material exploration phase was to understand how cellulose and lignin behave at different temperatures and how they react and combine with binding agents and solvents. The expected outcome was a recipe for a stable mix, bio-based, with optimal viscosity and bonding properties for extrusion through an LDM process.

At first, the lignocellulosic polymers were analysed individually. Their melting and degradation points were assessed and the behaviour when combined was analysed.

Subsequently, experiments with solvents were performed, reproducing the state-of-the-art recipe with acetone and testing different concentrations. The total removal of acetone and a mix with water only was also experimented, pushing to the limit to attest the hydrophobic and hydrophilic behaviours or lignin and cellulose respectively.

At last, a series of binding agents were studied, individually first to determine their consistency and, eventually, combined with the lignocellulosic polymers. Quantities were defined through proportions and eye-sight observations throughout the material mixing process. Material properties were observed and assessed to compare and evaluate the recipes, identifying the most promising ones, which were then refined and further characterised for comparison purposes.

### 2.2.2. Location

The experiments were executed at three different locations with similar environment conditions – room temperature between 20C and 23C and relative humidity between 37% and 45% - all measured with an Arduino kit connected to a DHT11 digital temperature and humidity sensor. The main location was the Laboratory for Additive Manufacturing in Architecture, hereinafter LAMA, located at the Faculty of Architecture and the Built Environment of TU Delft. The secondary locations were the Spray Room, located in the Model Hall of the aforementioned faculty – with enhanced exhaust and ventilation systems used for the experiments with risk of creating fumes and strong odours - and the Recycling Laboratory, located in the Stevin Laboratory at the Faculty of Civil Engineering and Geosciences of TU Delft – with larger countertops and precision scales used for the adjustment of the final recipes of the promising mixes and for large scale material production for the printability tests.

Fig 50 - LAMA workstation & material storage



SOLDERING TABLE
SOLDEER TAFEL
PLEASE NO PAINT
GEEN VERF AUB


Fig 51 - Spray booth workstation
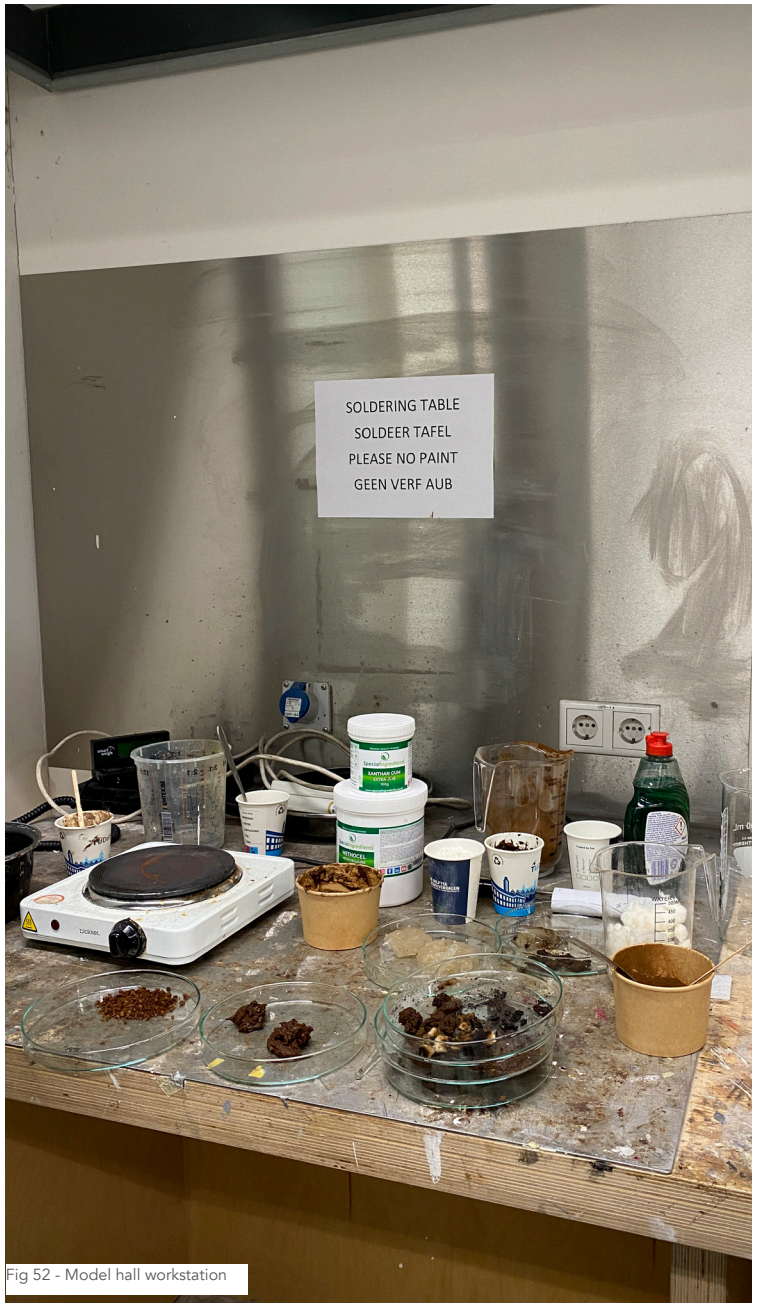
Fig 52 - Model hall workstation


Fig 53 - LAMA workstation & equipment display

### 2.2.3. Equipment

The list of equipment necessary for the material experiments combines specific glassware from chemistry laboratories with kitchenware and appliances commonly used in a residence.

A small part of the necessary equipment was already available from previous researches at LAMA, such as the electric caulking gun, hot plate and pans, and at the Stevin Lab, such as the scales with a 0.01g level of precision. All the beakers, petri dishes, pipettes, glass stirrers, syringes and thermometer were obtained from online stores specialised in laboratory supplies – Labbox & Neolab – procured through the Amazon.nl portal. Nozzles, icing gun and icing bags were found on online stores specialised in baking supplies. Coffee grinder, food dehydrator, mixer, scale, aluminium bowls, pans, spoons and glasses were obtained from local houseware shops – such as Lidl, Action and IKEA – and online, through the Amazon.nl portal.

Lastly, accessories such as sanding paper, spatulas and all the safety equipment were sourced from local hardware stores, such as Gamma, and all the cleaning supplies from local supermarkets.

### 2.2.4. Material

The base materials used in this research – cellulose and lignin – were provided by Wageningen University. The remaining materials were sourced from online stores specialised on either pharmaceutical or gastronomic products, through the Amazon.nl portal, and from local supermarkets.

Cellulose is from the kraft type, bleached, presented in A4 size sheets, from an unspecified supplier.

Lignin is from the sodium hydroxide type, hydrated, delivered in a 25kg package, batch number 11-0-044, from Greencone Environs Pvt Ltd.

Acetone is 99% pure, presented in 100mL bottles from local supermarket Kruidvat.

Dimethylsulfoxide is 99.9% pure, presented in 100mL bottles from WoldoHealth, obtained online through the Amazon.nl portal.

Methylcellulose is from the E461 food grade type, delivered in 500g packages from Special Ingredients, obtained online through the Amazon.nl portal.

Xanthan gum is 100% pure from the E415 food grade type, delivered in 100g packages from Special Ingredients, obtained online through the Amazon.nl portal.

Wood glue is from a polyvinyl acetate base, water resistant (EN 204 D3 classification), presented in 750g bottles from Bison, obtained from local hardware store Gamma.

Alginate is sea-weed based and mixed with sodium. It is cosmetic-grade and obtained in packages of 250g online from the jojoli.nl portal.

Beeswax used is cosmetic-grade and partially synthetic, composed of paraffin, glyceryl palmitate and stearate, beeswax and stearic acid. It was obtained online through the Amazon.nl portal.

Bone glue is from animal carcasses and presented in hard and gelatinous beads. It was obtained online from the Labshop.nl portal.

Sunflower oil and baking soda are standard culinary ingredients, presented in standard packaging and sourced from a local supermarket.

Fig 54 - Tools and equipments necessary - filtering & measuring


Fig 55 - Tools and equipments necessary - extruding
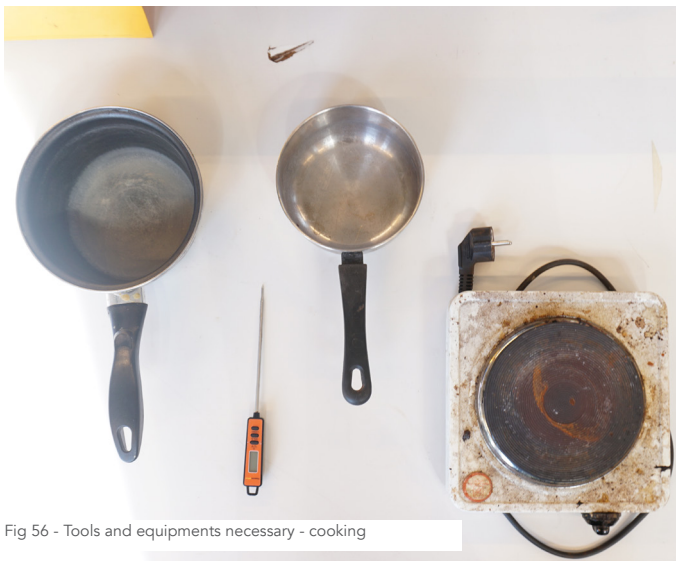

Fig 56 - Tools and equipments necessary - cooking


Fig 57 - Tools and equipments necessary - measuring


Fig 58 - Tools and equipments necessary - sieving


Fig 59 - Tools and equipments necessary - cleaning & safety

## TOOLS NECESSARY

| EQUIPMENT | KITCHEN TOOLS | LAB GLASSWARE | SAFETY & ACCESSORIES |
|---|---|---|---|
| – MIXER + PLASTIC LID | – POTS & PANS | – BEAKERS – 250ml, 600ml & 900ml | – APRON |
| – COFFEE GRINDER | – ALUMINIUM BOWLS | – PETRI DISHES | – MASKS |
| – FOOD DEHYDRATOR | – SIEVE | – PIPETTES | – LATEX GLOVES |
| – THERMOMETER | – SPOONS & SPATULAS | – GLASS STIRRERS | – COTTON CLOTHS |
| – SCALE (GENERAL & HIGH PRECISION – 0.01g) | – WHISK | – SYRINGES | |
| – HOT PLATE | – CUPS | | |
| – CAULKING GUN | – MEASURING CUPS | | |
| | – ICING GUN, BAGS AND NOZZLES | | |
| | – CUTTING KNIFE | | |

ACETONE

XANTHAN GUM

METHYLCELLULOSE

DMSO

GLYCERINE

CORN STARCH

ALGINATE

BEESWAX

BONE GLUE

WOOD GLUE

BAKING SODA

SUNFLOWER OIL

CELLULOSE & LIGNIN

Fig 60 - Materials necessary overview

## 2.3. Process

The material experiments were executed in three distinct phases – understanding the basics, exploring the binding agents and refining the recipes. At each phase the degree of precision was increased, and the analysis of the results enhanced, adding more parameters to the evaluation of each mix iteration.

The first phase focused solely on the cellulose fibres and lignin. Initial step was to identify the most effective pulping procedure. Cellulose sheets were cut into smaller chips and processed into four different methods: directly mixed with water, shredded with a blender, with a mixer and with a coffee grinder. Second step was to understand the hygroscopic and hydrophobic behaviour of both materials by mixing them with water both separately and combined. Third and final step was to test the melting and degradation points of the polymers in a pan on the hot plate.

The second phase focused on the binding agent, starting from acetone and investigating the different alternatives highlighted in the literature review as potential binders for lignocellulosic fibres – xanthan gum, methylcellulose, glycerine, DMSO, corn starch, alginate, bee wax, bone glue, wood glue, sunflower oil and baking soda. The initial step was to create a polymer matrix by mixing the lignin powder with water and the binder to be experimented. The second step was to combine, by hand with a spoon or spatula, the cellulose fibres already pulped. The final step, if feasible, was the manual extrusion with a syringe. At this phase, measurements were not precise and based on proportions between the different elements – lignin vs. binder and binder vs. water.

The third and final phase was the refinement of the mixes with the highest potential among the experiments from the previous phase. First step was to adjust the proportions between raw materials and define their quantities. Second step was to improve the mixing procedure by incorporating an electric mixer to evenly combine the ingredients. And the final step was to correct the mixing order. Cellulose should be blended separately at first to separate the fibres and increase the surface of contact. Adding lignin in the sequence covered evenly all fibres with the polymer. And finalising with water and the binding agent creates a matrix with uniform fibre distribution.


Fig 61 - Lignin melting & degrading


Fig 62 - Raw materials - cellulose & lignin


Fig 63 - Cellulose pulping


Fig 64 - Cellulose & lignin mixing


Fig 65 - Material paste


Fig 66 - Extrudability assessment

## 2.4. Evaluation

A criteria set with nine parameters was used to evaluate all the material mixes and the samples produced. This evaluation is preliminary and was performed based on eye-sight observations and manual assessment. The objective was to identify the mixes with the highest potential to be further investigated.

A value of -1, 0 or 1 was attributed to each parameter for a negative, indifferent, or positive performance, respectively. The total sum of grades offered a quick although comprehensive comparison among all samples produced. No weights were determined. The following parameters were applied:

– Homogeneity – relates to the structural stability (fibre distribution and incorporation to the matrix) and to the smoothness of the resulting extrusion. A homogeneous paste has a uniform colour and consistency and does not have chunks and agglomerated threads.

– Viscosity – relates to the material extrusion. The higher the viscosity, the less liquid the material. A moderate to high viscosity – dense, although not dry and not crumbly – is the ideal for extrusion.

– Adhesion – relates to the inter-layer bonding. The higher the adhesion, the stronger is the layered structure of the print. A moderate to high adhesion – sticky, although not blocking the movable parts and interfering on the equipment operation – is the ideal for additive manufacturing fabrication.

– Extrudability – a combination between adhesion and viscosity, it is experimented with a syringe operated manually or with the caulking gun.

– Bio-based content – relates to the amount of natural-based components in a material mix. If full bio-based, the grade is 1.

– Shrinkage – relates to the deformation inflicted on the samples after curing. Tends to be proportional to the water content of the mix. The more evident the shrinkage is, the less shape fidelity and geometrical stability a printed part would have.

– Brittleness – relates to the easiness of breaking a material sample by touching and applying small force to it or dropping it from a height of 1m.

– Curing time – relates to the drying period of a printed part. A short curing time typically allows for more efficiency with more extrusions in a limited amount of time, and higher multi-layered structures to be fabricated.

– Aesthetics – relates to the appearance of the material. This is supposed to be a 3D printable wood-based feedstock, therefore a natural and close look to wood, at least in terms of colour and texture, is an advantage in terms of acceptance in the building industry.

## 2.5. Results

Fig 67 - Material Exploration summary
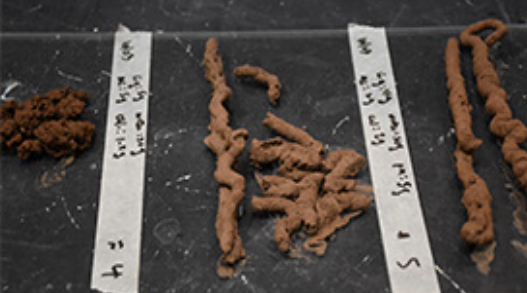
Fig 68 - Cellulose & lignin exploration - overview

Fig 69 - Lignin degradation (charred)

Fig 70 - Cellulose degradation (burned)

### 2.5.1.  Phase 1

#### 2.5.1.1.  Cellulose & Lignin

The most effective pulping method for cellulose was to reduce the large sheets to small 10x30mm chips and process them with a coffee grinder in small quantities, forcing the fibres to separate and gain volume, acquiring the appearance of cotton. The enlarged surface of contact increased the fibre coverage with the lignin polymer and favoured the bonding between matrix and fibres. Mixed with water they presented a hygroscopic behaviour and formed chunks. When heated above 180C they directly degraded.

Lignin powder when heated started to melt above 130C, before quickly degrading above 180C. When mixed with water, The soda type, used in this research, presented a partially hygroscopic behaviour when saturated and continuously stirred at temperatures between 80C and 130C, unlike the kraft type, forming a substance with low viscosity before quickly degrading above 180C and turning into char. When dried the mass turned brittle and crumbly.

ACETONE

Fig 71 - Acetone exploration - overview 1



Fig 72 - Acetone exploration - overview 2
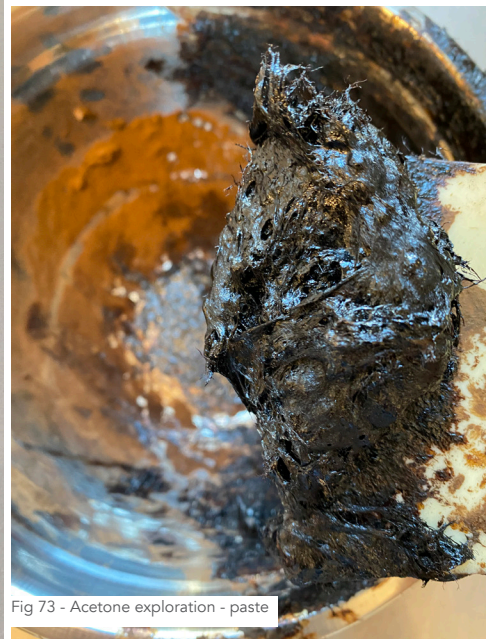


Fig 73 - Acetone exploration - paste

| MATERIAL EVALUATION – MIX 1 | | | | | | | | | | |
|---|---|---|---|---|---|---|---|---|---|---|
| MIX 1<br>ACETONE | HOMOGENEITY | VISCOSITY | ADHESION | EXTRUDABILITY | BIO-BASED | SHRINKAGE | BRITTLENESS | CURING TIME | AESTHETICS | TOTAL |
| | 1 | 1 | 1 | 1 | -1 | 0 | 1 | 1 | -1 | 2 |

Table 1 - Mix 1 Evaluation

## 2.5.2. Phase 2

### 2.5.2.1. Acetone

The alcohol mixed directly with lignin created a viscous paste highly adherent to the container walls and difficult to handle. When mixed with cellulose and water, the fibres created chunks and resulted in a non-homogeneous substance, difficult to extrude with a syringe. In subsequent iterations, increasing the amount of solvent and partially replacing the fibres with papier mache facilitated both the material mixing and extrusion processes, reducing the viscosity and resulting on a smooth and homogeneous paste with a dark and glossy appearance.

The extruded samples presented a rough surface with chunks of fibres and a long curing period – after 48h the surface dried but it was necessary one week for the sample to harden completely.

XANTHAN GUM

Fig 74 - Xanthan gum exploration - overview
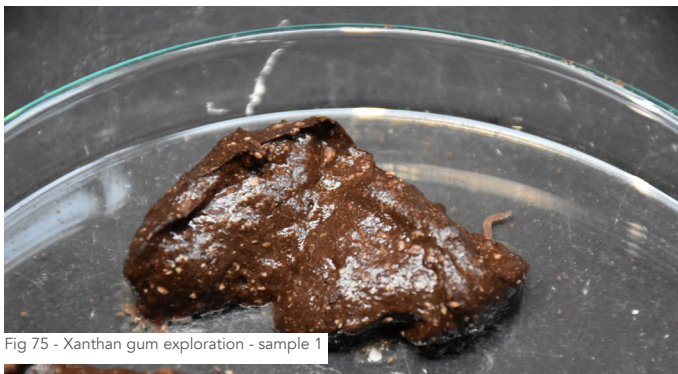


Fig 75 - Xanthan gum exploration - sample 1



Fig 76 - Xanthan gum exploration - sample 2

| MATERIAL EVALUATION – MIX 2 | | | | | | | | | | |
|---|---|---|---|---|---|---|---|---|---|---|
| MIX 2 XANTHAN | HOMOGENEITY | VISCOSITY | ADHESION | EXTRUDABILITY | BIO-BASED | SHRINKAGE | BRITTLENESS | CURING TIME | AESTHETICS | TOTAL |
| | -1 | -1 | -1 | -1 | 1 | 0 | 0 | -1 | -1 | -5 |

Table 2 - Mix 2 Evaluation

### 2.5.2.2. Xanthan Gum

Xanthan gum creates a gel-like matrix when dissolved in water in a 1:2 ratio. Combined with the lignin powder, it did not dissolve the polymer and created a non-homogeneous and non-viscous substance. When mixed with cellulose, it formed fibre clots precluding extrusion with a syringe. In subsequent iterations, the lignin powder mixed with the gum powder before adding water produced better results leading to a homogeneous gel-like substance with low viscosity and moderate bonding. When cellulose was added, no relevant changes to the consistency were observed, solely a reduction in the homogeneity of the material. Extrusion with a syringe was not feasible and after one week of curing time, the material samples retained the gel-like consistency, with a partially dry surface.

METHYLCELLULOSE
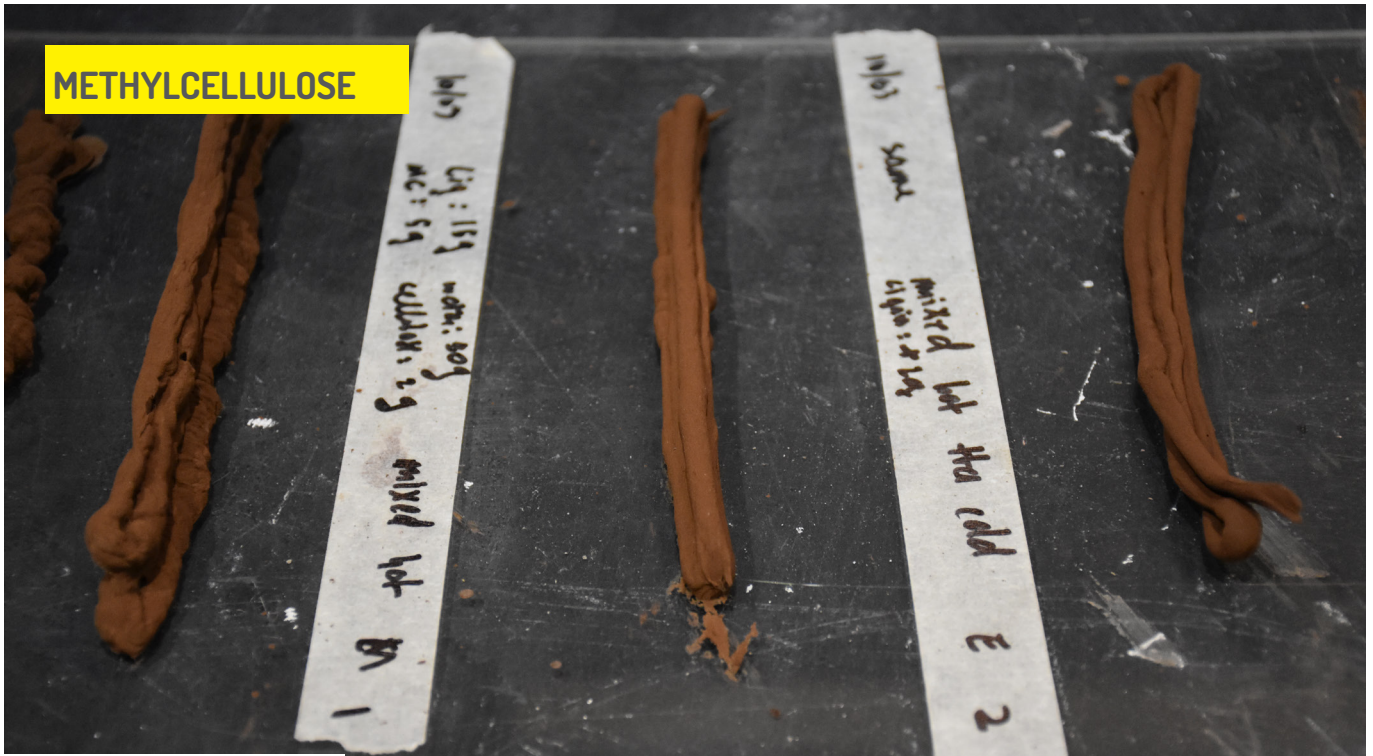
Fig 77 - Methylcellulose exploration - overview



Fig 78 - Methylcellulose exploration - final samples



Fig 79 - Methylcellulose exploration - initial samples

| MATERIAL EVALUATION – MIX 3 | | | | | | | | | |
|---|---|---|---|---|---|---|---|---|---|
| MIX 3 METHYLCELLULOSE | HOMOGENEITY | VISCOSITY | ADHESION | EXTRUDABILITY | BIO-BASED | SHRINKAGE | BRITTLENESS | CURING TIME | AESTHETICS | TOTAL |
| | 1 | 1 | 1 | 1 | 1 | -1 | 0 | 1 | 1 | 6 |

Table 3 - Mix 3 Evaluation

## 2.5.2.3.  Methylcellulose

Methylcellulose creates a paste-like substance when dissolved in hot water – temperature above 60C – in a 1:10 ratio and cooled down. Combined with the lignin powder when still in liquid state, it created a homogeneous mix, which turned into a paste with moderate bonding and viscosity when cellulose was added. The satisfactory results from the initial experiments led to two rounds of subsequent iterations. Quantities of lignin and fibres were studied and tested to retain the homogeneity of the material and maximise bonding and viscosity meanwhile preserving an extrusion flow by hand with a syringe. The material temperature was found to be an important threshold – ideal homogeneity, bonding and viscosity were reached once the mix's temperature dropped below 40C, leading to the methylcellulose solution to assume a paste consistency.

The extruded samples presented varying degrees of homogeneity and consistency according to the proportions among the raw materials. Overall, the curing time observed was short – within 24h the outer surfaces were dry and within three days they reached maximum hardening.

Fig 80 - DMSO exploration - overview


Fig 81 - DMSO exploration - sample 1


Fig 82 - DMSO exploration - sample 2

| MATERIAL EVALUATION – MIX 4 | | | | | | | | | | |
|---|---|---|---|---|---|---|---|---|---|---|
| MIX 4 DMSO | HOMOGENEITY | VISCOSITY | ADHESION | EXTRUDABILITY | BIO-BASED | SHRINKAGE | BRITTLENESS | CURING TIME | AESTHETICS | TOTAL |
| | 1 | 1 | 1 | 1 | 1 | 0 | 0 | –1 | 0 | 4 |

Table 4 - Mix 4 Evaluation

## 2.5.2.4.  Dimethylsulfoxide (DMSO)

DMSO mixed with lignin at a 1:1 ratio created a dark brown homogeneous paste, with low viscosity and moderate bonding. When cellulose was added, chunks of fibres were formed and the homogeneity lost even with the addition of water. Two rounds of subsequent iterations were performed. At first, the proportions between binder and polymer were studied to optimise the bonding and viscosity of the resulting paste. At last, the ratio between DMSO and water was studied to avoid the agglomeration of fibres when increasing the amount of cellulose, enhancing the paste homogeneity.

Extrusion with a syringe was feasible for most of the iterations, resulting in samples with varied degrees of smoothness. In terms of hardening, the outer surfaces were dried within 24h but their overall total curing time reached two weeks. In a few specific examples, thicker sections of a few samples demanded four weeks for total hardening.

Fig 83 - Glycerine exploration - overview


Fig 84 - Glycerine exploration - sample 1


Fig 85 - Glycerine exploration - sample 2

| MATERIAL EVALUATION – MIX 5 | | | | | | | | | |
|---|---|---|---|---|---|---|---|---|---|
| MIX 5 GLYCERINE | HOMOGENEITY | VISCOSITY | ADHESION | EXTRUDABILITY | BIO-BASED | SHRINKAGE | BRITTLENESS | CURING TIME | AESTHETICS | TOTAL |
| | -1 | -1 | -1 | -1 | 1 | 0 | 0 | -1 | 0 | -4 |

Table 5 - Mix 5 Evaluation

## 2.5.2.5. Glycerine

Lignin mixed solely with glycerine in a 1:1 ratio resulted in heterogeneous substance. When cellulose was added, it turned into a homogeneous gel with low viscosity and bonding. Increasing the quantities of lignin and fibres improved these properties although retaining the gel-like consistency. In subsequent iterations, different ratios between the raw materials were studied, obtaining similar results. The effect of heat on the glycerine matrix was also experimented, resulting on a homogeneous and crumbly mix.

Extrusion with a syringe was feasible, although the low adherence between layers is an obstacle to multi-layered structures and the gel-like consistency slowed the curing time. Outer surfaces required two weeks to dry and the overall sample retained the gel consistency.

63

Fig 86 - Corn starch exploration - overview


Fig 87 - Corn starch exploration - sample 1


Fig 88 - Corn starch exploration - sample 2

| MATERIAL EVALUATION – MIX 6 | | | | | | | | | | |
|---|---|---|---|---|---|---|---|---|---|---|
| MIX 6 CORN STARCH | HOMOGENEITY | VISCOSITY | ADHESION | EXTRUDABILITY | BIO-BASED | SHRINKAGE | BRITTLENESS | CURING TIME | AESTHETICS | TOTAL |
| | 0 | -1 | -1 | -1 | 1 | 0 | -1 | 0 | 1 | -2 |

Table 6 - Mix 6 Evaluation

## 2.5.2.6. Corn Starch

Corn starch mixed with water creates an opaque thick non-adherent solution which viscosity varies from low to moderate according to the ratio between ingredients. In the first round of iterations, performed with mixes at room temperature, when lignin was added the material remained homogeneous, the viscosity increased and the material showed a low adhesion to the container walls. When cellulose was added, it absorbed the water content transforming all solutions into crumbly and non-homogeneous mixes.

In a second round of experiments, the solution with corn starch and water was heated to 100C before mixing with lignin and cellulose in different concentrations. A ratio of 3:1 between starch and lignin proved successful at creating a relatively homogeneous mix, with moderate viscosity and low bonding.

All extrusions of the first round of experiments were precluded by the fibre chunks. From the second round, although less viscous, homogeneous and adherent than previous mixes, an extrusion with a syringe was successful.

Fig 89 - Alginate exploration - overview
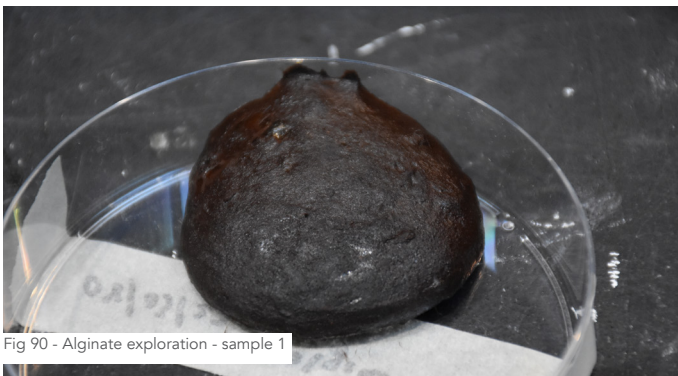

Fig 90 - Alginate exploration - sample 1
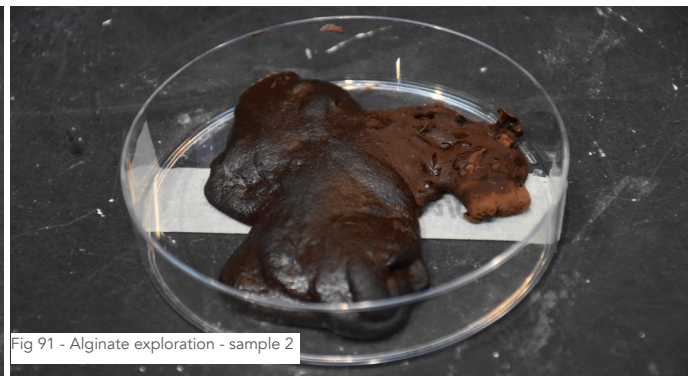

Fig 91 - Alginate exploration - sample 2

| MATERIAL EVALUATION – MIX 7 | | | | | | | | | |
|---|---|---|---|---|---|---|---|---|---|
| MIX 7 ALGINATE | HOMOGENEITY | VISCOSITY | ADHESION | EXTRUDABILITY | BIO-BASED | SHRINKAGE | BRITTLENESS | CURING TIME | AESTHETICS | TOTAL |
| | -1 | -1 | -1 | -1 | 1 | 0 | 0 | 0 | 0 | -3 |

Table 7 - Mix 7 Evaluation

### 2.5.2.7. Alginate

Alginate dissolves in water and creates a gel according to the material concentration. A 1:1 ratio solution resulted in a non-homogeneous mix with chunks of gel difficult to remove even by increasing the ratio to 1:5 and increasing the mix temperature to 80C. When adding lignin and cellulose it resulted in a homogeneous gel with low viscosity and bonding.

Extrusion with a syringe was not feasible and after two weeks of curing time, the material samples retained the gel-like consistency, with a partially dry surface.

Fig 92 - Beeswax exploration - overview


Fig 93 - Beeswax exploration - sample 1


Fig 94 - Beeswax exploration - sample 2

| MATERIAL EVALUATION – MIX 8 | | | | | | | | | |
|---|---|---|---|---|---|---|---|---|---|
| MIX 8 BEESWAX | HOMOGENEITY | VISCOSITY | ADHESION | EXTRUDABILITY | BIO-BASED | SHRINKAGE | BRITTLENESS | CURING TIME | AESTHETICS | TOTAL |
| | -1 | -1 | -1 | -1 | 0 | 0 | -1 | 1 | -1 | -5 |

Table 8 - Mix 8 Evaluation

### 2.5.2.8. Beeswax

Beeswax dissolved in hot water in a 1:1 ratio created a bright yellow and transparent liquid. When mixed with lignin it did not combine with the polymer and created chunks of fibres when cellulose was added. In a subsequent iteration, pure wax was melted in a water-bath and mixed with lignin, creating a homogeneous thick paste which quickly solidified when removed from the heat. When adding cellulose, fibres agglomerated and the mix lost homogeneity.

Extrusion with a syringe was not feasible. The curing time of the material sample was less than a minute for the outer surfaces and reached a maximum of 24h for the overall piece.

Fig 95 - Bone glue exploration - overview


Fig 96 - Bone glue exploration - sample 1


Fig 97 - Bone glue exploration - sample 2

| MATERIAL EVALUATION – MIX 9 | | | | | | | | | |
|---|---|---|---|---|---|---|---|---|---|
| MIX 9<br>BONE GLUE | HOMOGENEITY | VISCOSITY | ADHESION | EXTRUDABILITY | BIO-BASED | SHRINKAGE | BRITTLENESS | CURING TIME | AESTHETICS | TOTAL |
| | 1 | 1 | 1 | 0 | 1 | -1 | 0 | 0 | -1 | 2 |

Table 9 - Mix 9 Evaluation

### 2.5.2.9. Bone Glue

Bone glue dissolved in water created a thick liquid. When combined with lignin it created a homogeneous mix with low viscosity and low bonding. When combined with cellulose, it formed chunks of fibres and lost the homogeneity. In a subsequent iteration, pure bone glue was melted in a water-bath and mixed to lignin, creating a homogeneous paste with low viscosity and bonding. When combined with cellulose, it formed chunks of fibres and lost the homogeneity at first, demanding a longer mixing process to retrieve a smooth, although extremely sticky consistency, excessively adhering to the container walls.

Extrusion was feasible under intense pressure solely. The curing time of the material sample was 48h overall.

Fig 98 - Wood glue exploration - overview


Fig 99 - Wood glue exploration - sample 1


Fig 100 - Wood glue exploration - sample 2

| MATERIAL EVALUATION – MIX 10 | | | | | | | | | |
|---|---|---|---|---|---|---|---|---|---|
| MIX 10 WOOD GLUE | HOMOGENEITY | VISCOSITY | ADHESION | EXTRUDABILITY | BIO-BASED | SHRINKAGE | BRITTLENESS | CURING TIME | AESTHETICS | TOTAL |
| | 1 | 1 | 1 | 1 | -1 | 0 | 1 | 0 | 1 | 5 |

Table 10 - Mix 10 Evaluation

## 2.5.2.10.  Wood Glue

Wood glue mixed with lignin in a 3:1 ratio resulted in a homogeneous paste with moderate adhesion and viscosity. When cellulose was added the mixture retained its homogeneity and the viscosity and adhesion increased, without compromising the material extrudability.

Extrusion with a syringe was smooth and the material samples had a high layer definition and bonding. The curing time was 24h for the outer surfaces and one week for the overall samples.

SUNFLOWER OIL

Fig 101 - Sunflower oil exploration - overview


Fig 102 - Sunflower oil exploration - sample 1


Fig 103 - Sunflower oil exploration - sample 2

| MATERIAL EVALUATION – MIX 11 | | | | | | | | | | |
|---|---|---|---|---|---|---|---|---|---|---|
| MIX 11 SUNFLOWER OIL | HOMOGENEITY | VISCOSITY | ADHESION | EXTRUDABILITY | BIO-BASED | SHRINKAGE | BRITTLENESS | CURING TIME | AESTHETICS | TOTAL |
| | 1 | -1 | -1 | 1 | -1 | 0 | 0 | -1 | 1 | -1 |

Table 11 - Mix 11 Evaluation

## 2.5.2.11.  Sunflower Oil

Sunflower oil was tested as a potential replacement to water in the recipe resulting from the previous experiments with methylcellulose. In several iterations, different proportions were experimented. A total substitution resulted in a non-homogeneous and crumbly mix with chunks of fibres. In a ratio of 1:1 and 1:2 between oil and water, it resulted in greasy and homogeneous mixes with a glossy appearance and moderate viscosity and bonding. Extrusion with a syringe was difficult and the smoothness of the material samples was reduced when compared to the samples produced with the original recipe. Curing time was also increased to a week, with the outer surface retaining a greasy aspect even after hardened.

BAKING SODA

Fig 104 - Baking soda exploration - overview



Fig 105 - Baking soda exploration - sample 1



Fig 106 - Baking soda exploration - sample 2

| MATERIAL EVALUATION – MIX 12 | | | | | | | | | | |
|---|---|---|---|---|---|---|---|---|---|---|
| BAKING SODA | HOMOGENEITY | VISCOSITY | ADHESION | EXTRUDABILITY | BIO-BASED | SHRINKAGE | BRITTLENESS | CURING TIME | AESTHETICS | TOTAL |
| | -1 | 0 | -1 | -1 | 0 | 0 | 1 | 1 | 0 | -1 |

Table 12 - Mix 12 Evaluation

### 2.5.2.12. Baking Soda

Baking soda mixed with water creates an alkaline solution which facilitates the dissolution of lignin and its fixation to the matrix. It was used to replace water in the recipe resulting from the previous experiments with methylcellulose and created a crumbly and non-homogeneous mix. The quantity of water had to be increased two-fold the original recipe for a homogeneous paste with moderate viscosity and bonding to be created. In a subsequent iteration, baking soda was added directly to the mix with the lignin and methylcellulose powders, on a proportion of 1:1 to the binding agent. It resulted in a dry and homogeneous paste with high viscosity and bonding.

In both experiments the resulting material was not extrudable with a syringe. The samples showed similar smoothness and properties. Overall, the curing time was similar – within three days they reached maximum hardening.

### 2.5.3. Phase 3



Fig 107 - Acetone & methylcellulose samples overview

With the exploration phase of the material experimentation complete and all samples evaluated, two binders were selected for further refinement of their recipes – acetone and methylcellulose.

Acetone is the binding agent currently in use in terms of state-of-the-art material containing lignocellulosic fibres for additive manufacturing processes, therefore the benchmark for any alternative recipes. Methylcellulose presented the best results among all bio-based binders investigated. However further investigation in the mixing process and material concentrations was necessary to define the final recipes.

The extrusions were all performed with an electric caulking gun and a syringe adapted as a cartridge to ensure a continuous material flow and higher pressure when compared to a manual process.



ACETONE

Fig 108 - Acetone mix refinement - overview



Fig 109 - Acetone mix refinement - sample 1



Fig 110 - Acetone mix refinement - sample 2

#### 2.5.3.1. Acetone

Cellulose was blended first and then mixed with lignin to separate the fibres and enhance their coverage with the polymer. Water was used to reduce material dispersion. When acetone was added it formed a homogeneous paste with no fibre clots, moderate viscosity and high adhesion. In subsequent iterations, reducing the quantity of water resulted in a non-homogeneous mix with dry fibres agglomerated, meanwhile increasing the quantity of lignin reduced the viscosity and increased the adhesion.

Extrusion of multi-layered structures was successful with two nozzle sizes – 3.8mm and 2.9mm – with the latter offering higher definition and smoothness to the material samples. The surface required a 48h curing time and the overall pieces one week to harden completely.

**METHYLCELLULOSE**

Fig 111 - Methylcellulose mix refinement - overview

Fig 112 - Methylcellulose mix refinement - sample 1

Fig 113 - Methylcellulose mix refinement - sample 2

### 2.5.3.2. Methylcellulose

Cellulose was blended first and then mixed with lignin and methylcellulose to separate the fibres and enhance their coverage with both polymer and binder. Water at 80C was added and the material continuously mixed until reaching a homogeneous and moderately viscous paste. Adhesion and consistency varied according to the mix temperature, increasing as the temperature lowered below 40C.

Several iterations were performed to maximise the quantity of lignin and fibres and minimise the water content to optimise the material properties meanwhile keeping the binder quantity fixed. Lignin enhanced the adhesion and the viscosity, although it also increased the brittleness and turned it into a dry paste. Elevated quantity of fibres tended to reduce the homogeneity and form chunks. Reducing the water content resulted in a dry and crumbly mix and compromised the material extrudability.

From the experiments performed in this phase, a proportion of 6:1 between lignin and methylcellulose proved to be the most promising recipe, as well as a proportion of 1:20 between cellulose and lignin.

Extrusion of multi-layered structures was successful for most of the iterations with the smaller nozzle – diameter 2.9mm – creating smooth samples with highly defined layered structure. Curing time remained consistent from the previous experiments. Outer surfaces required 24h to dry and the overall pieces three days to harden completely.

## 2.6. Summary of Findings

From the material preparation aspect, blending the cellulose as the first step collaborated to reduce material clots and separate the fibres. Mixing them with the lignin powder before adding a binder resulted on a better coating on the fibres and improved its bonding with the polymer matrix, although increasing the material losses through dispersion. The powdery aspect of the lignocellulosic polymers increased waste which was difficult to quantify and avoid. An enclosed container was necessary to minimise it, as well as a compensation of 5% on the ingredients quantities.

Cellulose and lignin did not melt, quickly degraded when heated above 130C and required a binding agent to recombine into a viscous material. When mixed solely with water, lignin became brittle meanwhile the cellulose fibres quickly absorbed the liquid and agglomerated, creating clots if there was no bonding with the matrix or if the interaction between fibres and polymer-binder matrix was not strong.

Acetone dissolved lignin and created a viscous and adherent paste. Adding cellulose to the mix retained the homogeneity and increased the viscosity and adherence, forming long chains of microfibres. The material samples extruded showed a rough surface and an excellent interlayer bonding. The strong disadvantage is the hazardousness of the alcohol and its reaction with plastics, requiring aluminium containers for handling and glazed surfaces for extruding. Curing time is also a negative aspect, with a minimum of one week for the complete hardening of a sample.

In terms of homogeneity, viscosity and adherence, wood glue was one of the best binders among all. In a preliminary assessment, it also indicated the highest bending strength among all samples. Curing time was short for the outer surface – 24h it was dry – although the samples required one week for complete hardening. The small amount of water reduced the tendency to shrink and deform. However, the polyvinyl acetate base is a disadvantage, precluding the formulation of a bio-based material.

Most natural binders experimented did not produce tangible results in the development of a paste with adequate viscosity and adhesion for cold extrusion. Agents which activate with water at varied temperatures and form gel-like matrices – xanthan gum, glycerine and alginate – tended to form non-homogeneous mixes and retain their consistency after combined with fibres, failing at achieving a minimum viscosity for a successful extrusion and minimum bonding to build multi-layered structures.

Methylcellulose was one of the exceptions and the one with the highest score in the material exploration evaluation. Prepared at temperatures above 80C, with continuous mixing it assumed a homogeneous paste consistency with moderate viscosity and moderate to high adhesion at temperatures below 40C. The material samples manually extruded demonstrated the possibility of building multi-layered structures and showed a strong interlayer bonding and a natural wood-like appearance.

The other exception was DMSO. When combined with lignin, it created a homogeneous paste with moderate viscosity and bonding, similar to the results obtained with acetone. When mixing cellulose with the polymer beforehand, the fibres are homogeneously incorporated in the matrix, increasing the paste viscosity and adhesion. The disadvantage was the extended curing period which reached over four weeks to harden completely.

The summary table 13 comparing the results of all experiments executed combined with the observations above provide a solid background to define the most promising binding agents – acetone, DMSO, methylcellulose and wood glue – and their optimal recipes, described on the table below. These mixes were selected to be further studied and characterised in terms of material properties in the next chapter.

## MATERIAL EXPLORATION SUMMARY & COMPARISON

| | HOMOGENEITY | VISCOSITY | ADHESION | EXTRUDABILITY | BIO-BASED | SHRINKAGE | BRITTLENESS | CURING TIME | AESTHETICS | TOTAL |
|---|---|---|---|---|---|---|---|---|---|---|
| MIX 1 I ACETONE | 1 | 1 | 1 | 1 | -1 | 0 | 1 | 1 | -1 | 2 |
| MIX 2 I XANTHAN | -1 | -1 | -1 | -1 | 1 | 0 | 0 | -1 | -1 | -5 |
| MIX 3 I MC | 1 | 1 | 1 | 1 | 1 | -1 | 0 | 1 | 1 | 6 |
| MIX 4 I DMSO | 1 | 1 | 1 | 1 | 1 | 0 | 0 | -1 | 0 | 4 |
| MIX 5 I GLYCERINE | -1 | -1 | -1 | -1 | 1 | 0 | 0 | -1 | 0 | -4 |
| MIX 6 I CORN STARCH | 0 | -1 | -1 | -1 | 1 | 0 | -1 | 0 | 1 | -2 |
| MIX 7 I ALGINATE | -1 | -1 | -1 | -1 | 1 | 0 | 0 | 0 | 0 | -3 |
| MIX 8 I BEE WAX | -1 | -1 | -1 | -1 | 0 | 0 | -1 | 1 | -1 | -5 |
| MIX 9 I BONE GLUE | 1 | 1 | 1 | 0 | 1 | -1 | 0 | 0 | -1 | 2 |
| MIX 10 I WOOD GLUE | 1 | 1 | 1 | 1 | -1 | 0 | 1 | 0 | 1 | 5 |
| MIX 11 I OIL | 1 | -1 | -1 | 1 | -1 | 0 | 0 | -1 | 1 | -1 |
| MIX 12 I BS | -1 | 0 | -1 | -1 | 0 | 0 | 1 | 1 | 0 | -1 |

Table 13 - Material comparison

Among the four binders presented above, methylcellulose presented the highest score and the less disadvantages. It created a full bio-based mix which showed great extrudability with adequate viscosity and bonding properties for LDM additive manufacturing fabrication, similar to the clay feedstock commonly used in such processes. In terms of material development, it validates the potential of producing a full natural mix with cellulose and lignin.

For the subsequent printability exploration, this was the base material used to explore the limits of the additive manufacturing fabrication in terms of design and geometry and, consequently, it will also be applied on the fabrication of the final prototypes.

### ACETONE MIX RECIPE

| | QUANTITIES USED | WT % |
|---|---|---|
| LIGNIN | 60g | 58.25% |
| CELLULOSE | 5g | 4.85% |
| WATER | 10g | 9.71% |
| ACETONE | 28g | 27.19% |

### METHYLCELLULOSE MIX RECIPE

| | QUANTITIES USED | WT % |
|---|---|---|
| LIGNIN | 30g | 29.13% |
| CELLULOSE | 3g | 2.91% |
| WATER | 65g | 63.11% |
| METHYLCELLULOSE | 5g | 4.85% |

### DMSO MIX RECIPE

| | QUANTITIES USED | WT % |
|---|---|---|
| LIGNIN | 35g | 50.72% |
| CELLULOSE | 4g | 5.80% |
| WATER | 10g | 14.49% |
| DMSO | 20g | 28..99% |

### WOOD GLUE MIX RECIPE

| | QUANTITIES USED | WT % |
|---|---|---|
| LIGNIN | 10g | 24.39% |
| CELLULOSE | 1g | 2.44% |
| WATER | - | - |
| WOOD GLUE | 30g | 73.17% |

Table 14 - Material recipes - promising mixes

## 2.7. Conclusion

With an excuse to the scientific methodology, the material exploration phase could be compared to cooking without a recipe – even in terms of raw materials, procedures and equipment. The base materials and their limitations and challenges in terms of preparation, temperature and water affinity were well-known. Additives and binders were novelty, as well as their behaviour when combined with the first ones.

The process involved a repetitive series of iterations for each new binder until finding the best recipe – meaning, the best proportions. And, like in the culinary world, some concoctions were more successful than others and inspired a continuous process of refinements and a series of spin-off variations.

The material exploration phase aimed at fully understanding the base materials used in this research – cellulose and lignin – and how they react with potential binding agents, identifying the most promising ones and establishing a recipe. A successful result in the scenario of this research meant also a material with printability potential, attested with the extrudability, viscosity and adherence parameters, and a material which could be used in a sustainable building industry, assessed through the bio-based content and aesthetical factors.

It achieved its goal by successfully pointing towards the most promising binder – methylcellulose – and three high-score alternatives to be used in terms of comparison in the material properties investigation phase – acetone, wood glue and DMSO. Among these, two are not bio-based, although they offered outstanding adherence and strength scores and were chosen to create a benchmark for comparison and, potentially, directions for improvement of the methylcellulose mix.

The assessments from this chapter were already conclusive to define methylcellulose as the most promising binder and the one to be used for the printability tests and design exploration. Even though, the other three recipes were still assessed at the subsequent material properties exploration phase for comparison purposes. By understanding their different mechanical behaviours, the direction for further research and improvements could be outlined.

# 3. Printability Exploration

## 3.1. Overview

During the previous phase, the extrudability of each mix was tested with a syringe either manually or with an electric caulking gun. With the material exploration completed and the potential mixes defined, the printability exploration phase was the subsequent step, set to explore the additive manufacturing fabrication with the most promising mix among the short-listed ones.

From the four materials selected for further characterisation and investigation on their properties, the methylcellulose mix had the highest scores and less disadvantages. It is a full bio-based material and showed the best viscosity and adherence, fundamental for an LDM fabrication process, similar to the clay commonly used in such processes. In a short summary, acetone is hazardous and flammable, wood glue is chemically based and DMSO requires a long curing time, besides an excessive adherence, reinforcing methylcellulose as the material of choice for the printability testing.

All the additive manufacturing exploration was performed at LAMA, in the Faculty of Architecture and the Built Environment of TU Delft. A clay extruder from WASP was made available for the research as well as the two 6-axis robotic arms from Comau and Universal Robots.

The first step was the installation and setup of the extruder, the understanding of its operation and eventually a try-out before the installation onto the robotic arm. Second step was the installation and setup of the robotic arm, the understanding of its operation and eventually a try-out before the installation of the extruder. With the whole system set, basic geometries were designed with Rhinoceros and Grasshopper to experiment with the printing process and finally to execute the printability tests and assess the potential and limitations of the material and process.

The setup, including hardware, firmware and software, was designed and implemented by Christopher Biearch and can be followed in detail in Potential and Limitations to 3D print a window frame with cellulose and lignin (Biearch, 2022).

## 3.2. Planning & Preparation

### 3.2.1. Equipment Setup

An LDM extruder from Wasp – model Extruder XL 3.0 – commonly used for Delta 40100 Clay printers, was used for all the fabrication. It is operated by a 23 NEMA stepper motor and controlled by an Arduino Duet 3 6HC motherboard directly connected to a computer. Material is supplied from a 0.7l metallic cartridge attached by a plastic hose and connected to an air compressor with a maximum pressure of 6 bar.

The initial setup mounted the extruder on a 6-axis industrial robotic arm Comau NJ 60-2.2. Nevertheless, technical difficulties hindered the operation of the setup and forced a rearrangement of the extruder to the 6-axis collaborative robotic arm UR5 from Universal Robots.

Fig 114 - Extruder setup


Fig 115 - Robotic arm remote control setup
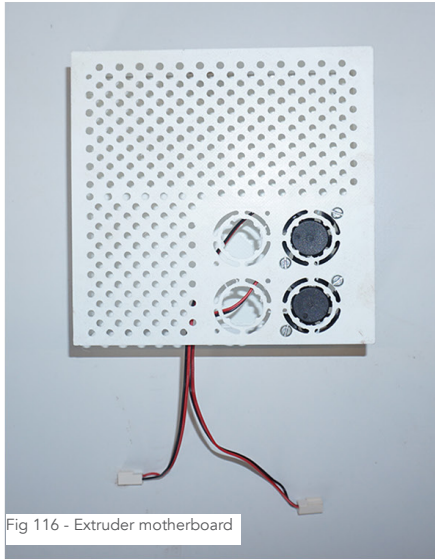

Fig 116 - Extruder motherboard
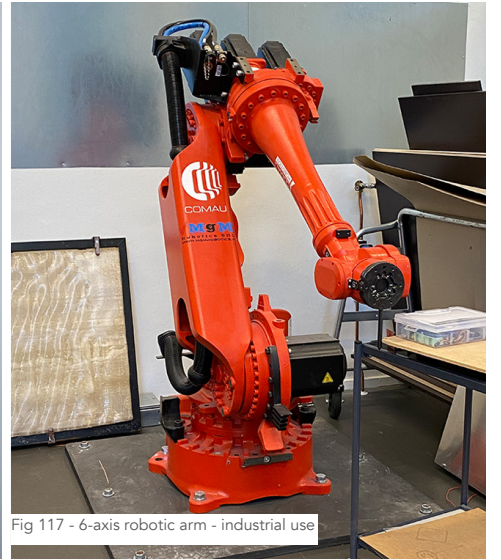

Fig 117 - 6-axis robotic arm - industrial use
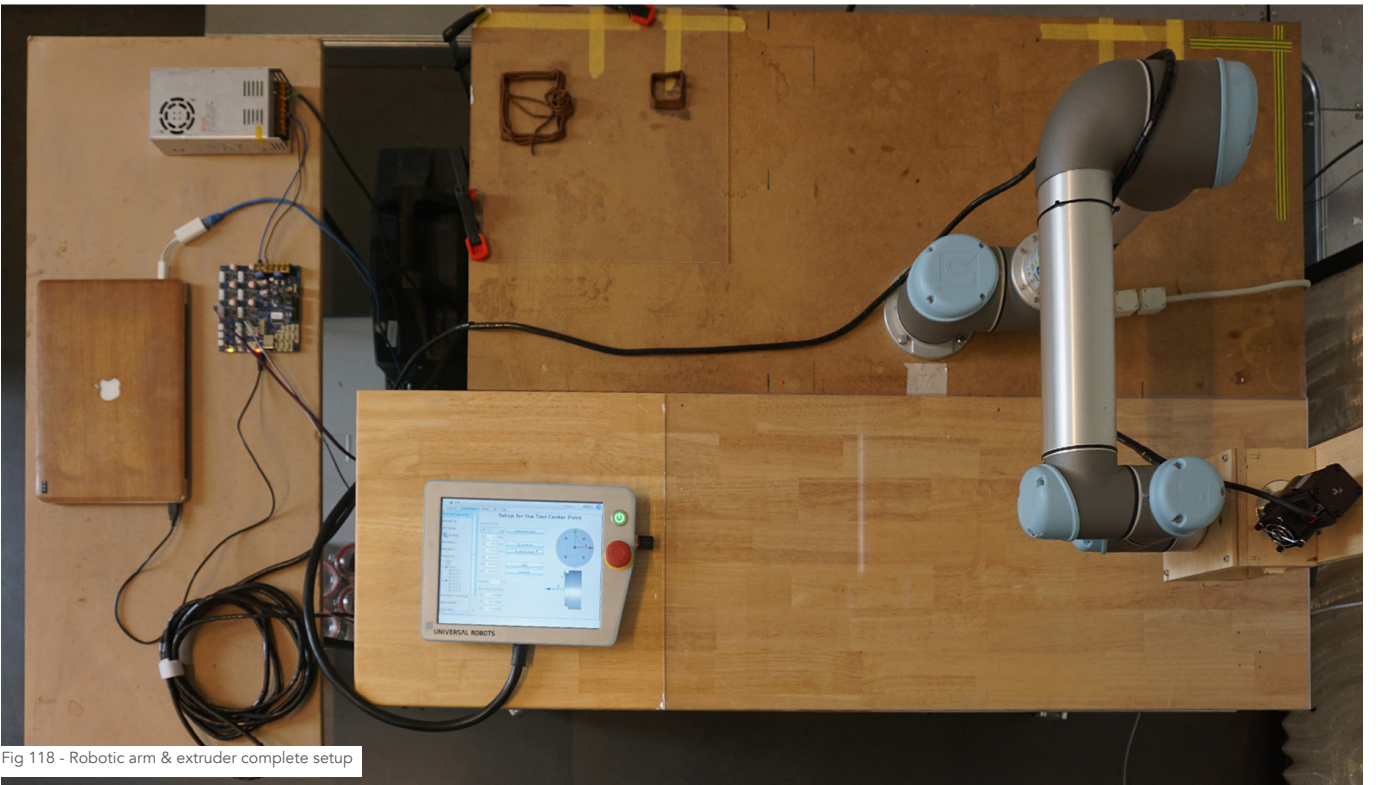

Fig 118 - Robotic arm & extruder complete setup

### 3.2.2. Software Setup

The extruder and the robotic arm are controlled and operated separately.

A slicing software – Simplify 3D – was used as the interface with the Arduino motherboard connected to the former and commands the start/stop, defines the speed and the number of rotations for the stepper motor.

The robotic arm was connected directly to the computer through a router and controlled by a program created with the plugin Robot for Grasshopper. Printing bed size and location relative to the robot were defined, as well as the tool installed onto it – wooden holder and extruder –, its TCP and the total payload. Movement types, speed and quantity of waypoints were adjusted according to the geometry to be extruded, with linear moves for straight lines and sharp corners and constant speed moves for curvilinear sections and smooth corners. A higher number of waypoints increases the smoothness although it slows the program.

Rhino and Grasshopper were used to create all the shapes to be fabricated. The joint surfaces were imported into the script developed with the Robot plugin, the geometry contour generated, and the printing parameters adjusted for simulation and printing.

### 3.2.3. Material Setup

The feedstock selected for the printability exploration was the one based on methylcellulose as a binder due to its performance and characteristics prone to extrusion. An additional advantage of this mix was the easiness to handle – it does not damage any tools or surfaces and does not require special products to clean.

The material batch was sized according to the extruder cartridge and should be sufficient to fill it entirely. The recipe followed the proportions established at the end of chapter 2 and resulted on the quantities showed on the table below for a mass of approximately 760g.

| BATCH – 1 CARTRIDGE | WT % | QUANTITIES USED |
|---|---|---|
| LIGNIN | 29.13% | 164.33g |
| CELLULOSE | 2.91% | 16.43g |
| WATER | 63.11% | 356.04g |
| METHYLCELLULOSE | 4.85% | 27.39g |
| TOTAL | 100% | 564.19g |

Table 15 - Material quantities - one cartridge

The mix is typically produced hot, and its temperature lowers during the process. Although viscous and adherent once the mixing is completed, it requires a complete and slow cooling down process for a minimum of 24h in an enclosed container, or covered with plastic film, to reach its optimal consistency. Prints executed with freshly produced material showed a high moisture content and resulted on collapsing geometries.

### 3.2.4. Exploration Setup

First phase of the printability tests was executed by manually handling the extruder before mounting it on the robotic arm. The objectives were to validate the extruder setup, operation, and control and to attest the extrudability of the material with the equipment, verifying the minimum pressure required for a successful print. No shapes were designed, or tool paths defined, only lines of code were used directly on the Arduino controller software to activate and deactivate the stepper motor.



Fig 119 - First extrusion tests

Second phase of the tests was executed after the extruder setup was finalised and it was mounted on the 6-axis robotic arm. Simple shapes were designed on Rhinoceros and imported into the Grasshopper/Robots script developed to generate the tool path and used to control the robotic arm operation. The models were divided into three groups with distinct printing parameters to investigate – geometry, overlapping and overhang. According to each model, parameters regarding the movement type, speed, number of waypoints and frames were adjusted on the tool path and simulations performed to validate it. With the program finalised, the robot was set to perform all the movements for a final visual check before proceeding with the extrusion.

## 3.3. Execution & Results

Prior all extrusions, the cartridge was filled to the maximum capacity with special attention to avoid air pockets. If excessively adherent or dry, a small amount of water was used to retrieve the necessary viscosity.

Successful extrusions and collapsed structures which offer relevant information regarding printing limitations and material behaviour were let to cure for a minimum of three days. Failed prints were aborted and the material reused on the subsequent extrusions. The design of the test subjects was constantly revised according to the input from each iteration.

### 3.3.1. Geometry

A set of simple geometrical shapes to verify the extrusion overall structure and stability were drawn – square, circle, diamond, olive, and oval – with a maximum length of 50mm on the longest side, and extruded 30mm. Models had a single-line wall and no infill and the prints were performed with a 4mm nozzle.

All extrusions, except the circle oval, collapsed either during the printing process or at the end of the process.
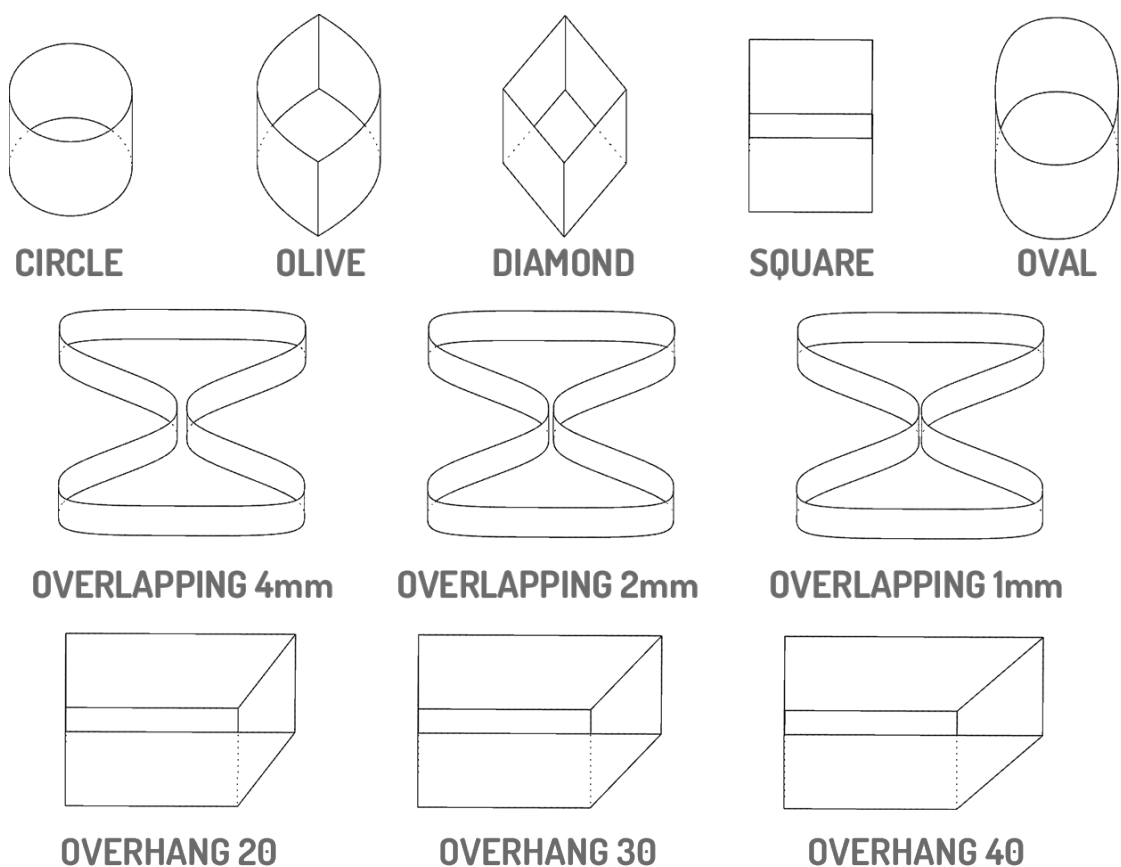


Fig 120 - Printability test design



Fig 121 - Geometry test outcome

### 3.3.2. Overlapping

Three curvilinear shapes resembling the number 8 were drawn with a continuous line and with a 4mm, 2mm and 1mm gap between the curves at their closest point, with a maximum length of 100mm on the longest side and extruded 30mm. Models had a single-line wall and no infill and the prints were performed with a 4mm nozzle.

All extrusions were successful and none collapsed. Only the 1mm spacing resulted in overlapping. With 2mm, the walls touched and with 4mm they were completely separated.

Fig 122 - Overlapping test outcome

### 3.3.3. Overhang

Three boxes 50x70x50mm (l*w*h) were designed with an inclination of 20, 30 and 40 degrees on the wall on one of the shortest sides. Models had a single-line wall and no infill and the prints were performed with a 4mm nozzle.

The first extrusion collapsed at the end of the process, leading to a design review and the incorporation of a zig-zag infill. The straight walls buckled and the second print also collapsed at the end of the process. Zig-zag infill and linear walls were replaced with curvilinear walls, nonetheless the material used – from a new batch – was heavy and not viscous enough, leading to the collapse of the third attempt.

From observations throughout the extrusion process, an overhang of 20 degrees with curvilinear walls is feasible, although the material must cool down and dry for at least 24h in the cartridge or covered in plastic film to reach the optimal viscosity.


Fig 123 - Overhang test outcome

# 3.4. Summary of Findings

### 3.4.1. Geometry, overlapping & overhang

Without infill and support structure, circular shapes proved to be more stable than straight walls. Linear extrusions with a 4mm nozzle tended to buckle at heights above 30mm due to the wall thickness and material weight.

With the same nozzle, a spacing of 1mm between walls created a half-layer overlapping, adequate for strong connections such as between infill walls. With a 2mm distance, the layers connected although did not overlap, adequate for connections between support structure and the shape outline.

Overhangs were challenging due to the material weight, however from observations on the failed prints, an inclination of 20 degrees would be feasible, although an infill must be added and designed to do not add weight to the projecting wall. A circular overhang with a curvilinear support structure would potentially increase the inclination to 30 or 40 degrees.

### 3.4.2. Infill

Hollow structures had the tendency to buckle, except circles, therefore demanding an infill. A zig-zag design with straight and tall walls must consider the grid density to also avoid buckling. Nonetheless, a curvilinear design proved to be more stable and allows for a lower density, less material usage and an overall lighter structure. Overlapping between infill and outline must be observed to ensure an efficient support and avoid punctual material excess and loss of smoothness.

### 3.4.3. Nozzle

The nozzle diameter had a direct influence on the overall resolution of the extrusion outcome and the level of details feasible to produce. Overall, it defines the minimum layer thickness achievable. During the short first phase of test prints, nozzles with diameters of 4, 6 and 8mm were used for multi-layered linear extrusions, all successfully producing smooth samples with no clogging due to fibre chunks or material viscosity. No limitations were documented to the printability, and the differences observed relate to the curing time and behaviour

With curvilinear geometries and corners, as explored during the second phase of the printability exploration, the nozzle diameter turned into a limitation. Wider meant more stability for linear walls, but less details and form freedom on the same scale. It must be proportional to the scale of the print and the expected level of details.

### 3.4.4. Shrinkage, warping & deformation

Shrinkage seemed to be similar on all directions and independent from thickness, height and weight. All samples presented a reduction of approximately 10% on their overall dimensions. They did not have a predominant fibre direction.

Deformation reached its maximum after three days of curing and loss of the moisture content of the

extruded part. It is less noticeable on heavier structures, either taller or printed with a wider nozzle. Long and linear extrusions, which have less structural stability when compared to closed geometrical shapes, showed significant alterations on their original form as observed during the first phase of tests, including sharp warping on single and double-layered extrusions.



Fig 124 - Sample warping effect

Curing conditions collaborated with the deformations. Samples dried from top to bottom due to uneven distribution of heat and ventilation of the environment. The ideal hardening process would be done on a mesh, elevated from the surface to create a circular air flow in a full-controlled environment in terms of humidity, temperature and ventilation.

## 3.5. Conclusion

The material exploration phase showed the challenges in handling the raw materials, mixing, and creating a viable feedstock for additive manufacturing. Extrudability had already been assessed, nonetheless, the printability exploration was the research phase designed to validate the material potential to successfully extrude geometrical shapes and identify its limitations and fabrication challenges.

The material created has an outstanding performance as an additive manufacturing feedstock. It can be produced in advance and conserved wrapped in plastic film and protected from the environment for up to one month (time frame experimented). Consistency, viscosity and adherence are great and did not offer resistance to extrusion even at low pressure – highest value used was 2 bar. A strong inter-layer bonding kept the structure stable and did not allow dragging during the extrusion. Finally, it showed a fast hardening period of 24h for the outer surfaces and an overall curing time of 3 to 7 days, depending on the thickness of the layers and walls.

Potential is clear, however the challenges are great still.

The high water content proved to be the source of increased deformation at hardening. Circular geometries are stable, although straight walls tended to buckle above 30mm of height, even in closed polygons like squares and diamonds. Material mass and the wall thickness demanded a balance to reach stability. Wider layers offered more stability, although they increased the weight and reduced the resolution of sharper corners. Reduced layer heights offered higher print resolution, however increased the weight and the tendency of straight walls to buckle and collapse. A well-thought infill design balancing structural stability and density, adjusted to each design approach, is necessary.

Overhangs are feasible, despite the failed tests, based on prior prints, although also require a customised infill design to provide adequate support without offering additional load on the inclined walls.

With the material recipe refined, the printability studied and a clear understanding of the potentials, limitations and challenges encountered, the main question of this research can be assessed and explored in the design of a prototype.

# 4. Material Properties Exploration

# 4.1. Overview

The material experimentation described in chapter 2 identified four promising binding agents to be combined with cellulose and lignin and their respective recipes. Conclusions were drawn based on manual testing and observations, although no mechanical properties were assessed. These had to be verified and documented for comparison purposes and to establish the potential of cellulose and lignin in the development of a feedstock for 3D printing.

Novel bio-based materials for additive manufacturing are not included in any specific codes that regulate material testing. Therefore, the test design, parameters, specimens and interpretation of the results followed the standards used for polymer testing and described in the NEN-EN-ISO-178 (CEN, 2019) and NEN-EN-ISO-527 (CEN, 2012) norms, however adaptations were made to suit the material and process limitations.

The characterisation of these materials started with the investigation of their mechanical properties through tensile and bending tests. The yield stress, ultimate tensile stress and modulus of elasticity – both at tensile and flexural situations – of each material were tabulated and compared with benchmark values from timber typically used in the building industry. Nonetheless, as preliminarily observed during the material exploration phase, no structural properties were expected from any of the material mixes. Among the four sets tested, the wood glue and methylcellulose mixes were expected to present the highest strength, and the DMSO mix the lowest.

The documentation of these properties aims at verifying the potential, advantages and disadvantages of each recipe and create a parallel with timber, establishing a direction for improvements and further research. Nevertheless, the current stage of development does not allow for maximum scientific rigor to be respected.

Based on the hydrophilic behaviour from wood and cellulose, the effect of water and the need of a repellent layer on these novel materials also had to be verified. Samples were tested for water absorption and retention, both with and without protective coatings and compared to the timber industry standards.

Finally, samples had their surfaces and cross sections analysed though the lenses of an electronic microscope. Detailed images in high resolution provided information regarding the porosity, homogeneity and fibres coating, length and direction. Previously assessed solely through macro-lens observations, this analysis collaborated to define the density and composition of the different mixes and the directions for further research and improvements.

| WOOD MECHANICAL PROPERTIES | | | | | |
|---|---|---|---|---|---|
| | FLEXURAL STRENGHT | MODULUS ELASTICITY (BENDING) | YIELD STRENGHT | MODULUS ELASTICITY (TENSION) | REFERENCE |
| BEECH, AMERICAN | - | 9.5 GPa | 86.2 MPa | - | (USDA Forest Service, 2010) |
| OAK, OVERCUP | - | 9.8 GPa | 77.9 MPa | - | (USDA Forest Service, 2010) |
| PINE, EASTERN WHITE | - | 8.5 GPa | 73.1 MPa | - | (USDA Forest Service, 2010) |
| SPRUCE, ENGELMANN | - | 8.9 GPa | 84.8 MPa | - | (USDA Forest Service, 2010) |
| PARTICLEBOARD | - | 2.8 – 4.1 GPa | 15 – 24 MPa | - | (USDA Forest Service, 2010) |
| MDF | - | 3.6 GPa | 36 MPa | - | (USDA Forest Service, 2010) |
| OSB | - | 4.4 – 6.3 GPa | 22 – 35MPa | - | (USDA Forest Service, 2010) |
| PLYWOOD | - | 7 – 8.6 GPa | 34 – 43 MPa | - | (USDA Forest Service, 2010) |
| GLULAM | - | 9 – 14.5 GPa | 29 – 63 MPa | - | (USDA Forest Service, 2010) |

Table 16 - Wood mechanical properties

## 4.2. Mechanical Test

The objective of the mechanical testing in this research was to outline the properties of the material mix identified as the most promising one in the material exploration phase – the methylcellulose mix. For comparison purposes, and to build a benchmark in terms of cellulose and lignin based materials, the properties of the other three mixes also selected as promising recipes were also assessed and documented.

### 4.2.1. Planning & Preparation

#### 4.2.1.1. Test Design

The development of bio-based materials specifically for additive manufacturing fabrication processes is a novel field. There are no unified codes and standards for mechanical tests and for the design and production of test specimens. Examples obtained from the literature are neither clear nor consistent. Therefore, to proceed with the material characterisation in this research the EN-ISO standards applied to the test of polymers were followed to define the test procedures and the geometry and dimensions of the test coupons.

Two tests were performed – tensile and three-point bending – to determine the material properties under direct tension and at tension-compression respectively. Five specimens of each composition were tested and documented to offer a minimum confidence on the results.

For the tensile test, a universal testing machine was fitted with clamps. A specimen was installed between them and load applied in tension, increasing the pressure until rupture. Force and displacement values were measured and, subsequently, transformed into a stress-strain graph to extract the relevant properties.

For the bending test, the same machine was fitted with two supports, where the specimen rests, and a centralised pin, which applies pressure until the maximum flexural strength is reached and the specimen continuously deforms. Force and displacement values were measured and, subsequently, transformed into a force-displacement graph to extract the relevant properties.

#### 4.2.1.2. Outcome

Due to the novel nature of the mixes and the inexistence of similar materials, it was difficult to estimate the expected results from the mechanical tests. The overall benchmark for this research is wood, therefore the properties of different types of timber applied in the building industry were used as reference values. As an educated guess based on the preliminary observations from the exploration phase, the wood glue mix was expected to present the best properties among the four materials to be characterised.

A data set with force and displacement values for each test iteration was created. Through graph analysis and calculations, a set of properties was defined and the data from the five specimens compiled. Wide variations between the specimens resulted on large deviations, therefore average values were not established. Instead, a range of values was defined for each property of each material mix.

From the tensile test results, the yield stress, modulus of elasticity, ultimate tensile stress were determined.

From the flexural test results, the flexural strength and the modulus of elasticity in bending were determined.

### 4.2.1.3. Location

The mechanical tests were performed at the Stevin Laboratory II, located in the Faculty of Civil Engineering and Geosciences of TU Delft through a collaboration with the group of Structural Design and Building Engineering.

### 4.2.1.4. Equipment

For all tests a universal testing machine from Instron was used, fitted with clamps for the tensile test and with a movable beam, equipped with two support pins and a pressure pin, for the flexural test. Maximum load limit of 1kN. t



Fig 126 - Tensile test setup



Fig 127 - Three-point bending test setup
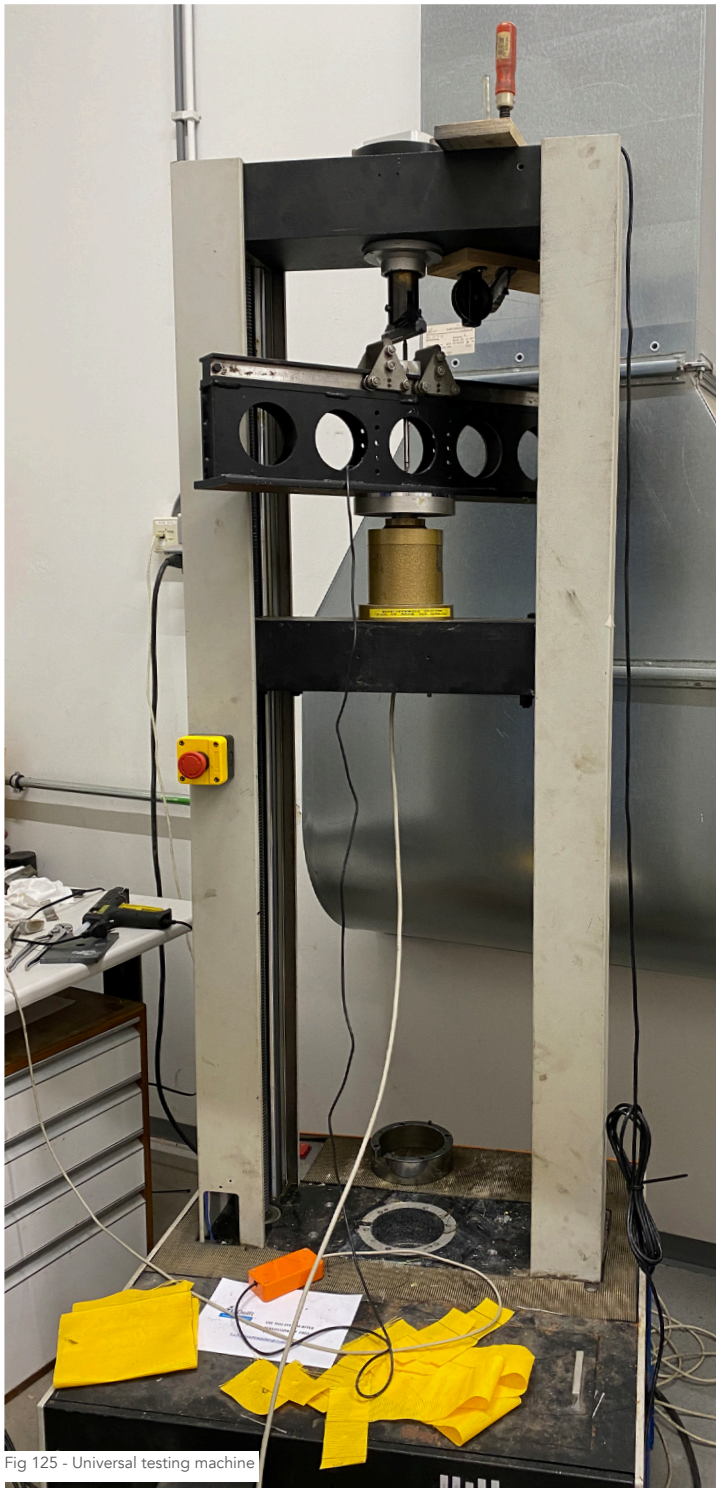


Fig 125 - Universal testing machine

### 4.2.1.5. Test Specimens

For the tensile test, the NEN-EN-ISO-527-2 (CEN, 2012) standard defines a minimum quantity of five dumbbell-type specimens to obtain results with a 95% level of confidence.

For the flexural test, the NEN-EN-ISO-178 (CEN, 2019) standard defines a minimum quantity of five beam-type specimens to obtain results with a 95% level of confidence.

All pieces were designed according to the guidelines presented in the NEN-EN-ISO-20753:2018 (CEN, 2018b) standard for plastic test specimens.
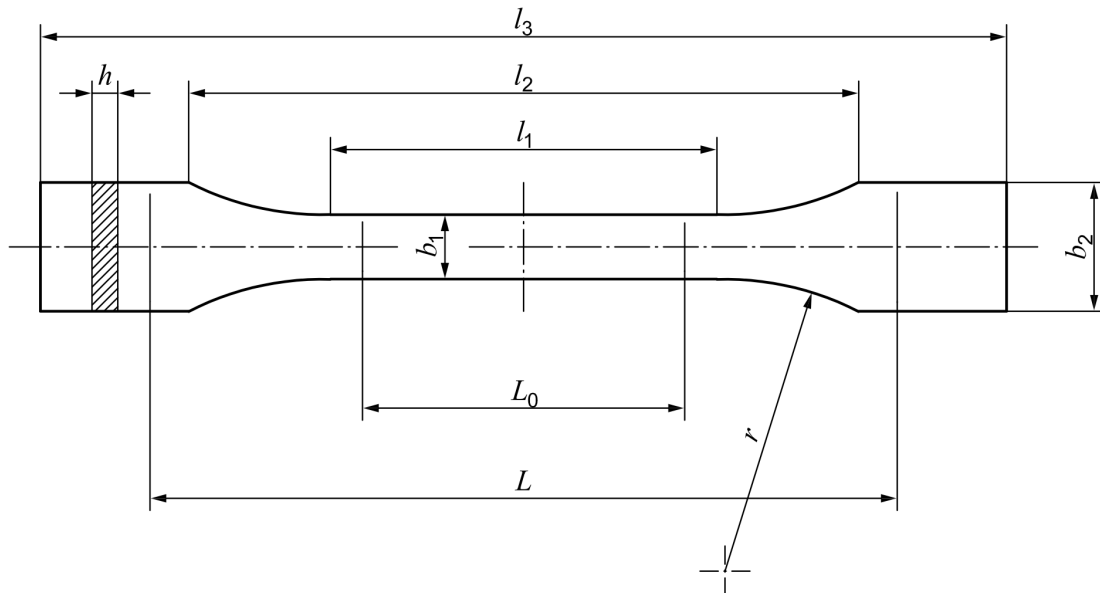


Fig 128 - Specimen Type A - Dumbbell (source: NEN-EN-ISO-527-2)
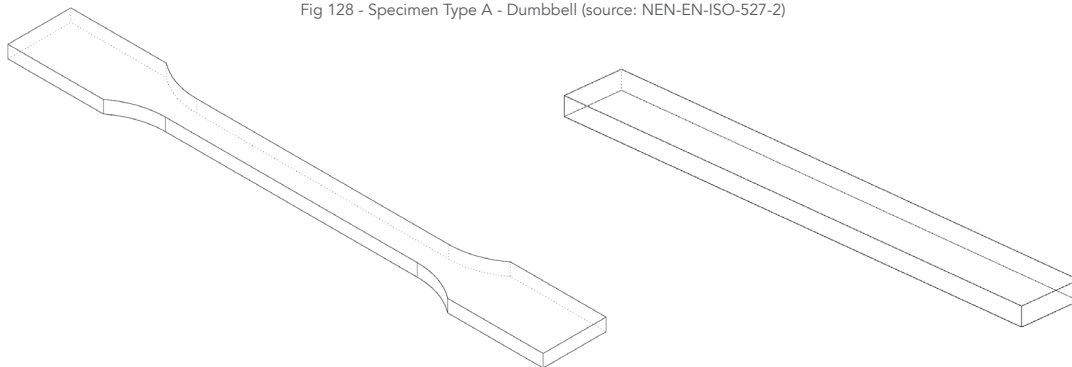


Fig 129 - Specimens type dumbbell & beam

Dimensions of the grip portion of the dumbbell and of the beam overall length had to be adjusted to better fit the test machine and the available support pins and clamps. However the dimensions of the test zone in both types remained within the specifications determined by the ISO standards.

For the water absorption test, due to an extended curing time estimated for the monolithic specimens specified in the ISO 62 (ISO, 2008) standard, the same beam-type geometry from the flexural test was selected.

For the microscope analysis, one of the additional beam-type specimens produced for the previous tests was used.

The standards above are specific for polymers and for an injection moulding fabrication process. They do not define tolerances and design compensations for material shrinkage, a behaviour observed in previous samples fabricate with three out of the four mixes selected from the material exploration phase. The average shrinkage was therefore estimated, through failed specimens produced in several iterations, and incorporated to the design.

### 4.2.1.5.a. Quantity

For the mechanical tests, five specimens of each type and from each material mix were produced, following the guidelines established in the ISO standards to reach a level of 95% of confidence in the test results. For the water absorption test, three specimens from each material mix were produced, also following the aforementioned norm. As contingency, one additional specimen was produced for each test to account for machine and operational errors, totalling six dumbbell-type pieces and ten beam-type pieces.

### 4.2.1.5.b. Specimens Production

According to the initial research plan, the test specimens would be produced in a subsequent phase to the printability exploration through additive manufacturing fabrication. Time constrains due to delays on the equipment setup and limitations to the use of a solvent – acetone – in its plastic container led to both phases printability exploration and material properties exploration to proceed in parallel. Therefore, an alternative production method was developed to fabricate the test coupons.

Based on the standards NEN-EN-ISO-294-1 (CEN, 2017) and NEN-EN-ISO-294-2 (CEN, 2018a) applied in polymer research and characterisation, a simplified compression mould was designed and fabricated in PLA using an FDM printer. Nevertheless, the overflow channels were insufficient to control the thickness of the piece, the lack of an air inlet and a curing strategy prevented hardening and the lack of ejection pins and the material mixes adhesive nature damaged the pieces during demoulding.
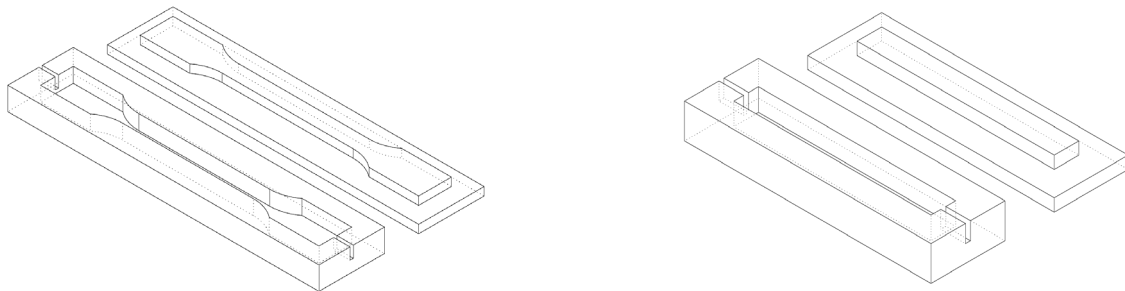


Fig 130 - Specimens mould - version 1

A revised version, produced with MDF boards and laser cut, transformed the bottom half into a panel with the shape cut out and carved overflow channels. The top half remained as the compression plate, with a guiding frame for the specimen thickness. Regardless the open frame bottom, the material did not harden. Coatings of wax, vaseline and vegetable oil on the surface and moulds were tested, nonetheless adhesion still damaged the pieces.

In the subsequent iteration, a single MDF panel with the shape cut out, similar to the one from the previous attempt, was designed. Material was spread on top with a rolling pin, nonetheless difficulties to evenly fill the moulds and continued excessive adhesion to the tools hindered the process.
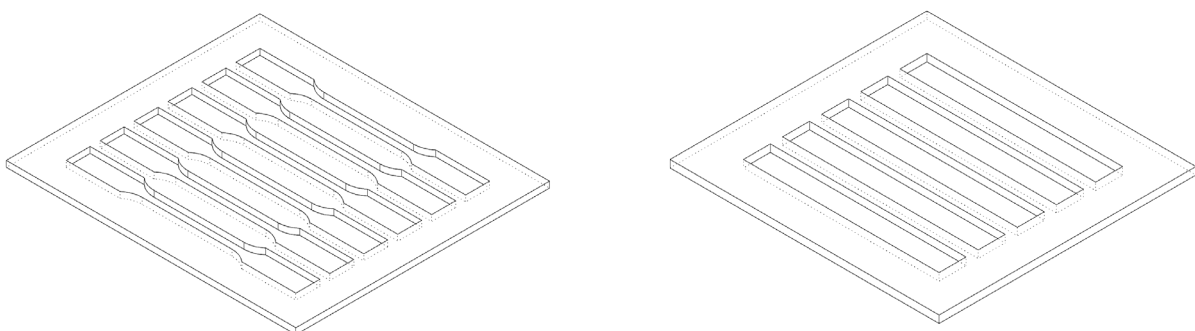


Fig 131 - Specimens mould - version 3

Alternatively to moulds, an outline cutter, similar to the ones commonly used in the pastry industry, was designed and fabricated in PLA with an FDM printer. Enlarged frame, crossed support elements and a 1.2mm thickness for the walls were used for overall stability. Material was spread with a rolling pin on a surface covered with plastic film and previously coated with demoulding wax and lignin, using guides to maintain a uniform height. The specimens were marked and cut on the material patches. After hardening for 24h, the excessive material was removed and the specimens let cure for one week.
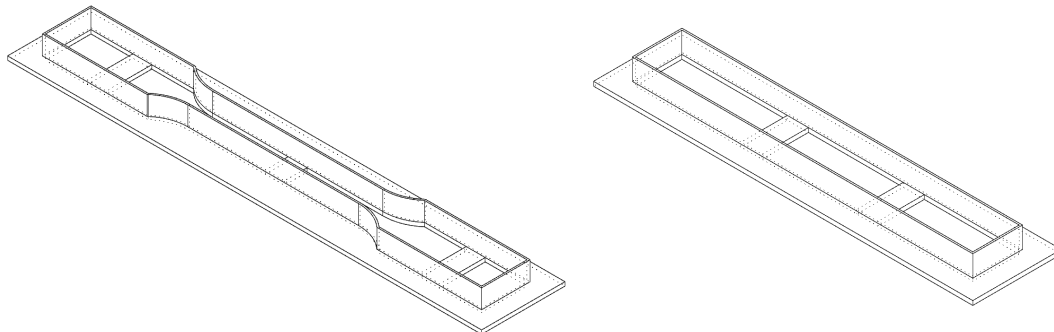


Fig 132 - Specimens mould - version 4

Such method was successful with the wood glue and methylcellulose mixes, although an average shrinkage of 10% on the overall dimensions of the latter was observed.

On a final iteration, the cutter design was revised to compensate the deformation and to reduce the wall thickness to 0.8mm to facilitate the cutting process. The tools were fabricated and all the methylcellulose and wood glue specimens produced and set to harden.



Fig 133 - Beam specimen - shrinkage effect



Fig 134 - Dumbbell specimen - shrinkage effect



Fig 135 - Methylcellulose pecimens fabrication

Fig 136 - Methylcellulose pecimens fabrication

For the acetone and DMSO specimens however, an alternative approach was necessary due to the excessive adhesion of the material to the surface and to the rolling pin. A cut out mould, similar to the ones previously used, was designed as a single-use tool. A flexible frame without top and bottom panels and a reduced infill grid of 10% was fabricated in PLA with an FDM printer. Material was spread evenly and let cure before breaking the moulds to release the specimens and finalise the hardening process.

After cured, all specimens were measured to document any dimensional variations, and sanded to reduce imperfections on the surface which could lead to failure and high imprecisions during the test execution.


Fig 137 - Specimens mould - version 5
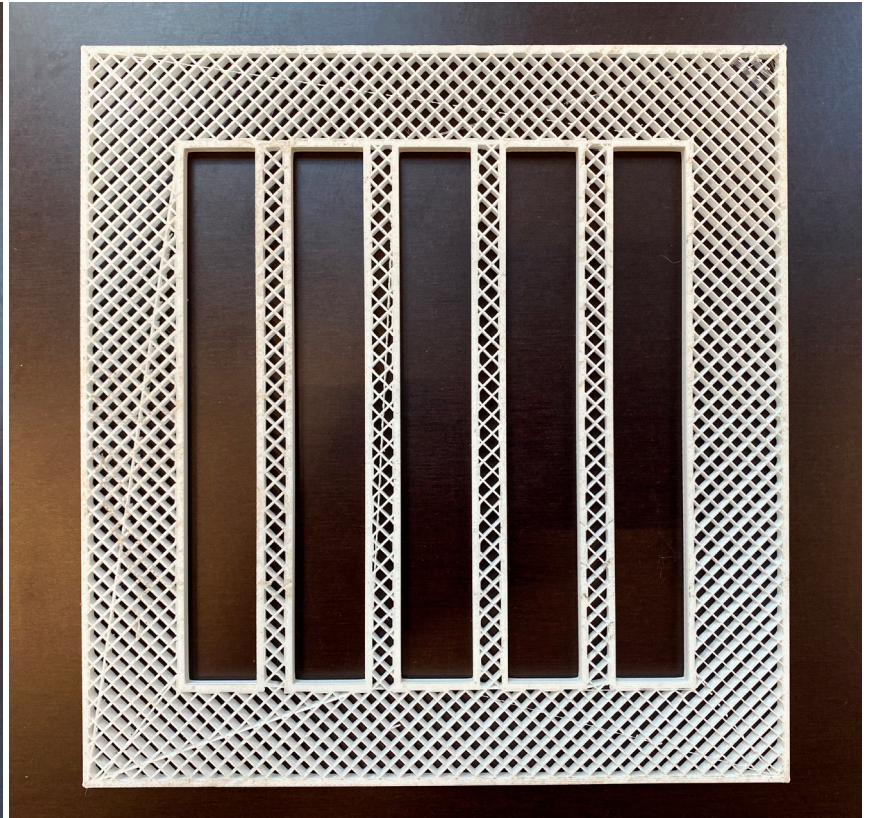

Fig 139 - DMSO specimens fabrication


Fig 138 - Acetone specimens fabrication


Fig 140 - DMSO specimens fabrication

### 4.2.2. Test Execution

#### 4.2.2.1. Tensile Test

The universal test machine was fitted with clamps at top and bottom. Load is applied and measured on the top clamp meanwhile the bottom clamp fixed to the movable beam lowers upon reaching maximum force and the rupture of the specimen. Both clamps are aligned on the same vertical axis and free to rotate around it to compensate for imperfections on the specimen geometry, requiring careful operation to avoid damage to the coupons. Two pieces were discarded due to premature cracking during the first test. The machine is connected to a proprietary software in the attached computer which controls the position of the bottom clamp, to be adjusted according to the specimen overall length, and the clamping pressure. At the start of the test, the applied pressure must be calibrated and set to zero.

The standard system measures the displacement of the clamp and is subject to imprecisions due to its assembly tolerances. In order to obtain accurate values for the specimen deformation, an LVDT (linear variable differential transformer) sensor was attached to the clamps and connected to the measurement software, calibrated at the start of each iteration.



Fig 141 - Universal test machine - tensile setup

Fig 142 - Specimen & LVDT sensor

Fig 143 - Specimen setup

#### 4.2.2.2. Three-point Flexural Test

The universal testing machine was fitted with a fixed loading pin at the top and a beam and two sliding support pins at the bottom. Load is applied and measured on the top pin meanwhile the bottom part of the machine moves upwards resulting on the deflection of the tested specimen.

Prior the test, each sample was measured and the geometrical central point marked, as well as the position of the equidistant supports. The sliding pins at the bottom part of the machine allow for an adjustable span according to the test specifications. For this research, a span of 80mm was defined following the NEN-EN-ISO-178 (CEN, 2019).

The standard system measures the dislocation of the supports. To precisely quantify the deflection, an LVDT sensor was installed underneath the specimen and connected to the controlling software, calibrated at the start of each iteration.

For the test execution, the specimen is centralised on the top pin, the supports adjusted, and the height calibrated and the force set to zero.
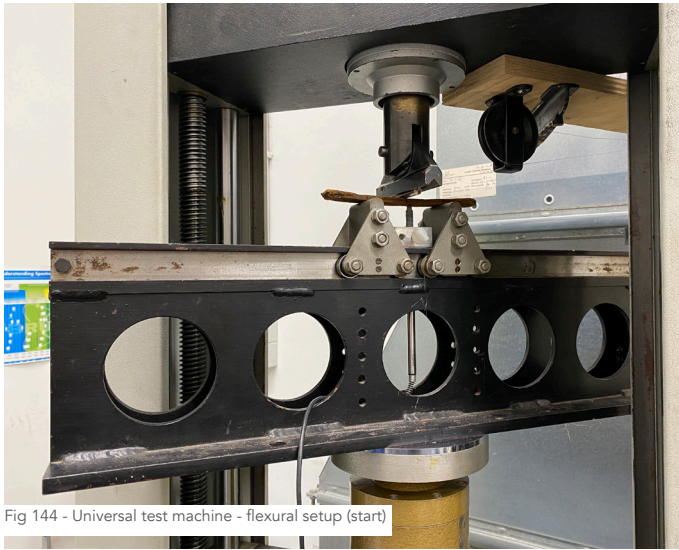

Fig 144 - Universal test machine - flexural setup (start)


Fig 145 - Universal test machine - flexural setup (end)

### 4.2.3. Test Results

A summary with the test results and findings for the methylcellulose, wood glue and acetone material mixes is presented below. The DMSO specimens failed prematurely at all attempts of performing the tensile and flexural tests, retaining an elastic aspect during the curing period and not offering any resistance to forces in tension and compression.

According to the literature, the solvent transitions from liquid to solid states at 18C, therefore attempts were made to put the pieces through a low temperature hardening process in a refrigerator at 5C, and in a freezer at -18C. Despite the success, the samples would quickly return to the elastic state after being transferred to room temperature, making the test execution unattainable. Therefore, no mechanical tests were performed with the DMSO mixture.


Fig 146 - DMSO beam samples - before


Fig 147 - DMSO beam samples - after


Fig 148 - DMSO dumbbell samples - before


Fig 149 - DMSO dumbbell samples - after

### 4.2.3.1. Tensile Test

The individual data sets for each test specimen can be found in the appendix 2. These include the "force x displacement" values and graphs, their dimensions at production and testing, a summary table with the individual properties and a graph showing their performance.

### 4.2.3.1.a. Methylcellulose

During the tensile test of the methylcellulose material, two specimens cracked at the machine setup (A1.5 and A1.6) and one presented an abnormal behaviour throughout the test (A1.2), visible on its graph, resulting on lower values for the documented properties. In order to obtain a minimum of five viable specimens and data sets from the same material to draw an effective comparison to the remaining materials, two other specimens (MC.01 and MC.02), produced from the same material batch although on a different date and with marginally different dimensions to the grip length, were included in the test. The specimens have the same gauge length and thickness on the zone subjected to the test.

The table 17 below shows the summary among all methylcellulose samples tested for a comparison. The range of values obtained is wide for all properties and a consequence of imperfections on the specimens (surface irregularities and shape deformations) due to non-standard fabrication methods and material curing behaviour. Stating an average value for the material properties would result on high deviation and imprecision. Establishing a range allows for a comparison with the other mixes and with the building industry benchmark materials.

The yield strength of the methylcellulose mix reached between 3.21 MPa and 4.06 MPa, a variation of approximately 26%. The modulus of elasticity reached between 0.33 GPa and 0.56 GPa, a variation of 67%. And the ultimate tensile strength reached between 3.37 MPa and 4.29 MPa, a variation of 27%.

| Methylcellulose Mix | | | | | | | |
|---|---|---|---|---|---|---|---|
| | Specimens | | | | | | |
| | A1.1 | A1.2 | A1.3 | A1.4 | A1.5 | A1.6 | MC.01 |
| $\sigma$ UTS Ultimate Tensile Strength [Mpa] | 3.60 | 2.94 | 4.29 | 4.07 | 0.00 | 0.00 | 3.37 |
| $\sigma$ YS Yield Strength [Mpa] | 3.51 | 2.89 | 3.79 | 4.06 | 0.00 | 0.00 | 3.21 |
| E Modulus of Elasticity [Gpa] | 0.37 | 0.25 | 0.56 | 0.45 | 0.00 | 0.00 | 0.33 |

Table 17 - Methylcellulose mix mechanical roperties - Tensile Test


Fig 150 - Methylcellulose dumbbell specimens - before


Fig 151 - Methylcellulose dumbbell specimens - after

### 4.2.3.1.b. Wood Glue

The wood glue specimens were all valid and none failed prematurely due to machine or production issues. Due to the extremely low water content, only a minimal shrinkage was observed, unlike the methylcellulose samples, resulting on overall larger specimens. Nevertheless, the gauge of each specimen, which is the tested area, had similar dimensions to all remaining samples from all different recipes.

The table 18 below shows the summary among all wood glue samples tested for a comparison. The range of values obtained is wide for all properties and a consequence of imperfections on the specimens production (surface irregularities, shape deformations and imprecise raw material mixing) due to non-standard fabrication methods. Stating an average value for the material properties would result on high deviation and imprecision. Establishing a range allows for a comparison with the other mixes and with the building industry benchmark materials.

The yield strength of the wood glue mix reached between 3.58 MPa and 4.81 MPa, a variation of approximately 34%. The modulus of elasticity reached between 0.30 GPa and 0.64 GPa, a variation of 113%. And the ultimate tensile strength reached between 6.66 MPa and 7.66 MPa, a variation of 15%.

| Wood Glue Mix | | | | | |
|---|---|---|---|---|---|
| | Specimens | | | | |
| | A3.1 | A3.2 | A3.3 | A3.4 | A3.5 |
| $\sigma_{UTS}$ Ultimate Tensile Strength [Mpa] | 6.99 | 6.69 | 7.66 | 7.04 | 6.66 |
| $\sigma_{YS}$ Yield Strength [Mpa] | 4.81 | 3.58 | 4.26 | 3.58 | 3.74 |
| E Modulus of Elasticity [Gpa] | 0.30 | 0.58 | 0.41 | 0.64 | 0.77 |

Table 18 - Wood glue mix mechanical properties - Tensile Test



Fig 152 - Wood glue dumbbell specimens - before



Fig 153 - Wood glue dumbbell specimens - after

### 4.2.3.1.c.  Acetone

The acetone specimens were all valid and none failed prematurely due to machine or production issues. However, similarly to the DMSO samples, they presented highly irregular surfaces and geometries, due to difficulties at handling the material and producing the specimens. The gauge of each specimen, although, had similar dimensions to the remaining pieces.

The table 19 below shows the summary among all acetone samples tested for a comparison. The range of values obtained is wide for all properties and possibly a consequence of the imperfections on the specimens production – inadequate moulding technique, extreme surface irregularities, shape deformations and imprecise raw material mixing, with occasional chunks of fibres – due to non-standard fabrication methods. Stating an average value for the material properties would result on high deviation and imprecision. Establishing a range allows for a comparison with the other mixes and with the building industry benchmark materials.

The yield strength of the acetone mix reached between 0.81 MPa and 1.51 MPa, a variation of approximately 86%. The modulus of elasticity reached between 0.11 GPa and 0.28 GPa, a variation of 94%. And the ultimate tensile strength reached between 0.98 MPa and 1.76 MPa, a variation of 79%.

| Acetone Mix | | | | | |
|---|---|---|---|---|---|
| | Specimens | | | | |
| | A2.1 | A2.2 | A2.3 | A2.4 | A2.5 |
| $\sigma$ UTS<br>Ultimate Tensile Strength [Mpa] | 1.76 | 1.26 | 1.70 | 1.09 | 0.98 |
| $\sigma$ YS<br>Yield Strength [Mpa] | 1.09 | 1.25 | 1.51 | 0.81 | 0.97 |
| E<br>Modulus of Elasticity [Gpa] | 0.28 | 0.11 | 0.20 | 0.13 | 0.13 |

Table 19 - Acetone mix mechanical roperties - Tensile Test



Fig 154 - Acetone dumbbell specimens - before

Fig 155 - Acetone dumbbell specimens - after

### 4.2.3.2. Flexural Test

The individual data sets for each test specimen can be found in the appendix 2. These include the "force x displacement" values and graphs, their dimensions at production and testing and a summary table with the individual properties.

### 4.2.3.2.a. Methylcellulose

During the flexural test, all specimens were viable and there were no failed iterations. Overall, their surfaces were smooth and the geometries regular, with moderate shrinkage and warping due to the curing process and the large amounts of water included in the recipe.

The table 20 below shows the summary among all methylcellulose samples tested for a comparison. The range of values obtained is wide, specially in terms of the flexural modulus, and a consequence of the uneven and warped surface of the specimens. Stating an average value for the material properties would result on high deviation and imprecision. Establishing a range allows for a comparison with the other mixes and with the building industry benchmark materials.

The flexural modulus of the methylcellulose mix reached between 0.67 GPa and 1.05 GPa, a variation of 56%. Specimen B1.2 showed an atypical value at the bottom of the spectrum, with the other samples grouped at the centre and top of the range. The flexural strength reached between 8.59 MPa and 10.85 MPa, a variation of 26% and values evenly spread in the range.

| Methylcellulose Mix | | | | | |
|---|---|---|---|---|---|
| | Specimens | | | | |
| | B1.1 | B1.2 | B1.3 | B1.4 | B1.5 |
| F<br>Failure Load [N] | 30.37 | 27.99 | 22.91 | 28.26 | 28.57 |
| $\sigma_{FS}$<br>Flexural Strength [Mpa] | 9.41 | 10.00 | 8.59 | 10.60 | 10.85 |
| E<br>Flexural Modulus [Gpa] | 0.90 | 0.67 | 0.82 | 1.02 | 1.05 |

Table 20 - Methylcellulose mix mechanical properties - Flexural Test



Fig 156 - Methylcellulose beam specimens - before

Fig 157 - Methylcellulose beam specimens - after

### 4.2.3.2.b. Wood Glue

All samples were viable and there were no failed iterations. Overall, the wood glue specimens had a smooth surface and a regular geometry. Due to the minimum amount of water content in the recipe, only a minimal shrinkage was observed, resulting on larger specimens than the remaining pieces tested. However, the testing area was the same for all samples, independent of their overall size.

The table 21 below shows the summary among all wood glue samples tested for a comparison. The range of values obtained is wide and possibly a consequence of the uneven and warped geometry of the specimens, associated to non-standard fabrication methods and irregularities in the material mixing process. Stating an average value for the material properties would result on high deviation and imprecision. Establishing a range allows for a comparison with the other mixes and with the building industry benchmark materials.

The flexural modulus of the wood glue mix reached between 0.64 GPa and 0.90 GPa, a variation of 40%. The flexural strength reached between 20.67 MPa and 28.89 MPa, a variation of 39%. Overall, the samples scored either at the lower or at the higher ends of the values spectrum for the flexural modulus and strength.

| Wood Glue Mix | | | | | |
|---|---|---|---|---|---|
| | Specimens | | | | |
| | B3.1 | B3.2 | B3.3 | B3.4 | B3.5 |
| F<br>Failure Load [N] | 122.78 | 143.36 | 173.33 | 166.05 | 158.29 |
| $\sigma$ FS<br>Flexural Strength [Mpa] | 20.67 | 23.89 | 28.89 | 27.28 | 27.06 |
| E<br>Flexural Modulus [Gpa] | 0.67 | 0.64 | 0.79 | 0.90 | 0.79 |

Table 21 - Wood glue mix mechanical roperties - Flexural Test



Fig 158 - Wood glue beam specimens - before



Fig 159 - Wood glue beam specimens - after

### 4.2.3.2.c. Acetone

All specimens were viable and there were no failed iterations. However, they presented the most irregular surfaces due to difficulties at handling the material and producing the specimens through a non-standard process. Chunks of fibres and areas with uneven thickness were found on most samples. The testing zone of each sample, although, had similar dimensions to all remaining units.

The table 22 below shows the summary among all acetone samples tested for a comparison. The range of values obtained is extremely wide and possibly a consequence of the overall irregularities of the specimens, associated to non-standard fabrication methods and to the material mixing process. Stating an average value for the material properties would result on high deviation and imprecision. Establishing a range already allows for a comparison with the other mixes and with the timber benchmark.

The flexural modulus of the acetone mix reached between 0.15 GPa and 0.37 GPa, a variation of 106%. The flexural strength reached between 4.77 MPa and 9.74 MPa, a variation of 104%. Overall, the samples scored either at the lower or at the higher ends of the spectrum for both flexural modulus and strength.

| Acetone Mix | | | | | |
|---|---|---|---|---|---|
| | Specimens | | | | |
| | B2.1 | B2.2 | B2.3 | B2.4 | B2.5 |
| **F** <br> Failure Load [N] | 61.87 | 37.16 | 61.37 | 38.48 | 30.04 |
| $\sigma$ FS <br> Flexural Strength [Mpa] | 9.37 | 6.86 | 9.74 | 5.70 | 4.77 |
| **E** <br> Flexural Modulus [Gpa] | 0.15 | 0.22 | 0.20 | 0.37 | 0.33 |

Table 22 - Acetone mix mechanical properties - Flexural Test



Fig 160 - Acetone beam specimens - before



Fig 161 - Acetone beam specimens - after

### 4.2.4. Summary of Findings

As a result from the non-standard fabrication methods – uneven mixing, inadequate moulds and irregular curing – as well as from the subtle although existing dimensional variations between specimens, the test results show a wide range of variation for all material mixes. Therefore, average values would not express a precise result, indicating strong deviations.

As expected, the results fall short from structural properties and from the values obtained by wood types typically used in the building industry, as exemplified in the table 23 below. When compared with other feedstocks with wood content already employed in additive manufacturing processes, the material mixes developed in this research still score below. However, all those options include either chemical binders – such as formaldehyde-based adhesives – or a polymer matrix such as PLA. When compared with another full bio-based material such as FLAM (Sanandiya et al., 2018), already used to extrude a column and a wind turbine component, the methylcellulose mix, showcased as the most promising outcome of this study, shows better results, attesting its potential as a new bio-based feedstock.

| MECHANICAL PROPERTIES COMPARISON | | | | |
|---|---|---|---|---|
| | FLEXURAL STRENGHT | MODULUS ELASTICITY (BENDING) | YIELD STRENGHT | MODULUS ELASTICITY (TENSION) | REFERENCE |
| BEECH, AMERICAN | - | 9.5 GPa | 86.2 MPa | - | (USDA Forest Service, 2010) |
| OAK, OVERCUP | - | 9.8 GPa | 77.9 MPa | - | (USDA Forest Service, 2010) |
| PINE, EASTERN WHITE | - | 8.5 GPa | 73.1 MPa | - | (USDA Forest Service, 2010) |
| SPRUCE, ENGELMANN | - | 8.9 GPa | 84.8 MPa | - | (USDA Forest Service, 2010) |
| PARTICLEBOARD | - | 2.8 – 4.1 GPa | 15 – 24 MPa | - | (USDA Forest Service, 2010) |
| MDF | - | 3.6 GPa | 36 MPa | - | (USDA Forest Service, 2010) |
| OSB | - | 4.4 – 6.3 GPa | 22 – 35MPa | - | (USDA Forest Service, 2010) |
| PLYWOOD | - | 7 – 8.6 GPa | 34 – 43 MPa | - | (USDA Forest Service, 2010) |
| GLULAM | - | 9 – 14.5 GPa | 29 – 63 MPa | - | (USDA Forest Service, 2010) |
| | | | | | |
| PLA + WOOD POWDER | - | 3 GPa | 30 MPa | - | (Gardner et al., 2019) |
| PLA + LIGNIN (40WT%) | - | 1.93 GPa | 29.25 MPa | - | (Tanase-Opedal et al., 2019) |
| WOOD POWDER + GLUE | - | 3 – 3.94 GPa | 30 – 57 MPa | - | (Das et al., 2021a) |
| TECNARO ARBOBLEND | - | 4.3 GPa | 58 MPa | - | (www.albis.com) |
| FLAM! | - | 0.26 GPa | 6.12 MPa | - | (Sanandiya et al., 2018) |
| | | | | | |
| METHYLCELLULOSE MIX | 8.59 – 10.60 MPa | 0.67 – 1.05 GPa | 3.21 – 4.06 MPa | 0.33 – 0.56 GPa | (own work) |
| WOOD GLUE MIX | 20.67 – 28.89 MPa | 0.64 – 0.90 GPa | 3.58 – 4.81 MPa | 0.30 – 0.77 GPa | (own work) |
| ACETONE MIX | 4.77 – 9.74 MPa | 0.15 – 0.37 GPa | 0.81 – 1.51 MPa | 0.11 – 0.20 GPa | (own work) |

Table 23 - Mechanical properties comparison

As predicted, the wood glue mix is the strongest material among the mixes tested, showing the highest values for flexural and yield strength. These are derived from the elevated adhesive content, as attested previously in the study of Kariž et al. (2016). In terms of stiffness, however, both the methylcellulose and the wood glue mixes presented similar results for their modulus of elasticity. Replacing the PVAc with a stronger formaldehyde-based adhesive would potentially increase its stiffness and enhance the mechanical properties of the wood glue mix (Kariž et al., 2016), although introducing a hazardous element to its composition.

At the other end of the spectrum, the results obtained by the acetone mix are far below the ones obtained by the methylcellulose and wood glue specimens. In general, their highest scores were still lower than the

minimum values reached by the other samples. From the broken specimens, it is possible to observe the crumbly, dry and brittle aspect of the material, not homogeneous and without a strong matrix covering the cellulosic fibres, an indication of its low performance.

The maximum modulus of elasticity reached by an elastomer is around 0.1 GPa. Between 0.1 and 1 GPa, rigid polymer foams, natural materials and polymers can be found. Ceramics, metals and composites typically present values starting at 10 GPa and above (Ashby et al., 2019).

In terms of yield strength, it is possible to find rigid polymer foams, natural materials, polymers, elastomers and ceramics between 1 and 10 MPa. Composites, such as carbon fibre reinforced polymers, and metals, such as steel, typically present values above 100 MPa, reaching close to 1000 MPa (Ashby et al., 2019).

Combining both properties, rigid polymer foams, such as rigid PU, and timber on the perpendicular direction of the fibres are the closest examples of materials with similar properties to the methylcellulose mix developed in this research. For comparison purposes, image 162 below shows a graph obtained from the Granta EduPack software with an overview of all materials available in the construction universe in the same range of properties as the methylcellulose mix.
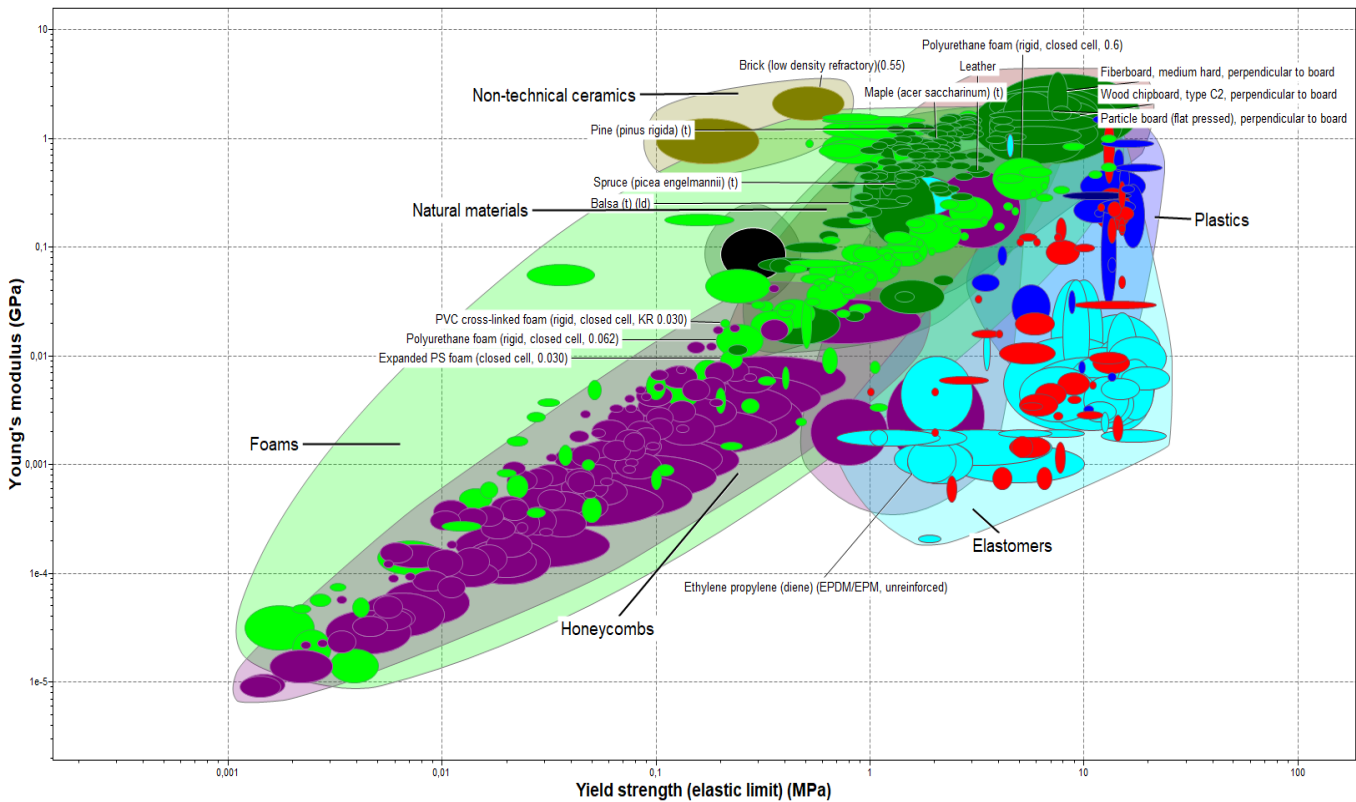


Fig 162 - Modulus of elasticity vs. yield strength graph - created with Granta EduPack 2021 software (Ashby et al., 2019)

## 4.3. Mechanical Test - Extruded Specimens

The previous material properties investigation was performed in parallel to the printability exploration, therefore the mechanical tests and the material properties documented were based on specimens produced with cut out and outline moulds. In additive manufacturing applications, variations on these results were expected due to the typical layered structure of the printed products and the fibre orientation forced by the extrusion process. Considering that this novel material was developed specifically for AM processes, additional tensile and flexural tests were necessary to assess the effect of fabrication on the material performance.

Dumbbell and beam-like specimens, with the same dimensions as the ones previously produced, were designed in Rhinoceros and adapted to generate the tool path for the robotic arm. The solid model was transformed in a continuous curve, extruded and imported into the Grasshopper script used for the slicing, simulation and control of the robotic arm.



Fig 163 - MC extruded beam specimens - before



Fig 164 - MC extruded dumbbell specimens - before



Fig 165 - MC extruded beam specimens - after



Fig 166 - MC extruded dumbbell specimens - after

Specimens had to be produced as solid elements for the execution of the tests. They were built with a total height of 6mm, divided into three layers of 2mm, the minimum feasible value considering the smallest nozzle available, with a diameter of 4mm. The tool paths were created to generate a 100% infill by allowing a constant overlapping between all curves.

The pieces were fabricated using the methylcellulose mix with the clay extruder and the 6-axis robotic arm already used for the printability exercises. They were left to cure and harden completely for a week, then sanded and prepared for testing. Due to material availability and fabrication time constraints, only five dumbbell and three beam-like specimens were produced.

The complementary mechanical tests were performed at the same laboratory formerly used for the other samples, with the same machine setup and following the same methodology, as described in chapter 4 of this report. For the tensile test, the machine speed was set to 0.005 mm/s and for the flexural test it was set to 0.02 mm/s.

All the tensile and flexural tests were successfully performed, and no samples failed prematurely. Below, the tables 24 and 25 present a summary of the test results.

| Methylcellulose Mix - EXTRUDED SPECIMENS | | | | | |
|---|---|---|---|---|---|
| | Specimens | | | | |
| | A5.1 | A5.2 | A5.3 | A5.4 | A5.5 |
| $\sigma$ UTS<br>Ultimate Tensile Strength [Mpa] | 3.14 | 3.45 | 3.23 | 2.43 | 2.64 |
| $\sigma$ YS<br>Yield Strength [Mpa] | 2.58 | 3.10 | 2.98 | 2.38 | 2.51 |
| E<br>Modulus of Elasticity [Gpa] | 0.42 | 0.46 | 0.52 | 0.44 | 0.40 |

Table 24 - Methylcellulose mix mechanical properties - Tensile Test (extruded specimens)

Similarly to the occurred in the previous tests, with the moulded specimens, the results obtained in the tensile test showed a large variation among samples, reaching a difference of approximately 30% between the lowest and highest scores observed. Therefore, to avoid high deviation and imprecision, the strategy previously applied of defining ranges of values was used. The yield strength reached values between 2.51 – 3.10 MPa and the modulus of elasticity between 0.40 – 0.52 GPa.

| Methylcellulose Mix - EXTRUDED SPECIMENS | | | |
|---|---|---|---|
| | Specimens | | |
| | B5.1 | B5.2 | B5.3 |
| F<br>Failure Load [N] | 68.77 | 62.35 | 68.51 |
| $\sigma$ FS<br>Flexural Strength [Mpa] | 9.55 | 8.48 | 9.52 |
| E<br>Flexural Modulus [Gpa] | 0.60 | 0.64 | 0.61 |

Table 25 - Methylcellulose mix mechanical properties - Flexural Test (extruded specimens)

Unlike the previous tests, with the moulded specimens, the results obtained in the flexural test showed a small variation among samples. This is a consequence of a consistent and standardised production process and less imperfections on the pieces. Even though, following the methodology applied to all previous iterations, ranges of values were defined for each parameter. The flexural strength reached values between 8.48 – 9.55 MPa, a difference of 12%, and the flexural modulus between 0.60 – 0.64 GPa, a difference of 7%.

| MECHANICAL PROPERTIES COMPARISON – MOULDED SPECIMENS vs. EXTRUDED SPECIMENS | | | | | |
|---|---|---|---|---|---|
| | FLEXURAL STRENGHT | MODULUS ELASTICITY (BENDING) | YIELD STRENGHT | MODULUS ELASTICITY (TENSION) | REFERENCE |
| METHYLCELLULOSE MIX – MOULDED | 8.59 - 10.60 MPa | 0.67 - 1.05 GPa | 3.21 - 4.06 MPa | 0.33 - 0.56 GPa | (own work) |
| METHYLCELLULOSE MIX – EXTRUDED | 8.48 - 9.55 MPa | 0.60 - 0.64 GPa | 2.38 - 3.10 MPa | 0.40 - 0.52 GPa | (own work) |

Table 26 - Methylcellulose mix mechanical properties comparison - moulded specimens vs. extruded specimens

Summarising all the mechanical properties and comparing the extruded specimens to the moulded pieces, they presented similar values for modulus of elasticity and flexural strength but lower values for yield strength, ultimate tensile stress and flexural modulus. Such inconsistency in the results can be a consequence of the squared layered structure of the extruded samples and the irregularities created by shrinkage during the curing process. Gaps, depressions and detaching between layers affected the overall strength of the pieces. The gaps encountered between the gauge and the grip of the dumbbell samples, as illustrated below, also created a weak point and potentially led to an early rupture during the test.

# 4.4. Water Absorption Test

### 4.4.1. Planning & Preparation

#### 4.4.1.1. Test Design

The water absorption test was based on the ISO 62 (ISO, 2008) standards used for plastics and adjusted to the material limitations. The test samples were reduced and simplified to a 1/3 section of a beam-type specimen. They were prepared and dried for a week at room temperature and were not desaturated in the oven. And lastly, the entire specimens were submerged in water instead of one face only.

This test was also designed to allow for the exploration of pertinent material properties for their use in the building industry. In parallel to the pure material samples, two additional sets of specimens for each mix were tested with different coatings to draw a comparison and validate their water repellent potential.

#### 4.4.1.2. Outcome

Two results were expected from this test. Firstly, the material tendency to absorb water and at which ratio it does, drawing a comparison among the four mixes and timber and determining the potential and challenges for their outdoor use. Secondly, the validation or not of the water repellent potential of both bee wax and linseed oil as coatings, determining how much a coating interferes on the water absorption in terms of absolute values and ratios.

#### 4.4.1.3. Location

The water absorption test was executed at LAMA in the Faculty of Architecture and the Built Environment of TU Delft. The room temperature oscillated between 20C and 23C and the relative humidity remained at 40% – all measured with an Arduino kit connected to a DHT11 digital temperature and humidity sensor.

#### 4.4.1.4. Equipment

No specific equipment is necessary for this test. A precision scale was used to weigh all specimens at the start and at the end of the test. For the water saturation, paper cups were used as individual containers for each specimen.

#### 4.4.1.5. Test Specimen

The specimens determined by the ISO-62 (ISO, 2008) and NEN-EN-ISO-294 (CEN, 2018a) standards – hollow squared geometries – were not feasible to produce due to the nature of the materials, current development status and the available fabrication methods. Monolithic structures were also not feasible due to the extended curing period necessary. As an alternative solution, the same beam-type design used for the flexural test was selected.

Three specimens from each material were produced, with one additional piece as contingency. All samples used in all tests were fabricated at once and followed the process formerly described.


Fig 167 - Test specimens - no coating


Fig 168 - Test specimens - linseed oil coating


Fig 169 - Test specimens - beeswax coating

### 4.4.2. Test Execution

Each specimen was divided in three equal parts approximately. Two parts were evenly covered with the selected coatings – linseed oil and bee wax – and one was kept without any additives. After a 72h curing time, all parts were weighed, documented and submerged in water in individual vessels. After a period of 24h, all specimens were removed from water and once again weighed and documented. Such process was repeated twice again, after 1h and 3h, to evaluate the water retention of each sample.


Fig 170 - Test preparation - specimens placement


Fig 171 - Test commencement - specimens in water at 0h


Fig 172 - Test conclusion - specimens in water at 24h

## 4.4.3. Results

Among the specimens with no coating, the methylcellulose mix presented the highest rate of water absorption with approximately 134% of its original weight in average, meanwhile the wood glue ones had the lowest, with approximately 10%. In terms of water retention, after 3h the methylcellulose samples still contained almost half of the liquid absorbed, meanwhile the acetone mix samples had lost almost all.

| No Coating - Pure Material | | | | | | | | | | | | | | |
|---|---|---|---|---|---|---|---|---|---|---|---|---|---|---|
| | | Weight (g) | | | | Water Absorption | | | Water Retention (after 1h) | | | Water Retention (after 3h) | | |
| | | Initial | After 24h | After 1h | After 3h | Quantity (g) | Weight Ratio | Average | Quantity (g) | Weight Ratio | Average | Quantity (g) | Weight Ratio | Average |
| Methylcellulose | C1.1 | 2.00 | 4.90 | 4.40 | 3.22 | 2.90 | 145.00% | | 2.40 | 120.00% | | 1.22 | 61.00% | |
| | C1.2 | 2.41 | 5.45 | 4.99 | 3.87 | 3.04 | 126.14% | 134.91% | 2.58 | 107.05% | 114.22% | 1.46 | 60.58% | 58.79% |
| | C1.3 | 2.50 | 5.84 | 5.39 | 3.87 | 3.34 | 133.60% | | 2.89 | 115.60% | | 1.37 | 54.80% | |
| Wood Glue | C2.1 | 6.50 | 7.15 | 6.96 | 6.81 | 0.65 | 10.00% | | 0.46 | 7.08% | | 0.31 | 4.77% | |
| | C2.2 | 5.78 | 6.37 | 6.21 | 6.06 | 0.59 | 10.21% | 10.35% | 0.43 | 7.44% | 7.33% | 0.28 | 4.84% | 4.82% |
| | C2.3 | 5.35 | 5.93 | 5.75 | 5.61 | 0.58 | 10.84% | | 0.40 | 7.48% | | 0.26 | 4.86% | |
| Acetone | C3.1 | 3.46 | 4.34 | 4.13 | 3.48 | 0.88 | 25.43% | | 0.67 | 19.36% | | 0.02 | 0.58% | |
| | C3.2 | 5.38 | 6.66 | 6.39 | 5.55 | 1.28 | 23.79% | 24.62% | 1.01 | 18.77% | 19.31% | 0.17 | 3.16% | 2.16% |
| | C3.3 | 6.21 | 7.74 | 7.44 | 6.38 | 1.53 | 24.64% | | 1.23 | 19.81% | | 0.17 | 2.74% | |
| DMSO | C4.1 | 4.37 | 5.54 | 5.34 | 4.43 | 1.17 | 26.77% | | 0.97 | 22.20% | | 0.06 | 1.37% | |
| | C4.2 | 6.58 | 8.55 | 8.26 | 7.36 | 1.97 | 29.94% | 28.23% | 1.68 | 25.53% | 23.82% | 0.78 | 11.85% | 7.12% |
| | C4.3 | 5.90 | 7.55 | 7.30 | 6.38 | 1.65 | 27.97% | | 1.40 | 23.73% | | 0.48 | 8.14% | |

Table 27 - Water absorption summary - no coating

Among the specimens with a bee wax coating, the methylcellulose mix presented the highest rate of water absorption with approximately 69% of its original weight in average, meanwhile the wood glue ones had the lowest, with approximately 3.60% only. In terms of water retention, after 3h the methylcellulose samples still had around 2/3 of the liquid originally absorbed, meanwhile the acetone and the wood glue ones had retained only approximately 1/3 of the total absorbed.

| Bee Wax Coating | | | | | | | | | | | | | | |
|---|---|---|---|---|---|---|---|---|---|---|---|---|---|---|
| | | Weight (g) | | | | Water Absorption | | | Water Retention (after 1h) | | | Water Retention (after 3h) | | |
| | | Initial | After 24h | After 1h | After 3h | Quantity (g) | Weight Ratio | Average | Quantity (g) | Weight Ratio | Average | Quantity (g) | Weight Ratio | Average |
| Methylcellulose | C1.4 | 4.69 | 7.89 | 7.68 | 7.01 | 3.20 | 68.23% | | 2.99 | 63.75% | | 2.32 | 49.47% | |
| | C1.5 | 3.00 | 5.05 | 4.89 | 4.34 | 2.05 | 68.33% | 69.61% | 1.89 | 63.00% | 64.40% | 1.34 | 44.67% | 46.75% |
| | C1.6 | 3.10 | 5.34 | 5.16 | 4.53 | 2.24 | 72.26% | | 2.06 | 66.45% | | 1.43 | 46.13% | |
| Wood Glue | C2.4 | 7.14 | 7.47 | 7.31 | 7.25 | 0.33 | 4.62% | | 0.17 | 2.38% | | 0.11 | 1.54% | |
| | C2.5 | 6.53 | 6.71 | 6.59 | 6.57 | 0.18 | 2.76% | 3.60% | 0.06 | 0.92% | 1.41% | 0.04 | 0.61% | 0.98% |
| | C2.6 | 7.59 | 7.85 | 7.66 | 7.65 | 0.26 | 3.43% | | 0.07 | 0.92% | | 0.06 | 0.79% | |
| Acetone | C3.4 | 6.28 | 7.61 | 7.38 | 6.68 | 1.33 | 21.18% | | 1.10 | 17.52% | | 0.40 | 6.37% | |
| | C3.5 | 5.55 | 6.66 | 6.55 | 6.02 | 1.11 | 20.00% | 20.35% | 1.00 | 18.02% | 17.52% | 0.47 | 8.47% | 7.13% |
| | C3.6 | 5.64 | 6.76 | 6.60 | 6.01 | 1.12 | 19.86% | | 0.96 | 17.02% | | 0.37 | 6.56% | |
| DMSO | C4.4 | 6.99 | 7.82 | 7.60 | 7.47 | 0.83 | 11.87% | | 0.61 | 8.73% | | 0.48 | 6.87% | |
| | C4.5 | 7.34 | 8.22 | 8.01 | 7.86 | 0.88 | 11.99% | 10.44% | 0.67 | 9.13% | 7.83% | 0.52 | 7.08% | 6.15% |
| | C4.6 | 7.10 | 7.63 | 7.50 | 7.42 | 0.53 | 7.46% | | 0.40 | 5.63% | | 0.32 | 4.51% | |

Table 28 - Water absorption summary - beeswax coating

Among the specimens with a linseed oil coating, the methylcellulose mix presented the highest rate of water absorption with approximately 70% of its original weight in average, meanwhile the wood glue ones had the lowest, with approximately 8%. In terms or water retention, after 3h the methylcellulose samples still had the highest water ratio among all samples, although the wood glue ones retained more, approximately half of the absorbed liquid, meanwhile the acetone samples retained approximately only 1/5 of the total absorbed.

| Linseed Oil Coating | | | | | | | | | | | | | | |
|---|---|---|---|---|---|---|---|---|---|---|---|---|---|---|
| | | Weight (g) | | | | Water Absorption | | | Water Retention (after 1h) | | | Water Retention (after 3h) | | |
| | | Initial | After 24h | After 1h | After 3h | Quantity (g) | Weight Ratio | Average | Quantity (g) | Weight Ratio | Average | Quantity (g) | Weight Ratio | Average |
| Methylcellulose | C1.7 | 2.43 | 4.42 | 4.05 | 3.24 | 1.99 | 81.89% | | 1.62 | 66.67% | | 0.81 | 33.33% | |
| | C1.8 | 3.14 | 5.20 | 4.86 | 4.07 | 2.06 | 65.61% | 70.89% | 1.72 | 54.78% | 58.64% | 0.93 | 29.62% | 30.52% |
| | C1.9 | 2.90 | 4.79 | 4.48 | 3.73 | 1.89 | 65.17% | | 1.58 | 54.48% | | 0.83 | 28.62% | |
| Wood Glue | C2.7 | 5.39 | 5.81 | 5.69 | 5.60 | 0.42 | 7.79% | | 0.30 | 5.57% | | 0.21 | 3.90% | |
| | C2.8 | 5.69 | 6.21 | 6.05 | 5.94 | 0.52 | 9.14% | 8.27% | 0.36 | 6.33% | 5.73% | 0.25 | 4.39% | 3.91% |
| | C2.9 | 6.97 | 7.52 | 7.34 | 7.21 | 0.55 | 7.89% | | 0.37 | 5.31% | | 0.24 | 3.44% | |
| Acetone | C3.7 | 3.40 | 4.19 | 3.92 | 3.53 | 0.79 | 23.24% | | 0.52 | 15.29% | | 0.13 | 3.82% | |
| | C3.8 | 4.60 | 5.69 | 5.40 | 4.81 | 1.09 | 23.70% | 20.74% | 0.80 | 17.39% | 14.57% | 0.21 | 4.57% | 3.48% |
| | C3.9 | 5.89 | 6.79 | 6.54 | 6.01 | 0.90 | 15.28% | | 0.65 | 11.04% | | 0.12 | 2.04% | |
| DMSO | C4.7 | 5.12 | 6.63 | 6.38 | 5.79 | 1.51 | 29.49% | | 1.26 | 24.61% | | 0.67 | 13.09% | |
| | C4.8 | 5.21 | 6.90 | 6.67 | 6.20 | 1.69 | 32.44% | 30.80% | 1.46 | 28.02% | 26.06% | 0.99 | 19.00% | 14.85% |
| | C4.9 | 4.89 | 6.38 | 6.14 | 5.50 | 1.49 | 30.47% | | 1.25 | 25.56% | | 0.61 | 12.47% | |

Table 29 - Water absorption summary - linseed oil coating

### 4.4.4. Summary of Findings

As expected due to the hydrophilic behaviour of cellulose, all material mixes are prone to water absorption to a certain extent, and require a protective layer to avoid degradation, similar to wood. Regarding the coatings, linseed oil had less impact on the aesthetics of the material and resulted on a uniform thin coverage, meanwhile bee wax created a light yellow opaque layer, thick and uneven, affected by surface imperfections.

Methylcellulose was the less dense material observed, with its samples floating in the water containers. In terms of water absorption, it performed poorly, explained by its porosity and by the hydrophilic properties of both methylcellulose and cellulose. Specimens did not degrade, although there was a marginal change of colour in the water, implying part of the material being dissolved in it. A great difference was observed between the pure material and the samples with a protective coating, validating the importance of a water resistant layer on future applications.

Wood glue was the denser material observed, instantly submerging in the water. In terms of absorption, it showed the best performance in all tests, despite the porosity identified in its cross section. The smoother surface, with less porous, collaborates to the behaviour observed.

Acetone showed constant results among all tests in terms of water absorption, not being significantly affected by any coatings. Specimens also did not retain the liquid absorbed, unlike the methylcellulose ones, consistently losing most of it after 3 hours drying.



Fig 173 - Test conclusion - specimens after 3h drying

# 4.5. Microscope Analysis

### 4.5.1. Analysis Overview

The analysis of the material samples through the microscope was designed to investigate the homogeneity, porosity and the fibre behaviour – coating, length and direction – through observation. During the material exploration phase, part of these properties were visually assessed, superficially, through photographs taken with macro-lenses. Enhanced images allowed for a validation of these preliminary observations.

Matrix homogeneity and the fibre coating and concentration are the most relevant data collected through the amplified photographs.

### 4.5.2. Planning & Preparation

#### 4.5.2.1. Location

The microscope analysis was performed at the Faculty of Architecture and the Built Environment of TU Delft through a collaboration with the master students from the recycled glass group led by Telesilla Bristogianni.

#### 4.5.2.2. Equipment

For all the analysis it was used a digital microscope from Keyence, model VHX-7000N, with a 20x to 200x lens.

#### 4.5.2.3. Analysis Execution

A beam-type specimen from each mix, produced as contingency for the mechanical and water tests, was used for the analysis. Three samples were prepared for each material – a large portion of the surface, a cross section and a partial longitudinal section. For the homogeneity and porosity, the surface and cross section were examined. For the fibre behaviour, the cross section and longitudinal section were analysed and compared in terms of thread length and direction.

At each iteration, images were generated with the minimum and maximum magnification – 20x and 200x – for a general view at first and to capture the highest level of details at last. An intermediate scale between 70x and 120x was also used for an overall understanding of specific zones.

### 4.5.3. Summary of Findings

### 4.5.3.1. Methylcellulose

### 4.5.3.1.a. Homogeneity

The cross section images showed the highest homogeneity among the four samples analysed, with evenly distributed fibres in a homogeneous matrix. No patches with different colours were identified and no different zones across the sample cross section, only few spots on the surface with exposed fibres with scarce coating.

### 4.5.3.1.b. Porosity

Cross section images showed a material with low density and high porosity, highlighted by the contrast between the surface and the pores depth, the holes and depressions on the surface.

### 4.5.3.1.c. Fibres

Images showed fibres with an overall strong and homogeneous lignin coating, with a few exceptions spotted with brighter colour on the surface. Organisation was irregular and no predominant direction was identified, despite attempts to direct them using a rolling pin during fabrication. The documented fibre length on the sample was 1.2mm, placing it just above acetone as the second best sample in terms of fibre length.
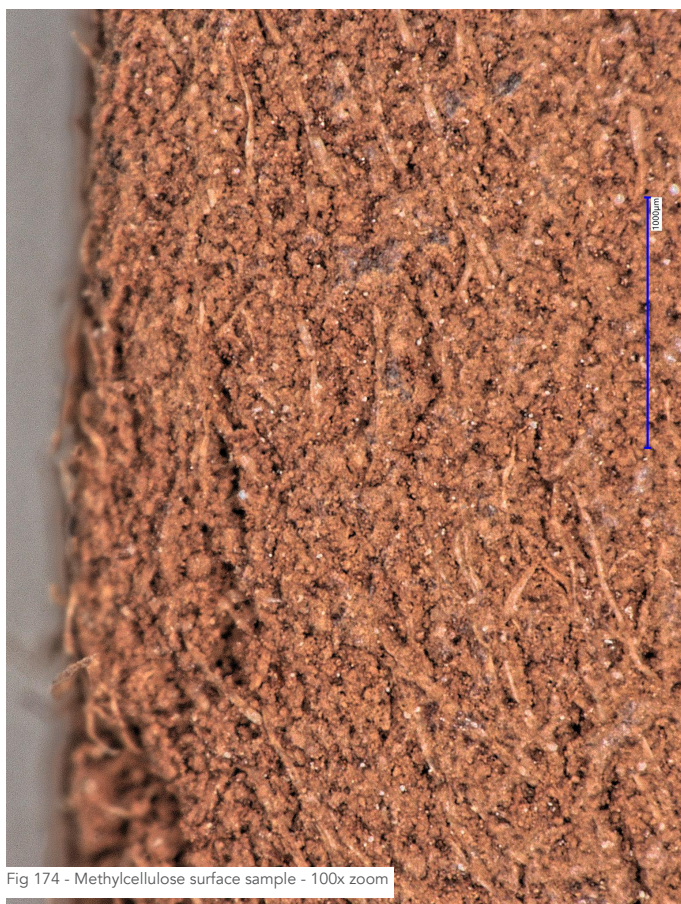


Fig 174 - Methylcellulose surface sample - 100x zoom

Fig 175 - Methylcellulose cross section sample - 200x zoom

### 4.5.3.2.  Wood Glue

### 4.5.3.2.a.  Homogeneity

The cross section images showed the material was not homogeneous overall, with different colour patches indicating zones where the matrix had different concentrations of lignin. As an educated guess, the higher density of the wood glue interfered on the curing process, leading to a separation between a top zone, richer in lignin and fibres, and a heavier matrix at the bottom, with lower concentration of fibres and higher concentration of adhesive.

### 4.5.3.2.b.  Porosity

Surface images showed a high degree of imperfections on the material surface. The cross section showed a denser material than acetone and DMSO, although pores, depressions and holes could still be identified through a depth analysis of the high resolution imagery.

### 4.5.3.2.c.  Fibres

The images showed the fibres with a white colour overall, indicating a scarce lignin coating, with a few exceptions on the surface. Organisation was irregular and no predominant direction was identified, despite an attempt to direct the fibres during the sample fabrication with the rolling pin. Fibre length documented was shorter when compared to acetone and DMSO, ranging from 0.4 to 0.8mm.



Fig 176 - Wood glue surface sample - 50x zoom
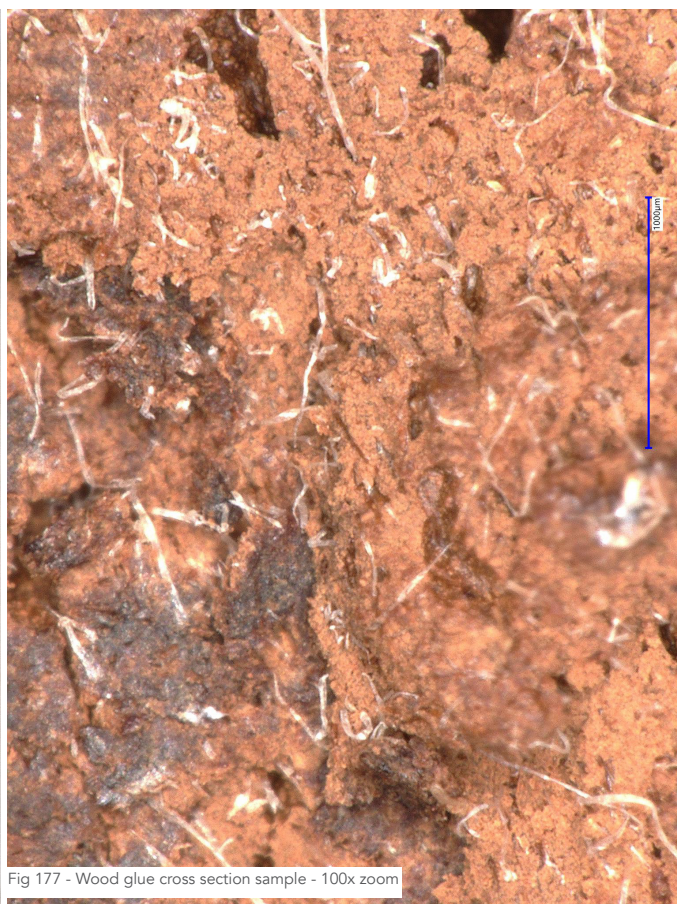
Fig 177 - Wood glue cross section sample - 100x zoom

### 4.5.3.3.  Acetone

### 4.5.3.3.a.  Homogeneity

The images from the material surface and cross section showed the material was not homogeneous, with different colour patches indicating zones where the polymer matrix was stronger – dark brown and black colour – and the fibre concentration was smaller, and zones where the quantity of fibres was higher and the matrix was weaker – brown colour – with lower concentration of acetone due to hardening or faulty mixing.

### 4.5.3.3.b.  Porosity

The cross section images showed a high degree of porosity and low density, attested with the high contrast images highlighting the depth of the pores and the flaws and depressions on the surface.

### 4.5.3.3.c.  Fibres

The cross section images showed the cellulose fibres with a homogeneous and continuous lignin coating. Nevertheless, ethere was no predominant direction and the fibre organisation was irregular despite an attempt to direct the fibres during the sample fabrication with a spatula. The overall fibre length was shorter than 1mm, ranging from 0.6mm to 1.14mm on the sample documented, despite the long chains of fibres observed at mixing and moulding the test specimens.
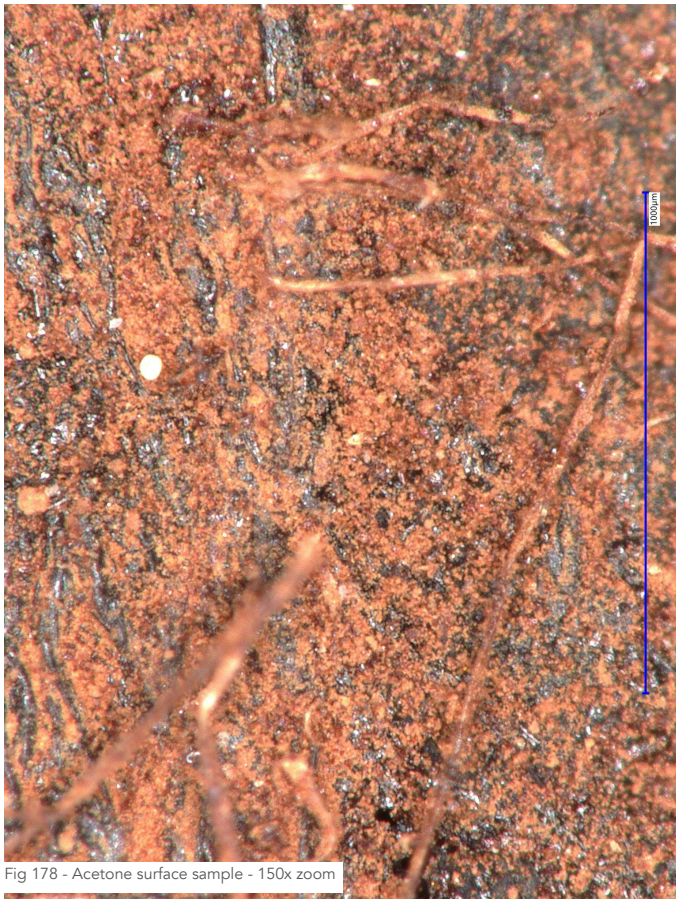


Fig 178 - Acetone surface sample - 150x zoom

Fig 179 - Acetone cross section sample - 200x zoom

### 4.5.3.4. Dimethylsulfoxide (DMSO)

#### 4.5.3.4.a. Homogeneity

The images from the surface and cross section showed a material more homogeneous than the acetone mix, with a uniform pattern and colour throughout the images. Nevertheless, spots with a light brown colour in the cross section and patches with brown colour on the surface pointed to zones with different concentration of lignin in the matrix.

#### 4.5.3.4.b. Porosity

The dark and glossy colour of the sample hindered the visualisation of pores and depressions on the material surface. Density wase higher and porosity lower when compared to the acetone mix, with a rough albeit smoother surface.

#### 4.5.3.4.c. Fibres

Overall the images showed fibres with a strong homogeneous and continuous coating with the lignin matrix. Nevertheless, on the surface a few fibres with lighter colour indicating a weaker coverage could be found. Organisation was irregular and no predominant direction could be identified, despite the attempt to direct the fibres during the sample fabrication with a spatula. Fibres formed longer chains when compared to the remaining samples, reaching 1.7mm on the specimen documented.



Fig 180 - DMSO surface sample - 20x zoom

Fig 181 - DMSO cross section sample - 100x zoom
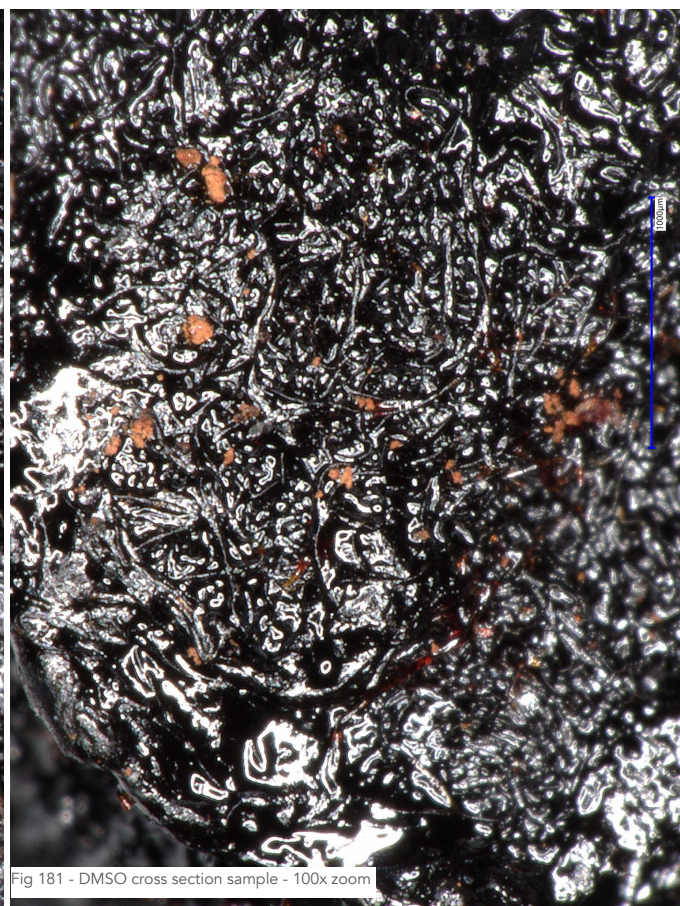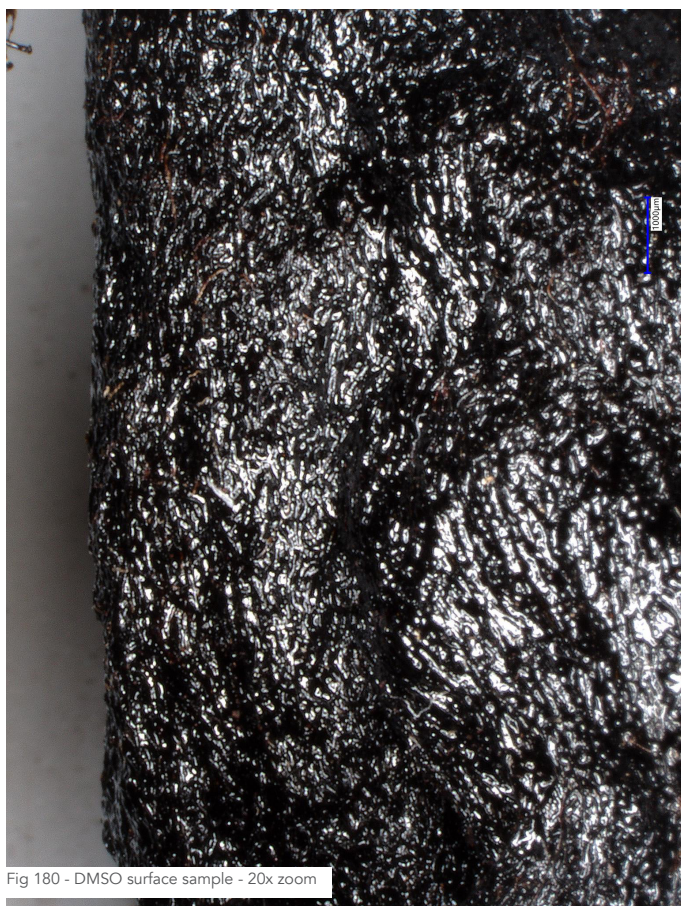
# 4.6. Conclusion

In terms of the mechanical properties investigation, the results are the initial step towards the characterisation of these innovative materials, and a fundamental approach towards objective improvements. From the start, no structural values were expected due to the novel nature of the material, the literature research and the initial assessments. Nevertheless, the proximity to the results obtained by the only other full bio-based material identified in the background research – FLAM (Sanandiya et al., 2018) – is a great outcome and attests the potential in the fabrication of architectural elements. The material developed by SUTD has already been used to fabricate a column and a wind turbine, an indication that the methylcellulose mix, with better mechanical performance, could also be used for similar applications.

The challenges posed here for an immediate use of this material in the building industry are the low values for the modulus of elasticity and for the tensile and flexural strength. Target values are the ones showcased by the different types of timber, and could be achieved through a higher fibre concentration, lower water content and a denser matrix, paving the way for a future line of research.

In terms of the water absorption study, the results showed an already expected hydrophilic behaviour from the material due to its wood-sourced components. The methylcellulose mix was also expected to perform poorly due to its anticipated porosity and the water soluble binder. Nonetheless, the low water retention was a positive result, meaning that the dissolution and loss of the original shape is unlikely.

The necessity of a water repellent layer has been implied from the start, based on the same requirement for timber elements. The choice of material is the challenge to be approached since the majority of the veneers available for wood are chemically-based. Beeswax alters the aesthetics, therefore linseed oil would be a better option. The validation of this coating and the search for other bio-based alternatives with better performance are also part of the future researches to be developed.

In terms of understanding the mixes and validating initial observations from the material exploration phase, the microscope images offered an insight in the material morphology. Methylcellulose proved to be the most homogeneous, with a consolidated matrix and an even distribution of fibres throughout its cross section, uniformly coated with lignin, validating the initial assessment.

The challenges that rise from this analysis relate to the concentration and the orientation of the fibres. More fibres could improve the poor mechanical properties, however it could excessively dry the material and form chunks. A predominant direction and longer threads could have positive effect as well, although it might raise printability issues and it should be along the tensile stress direction to be efficient. These are considerations for the upcoming design and prototyping phase and for future researches and investigations.

# 5. Design & Prototyping

# 5.1. Overview

In the previous chapters, the development and testing of a novel material for additive manufacturing based on cellulose and lignin was documented. Its printability was explored and the challenges and limitations of its use were analysed, showing great potential as a feedstock for LDM fabrication. The homogeneity and viscosity observed are similar to the clay commonly used in such processes, resulting in smooth extrusions and products. The high adhesion capability presented results in a strong interlayer bonding, forming stable structures. Above all, its recipe achieved a full bio-based content and its raw components are sourced from waste material from the wood, paper and construction industries, a relevant feature in the advancement of a carbon neutral building industry.

Nevertheless, its mechanical properties are still poor and, in the tensile and flexural tests performed, the results obtained are a strong limitation to its use in the fabrication of structural components. For comparison purposes, in terms of yield strength and modulus of elasticity, the methylcellulose mix behaves similarly to rigid polymer foams, commonly used as insulation and other non-structural applications, and low strength wood in the perpendicular direction of the fibres.

These findings hinder the possibility of using this material in the fabrication of a functional structural node at its current stage of development. However, they do not eliminate its potential. Additional research and improvements are detrimental to its use for any applications in the building industry. Fibres, additives and adjustments to the fabrication process are some of the directions for future studies and investigations towards the ultimate goal of creating a strong and stiff bio-based material for structural applications.

Therefore, designing and producing a simple prototype of a structural node without first exploring possible improvements to the material would not have a strong value to this research.

The first step for a relevant result for this research out of this phase was to enhance the material properties to allow for higher and stronger prints to be produced. An additive – bentonite – and a reinforcement with long fibres – flax – were explored and added to the mix, testing the limits of the extruder with drier, denser and more viscous pastes.

With a potentially improved material, a simplified design for a structural node was developed and used as a case study to produce a prototype. No additional mechanical tests were performed, but the printability of the new mix, the limits of the equipment and the capability in fabricating higher and more stable structures were attested.

# 5.2. Material Enhancement

### 5.2.1. Planning & Preparation

The material properties documented for the methylcellulose mix were at the top of the spectrum among all the material mixes tested. However, they were still low when compared to standard types of timber commonly used in the building industry. Therefore, three directions were established towards the enhancement of the material. First attempt was to incorporate an additive to the mix, making it denser

and stronger, accelerating the hardening process and increasing its stiffness. The second attempt was to add a natural fibre reinforcement with long threads – length above 10mm. The third and final attempt was to combine both and test the limits of the extruder and the potential of the material at successfully producing geometries previously not feasible.

Bentonite was selected as the additive to be included in the mix, based on the testimonials and recipe developed at Umea School of Architecture, Sweden. The research developed by Peeters et al. (2019) described the experience with the development of a wood-based mix with methylcellulose as a binding agent and bentonite as an additive. Bentonite is a non-toxic type of clay from volcanic ashes, typically found in the United States (IMA-NA, 2022). Mixed with cement in small quantities, it increases the material viscosity and improves its extrudability in additive manufacturing process (Chen et al., 2020).

As fibre reinforcement, flax was chosen due to its popular use in natural-fibre reinforced composites, availability and thin and lightweight aspects, combined with high strength and stiffness (Ahmad et al., 2015). In additive manufacturing, its potential has already been attested when blended with a thermoplastic matrix such as PLA in the production of filaments (Tonk, 2020).

Bentonite was procured through an online shop specialised in artistic supplies through the online portal amazon.nl. Flax was obtained from EasyComposites, a specialised supplier of natural fibres and raw materials for composites. The material preparation was once again performed at LAMA and followed the same procedures and methodology applied during the material exploration phase, described in detail in chapter 2 of this report.


Fig 182 - Flax fibre sheet


Fig 183 - Bentonite clay powder


Fig 184 - Material mix with benotnite & flax

### 5.2.2. Execution

A batch of the methylcellulose mix previously prepared, sufficient for one cartridge, was used for the first iteration. A ratio of 1:5 of bentonite to methylcellulose was added directly to the material paste and thoroughly mixed by hand and with an electric mixer until it reached a homogeneous state. The result was a denser and drier paste, requiring an additional, although marginal, amount of water to achieve a similar consistency to the original recipe and established as the optimal for extrusion.

The second iteration was also based on an existing batch of methylcellulose mix. A ratio of 1:5 of flax to cellulose was added directly to the material paste and thoroughly mixed by hand and with an electric mixer. The fibres were cut with a length of approximately 10mm and, before being combined with the paste, blended alone in a recipient to separate the threads and avoid clusters and clots. Despite being more difficult to mix than the bentonite powder, the result was also a homogeneous paste, denser and drier than the original mix. No additional water was required to maintain the original viscosity and consistency.

For the final iteration, a new batch of material was prepared from scratch to incorporate both bentonite and flax into the recipe. The original recipe and procedure were followed, combining the clay powder at the beginning of the process, together with the lignin and methylcellulose, and the flax at the end of the process, just before the paste reached its optimal consistency. As expected, a higher amount of water was necessary to control the viscosity of the material and avoid it to crumble and lose its adhesion properties.

The three new material batches were allowed to cool down and rest for 24 hours before its extrudability could be assessed. No additional mechanical tests were planned, and instead a simplified prototype of a structural node was developed to be fabricated with the three mixes and compared, highlighting the potential of the material, the challenges and the direction towards future research and additional improvements.

### 5.2.3. Results

In terms of appearance, consistency, viscosity and homogeneity, the three variations of the methylcellulose mix produced were similar, and resembled the original mix previously developed.

The mixes containing bentonite are marginally drier, although viscous and suitable for extrusion. Adhesion increased, both to the surfaces and between layers, improving the stability of multi-layered structures. They also showed more resistance to pressure when touched and manipulated in comparison to the original methylcellulose-only mix.

The mixes containing flax also retained the viscosity and consistency from the original material. The fibre reinforcement, although in small quantities, was clearly observed, with the formation of long chains with threads fully covered by the material matrix and with a remarkable potential for directional orientation through the extrusion process.

The mechanical properties of this enhanced material will not be assessed at this stage. Strength and stiffness of the three iterations are expected to be higher when compared to the original recipe. The recipe containing both bentonite and flax showed the highest potential as an enhanced version of the methylcellulose mix since it combines the improved stiffness from the bentonite with the improved strength from the flax fibres.

# 5.3. Design

### 5.3.1. Planning & Preparation

A structural node as a design problem offers a wide range of approaches. Starting from the principle that this exercise aims at showing a combined proof of concept of a novel material and fabrication process, the prototype must be a simple shape pushing the limits of the printing parameters.

The scope of design is a node with three branches for a fictional free-form structure, with no case load applied to it. Details for (rain)water drainage, installation of panels, sealants and weatherproofing were disregarded.

The initial design had three variations and it was intended to explore different types of infill and the overhang limits of both material and fabrication. The prototypes were planned on a 1:1 scale, with branches with a 50x100mm (w*h) cross section and a length of 100mm.

The first iteration was a flat node with the same angle between branches. The tall and straight walls would require either a 100% infill or double-line walls and a grid-type infill, potentially built with curved lines to enhance stability. The second iteration was a spatial node with a flat top and the same angle between branches on its lateral elevation. Nozzle width and infill properties would follow the parameters used for the previous prints, and the challenge to be overcome would be the overhang limitations from the material. The final variation was a revised version of the first design, however with curved lines and surfaces, simulating a topological optimisation. The non-linear walls would collaborate in creating a stable and smooth structure.



Fig 185 - Structural node initial design - iteration 1



Fig 186 - Structural node initial design - iteration 2



Fig 187 - Structural node initial design - iteration 3

Based on the limitations observed on the material extrusion during the printability phase, however, the design originally developed for the prototype had to be adjusted and re-worked.

Linear and straight walls showed a lack of stability in general and a reduced infill was not sufficient to avoid buckling, even with a zig-zag design. Overhangs, even with curved walls, were also proven to not have stability without a solid infill or thick double-line walls.

### 5.3.2. Results

Starting from the constraints described above, a linear outline and a material optimisation with a reduced infill were eliminated. The rectilinear and traditional design, as initially proposed, was replaced by a new version with predominantly curved lines and a minimum although frequent overlapping to ensure stability and reduce buckling.

The design is still simple, and follows the same dimensions initially proposed. It is composed by three branches with a length of 100mm and a cross section of 50x100mm (w*h). It is formed by a continuous curvilinear zig-zag, populated with multiple overlapping points, and vertically extruded.

Taking advantage of the required curvilinear design for stability, an indent was created on the face of the three branches to allow for an interlocking connection with the adjacent structural members.

outline & no infill        outline & curvilinear infill        no outline & curvilinear infill
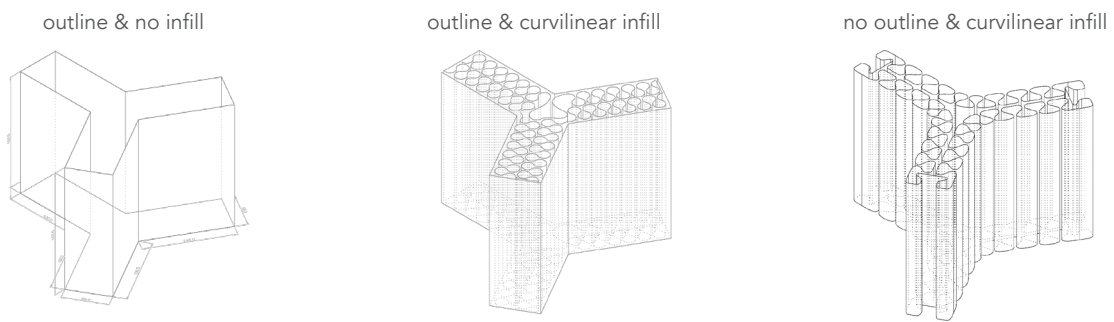


Fig 188 - Structural node design evolution
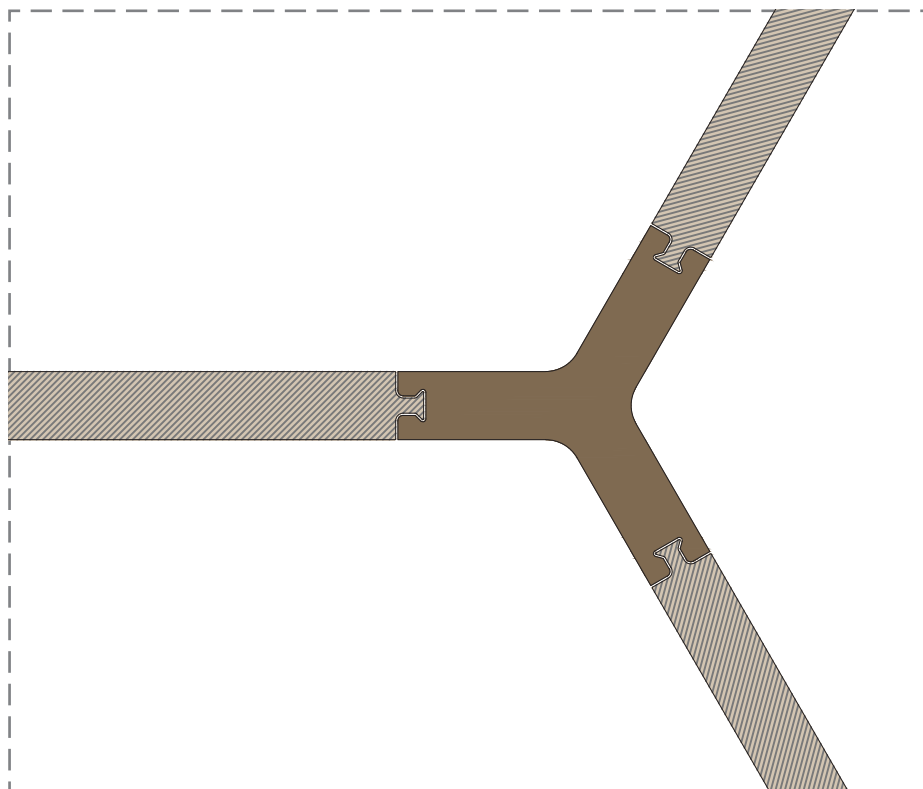


Fig 189 - Structural node concept design - top view (scale 1:5)

121

simulation of the expected outcome from extrusion following the tool path

interlocking to structural element

timber structural element
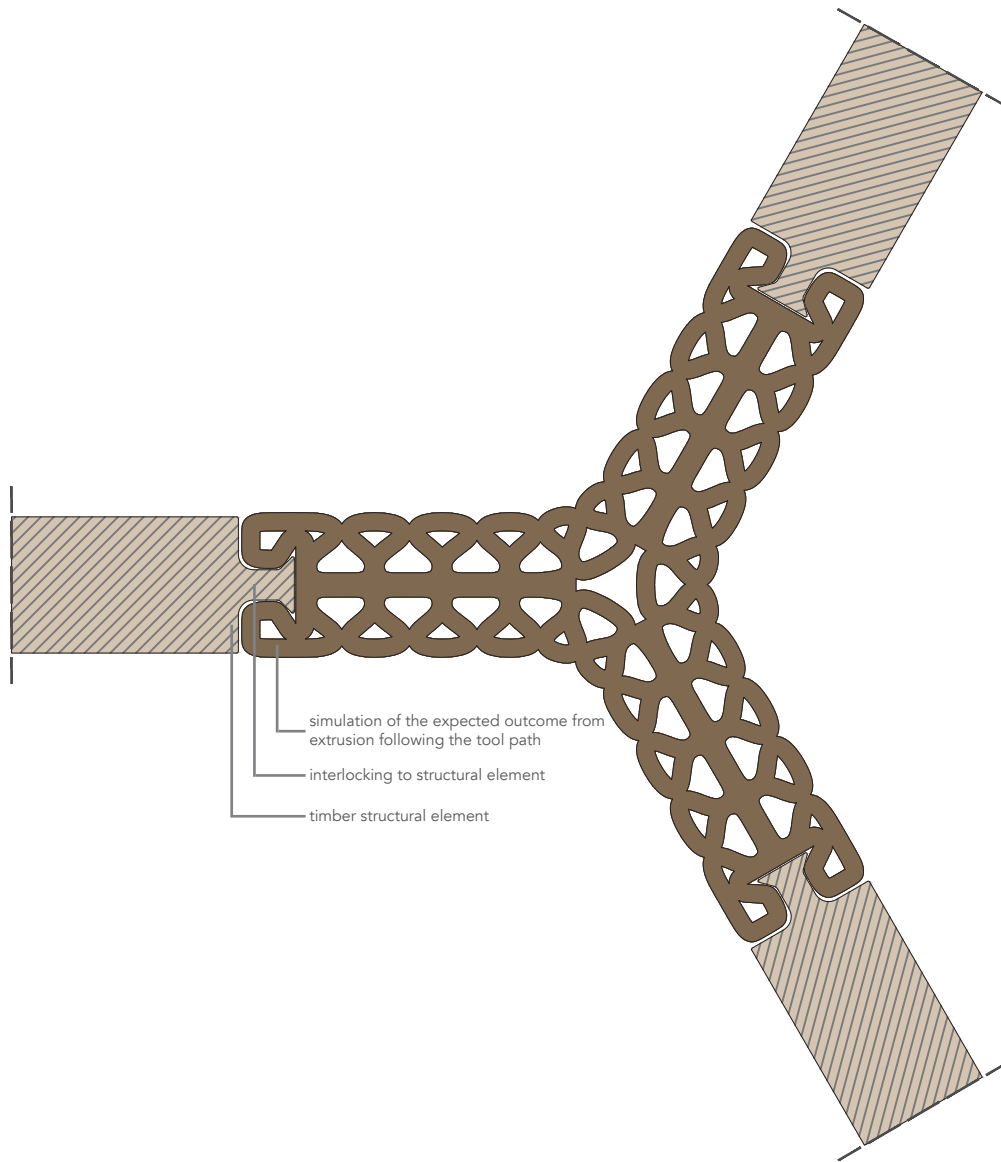
Fig 190 - Structural node design for fabrication - top view (scale 1:5)



100.00

100.00

100.00

100.00

50.00

50.00

100.00

100.00

120°  120°
120°  120°

DET 1

tool path

final product estimated boundaries

extrusion start point
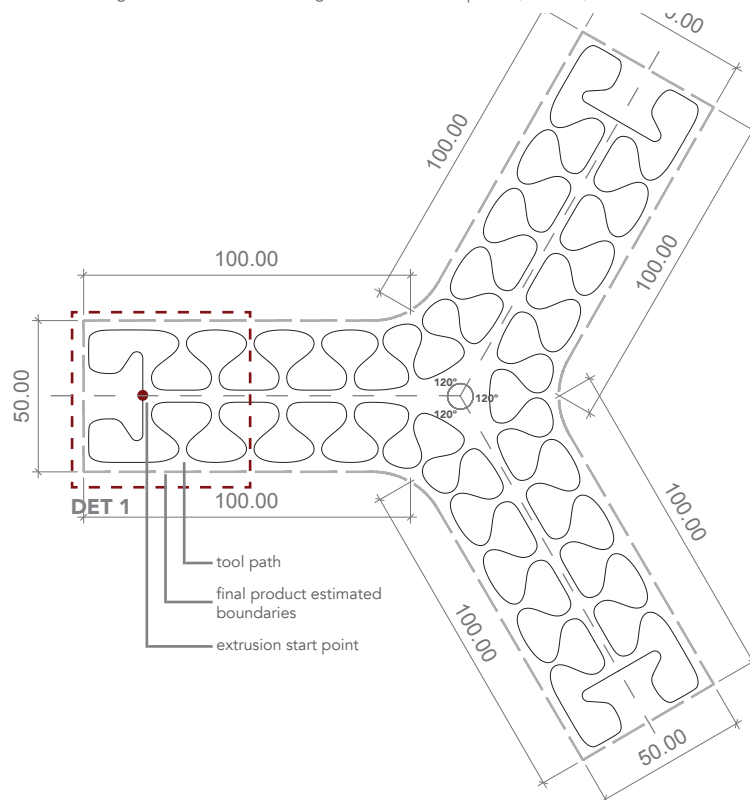
Fig 191 - Structural node - tool path view (scale 1:2.5)
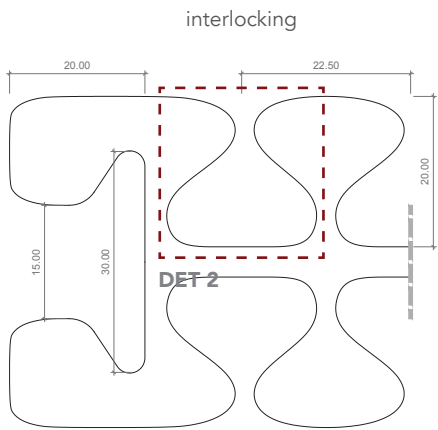
interlocking



Fig 192 - Detail 1 - Interlocking connection (scale 1:1)

tangents
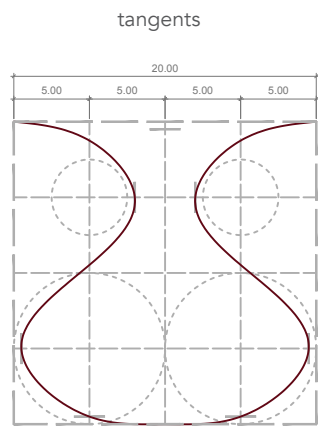


Fig 193 - Detail 2 - Curve generation (scale 2:1)

overlappings
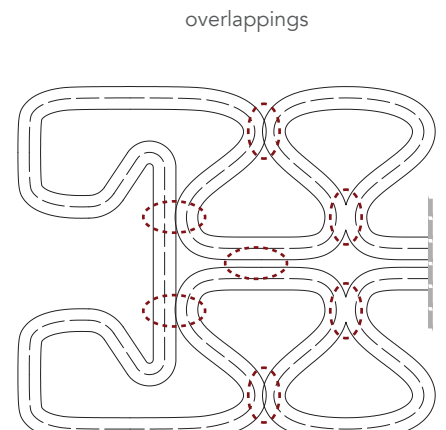


Fig 194 - Layer width simulation (scale 1:1)
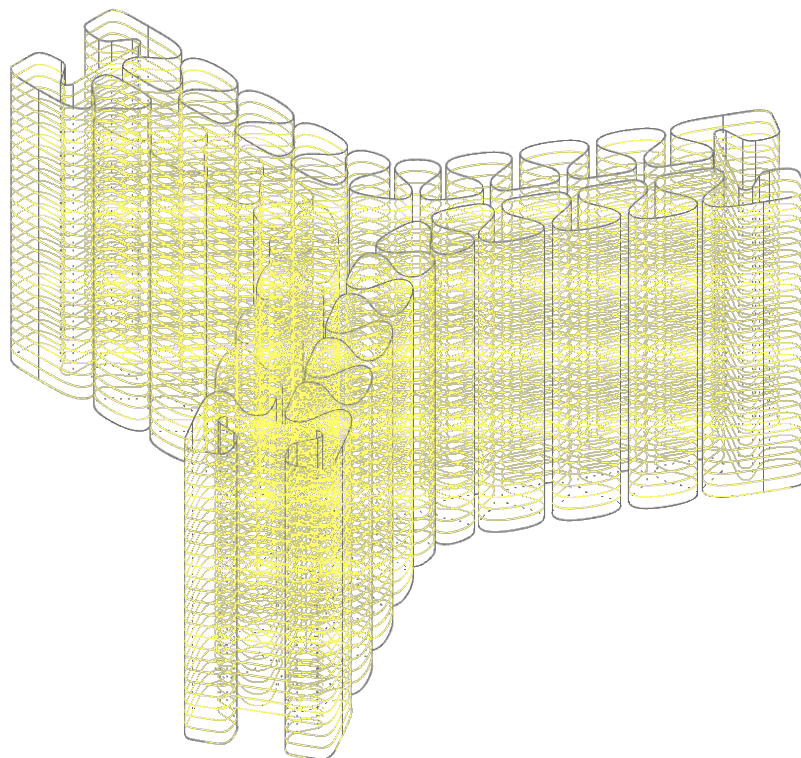


Fig 195 - Model sliced for fabrication - tool path
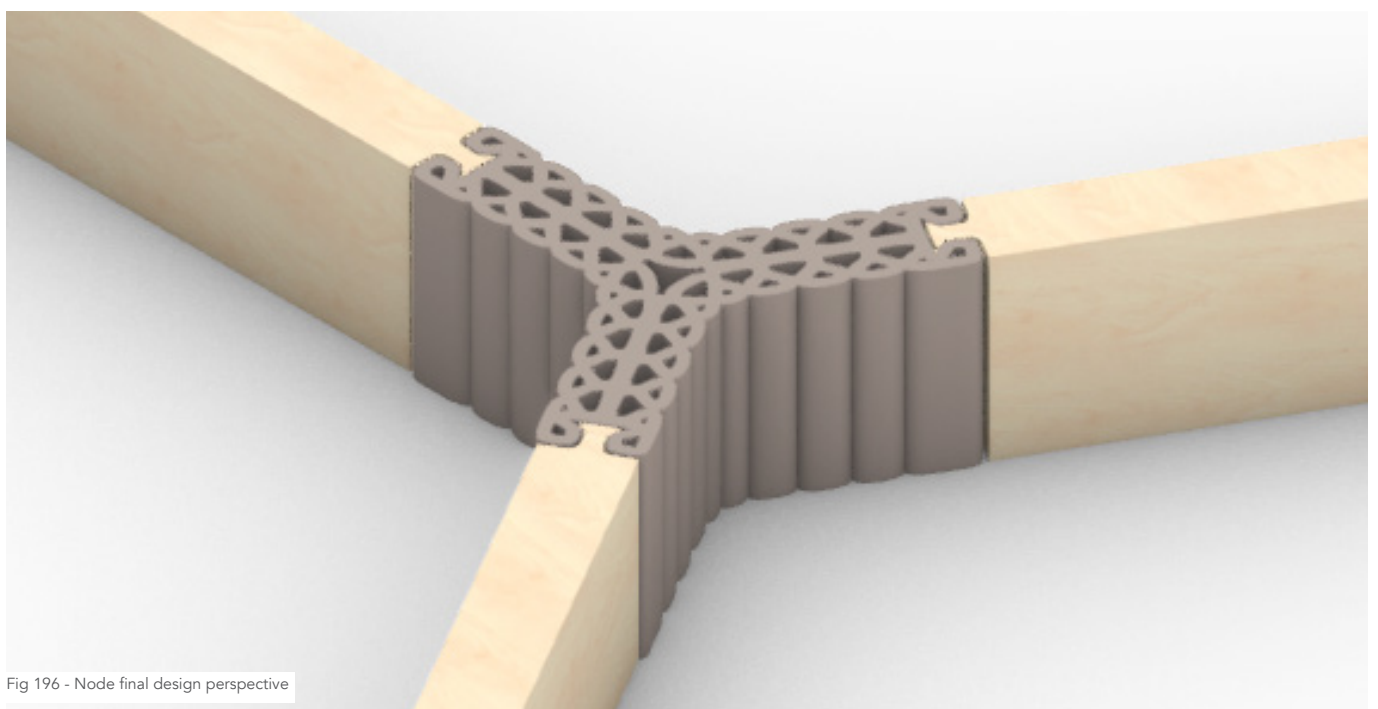


Fig 196 - Node final design perspective

123

# 5.4. Prototyping

### 5.4.1. Planning & Preparation

With the material enhanced and a design defined, a prototype could be fabricated to evaluate the printability, the potential and the limitations of this material and to compare its outcome to the original material mix resulting from the material exploration phase. The same geometry was intended to be produced with the three different materials, resulting in three pieces out of which the processes and outcomes could be compared.

The model was designed to be extruded in four stages, each with 8 layers with a height of 3mm. Each part is the equivalent to a full cartridge, which was demounted and refilled three times throughout the whole process. Between the stages, a drying time of 30 minutes was adopted, allowing the extrusion to settle and reducing the possibility of buckling and loss of stability.

Before each print, a simulation in Rhinoceros was performed, to verify the tool path and any possible collisions between the equipment components. With the tool path confirmed, a simulation with the robotic arm was performed to confirm the height of the first layer and the smoothness of the movements. With all the parameters confirmed, the extrusion could be performed.
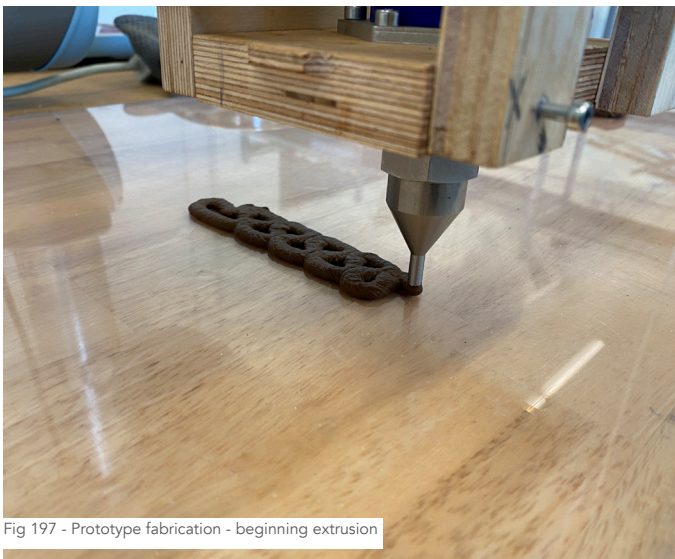

Fig 197 - Prototype fabrication - beginning extrusion
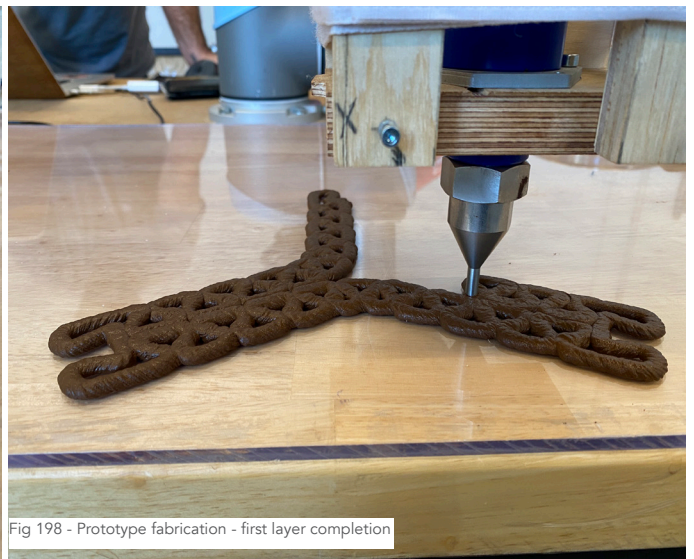

Fig 198 - Prototype fabrication - first layer completion
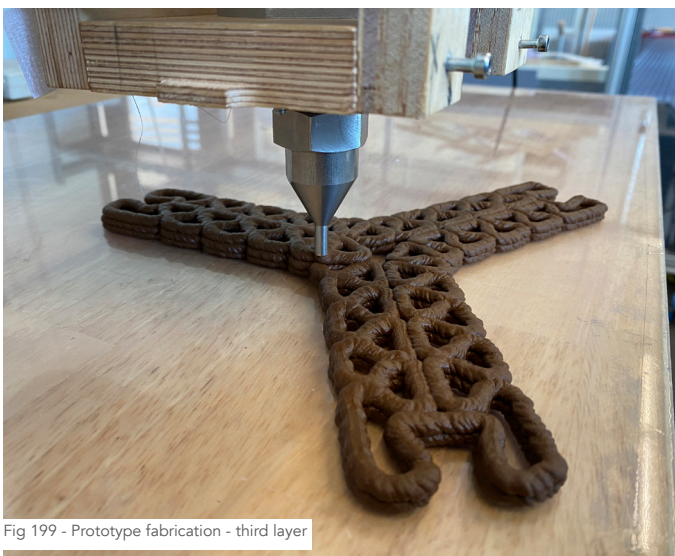

Fig 199 - Prototype fabrication - third layer
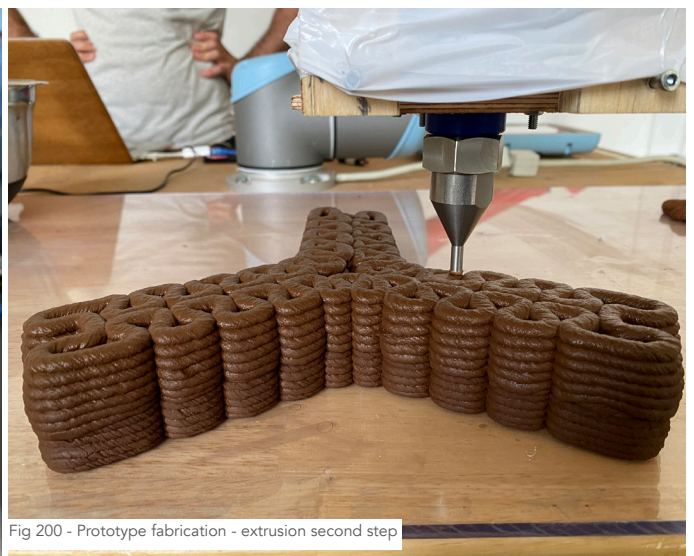

Fig 200 - Prototype fabrication - extrusion second step

### 5.4.2. Execution

The same node design, model and equipment were used for all the attempts at producing the prototype. The variables in each were the material and a few printing parameters – pressure and number of steps per revolution of the extruder's stepper motor – adjusted accordingly to the extrusion issues encountered throughout the process.

The first attempt was with the material mix expected to be the strongest among the new iterations, with bentonite and flax. The viscosity and homogeneity were similar to the original mix, however marginally denser and drier. A marginal amount of water was added to the batch when filling the cartridge to facilitate extrusion. No fibre clots were found and the overall aspect of the material resembled the original paste.

The extruder successfully printed the first layer of the prototype, however, the material density and the fibre content possibly created a constant force pulling the extruder's spiral piston and disconnecting it from the motor. Attempts of adding an adhesive on the equipment and increasing the water content of the material to reduce viscosity and increase the flow were only marginally successful, extruding two additional layers before failing and deeming the material non-extrudable with the available equipment.

The second attempt was with the material reinforced with flax fibres only, less dense and viscous than the batch prepared with bentonite. A marginal amount of water was still added to the mix when filling the cartridge to avoid the same issues encountered previously. No fibre clots were found, and the overall aspect of the material also resembled the original paste.

The extrusion started with the same printing parameters previously used – 2 bars of pressure and 2000 steps per revolution of the stepper motor – smoothly printing the first layer of the prototype before encountering the same issues observed previously. The number of steps of the extruder motor and the pressure were raised, however the equipment was not strong enough to push the material. The thin fibres created an additional resistance to the extrusion, entangling around the piston and between the spiral and the extruder container walls.

A final attempt was performed with the material mix enhanced only with bentonite, expected to offer less resistance to the extrusion and without long fibres to force the motor. The material viscosity and homogeneity were similar to the original mix and no additional water was necessary to reach the optimal conditions for extrusion.

The same printing parameters previously defined were used and the extrusion was performed seamlessly, resulting on a smooth layer sequence and without unforeseen events until the end of the fabrication process. With an enhanced material successfully extruded, the prototyping process could be executed.

After completion, the final product was placed on a well-ventilated surface to dry and cure for a week, until its surface hardened completely.

### 5.4.3. Results

The outcome was three models – two failed extrusions and one successful prototype. The material mixes containing flax were too heavy and the fibres too long, entangling in the spiral piston and leading to a forced stop of the extruder's stepper motor.

The failed models can still be used for comparison purposes. The extrusion with bentonite and flax does have a stronger and stiffer aspect when compared to the extrusions with methylcellulose only. It also shows a higher potential at producing successful overhangs, although this part was not finalised.

The extrusion with flax only, however, does not show significant differences when compared to the methylcellulose samples. Possibly, the fibre content could be increased, improving its stiffness. Even though on a broken part of the prototype it is already possible to identify the fibres with an oriented direction following the tool path of the extruder.

The complete prototype validates the potential of this material in building multi-layer structures of 100mm or more in height, a significant improvement from the original mix, which prints would collapse after 30mm.

It also required an extended curing time, a function of its size and infill density. Throughout the process, it showed a significant shrinkage. When printed, the total height was close to 100mm, meanwhile after one week of hardening, the final height reduced to 90mm. The transition layers between the different printing steps – every eighth layer – were also highlighted after a week, due to the small difference in curing time and conditions when compared to the subsequent layers and to the marginal differences in the material batches.

Overall, the strategy of extruding in steps of eight layers each was successful at reducing the risk of buckling and increasing the structural stability. However, the final model did present a conical aspect, with the top width smaller than the bottom, indicating that the lower layers were still stretched and compressed due to the excessive weight.

It was also clear to observe the vocation of this material and fabrication process to curves and non-linear designs. The short and few linear sections of the model were frequently misaligned and tended to lose their vertical stability if not followed or overlapped by a curve.

Overall, the resulting extrusions from the prototyping phase showed improvements to the material and attested its potential at fabricating multi-layered structures. The effects of these material enhancements to the mechanical properties and improvements to the fabrication processes to match the material advancements, are topics for future research.



Fig 201 - Prototype fabrication - extrusion completion

Fig 202 - Final prototype - start of curing period
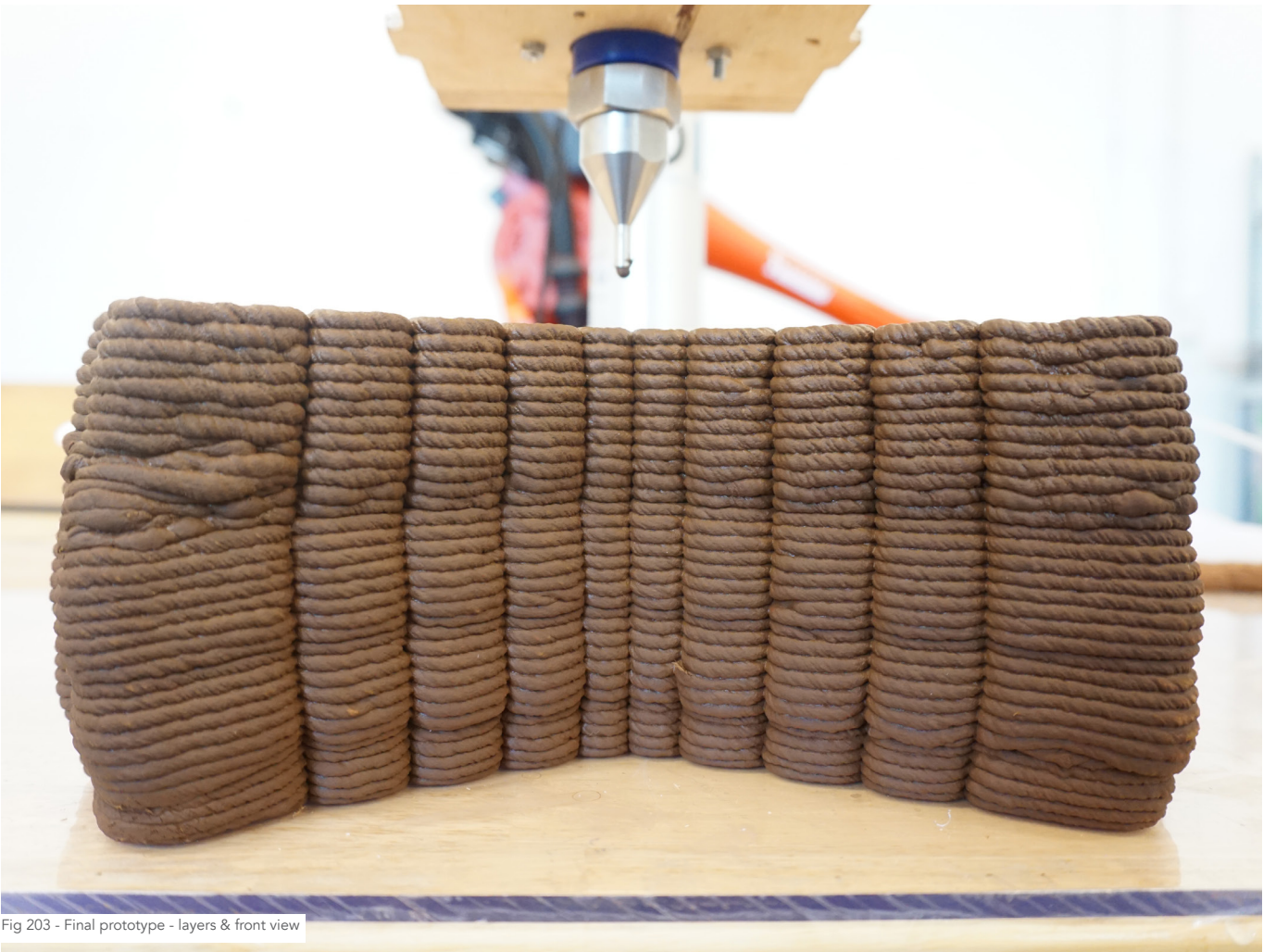


Fig 203 - Final prototype - layers & front view

## 5.5. Conclusion

At the start of this chapter, the relevance of producing a prototype of a structural node with a material without structural properties was questioned. The data available from the studies in printability and material properties indicated the prototype would either fail or be restrict to a merely geometrical study.

Therefore, the first step into a prototyping phase had to focus on the enhancement of the methylcellulose mix. Additives and fibres were studied, proposed and executed, creating variations to the material previously developed, but with presumed higher strength and stiffness. A refined recipe meant that limitations and challenges previously identified, such as extruding more than 30mm in height, could be overcome and a prototype would have a value at validating these improvements.

The failed models and the successful one showed that additives and fibre reinforcements did improve the methycellulose mix. The material became denser, heavier, more resistant to the touch and to pressure, and it successfully printed a 100mm tall stable structure, which hardened and did not collapse.

The prototype design validated the geometrical stability of curvilinear structures and the relevance of overlapping for long and tall pieces. It showed the importance of cavities for the curing process and the stretching of the hardening time caused by a dense infill. It also showcased how the additive manufacturing fabrication process affects the design outcome by eliminating straight outlines and adding curves and indents.

In terms of mechanical properties, no additional tensile and flexural tests were performed on the enhanced material. Its characterisation and further development are topics for an in-depth future research.

# 6. Conclusion & Reflection

## 6.1. Research & Results

Returning to the beginning, the objective of this thesis was the developing an application of a wood-like natural feedstock from recycled sources, man-made and tailored to high-tech production methods. Throughout this research, material, printability, and material properties were explored and documented, approaching different aspects of the initially proposed research question, and building up the necessary foundation to answer it.

From the material research, the main outcome was a full bio-based recipe based on a natural binding agent – methylcellulose – which, when mixed with cellulose and lignin, creates a homogeneous paste with great viscosity and adherence, resulting on smooth and well-structured extrusions. To reach this conclusion, extensive experiments were conducted with natural and non-natural binders, that were evaluated, graded and compiled in a comparative table, the first benchmark in terms of cellulose and lignin based materials.

From the fabrication, from the start of the material exploration, it was clear that LDM was the most suitable process. Filaments and pellets were briefly considered, nonetheless the degradation inflicted on a material by re-heating it associated to an already great viscosity and adherence in a paste consistency, defined extrusion with a clay extruder as the process to use.

From the mechanical properties, the main outcome was the outline of a material characterisation. Yield strength and modulus of elasticity were defined, nonetheless no structural properties were expected due to the novelty of the feedstock. Even though, the values obtained already placed it higher than the only other full bio-based material used in additive manufacturing mentioned in the literature review.

From the design and prototyping phase, the poor mechanical properties, combined with the limitations in height, overhang and stability of linear structures, raised questions about the relevance of designing and producing a node with such material. A quest for alternatives to improve the mix with additives and fibres was launched and led to new findings and a relevant outcome. The addition of flax helped hitting and understanding the limits of the extruder, and the incorporation of bentonite allowed for the first successful continuous print above 30mm, reaching 100mm.

After all the experiments and explorations, all the information gathered provides the means to answer the main research question:

> What are the **potential** and **challenges** of a material made of **cellulose** and **lignin** as feedstock for additive manufacturing processes in the fabrication of **structural nodes** for free-form structures?

The full bio-based nature of the material, combined with its homogeneity and great viscosity and adherence, successfully attested at the printability testing, and the smooth and stable structures produced, are the showcase of the potential of this material as an additive manufacturing feedstock.

The limitations lie on the combination between material behaviour and printability, typically addressed through design decisions and extrusion parameters. Curvilinear structures are steadier meanwhile straight walls tend to buckle. Overhang angles are limited. Heavy and thick geometries tend to collapse. Infills must be as carefully designed as the geometries itself, and do not overload any inclined surfaces. All of these are the challenges in obtaining a successful extrusion. And all of these have been approached and somehow overturned in the design and prototyping phase.

However, it is not possible to abstract the lack of structural properties of this material. Even with a successful printed prototype of a structural node, the material is not ready to be used in applications that demand high strength and stiffness. Attempts at enhancing these properties allowed for a fruitful prototyping phase, although the material properties have not been further assessed. Presumably, they surpass the values previously established, although there is still a long way of material characterisation and improvements for it to be a feasible choice to fabricate a strength-stiffness driven design piece.

The main outcome of this research, as expected from the beginning, was the development of a full bio-based material from the building blocks of wood with binders and additives. It has a good potential in the building industry, although for structural applications it still requires further research and refinement of its properties.



Fig 204 - Prototype fabrication - extrusion completion

## 6.2. Future Research

This research is already a continuation into the Wood Without Trees research line, started in 2018 with Thomas Liebrand and the use of acetone as a binding agent. Significant advances have been made, although the general feeling is that only the surface has been scratched and there is much more research to be done.

As stated above, the outcome of this thesis is a material recipe, a series of printability tests that explore its limitations and the outline of its properties. The ultimate goal of this research line is to develop a functional material based on cellulose and lignin for additive manufacturing fabrication and applications in the architectural universe. The potential and challenges have been stated through a combination of material, printability and design explorations. The follow-up investigations can be more specific and approach one area in detail, improving it significantly.

From the material side, the first step is to consolidate the material characterisation. Refine the concentrations, the mixing process, scale it up and repeat the mechanical testing with more accuracy to document the material properties. Additives to enhance the matrix strength and additional fibre reinforcements, finally reaching structural-grade properties, are also areas which require further investigation, especially towards bio-based elements.

From the fabrication side, a spin-off research could approach two different areas. First, the method itself, by investigating a hot extrusion process which would start from the production of pellets out of the viscous material. The second is the design for fabrication, by investigating further all the limitations imposed by the combination between material and equipment. Extrapolating the overhang and infill limitations could unleash more design possibilities. Alternative processes, use of scaffolding structures and even mixing other materials could be points to be explored.

From the design side, all sorts of applications in the architectural scenario could be explored, not only on the exterior of the building but also in the interior and for decoration purposes. Wood is the most welcomed bio-based material in the architect's palette, therefore a liquid version, which offers total freedom, unleashes all possibilities of design application.

## 6.3. Reflection

### 6.3.1. Graduation Process

**Topic**

The original intent of this research was to approach three areas – material, fabrication and design – with a stronger focus on the second and third, hence the combination between the chairs of Design Informatics and Façade Products. Throughout the process, the realisation of the importance of the material development prior exploring a fabrication process in depth and elaborating an optimised design, led to a refocus.

The revised outcome can be described as a material science exploration targeted on a specific fabrication process, the additive manufacturing, and a specific design application, a structural node. The focus might have been adjusted but the robotic fabrication remains and justifies the material investigation.

## Methodology

The methodology chosen at the beginning of the thesis focused on a design by research approach, with an extensive literature review and interviews to understand the field of study and the technology involved before switching to a practical phase of experiments and exploration. A solid foundation was indeed necessary, however the subsequent phase of material and printability explorations required so many iterations and additional literature investigation, and offered so much output and knowledge, that a design by research approach could have offered a better path forward. The project outcome was not affected negatively, however parts of the initial studies were not fundamental for the practical phases, meanwhile additional time would have been beneficial for the final material characterisation. An approach of literature research and practical exploration from the early stages of the thesis would have offered a more guided and effective process. Through exploration, the weaknesses and obstacles were identified and the investigation, realigned.

This project is part of the Wood Without Trees research line from the Design Informatics Chair, and it was developed in partnership with another student from the same Building Technology track, Christopher Biearch. Total freedom was offered to define the shape, goals and directions of this study, since no other researches were being developed in this topic at this time.

## Design

The design component of this research is limited and occupied only a few weeks out of the whole process. The importance of the material development greatly surpasses it since this is a novel field, with no standards and benchmarks for comparisons except conventional materials such as wood. The design component is expressed in the prototyping phase as a showcase of the research results. Rather than an outstanding and innovative piece, it is a proof of concept of material and fabrication process, only driving the focus to the research outcome.

## Collaboration

No moral or ethical issues were encountered, only a lack of collaboration between departments and between faculties was observed. This research has an extensive list of collaborators and partners due to the unwavering support from the mentors and their extensive network. At times when the resources were not accessible in-house, there was always an alternative to ensure the continuation of the exploratory work. It is noticeable as well how many research lines in the same field of bio-based materials are open in other faculties, although there is no acknowledgement or multi-disciplinary research teams. All students and their work would benefit greatly from better inter-faculty collaborations. Tentatively, a bridge with researchers in the field of bio-based materials from the Faculty of Civil Engineering was initiated to support the material characterisation developed in this research.

### 6.3.2. Societal Impact

## Results

TThe outcome of this thesis is a solid direction towards the development a new material for the building industry. It defines a recipe and its properties, and assesses its potential, limitations and challenges combined with a fabrication process. A proof of concept has been produced, now further research to characterise and improve it can be developed starting from this recipe. It demands additional and extensive research to reduce its limitations, nevertheless it shows that a bio-based material as an additive

manufacturing feedstock is feasible and that alternatives to chemical-based materials do exist.

## Innovation

The proof of concept achieved at the end of this research attests that the innovation projected at the start has been achieved to its fullest. An extensive material exploration phase was performed and documented, creating comparisons out of which the best binders for cellulose and lignin were identified, as well as the most promising recipe for an additive manufacturing feedstock. Printability was explored and extrusions were successful. Specimens were produced and the material properties documented. Compiling all this information creates a complete and unique data set with no parallel that validates this new material potential and paves the way for further investigation into its characterisation.

## Sustainability

The construction sector is one of the largest contributors to the greenhouse gases emissions. To reduce its carbon footprint and increase the energy efficiency towards the zero-energy goals proposed by the European Union, it must undergo a transformation. On one side, there is an increasing demand for bio-based construction materials, specially from recycled resources. On the other, innovative and more efficient fabrication processes are necessary to reduce the waste without adding design limitations.

This research successfully achieved the purpose of proofing that wood, one of the most sought-after natural materials in the building industry, can be combined with the most efficient fabrication method. It shows that mixing the building components of wood, which could potentially be extracted from the agricultural, wood and paper industry waste, through material science studies, can recreate a viable bio-based feedstock for additive manufacturing.

## Impact

The first impact would be the break of a paradigm with the development of "liquid wood" – a material traditionally seen as a natural, prismatic, solid and sturdy element now can be seen as a paste with a viscous consistency being fed into an extruder. It is a merger between natural and the highest technology in terms of fabrication. Total design freedom with minimal waste is now feasible also with a bio-based material. Challenges and limitations still exist, but the potential is clear and the directions to improve have been established.

Raw material found in waste can now be seen as more than merely residue and landfill fuel. It can be upcycled and recombined into a feedstock for the most efficient and innovative fabrication process. This proof of concept paves the way for a new understanding of wood in the building environment. Excessive waste and deforestation will not be concerns anymore.

As a direct impact, the result of this research proves the potential of this new material based on cellulose and lignin. The limitations and challenges establish the directions where further research is necessary for a full characterisation and improvement. And the prototype sheds a light on possible applications in the architecture universe.

Fig 205 - Prototype - completed extrusion

# 7. References

# 7.1. Bibliography

Ahmad, F., Choi, H. S., & Park, M. K. (2015). A Review: Natural Fiber Composites Selection in View of Mechanical, Light Weight, and Economic Properties. Macromolecular Materials and Engineering, 300, 10-24.

Alén, R. (2018). Characteristic Testing of Pulp and Paper. In: Elsevier.

Arantes, V., Dias, I. K. R., Berto, G. L., Pereira, B., Marotti, B. S., & Nogueira, C. F. O. (2020). The current status of the enzyme-mediated isolation and functionalization of nanocelluloses: production, properties, techno-economics, and opportunities. In (Vol. 27, pp. 10571-10630).

Aronson, J. K., & Dukes, M. N. G. (2006). Meyler's side effects of drugs : the international encyclopedia of adverse drug reactions and interactions.

Ashby, M. F., Shercliff, H. R., & Cebon, D. (2019). Materials: Engineering, Science, Processing and Design.

Ayrilmis, N., Kariž, M., & Kitek Kuzman, M. (2019). Effect of wood flour content on surface properties of 3D printed materials produced from wood flour/PLA filament. International Journal of Polymer Analysis and Characterization, 24, 659 - 666.

Ayrilmis, N., Kariž, M., Kwon, J.-h., & Kitek Kuzman, M. (2019). Effect of printing layer thickness on water absorption and mechanical properties of 3D-printed wood/PLA composite materials. The International Journal of Advanced Manufacturing Technology, 102, 2195-2200.

CEN, E. C. F. S.-. (2012). NEN-EN-ISO-527-2.

CEN, E. C. F. S.-. (2017). NEN-EN-ISO 294-1.

CEN, E. C. F. S.-. (2018a). NEN-EN-ISO 294-2.

CEN, E. C. F. S.-. (2018b). NEN-EN-ISO 20753.

CEN, E. C. F. S.-. (2019). NEN-EN-ISO 178.

Chen, M., Liu, B., Li, L., Cao, L., Huang, Y., Wang, S., Zhao, P., Lu, L., & Cheng, X. (2020). Rheological parameters, thixotropy and creep of 3D-printed calcium sulfoaluminate cement composites modified by bentonite. Composites Part B-engineering, 186, 107821.

Christ, J. F., Koss, H., & Ottosen, L. M. (2019). A concrete composite from biologically based binders and mineral aggregates for constructional 3D-printing.

Chung, H., & Washburn, N. R. (2016). Extraction and Types of Lignin. In (pp. 13-25). Elsevier. https://doi.org/10.1016/B978-0-323-35565-0.00002-3

Clemons, C. M., & Caulfield, D. F. (2005). Wood Flour. In Functional Fillers for Plastics (pp. 249-270). Wiley-VCH Verlag GmbH & Co. KGaA. https://doi.org/10.1002/3527605096.ch15

Couret, L., Irle, M., Belloncle, C., & Cathala, B. (2017). Extraction and characterization of cellulose nanocrystals from post-consumer wood fiberboard waste. In (Vol. 24, pp. 2125-2137).

Das, A. K., Agar, D. A., Rudolfsson, M., & Larsson, S. H. (2021). A review on wood powders in 3D printing: processes, properties and potential applications. Journal of materials research and technology, 15, 241-255.

Delgado Camacho, D., Clayton, P., O'Brien, W. J., Seepersad, C., Juenger, M., Ferron, R., & Salamone, S. (2018). Applications of additive manufacturing in the construction industry – A forward-looking review

Dimethyl Sulfoxide. (2022). Retrieved 14/06/2022 from https://en.wikipedia.org/wiki/Dimethyl_sulfoxide

Duigou, A. L., Castro, M., Bevan, R., & Martin, N. (2016). 3D printing of wood fibre biocomposites: From mechanical to actuation functionality. Materials & Design, 96, 106-114.

Ebers, L. S., Arya, A., Bowland, C. C., Glasser, W. G., Chmely, S. C., Naskar, A. K., & Laborie, M. P. (2021). 3D printing of lignin: Challenges, opportunities and roads onward. 112. https://doi.org/10.1002/bip.23431

EuropeanComission. (2019). The European Green Deal. Brussels

Evstigneev, E. I. (2011). Factors affecting lignin solubility. Russian Journal of Applied Chemistry, 84, 1040-1045.

FAOSTAT. (2020). Forestry Production and Trade. Retrieved 07/06/2022 from https://www.fao.org/faostat/en/#data/FO

Ferdosian, F., Pan, Z., Gao, G., & Zhao, B. (2017). Bio-Based Adhesives and Evaluation for Wood Composites Application. Polymers, 9.

Galjaard, S., Hofman, S., Perry, N., & Ren, S. (2015). Optimizing Structural Building Elements in Metal by using Additive Manufacturing.

Gardner, D., Wang, L., & Wang, J. (2019, 12). Additive Manufacturing of Wood-based Materials for Composite Applications.

Gardner, D. J., Anderson, J., Tekinalp, H., Ozcan, S., & Sauerbier, P. (2018, 26–29 September 2018). Lignocellulosic-filled polymer feedstocks for large scale additive manufacturing of low cost composites. Proceedings of the Internaional Forest Products Congress, Trabzon, Turkey.

Gauss, C., Pickering, K. L., & Muthe, L. P. (2021). The use of cellulose in bio-derived formulations for 3D/4D printing: A review. 4, 100113. https://doi.org/10.1016/j.jcomc.2021.100113

Gholamipour-Shirazi, A., Kamlow, M.-A., T Norton, I., & Mills, T. (2020). How to Formulate for Structure and Texture via Medium of Additive Manufacturing-A Review. Foods, 9.

Gibson, I., Rosen, D., Stucker, B., & Khorasani, M. (2021). Additive Manufacturing Technologies. Springer International Publishing. https://doi.org/10.1007/978-3-030-56127-7

GlobalABC. (2019). 2019 Global Status Report for Buildings and Construction.

Gosselink, R. (2011). Lignin as a Renewable Aromatic Resource for the Chemical Industry

Grigsby, W. J., Scott, S. M., Plowman-Holmes, M. I., Middlewood, P. G., & Recabar, K. (2020). Combination and processing keratin with lignin as

biocomposite materials for additive manufacturing technology. 104, 95-103. https://doi.org/10.1016/j.actbio.2019.12.026

Grover, J. A. (1993). CHAPTER 18 – METHYLCELLULOSE AND ITS DERIVATIVES.

Gunasekera, D. H. A. T., Kuek, S. Y., Hasanaj, D., He, Y., Tuck, C. J., Croft, A. K., & Wildman, R. D. (2016). Three dimensional ink-jet printing of biomaterials using ionic liquids and co-solvents. Faraday discussions, 190, 509-523.

Haeusler, M. H., Muehlbauer, M., Bohnenberger, S., & Burry, J. R. (2017). Furniture Design Using Custom-Optimised Structural Nodes. Proceedings of the 22nd Conference on Computer Aided Architectural Design Research in Asia (CAADRIA).

Hecht, H., & Srebnik, S. (2016). Structural Characterization of Sodium Alginate and Calcium Alginate. Biomacromolecules, 17 6, 2160-2167.

Henke, K., & Treml, S. (2013). Wood based bulk material in 3D printing processes for applications in construction. In (Vol. 71, pp. 139-141).

Hu, X., Yang, Z., Kang, S., Jiang, M., Zhou, Z., Gou, J. H., Hui, D., & He, J. (2020). Cellulose hydrogel skeleton by extrusion 3D printing of solution. Nanotechnology Reviews, 9, 345 - 353.

IMA-NA. (2022). What is Bentonite? . https://www.ima-na.org/page/what_is_bentonite

Ingtipi, K., Boro, U., & Moholkar, V. S. (2022). Chapter 15 - Lignin in nanocomposite hydrogels. In D. Puglia, C. Santulli, & F. Sarasini (Eds.), Micro and Nanolignin in Aqueous Dispersions and Polymers (pp. 459-484). Elsevier. https://doi.org/https://doi.org/10.1016/B978-0-12-823702-1.00002-5

ISO. (2008). ISO 62.

Kariž, M., Šernek, M., & Kuzman, M. K. (2016). Use of wood powder and adhesive as a mixture for 3D printing. In (Vol. 74, pp. 123-126).

Kariž, M., Šernek, M., & Kuzman, M. K. (2018). Effect of humidity on 3D-printed specimens from wood-pla filaments. Wood Research, 63, 917-922.

Kariž, M., Šernek, M., Obućina, M., & Kuzman, M. K. (2018). Effect of wood content in FDM filament on properties of 3D printed parts. Materials today communications, 14, 135-140.

Konnerth, J., Hahn, G., & Gindl, W. (2009). Feasibility of particle board production using bone glue. European Journal of Wood and Wood Products, 67, 243-245.

Li, H., Tan, Y. J., Leong, K. F., & Li, L. (2017). 3D Bioprinting of Highly Thixotropic Alginate/Methylcellulose Hydrogel with Strong Interface Bonding. ACS applied materials & interfaces, 9 23, 20086-20097.

Liebrand, T. (2018). 3D printed fiber reinforced lignin: Exploring the options to use wood in an additive manufacturing process

Liu, Z., Bhandari, B. R., Prakash, S., Mantihal, S., & Zhang, M. (2019). Linking rheology and printability of a multicomponent gel system of carrageenan-xanthan-starch in extrusion based additive manufacturing. Food Hydrocolloids.

Mohan, D., Teong, Z. K., Bakir, A. N., Sajab, M. S., & Kaco, H. (2020). Extending Cellulose-Based Polymers Application in Additive Manufacturing Technology: A Review of Recent Approaches. Polymers, 12.

Nguyen, N. A., Barnes, S. H., Bowland, C. C., Meek, K. M., Littrell, K. C., Keum, J. K., & Naskar, A. K. (2018). A path for lignin valorization via additive manufacturing of high-performance sustainable composites with enhanced 3D printability. 4. https://doi.org/10.1126/sciadv.aat4967

Nishimura, H., Kamiya, A., Nagata, T., Katahira, M., & Watanabe, T. (2018). Direct evidence for  ether linkage between lignin and carbohydrates in wood cell walls. Scientific Reports, 8.

Norström, E., Demircan, D., Fogelström, L., FaridehKhabbaz, & Malmström, E. (2017). Green Binders for Wood Adhesives.

Onusseit, H. (1992). Starch in industrial adhesives: new developments. Industrial Crops and Products, 1, 141-146.

Open3DP. (2011). Woodn't You Know It - 3DP in wood. Retrieved 21/01/2022 from https://depts.washington.edu/open3dp/2011/04/woodnt-you-know-it-3dp-in-wood/

Pavon, C., Aldas, M., López-Martínez, J., & Ferrándiz, S. (2020). New Materials for 3D-Printing Based on Polycaprolactone with Gum Rosin and Beeswax as Additives. Polymers, 12.

Peeters, J., van der Veen, R., Helgers, R., Långström, O., Bambi, M., Papworth, N., & Trotto, A. (2019). Resisting plastics for ambiguous results. Proceedings of the 4th Biennial Research Through Design Conference, Delft & Rotterdam, The Netherlands

Petit-Conil, M., Bertaud, F., Tapin-Lingua, S., Pizzi, A. P., & Navarette, P. (2011). Development of green adhesives for fibreboards manufacturing, using tannins and lignin from pulp mill residues. In (Vol. 65, pp. 6-12).

Podstawczyk, D. A., Nizioł, M., Szymczyk, P., Wiśniewski, P., & Guiseppi-Elie, A. (2020). 3D printed stimuli-responsive magnetic nanoparticle embedded alginate-methylcellulose hydrogel actuators. Additive manufacturing, 34, 101275.

Rajinipriya, M., Nagalakshmaiah, M., Robert, M., & Elkoun, S. (2018). Importance of Agricultural and Industrial Waste in the Field of Nanocellulose and Recent Industrial Developments of Wood Based Nanocellulose: A Review. In (Vol. 6, pp. 2807-2828).

Rana, V., Malik, S., Joshi, G., Rajput, N. K., & Gupta, P. K. (2021). Preparation of alpha cellulose from sugarcane bagasse and its cationization: Synthesis, characterization, validation and application as wet-end additive. In (Vol. 170, pp. 793-809).

Rschip, I. E., Vasile, C., Ciolacu, D. E., & Cazacu, G. (2007). Semi-interpenetrating Polymer Networks Containing Polysaccharides. I Xanthan/Lignin Networks. High Performance Polymers, 19, 603 - 620.

Reineke, L. H. (1966). Wood Flour. In U.S. Forest Service Research Note FPL-0113. U.S. Dept. of Agriculture, Forest Service, Forest Products Laboratory.

Rosenthal, M., Henneberger, C., Gutkes, A., & Bues, C.-T. (2018). Liquid Deposition Modeling: a promising approach for 3D printing of wood. In (Vol. 76, pp. 797-799).

Rumpf, J., Korte, I., Kreyenschmidt, J., Dreier, T., & Schulze, M. (2020, September 2020). Novel cellulose-beeswax-lignin composites as coating material for paper packaging European Technical Coatings Congress (ETCC) 2020, Krakow, Poland.

Runberger, J., & Lundberg, J. (2019). Material & Detail 2019 https://www.wouldwood.se/news/

Sain, M. M., Ghosh, A., & Banik, I. (2007). Effect of Propylene Carbonate on the Properties of Composite Fiberboard from Wood Fiber Bonded with Renewable Wood Resin. Journal of Reinforced Plastics and Composites, 26, 705 - 713.

Samarth, N., & Mahanwar, P. A. (2015). Modified Vegetable Oil Based Additives as a Future Polymeric Material—Review.

Sanandiya, N. D., Vijay, Y., Dimopoulou, M., Dritsas, S., & Fernandez, J. G. (2018). Large-scale additive manufacturing with bioinspired cellulosic materials. 8, 8642. https://doi.org/10.1038/s41598-018-26985-2

Sauerwein, M., Zlopaša, J., Doubrovski, Z., Bakker, C., & Balkenende, R. (2020). Reprintable Paste-Based Materials for Additive Manufacturing in a Circular Economy. Sustainability, 12, 1-15.

Seifi, H. (2019). Topology optimisation and additive manufacturing of structural nodes of gridshell structures.

Senthilkumar, K., Jeevith, K., Geyandraprasath, K., Roy, B., & Samraj, S. (2021). Extraction of cellulosic fibres from agricultural waste and its applications. In (pp. 040003).

Sjöström, E. (1993). Wood Chemistry. Academic Press. https://doi.org/https://doi.org/10.1016/B978-0-08-092589-9.50005-X

Sridhar, V., & Park, H. (2020). Extraction of Microfibrillar Cellulose From Waste Paper by NaOH/Urethane Aqueous System and Its Utility in Removal of Lead from Contaminated Water. In (Vol. 13, pp. 2850).

Tanase-Opedal, M., Espinosa, E., Rodríguez, A., & Chinga-Carrasco, G. (2019). Lignin: A Biopolymer from Forestry Biomass for Biocomposites and 3D Printing. 12, 3006. https://doi.org/10.3390/ma12183006

Tao, Y., Wang, H., Li, Z., Li, P., & Shi, S. Q. (2017). Development and Application of Wood Flour-Filled Polylactic Acid Composite Filament for 3D Printing. Materials, 10.

Tonk, R. (2020). Natural fibers for sustainable additive manufacturing: A state of the art review. Materials Today: Proceedings.

UNFCCC. (2015, December 2015). Paris Agreement United Nations Framework Convention on Climate Change,

USDA Forest Service, F. P. L. (2010). Wood handbook: wood as an engineering material. https://doi.org/10.2737/FPL-GTR-190

Vazquez-Martel, C., Becker, L., Liebig, W. V., Elsner, P., & Blasco, E. (2021). Vegetable Oils as Sustainable Inks for Additive Manufacturing: A Comparative Study. ACS Sustainable Chemistry & Engineering.

Vieira, J. G., Oliveira, G., Filho, G. R., Assunção, R. M. N., Meireles, C. d. S., Cerqueira, D. A., Silva, W. G., & Motta, L. A. C. (2009). Production, characterization and evaluation of methylcellulose from sugarcane bagasse for applications as viscosity enhancing admixture for cement based material. Carbohydrate Polymers, 78, 779-783.

Wetterlund, E., Pettersson, K., Lundmark, R., Lundgren, J., Athanassiadis, D., Mossberg, J., Torén, J., Schenck, A. v., & Berglin, N. (2013). Optimal localisation of next generation biofuel production in Sweden – Part II.

WouldWood. (2018). Retrieved 07/06/2022 from https://www.wouldwood.se

Wu, B., Sufi, A., Ghosh Biswas, R., Hisatsune, A., Moxley-Paquette, V., Ning, P., Soong, R., Dicks, A. P., & Simpson, A. J. (2019). Direct Conversion of McDonald's Waste Cooking Oil into a Biodegradable High-Resolution 3D-Printing Resin. ACS Sustainable Chemistry & Engineering, 8, 1171-1177.

Yang, J., An, X., Liu, L., Tang, S., Cao, H., Xu, Q., & Liu, H. (2020). Cellulose, hemicellulose, lignin, and their derivatives as multi-components of bio-based feedstocks for 3D printing. 250, 116881. https://doi.org/10.1016/j.carbpol.2020.116881

Zarna, C., Opedal, M. T., Echtermeyer, A. T., & Chinga-Carrasco, G. (2021). Reinforcement ability of lignocellulosic components in biocomposites and their 3D printed applications – A review. 6, 100171. https://doi.org/10.1016/j.jcomc.2021.100171

Zhao, H., Zhu, H. Y., Zhou, Y. L., & Wang, Q. W. (2011). Reasearch of Wood Plastic Composites application based on Fused Deposition Modeling technology. In (pp. 1560-1562): IEEE.

Zhao, X., Tekinalp, H. L., Meng, X., Ker, D., Benson, B., Pu, Y., Ragauskas, A. J., Wang, Y., Li, K., Webb, E. G., Gardner, D. J., Anderson, J., & Ozcan, S. (2019). Poplar as Biofiber Reinforcement in Composites for Large-Scale 3D Printing. ACS Applied Bio Materials.

# 7.2. List of Figures

All images obtained from books and articles have been referenced to their original sources. The images without any references were produced by the author of this thesis throughout the research process.

# 7.3. List of Tables

All tables were produced by the author of this thesis throughout the research process.

# 8. Appendices

## 8.1. Material Diary

# Cellulose & Lignin in Additive Manufacturing

Potential and challenges in the fabrication of structural nodes for free-form building envelope structures

Material Exploration Diary – "Cook Book"

**MIX 1**

### Recipe

5g Cellulose

60g Lignin

10g Water

28g Acetone

### Process

The experiments start with the reproduction of the recipe developed in Liebrand (2018), using *acetone* as the binding agent, and presented as the most promising among several iterations with different proportions of ingredients.

The first attempt at pulping the cellulose obtained in the shape of card paper sheets failed at completely separating the fibres. Pieces of paper and chunks of fibres could still be found in the recipient, creating a non-homogeneous mixture once the lignin powder was combined. The materials did not mix well, resulting in chunks of cellulose fibres and vast amounts of wasted lignin powder suspended in the air and adhered to the recipient walls. Water was added to reduce the material losses and combine them, however little effect was observed.

At last the acetone was added, reacting with the lignin and forming an extremely sticky paste difficult to mix and manipulate with wooden stirrers and spoons. A plastic spatula was the best tool to handle the mix, which seemed to become more viscous as the acetone would evaporate and the paste would dry.

### Outcome

The result was a paste with high viscosity and bonding and low homogeneity. It was difficult to extrude by hand, requiring high pressure to extrude manually. Chunks of fibres could be seen on the material sample, resembling hair knots, and remains of lignin powder would resurface as the material would start to dry.

## MIX 2

### Recipe

30g Papier Mache

60g Lignin

20g Water

38g Acetone

### Process

Since the pulping of cellulose from the previous experiment left residues of paper chips and agglomerated fibres, an attempt to replace it with papier mache was investigated. Easier to obtain than pure cellulose, its powder form made it better to combine with the lignin powder, creating a homogeneous powder mix.

However when water was added, it combined with the papier mache powder and not the lignin, creating chunks and a non-homogeneous mix. At last, with the addition of acetone it resulted in a sticky and viscous paste, as difficult to handle as the one from the previous experiment. The more acetone incorporated to the material, the more homogeneous and less viscous it would become, making it easier to manipulate and eventually extrude – final concentration of acetone/lignin is 35% higher than in the previous experiment.

### Outcome

The result was a paste with moderated viscosity and bonding and high homogeneity. A sample was extruded by using the caulking gun available at the laboratory. Although the different extrusion methods does not allow to compare the experiments in terms of extrudability and printability, this mix also appears to be easier to extrude by hand, and resulted in a more porous and less dense sample.

## ROUND 3 – Hot Mixes & Alternative Binding Agents

### MIX 3

### Recipe

Lignin

Cellulose

Papier Mache

Xanthan Gum

Methylcellulose

Water

### Process

The first step for the experiments with hot material mixes was to understand the behaviour of the different materials when heated up and the threshold before any degradation would commence. Once this was clear, the activation temperatures were studied for methylcellulose and xanthan gum, and the differences between manipulating them cold, at room temperature, and hot, close to the boiling temperature of water, were observed. At last, different proportions between the ingredients were investigated to analyse the viscosity, bonding and homogeneity of the mixtures to identify the most promising ones to be used as feedstock for additive manufacturing processes.

Since the purpose of this experiments was to understand the behaviour of the materials and how they react when combined, no fixed measurements were used, only the recommended proportions of 1:10 for the methylcellulose/water solution and 1:2 for the xanthan gum/water solution.

### Outcome

Cellulose did not melt and when heated up to 180C it started to degrade, changing from white to shades of yellow and brown until it burned and turned dark. Lignin started to melt when the temperature reached 130C and quickly degraded when it

passed over 180C, drying and turning into a brittle charred material even before removing it from the heat. Dissolving the lignin in water at the beginning (soda lignin is soluble in water) and heating it up avoided degradation and resulted in a homogeneous liquid with low viscosity. Adding cellulose turned it into a non-homogeneous paste full of chunks formed by fibres absorbing water, which quickly dried once removed from the heat.

Papier mache created a homogeneous mix with boiling water, with viscosity increasing proportionally to the amount of powder used. With lignin it became a non-homogeneous paste that quickly dried and turned brittle when removed from heat. Xanthan gum mixed with water created a gel and did not mix well with lignin, creating a non-homogeneous gel covered in residual lignin powder which retained the gel consistency and did not solidify.

Xanthan gum needs to be mixed with water to be activated and turn into a gel consistency. Combined solely with lignin, it resulted in a homogeneous gel with high viscosity and moderated bonding. Mixing it also with cellulose and/or papier mache did not change the consistency, but made it less homogeneous, with chunks of fibres – the more fibres, the less homogeneous. All experiments with xanthan gum, independent of the material and water proportions, resulted in gel-like samples which do not completely solidify.

In general, xanthan gum mixed with water does not create a solid structure, preserving the gel consistency and a white and opaque appearance. However, methylcellulose, which also needs to be mixed and activated with water just below boiling temperature, becomes transparent once the mixture cools down, solidifying and creating a plastic-like membrane.

A methylcellulose solution with lignin created a full homogeneous paste, with varying levels of viscosity and bonding depending on the mixture temperature and the amount of lignin. Adding cellulose made it less viscous and increased the bonding, with varying levels of homogeneity depending on the mixture temperature and the amount of cellulose. Adding papier mache also made it less viscous and more malleable but decreased the bonding and made the mix dry and crumbly.

Overall, methylcellulose resulted in a promising binding agent. Working temperature should start at around 80C and gradually decrease to reduce the viscosity after adding lignin. Cellulose should be mixed in the sequence and stirred until the material is homogeneous and without chunks of fibres, bonding is high and viscosity is low, with an adequate flow to extrude and allow for a stable layer structure.

**ROUND 4 – Lignin & Recipe Refinement**

**MIX 4**

Recipe

Lignin
Water

Process

This experiment was another attempt at melting the lignin powder without any additives or solvents, either pure or mixed with water at the proportions of 1:1 and 1:2, keeping the temperature at around 130C and analyse its behaviour and properties.

Outcome

The lower temperature avoided the material degradation and formation of char. However, there is a short window between melting and degrading, and once melted, the lignin dried in few seconds if stirring stopped or if removed from heat. Once cured, the samples were extremely brittle and showed no strength.

**MIX 5**


## Recipe

Lignin

Cellulose

Papier Mache

Methylcellulose

Water


## Process

The purpose was to define the best proportions between the ingredients for the most promising mix identified previously, using methylcellulose as the binding agent, and execute a first extrudability test with a syringe. Using the same base - a solution of 1:10 of methylcellulose in water at 80C with 5g methylcellulose and 50g water – two recipes were experimented. First attempt was 5g lignin + 1g cellulose and the second was 20g of lignin (started with 7g + increments until reached 20g) + 1g cellulose + 1g papier mache + 25g water.


## Outcome

The first attempt resulted in a weak mix, non-homogeneous with high viscosity and low bonding. Fibres were clearly not mixed well and large chunks could be seen in the material. The second attempt was improved during the execution of the recipe, with the addition of more lignin and fibres, and resulted in more successful samples. Result was a relatively homogeneous material with low viscosity and high bonding, but overall too dry and still with a few chunks which clogged the syringe during the extrusion.

**ROUND 5 – Methylcellulose, DMSO and Glycerine**

**MIX 5**

Recipe

Samples from previous experiments

Process

The working temperature of 80C for all methylcellulose mixes makes them good options for a hot extrusion process. However, this requires either filaments or pellets to feed the printer. Therefore, a re-melting experiment with cured methylcellulose samples, simulating the material during the printing process, was necessary to validate its feasibility.

Two samples from DAY 3 were selected for the experiment – XXX and XXX – and manipulated in a pan over a heat plate, at first with no water and after with increasing amounts of water.

Outcome

When directly heated, the material started to degrade instead of changing phase and becoming malleable or turning into a paste. Portions of the sample turned darker and charred instead of melting. Adding water did not make a big difference. It evaporated completely and no significant alterations were observed to the material sample. Similar procedure was followed for both material samples, and the overall conclusion was that outer layers of the material would react and dissolve in the water, but no significant melting was occurring. Additional experiments should be executed using an oven and prolonged exposition to constant heat.

## Recipe

Lignin

Cellulose

DMSO

Water

## Process

At first, to understand the material, started with a 1:1 proportion - 2g DMSO and 2g lignin - resulting in a dark brown and homogeneous paste, with low viscosity and low bonding. Adding 1g lignin turned it into a dry and disperse non-homogeneous mix with remains of lignin on the walls.

Second attempt started with a 1:2 proportion – 5g DMSO and 10g lignin. Mix was as homogeneous as the previous one, but drier and with higher viscosity. Adding 0.5g cellulose turned it non-homogeneous and created chunks, demanding for more DMSO to be incorporated (5g). Result was still a non-homogeneous paste with chunks and portions of liquid which do not mix well with the fibres.

Last attempt changed the proportions to 1:1.5 and raised the quantities to 20g DMSO and 30g lignin, turning into a homogeneous and highly viscous paste. Continued by adding 5g papier mache, 1g cellulose and 30g water to facilitate mixing, resulting in a homogeneous paste with moderated viscosity and high bonding.

## Outcome

DMSO proved to be an effective binding agent when combined with lignin, forming homogeneous mixes. With cellulose, the proportions still must be refined to avoid agglomeration of fibres. From the last iteration, a homogeneous paste could be easily extruded by hand with a syringe, although it could not keep a stable layer structure. More cellulose and lignin are necessary to create a less viscous material.

**MIX 7**

## Recipe

Lignin

Cellulose

Glycerine

Water

## Process

At room temperature, a 1:1 ratio mix was prepared with 10g glycerine and 10g lignin, which did not combine until 1g cellulose was added, resulting in a homogeneous gel with low viscosity and bonding. More lignin (5g) and cellulose (1g) were added, finalising with a homogeneous and extrudable paste.

To assess the influence of heat, glycerine (25g) was mixed with hot water (100g) at a 1:4 ratio, creating a non-homogeneous solution. Added 25g lignin – in increments of 5g – continued with 5g papier mache and finally 2g cellulose, resulting in a homogeneous, dry and crumbly mix.

## Outcome

There were no significant differences in the material behaviour between cold and hot processes. Both resulted in homogeneous pastes with moderated to low viscosity and bonding, extrudable by hand with a syringe. Overloading it with cellulose and papier mache fibres (second iteration) turned it into a dry material with a crumbly aspect and a gel-like consistency, not extrudable.

**MIX 8**

Recipe

Lignin

Cellulose

DMSO

Water

Process

DMSO was identified as a promising binding agent in the previous experiments, and to refine the recipe, the material ratio had to be studied.

First iteration was a 1:1 ratio of DMSO and water – 10g each. Mixing it with 10g lignin and 1g cellulose formed a non-homogeneous paste with chunks of fibres, moderated viscosity and low bonding, but still easy to extrude with a syringe. Adding 5g papier mache improved the homogeneity and bonding and maintained the extrudability.

As an extra step, to evaluate the necessity and minimum amount of water, the experiment was repeated with DMSO only. It resulted in a dry and non-homogeneous mix, too viscous and with large chunks of fibres making it difficult to extrude.

Second iteration was a 0.5:1 ratio of DMSO and water – 5g and 10g respectively. Mixing it with 10g lignin and 1g cellulose formed a watery non-homogeneous paste with large chunks of fibres, low viscosity and bonding. Adding 2g papier mache improved it slightly but it was not extrudable by hand.

Third iteration was a 0.25:1 ratio of DMSO and water – 2.5g and 10g respectively. Mixing it with 5g lignin and 1g cellulose formed a non-homogeneous paste with large chunks of fibres dissociated from the lignin/DMSO mix, with low viscosity and no bonding.

Fourth iteration was a 1.5:1 ratio of DMSO and water – 15g and 10g respectively. Mixing it with 20g lignin and 1g cellulose formed a homogeneous paste with moderated viscosity and high bonding, easy to extrude. Adding 5g lignin and 2g

cellulose kept the homogeneity and increased the viscosity and bonding, still within the threshold for a smooth extrusion.

At last, the fifth iteration was a 2:1 ratio of DMSO and water – 20g and 10g respectively. Mixing it with 30g lignin and 2g cellulose formed a homogeneous paste with moderated viscosity and high bonding, easy to extrude. Continued by adding 5g lignin and 2g cellulose, resulting in a homogeneous paste with high viscosity and bonding, difficult to handle but smooth to extrude.

## Outcome

DMSO reacts on a similar manner as acetone when mixed with lignin, creating a paste with high bonding and moderated to high viscosity, depending on the material ratio, but without the hazardous aspect. Water is still necessary to dilute the binder, avoid material dispersion and to humidify the fibres, but in small quantities to avoid chunks and watery mixes. From these experiments, the ideal material ratios can be defined as 2:1 for DMSO/water, 1:1.75 for DMSO/lignin and 1:8.75 for cellulose/lignin. As observed, higher quantities of lignin improve the bonding and viscosity even though turning the extrusion harder by drying the material and favouring the creation of chunks of fibres not homogeneously mixed. Recipe is promising as it deliver stable and structured extrusions, however it still needs refinements according to the available printing setup – nozzle size, pressure and speed.

**ROUND 7 – Alginate & Corn Starch**


**MIX 9**


**Recipe**


Lignin

Cellulose

Corn Starch

Water


**Process**


First iteration was a 1:1 ratio of corn starch and water – 10g each. Mixing it with 10g lignin and 1g cellulose resulted on a non-homogeneous, crumbly and dry mix. Added 10g water and it transformed into a paste, still non-homogeneous and with chunks of fibres agglomerated with water, non-viscous and non-bonding.

Second iteration was a 0.5:1 ratio of corn starch and water – 5g and 10g respectively. Mixing it with 5g lignin and 1g cellulose resulted in a non-homogeneous and dry mix which would quickly solidify under pressure or if not constantly stirred. Added 5g water to facilitate the handling but paste remained non-homogeneous with chunks of fibres, non-viscous and non-bonding.

Third iteration was a 0.25:1 ratio of corn starch and water – 2.5g and 10g respectively. Mixing it with 5g lignin and 1g cellulose resulted in a non-homogeneous and dry mix similar to the previous ones. Added 5g water and it became easier to handle, although still non-homogeneous, non-viscous and non-bonding.

Fourth iteration was a 1.5:1 ratio of corn starch and water – 15g and 10g respectively. Mixing 5g lignin resulted in a homogeneous paste with low viscosity and non-bonding. Adding 5g water and 1g cellulose, once again turned the mix into a dry and non-homogeneous paste, non-viscous and non-bonding.

The fifth iteration was a 2:1 ratio of corn starch and water – 20g and 10g respectively. The small amount of water made it powdery from the start, worsening once 5g lignin were added. Adding 10g water made it similar to the previous experiments, drying out and forming chunks once 1g cellulose was mixed. Non-viscous and non-bonding outcome.

As a final attempt to create an extrudable mix, the experiment with a 1:1 ratio of corn starch and water was replicated at high temperatures. After a few more failed trials, which also resulted in non-homogeneous pastes, mixing the corn starch and lignin before adding water at a 3:1 ratio – 30g corn starch and 10g lignin – delivered a homogeneous paste. When mixed with 1g cellulose, it resulted in an extrudable material with moderated viscosity and bonding.

## Outcome

All cold mixes with corn starch failed at creating an extrudable paste. Materials did not bind well and the result was constantly a non-homogeneous paste with chunks of fibres agglomerated with water. Lignin did not build strong bonds with any of the ingredients, becoming brittle and powdery once the samples dried.

The final attempt with a hot mix proved to be successful at delivering an extrudable material. However, the homogeneity, viscosity and bonding characteristics are not as promising as previous mixes with DMSO and other binding agents.

**MIX 10**

### Recipe

Lignin

Cellulose

Alginate

Water

### Process

A mix with ratio of 1:1 of alginate and water – 10g of each – was prepared, resulting in a non-homogeneous solution with chunks of gel. Additional 40g water were mixed until the liquid mixed more, still with chunks, which would not dissolve even when heated. Added 5g lignin and 1g cellulose, however the material consistency remained similar to a gel, homogeneous but with extremely low viscosity and bonding.

### Outcome

The experiments were planned on a similar structure as the previous ones, with ratios of 1:1, 0.5:1, 0.25:1, 1.5:1 and 2:1 of alginate and water to be studied. Although, the first iteration already showed the material would have a similar behaviour to xanthan gum and glycerine, which did not present promising results, therefore, the remaining experiments were scrapped.

## ROUND 8 – Bone Glue & Bee Wax

### MIX 11

### Recipe

Lignin

Cellulose

Bee Wax

Water

### Process

At first, bee wax was mixed with hot water in a 1:1 ratio – 100g each – and melted using a recipient in a water bath, to keep a constant and high temperature without the risk of burning the mix.

For the first experiment, 50g of wax/water solution were mixed to 10g of lignin – a ratio of 5:1 respectively – and 1g cellulose. The result is a completely heterogeneous thick liquid with chunks of fibres partially covered in lignin and chunks of wax.

For the next experiments, 30g bee wax were melted pure and directly in a recipient in a water bath and mixed with 30g lignin, in a 1:1 ratio. The result was a homogeneous thick liquid, to which 2g cellulose were added. Fibres did not mix completely, creating a non-homogeneous paste with moderated viscosity and low bonding.

### Outcome

Despite mixing well with lignin, it created large chunks with cellulose and dried quickly, compromising the material extrudability. The small samples were also brittle and appeared to be porous.

**MIX 12**

## Recipe

Lignin

Cellulose

Bone Glue

Water

## Process

At first, bone glue beads were soaked in water for a week to absorb liquid and soften. From these, 100g were mixed to 100g of water at 80C and kept under constant heat until fully diluted into a 1:1 ratio bone glue and water solution.

For the first experiment, 50g of this solution were added to 10g lignin – a ratio of 5:1 respectively – and 2g cellulose by using a recipient in a water bath. The result was a watery and non-homogeneous paste, with low viscosity and bonding.

For the next attempt no water was used, melting 50g of soften glue directly in a recipient in a water bath, and mixing it with 10g lignin and 2g cellulose at constant heat. The result was a homogeneous paste, with high viscosity and bonding, but still easy to extrude by hand.

## Outcome

The soften glue had already a large amount of water incorporated and did not require any additional liquid to melt. Once that was understood, the mix resulted in a stable and homogeneous paste. The disadvantage of bone glue is the strong smell and the appearance, far from wood.

### Recipe

Lignin
Cellulose
Wood Glue

### Process

In a recipient in a water bath, 30g wood glue were mixed to 10g lignin, in a 3:1 ratio respectively, resulting in a homogeneous paste with a high viscosity and high bonding. No fibres were added, since the mix was already difficult to handle and extrude.

The experiment was replicated at cold and presented similar results, with only the sample colour varying. Added 1g cellulose and resulted in a homogeneous paste with high viscosity and bonding.

### Outcome

Wood glue created some of the most stable and strongest samples from all the materials experimented until this stage. Despite the chemical origins, which could also be bio-based, pending further research, it created a homogeneous material with the adequate properties for a cold extrusion process.

## ROUND 9 – Methylcellulose

## MIX 14

### Recipe

Lignin

Cellulose

Methylcellulose

Water

### Process

The base for all these experiments was a 1:10 solution of methylcellulose in hot water – 5g and 50g respectively – mixed in a recipient in a water bath until forming a homogeneous and opaque liquid.

For the first iteration, 15g lignin and 2g cellulose were mixed, still in a water bath, resulting in a non-homogeneous paste, with moderate viscosity and bonding, possible to extrude. Continued by adding 5g lignin and 10g water until the paste became homogeneous and the viscosity and bonding increased. Extrusion was easier than the previous one since the chunks of fibres were dissolved, and the outcome sample had a smooth finishing and a more structured layer composition with the higher amount of lignin.

For the second iteration, 10g lignin and 1g cellulose were mixed to the methylcellulose solution, still in a water bath. The result was a homogeneous mix with moderated viscosity and bonding, easy to extrude and with no chunks.

Third iteration was a trial with only 1g cellulose to verify the reaction with methylcellulose, forming a non-homogeneous white paste. Continuing, 2g lignin were added, resulting in a non-homogeneous and crumbly mix, not extrudable.

The fourth iteration was a combination of 15g lignin, 5g papier mache and 2g cellulose, mixed until becoming homogeneous. Result was a dry paste, with high viscosity and moderated bonding, difficult to extrude. Continuing, 10g lignin and 20g water were added, improving the homogeneity, viscosity and bonding, although not enough for a smooth extrusion, remaining dry and brittle.

For the fifth iteration, 25g lignin were mixed with 2g cellulose, leading to a non-homogeneous and dry paste, non-extrudable. Added 15g water, 3g lignin and 1g cellulose, improving the paste but still too hard to extrude, with chunks of fibres and low bonding properties.

The sixth and last iteration started with 15g lignin only, mixed until forming a homogeneous paste, before adding 2g cellulose with well grinded and separated fibres. Result was a paste with moderated viscosity and high bonding, hard to extrude but with smooth appearance. Continued by adding 10g lignin and 10g water, increasing the viscosity and bonding although reducing the extrudability.

## Outcome

Methylcellulose is a promising binding agent which generally results in homogeneous and viscous pastes with good extrudability and bonding when combined with lignin. It is activated at 80C and becomes viscous once the mix temperature drops. Increasing the amount of lignin improves the bonding properties of the mix, but also makes it harder to extrude and brittle once dry, hence the role of cellulose fibres to reduce the brittleness and increase the material tensile strength.

The amount of cellulose should also be controlled to avoid the formation of fibre clots reducing the extrudability and homogeneity. As an alternative, papier mache initially makes the material more malleable and homogeneous, however it results in a dry and crumbly material, with low bonding properties.

## ROUND 10 – Acetone & Methylcellulose

## MIX 15

## Recipe

24g Lignin

2g Cellulose

11.2g Acetone

8g Water

## Process

This experiment was a complete reproduction of the state of the art mix developed by Thomas Liebrand, the start point of this research, from recipe to process and outcome. Cellulose was grinded and blended first, to separate the fibres, then mixed with lignin. Water was added during the process to avoid material losses through dispersion, although impossible to avoid entirely and quantify. Once the fibres were completely covered with the lignin powder, acetone was added and mixed until forming a homogeneous paste with no chunks, high bonding and moderated viscosity.

For the second iteration, water was removed from the recipe to reduce the possibility of forming fibre chunks. Experiment did not work, cellulose fibres were too dry and did not react with the lignin and acetone mix, resulting in a portion of lignin partially combined with acetone and covered in scarce fibres.

For the final iteration, the initial recipe was followed and 2-3g lignin were added to compensate for the material loss during mixing. Resulting mix was similar to the first attempt, a bit less viscous and more suitable for layered structures.

## Outcome

Mixes 1 and 3 were easy to extrude with the caulking gun and produced wall-like layered structures. The differences between both outcomes are mainly the extrusion speed – high and low respectively – and the nozzle size – 3.8mm and 2.9mm

respectively. Due to these settings, the last experiment produced a higher definition structure, smoother and with more refined details such as layer boundaries and more precise angles. Acetone is a promising binding agent, although its hazardous behaviour makes it difficult to manipulate in large quantities and its reaction with plastic demands glassware and metallic equipment instead of plastic tubes and plates, creating an obstacle to the operation of the material extruder.

**MIX 16**

## Recipe

Lignin

Cellulose

Methylcellulose

Water

## Process

The aim of this experiment was to refine the recipe and the proportions between raw materials. As verified prior, a 1:10 solution of methylcellulose and water offered the best results. For this experiment, to maximize the material strength and increase the amount of lignin, more water was added to the recipe from the beginning at a ratio of 1:12 – 5g methylcellulose and 60g water.

For all iterations, cellulose was first grinded then blended to separate the fibres. Lignin and methylcellulose were then added and blended – in an enclosed recipient to reduce material losses – until all fibres were fully covered with the powdery mix. At last, hot water at 80C minimum was added and the mix continuously blended until forming a watery and homogeneous paste with consistency, viscosity and bonding properties variable according to the mix temperature.

For the first iteration, a ratio of 4:1 of lignin and methylcellulose – 20g and 5g respectively – was used, combined with 2g cellulose. However, it was blended for too long, resulting in a dry and crumbly mix. Added more water, methylcellulose and lignin at unmeasured quantities to evaluate if it could be improved, but the outcome was not good and the paste remained too liquid, forming structures that would lose their layer structure once manually extruded.

For the second iteration, the same recipe was followed – 20g lignin, 5g methylcellulose and 2g cellulose – however the mix temperature was kept at a minimum of 50C until homogeneous, reaching a moderated viscosity and high bonding properties, suitable for extruding and forming wall-like structures.

For the third iteration, a ratio of 5:1 of lignin and methylcellulose – 25g and 5g respectively – was used, combined with 3g cellulose. Resulting mix showed moderated to high viscosity and high bonding, drier and denser than the previous one due to the increased amount of lignin. Harder to extrude although successful at building layered structures.

At last, for the fourth iteration, a ratio of 6:1 of lignin and methylcellulose – 30g and 5g respectively – was used, combined with 3g cellulose. Result was dry and dense paste which required additional 5g water, transforming it into a mix with even higher bonding and viscosity than the previous one. Harder to extrude, it formed well defined layered structures, with promising interlayer bonding.

## Outcome

As expected, increasing the amount of lignin in the mix improves the viscosity and bonding properties of the material, although it also increases its brittleness and tends to transform it into a crumbly and dry paste. Water and cellulose fibres keep the mix homogeneous and the paste consistency necessary for a successful extrusion and product, however the amount of fibres and the blending with the remaining raw materials will determine if it is a homogeneous material or if fibre clots will be disperse in the paste. From the experiments above, the outcome is that a proportion of 6:1 between lignin and methylcellulose proved to be the most promising recipe, as well as a proportion of 1:20 between cellulose and lignin. Additional experiments with increased amounts of fibres should be executed to potentially increase the material strength and flexibility.

## ROUND 11 – Baking Soda & Sunflower Oil


## MIX 17


### Recipe

Lignin

Cellulose

Methylcellulose

Baking Soda

Water

Sunflower Oil


### Process

For the last round of experiments, the objective was to improve the dissolution of lignin in the aqueous mixture and at the same time to investigate a way of reducing the amount of water necessary, consequently avoiding issues with shrinkage and deformation at curing.

At first, methylcellulose was mixed with alkaline water and with sunflower oil, in different proportions, to analyse the behaviour of such mixes and the potential at combining it with cellulose and lignin. Oil made the material greasy and delayed the curing time. Baking soda seemed to make the material less brittle, but also demanded more water to result in a homogeneous paste.

For the following part of the study, baking soda and water were mixed in a ratio of 1:125 – 2g and 250g respectively – to create alkaline water, which was used instead of pure water to reproduce the last recipe from the previous experiment. A mix of 30g lignin, 5g methylcellulose and 3g cellulose was blended and combined with 60g alkaline water, heated at 80C, resulting in a dry and crumbly material. Added 40g more alkaline water – 10g at a time – until it formed a dry and partially homogeneous paste with moderated viscosity and bonding, difficult to extrude by hand.

Continuing with the same mix, more alkaline water was added to improve the flow, losing the adhesion between matrix and fibres. More lignin was added, to reinforce the matrix, but the material bonding did not improve significantly. At last, more

cellulose was added, which only formed chunks and resulted in a non-homogeneous mix.

The next experiment was to mix oil with methylcellulose, lignin and cellulose, in unmeasured quantities at first, to understand the materials' behaviour. In general, the fibres created chunks and the oil just made the material greasy and delayed the curing time, proving it cannot completely replace water.

Following the study, a balance between oil and water was attempted at an initial ratio of 1:1 – 25g of each. Mixed and blended 20g lignin, 5g methylcellulose and 2g cellulose and added to the liquid mix, continuously blending it. The result was a well mixed although dry and crumbly material. Half of it was then mixed with 20g water and the other half with 20g oil, creating two homogeneous and extrudable mixes, with moderated viscosity and bonding. Added 10g lignin and 10g water, resulting in a less greasy and more homogeneous mix, with moderated viscosity and high bonding, dense, difficult to extrude.

At last, one final experiment with a ratio of 1:1:12 of baking soda, methylcellulose and water – 5g, 5g and 60g respectively – was executed. Following the mixing procedure adopted at the previous experiments, 20g lignin and 2g cellulose were blended together with baking soda and methylcellulose until well mixed and fibres had a good coverage. Added water and blended continuously until a dry, dense and homogeneous paste was formed, too viscous and difficult to extrude.


## Outcome


In general, adding baking soda in the recipe, either in the form of alkaline water or directly as an additive with the remaining raw materials, made the mix dry and crumbly, demanding more water to be added in order to create an extrudable paste. It alters the colour of the material, resulting on a dark brown matte exterior and a medium brown interior. In terms of properties, it reduced the curing time and seemed to create a hard exterior, although the excessive water most likely would create shrinkage and porosity issues.

Oil, however, made the mix less viscous in general, increasing the curing time and resulting in greasy and gelatinous mixes instead of pastes. It partially facilitates the extrusion, but does not provide a good option at replacing the water in the mix.

## 8.2. Mechanical Tests Data Sets

| Specimen A1.1 | | | |
|---|---|---|---|
| | Unit | Initial | Tested |
| Area | | | |
| Length - total | mm | 230 | 218 |
| Length - gauge | mm | 90 | 87 |
| Width - grip | mm | 24 | 21 |
| Width - gauge | mm | 12 | 8.5 |
| Thickness | mm | 6 | 4.5 |
| Cross Section Area | mm² | 72 | 38.25 |

STRAIN | Elongation divided by length

$$\varepsilon = \frac{\delta}{L}$$

STRESS | Axial force divided by cross section area

$$\sigma = \frac{P}{A}$$

MODULUS OF ELASTICITY | Stress divided by strain

$$\sigma = E\varepsilon$$

MODULUS OF ELASTICITY | Constant in graph's equation

| Specimen A1.1 | | |
|---|---|---|
| | Unit | Value |
| $\delta$ at $\sigma$ max | mm | 1.18694 |
| $\varepsilon$ at $\sigma$ max | - | 0.013643 |
| $\sigma$ max | MPa | 3.596052 |
| Yield Stress | MPa | 3.508261 |
| Young's Modulus | MPa | 374.16 |

Specimen A1.1 | Stress - Strain

y = 374.16x + 0.0751
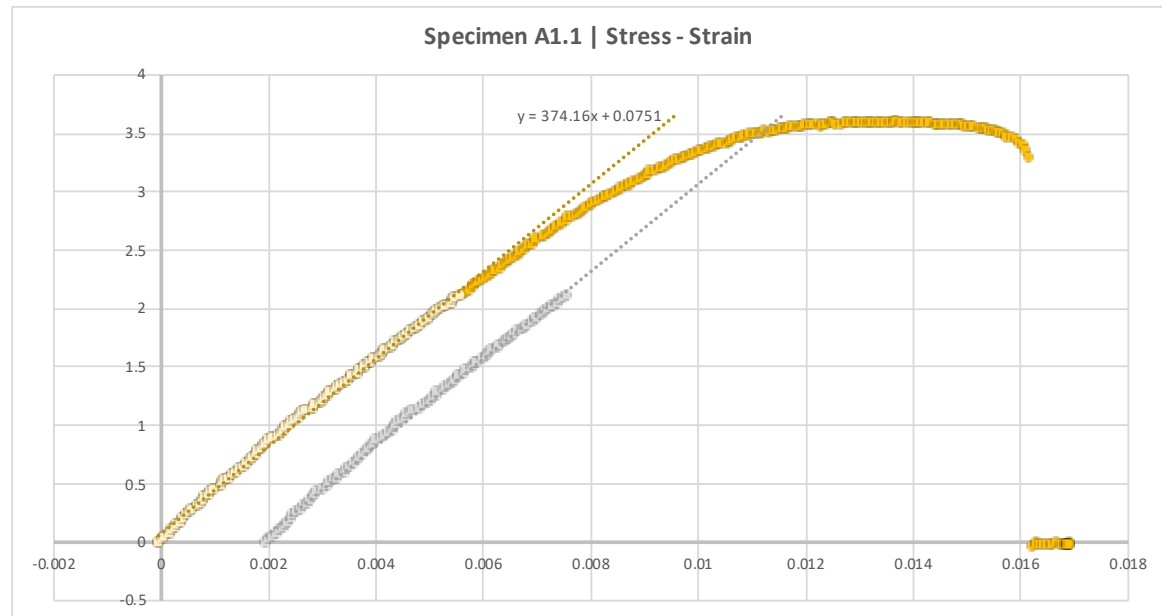
## Specimen A1.2

| | Unit | Initial | Tested |
|---|---|---|---|
| **Area** | | | |
| **Length - total** | mm | 230 | 218 |
| **Length - gauge** | mm | 90 | 87.5 |
| **Width - grip** | mm | 24 | 21 |
| **Width - gauge** | mm | 12 | 10 |
| **Thickness** | mm | 6 | 4.5 |
| **Cross Section Area** | mm² | 72 | 45 |

STRAIN | Elongation divided by length

$$\varepsilon = \frac{\delta}{L}$$

STRESS | Axial force divided by cross section area

$$\sigma = \frac{P}{A}$$

MODULUS OF ELASTICITY | Stress divided by strain

$$\sigma = E\varepsilon$$

MODULUS OF ELASTICITY | Constant in graph's equation

## Specimen A1.2

| | Unit | Value |
|---|---|---|
| **$\delta$ at $\sigma$ max** | mm | 1.23773 |
| **$\varepsilon$ at $\sigma$ max** | - | 0.014145 |
| **$\sigma$ max** | MPa | 2.944867 |
| **Yield Stress** | MPa | 2.888644 |
| **Young's Modulus** | MPa | 249.61 |



Specimen A1.2 | Stress - Strain

y = 249.61x + 0.0609
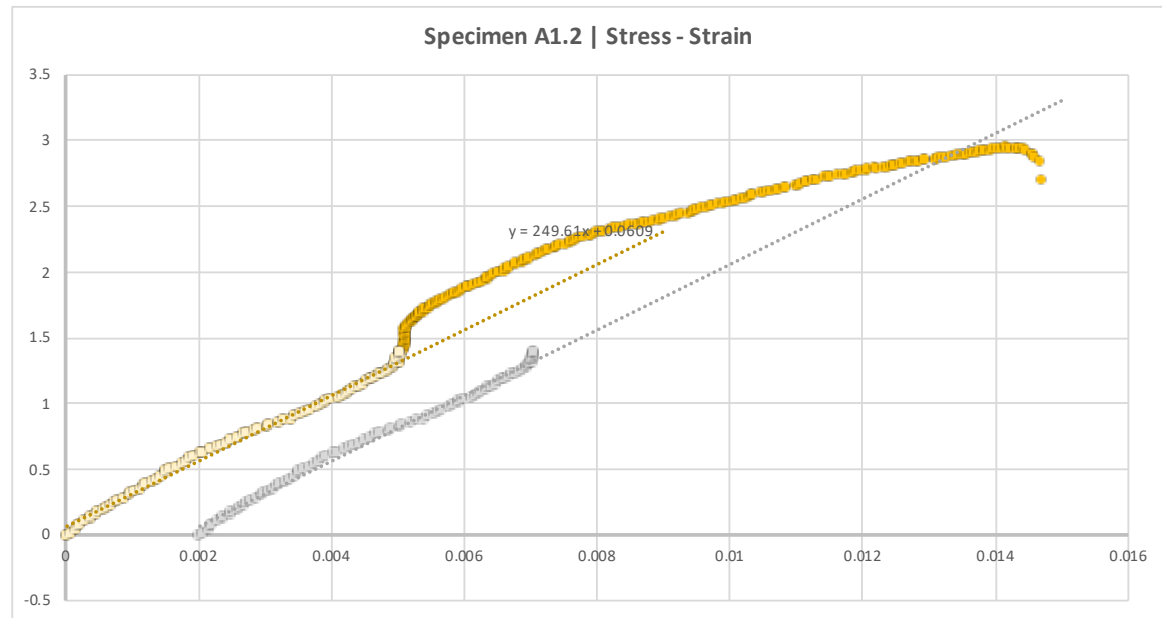
| Specimen A1.3 | | | |
|---|---|---|---|
| | **Unit** | **Initial** | **Tested** |
| **Area** | | | |
| **Length - total** | mm | 230 | 216 |
| **Length - gauge** | mm | 90 | 85 |
| **Width - grip** | mm | 24 | 20 |
| **Width - gauge** | mm | 12 | 9 |
| **Thickness** | mm | 6 | 4.1 |
| **Cross Section Area** | mm² | 72 | 36.9 |

STRAIN | Elongation divided by length

$$\varepsilon = \frac{\delta}{L}$$

STRESS | Axial force divided by cross section area

$$\sigma = \frac{P}{A}$$

MODULUS OF ELASTICITY | Stress divided by strain

$$\sigma = E\varepsilon$$

MODULUS OF ELASTICITY | Constant in graph's equation

| Specimen A1.3 | | |
|---|---|---|
| | **Unit** | **Value** |
| $\delta$ at $\sigma$ max | mm | 0.979081 |
| $\varepsilon$ at $\sigma$ max | - | 0.011519 |
| $\sigma$ max | MPa | 4.289946 |
| **Yield Stress** | MPa | 3.793306 |
| **Young's Modulus** | MPa | 558.97 |

**Specimen A1.3 | Stress - Strain**

y = 558.97x + 0.0991
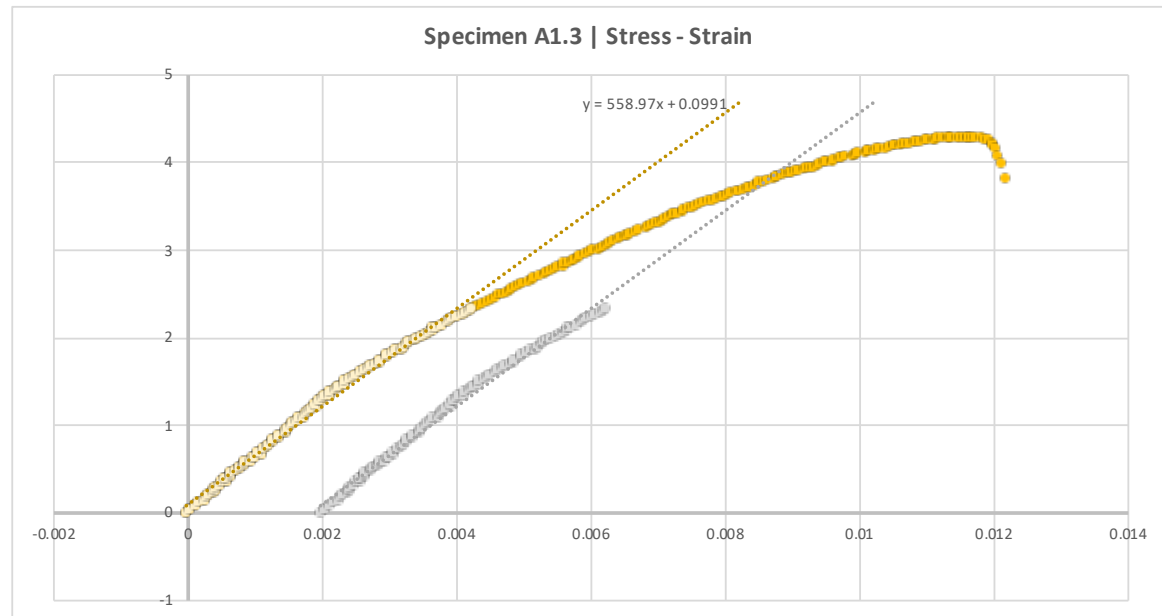
### Specimen A1.4

| | Unit | Initial | Tested |
|---|---|---|---|
| **Area** | | | |
| **Length - total** | mm | 230 | 219 |
| **Length - gauge** | mm | 90 | 87 |
| **Width - grip** | mm | 24 | 21 |
| **Width - gauge** | mm | 12 | 10 |
| **Thickness** | mm | 6 | 4.1 |
| **Cross Section Area** | mm² | 72 | 41 |

STRAIN | Elongation divided by length

$$\varepsilon = \frac{\delta}{L}$$

STRESS | Axial force divided by cross section area

$$\sigma = \frac{P}{A}$$

MODULUS OF ELASTICITY | Stress divided by strain

$$\sigma = E\varepsilon$$

MODULUS OF ELASTICITY | Constant in graph's equation

### Specimen A1.4

| | Unit | Value |
|---|---|---|
| $\delta$ at $\sigma$ max | mm | 0.964283 |
| $\varepsilon$ at $\sigma$ max | - | 0.011084 |
| $\sigma$ max | MPa | 4.072341 |
| **Yield Stress** | MPa | 4.063 |
| **Young's Modulus** | MPa | 449.6 |



**Specimen A1.4 | Stress - Strain**

y = 449.6x + 0.0207
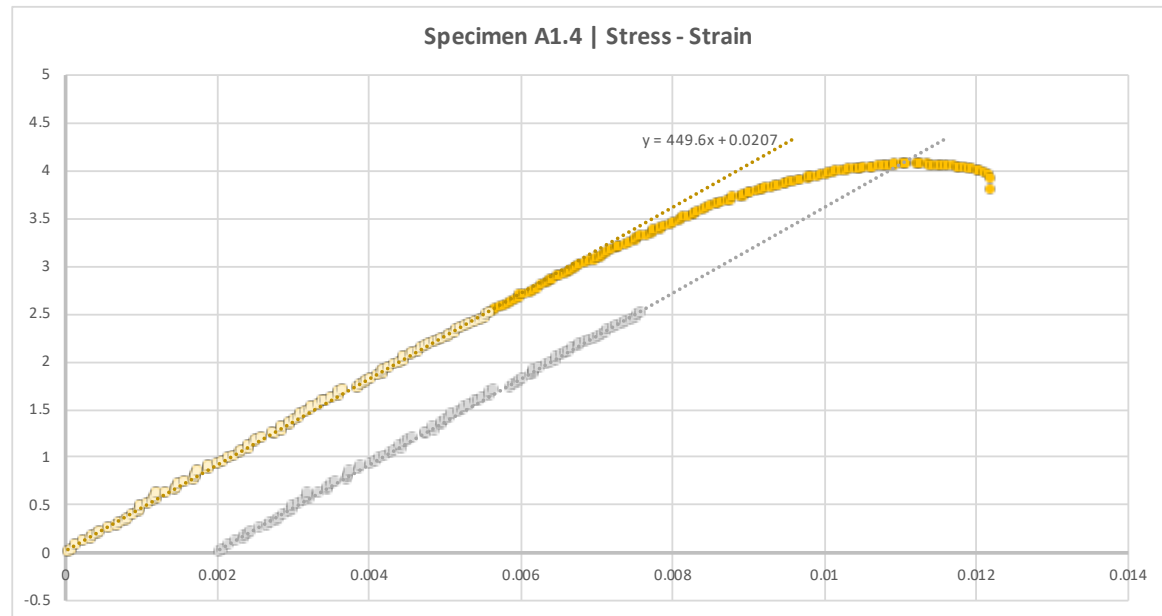
| Specimen 01 | | | |
|---|---|---|---|
| | Unit | Initial | Tested |
| Area | | | |
| Length - total | mm | 210 | 196.5 |
| Length - gauge | mm | 80 | 75 |
| Width - grip | mm | 22 | 20 |
| Width - gauge | mm | 10 | 8.5 |
| Thickness | mm | 4 | 4 |
| Cross Section Area | mm² | 40 | 34 |

STRAIN | Elongation divided by length

$$\varepsilon = \frac{\delta}{L}$$

STRESS | Axial force divided by cross section area

$$\sigma = \frac{P}{A}$$

MODULUS OF ELASTICITY | Stress divided by strain

$$\sigma = E\varepsilon$$

MODULUS OF ELASTICITY | Constant in graph's equation

| Specimen 01 | | |
|---|---|---|
| | Unit | Value |
| $\delta$ at $\sigma$ max | mm | 0.899369 |
| $\varepsilon$ at $\sigma$ max | - | 0.011992 |
| $\sigma$ max | MPa | 3.369765 |
| Yield Stress | MPa | 3.207559 |
| Young's Modulus | MPa | 333.78 |



Specimen 01 | Stress - Strain

y = 333.78x + 0.0878
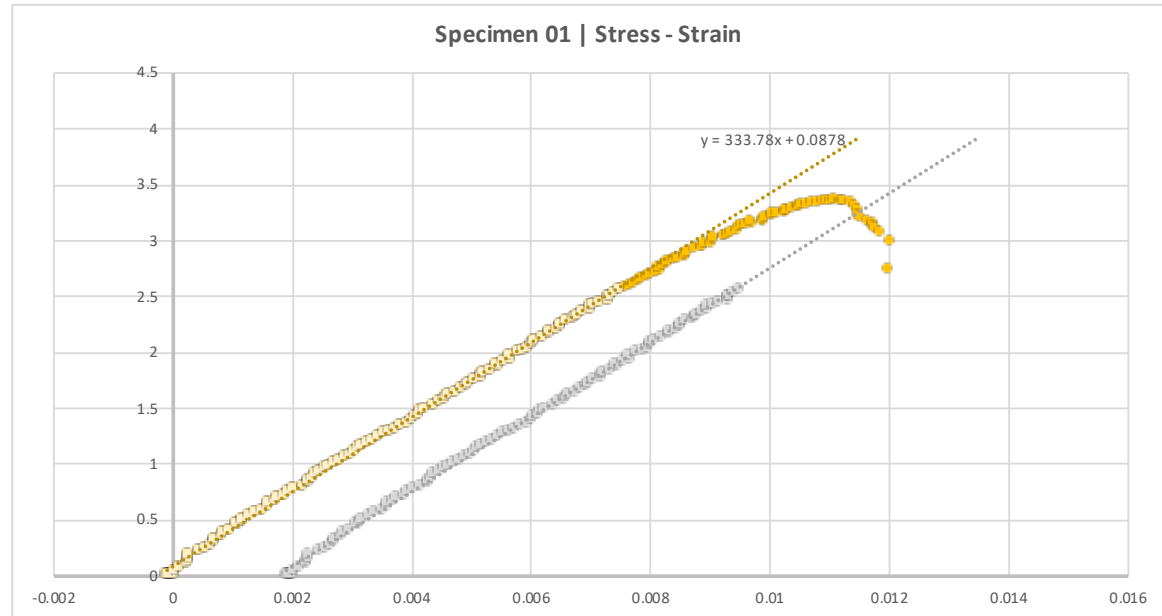
## Specimen 04

| | Unit | Initial | Tested |
|---|---|---|---|
| Area | | | |
| Length - total | mm | 210 | 196.5 |
| Length - gauge | mm | 80 | 75 |
| Width - grip | mm | 22 | 19.5 |
| Width - gauge | mm | 10 | 8.5 |
| Thickness | mm | 4 | 4 |
| Cross Section Area | mm² | 40 | 34 |

STRAIN | Elongation divided by length

$$\varepsilon = \frac{\delta}{L}$$

STRESS | Axial force divided by cross section area

$$\sigma = \frac{P}{A}$$

MODULUS OF ELASTICITY | Stress divided by strain

$$\sigma = E\varepsilon$$

MODULUS OF ELASTICITY | Constant in graph's equation

## Specimen 04

| | Unit | Value |
|---|---|---|
| $\delta$ at $\sigma$ max | mm | 0.76517 |
| $\varepsilon$ at $\sigma$ max | - | 0.010202 |
| $\sigma$ max | MPa | 3.737382 |
| Yield Stress | MPa | 3.634824 |
| Young's Modulus | MPa | 518.57 |

### Specimen 01 | Stress - Strain

y = 518.57x + 0.0146
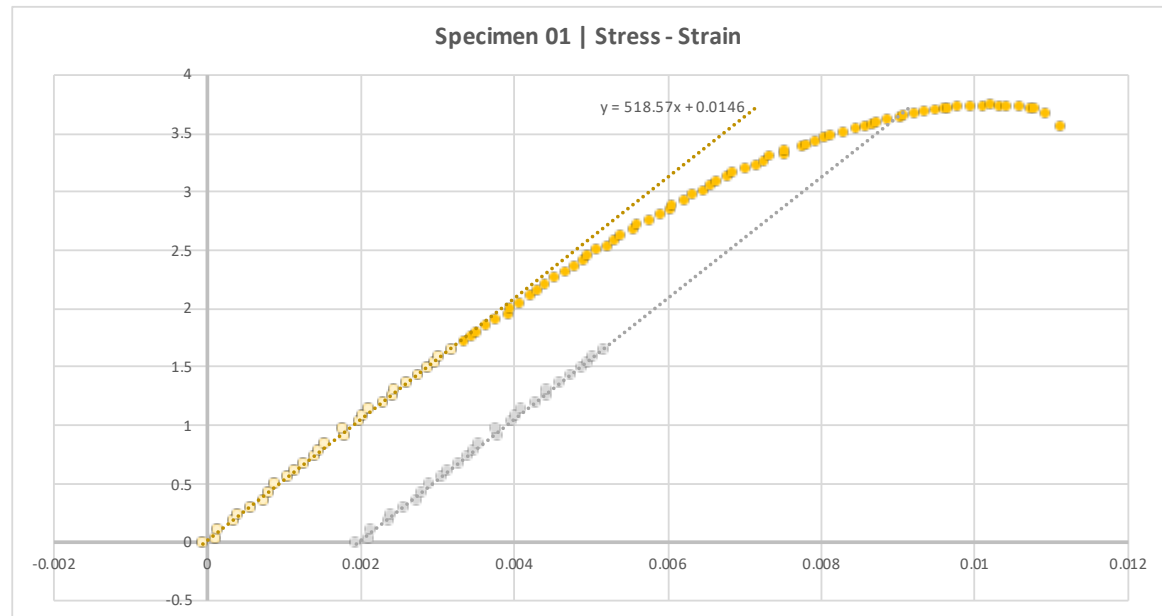
| Specimen A2.1 | | | |
|---|---|---|---|
| | Unit | Initial | Tested |
| Area | | | |
| Length - total | mm | 230 | 227 |
| Length - gauge | mm | 90 | 85 |
| Width - grip | mm | 24 | 24 |
| Width - gauge | mm | 12 | 11 |
| Thickness | mm | 6 | 6 |
| Cross Section Area | mm² | 72 | 66 |

STRAIN | Elongation divided by length

$$\varepsilon = \frac{\delta}{L}$$

STRESS | Axial force divided by cross section area

$$\sigma = \frac{P}{A}$$

MODULUS OF ELASTICITY | Stress divided by strain

$$\sigma = E\varepsilon$$

MODULUS OF ELASTICITY | Constant in graph's equation

| Specimen A2.1 | | |
|---|---|---|
| | Unit | Value |
| $\delta$ at $\sigma$ max | mm | 1.55052 |
| $\varepsilon$ at $\sigma$ max | - | 0.018241 |
| $\sigma$ max | MPa | 1.756197 |
| Yield Stress | MPa | 1.093336 |
| Young's Modulus | MPa | 275.39 |

**Specimen A2.1 | Stress - Strain**

y = 275.39x + 0.0178
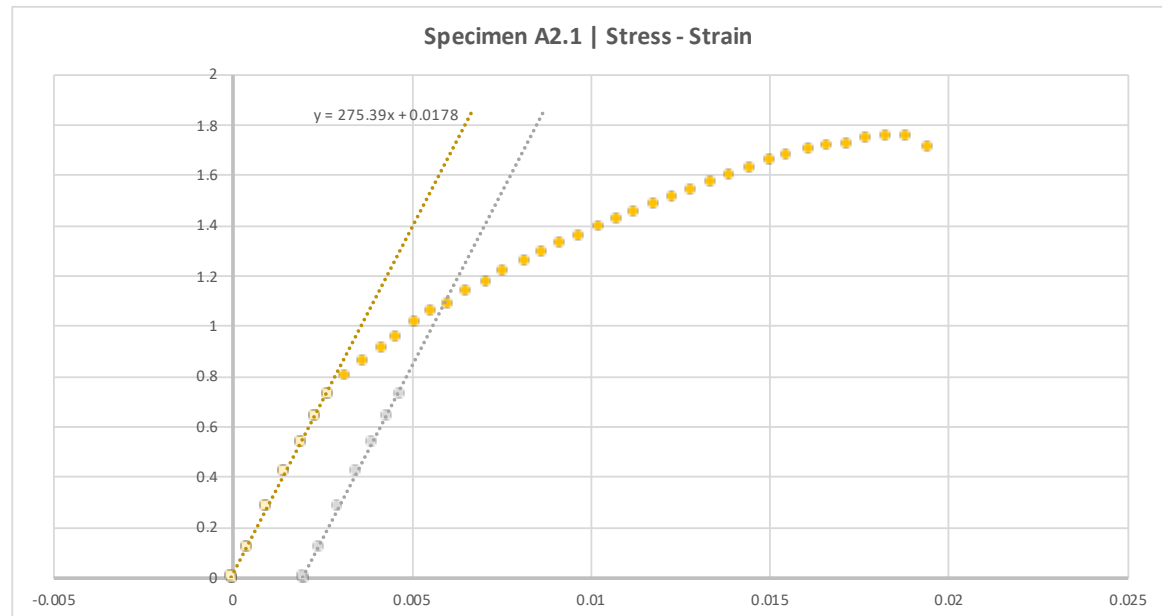
| Specimen A2.2 | | | |
|---|---|---|---|
| | Unit | Initial | Tested |
| Area | | | |
| Length - total | mm | 230 | 225 |
| Length - gauge | mm | 90 | 85 |
| Width - grip | mm | 24 | 23 |
| Width - gauge | mm | 12 | 12 |
| Thickness | mm | 6 | 6 |
| Cross Section Area | mm² | 72 | 72 |

STRAIN | Elongation divided by length

$$\varepsilon = \frac{\delta}{L}$$

STRESS | Axial force divided by cross section area

$$\sigma = \frac{P}{A}$$

MODULUS OF ELASTICITY | Stress divided by strain

$$\sigma = E\varepsilon$$

MODULUS OF ELASTICITY | Constant in graph's equation

| Specimen A2.2 | | |
|---|---|---|
| | Unit | Value |
| $\delta$ at $\sigma$ max | mm | 1.12942 |
| $\varepsilon$ at $\sigma$ max | - | 0.013287 |
| $\sigma$ max | MPa | 1.257501 |
| Yield Stress | MPa | 1.253636 |
| Young's Modulus | MPa | 105.35 |

**Specimen A2.2 | Stress - Strain**

y = 105.35x + 0.0274
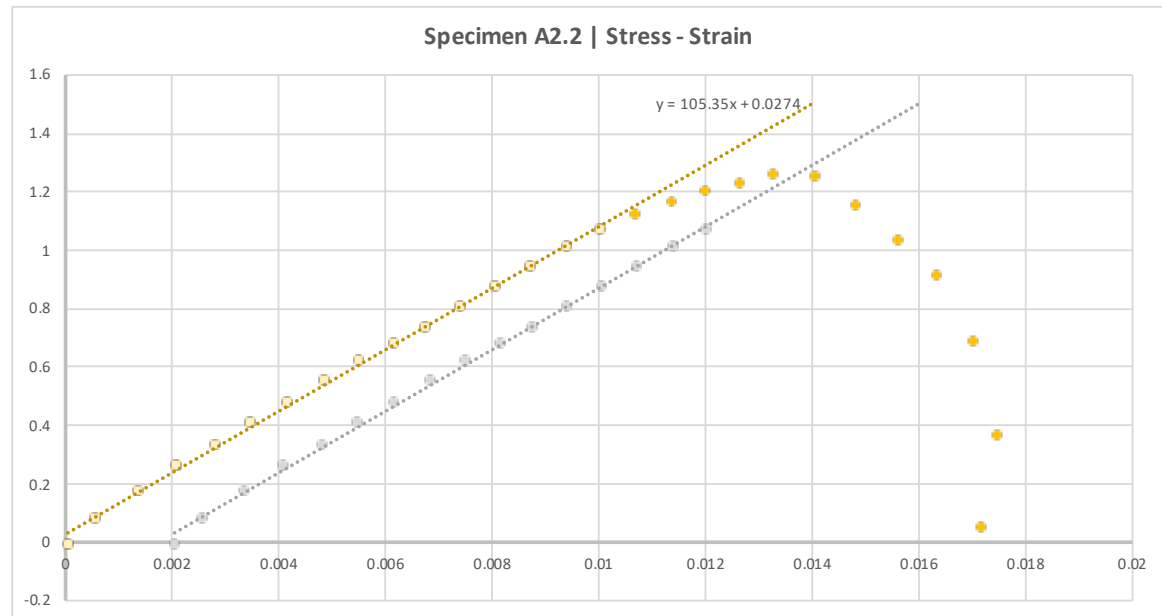
| Specimen A2.3 | | | |
|---|---|---|---|
| | Unit | Initial | Tested |
| Area | | | |
| Length - total | mm | 230 | 226 |
| Length - gauge | mm | 90 | 85 |
| Width - grip | mm | 24 | 25 |
| Width - gauge | mm | 12 | 11 |
| Thickness | mm | 6 | 6 |
| Cross Section Area | mm² | 72 | 66 |

STRAIN | Elongation divided by length

$$\varepsilon = \frac{\delta}{L}$$

STRESS | Axial force divided by cross section area

$$\sigma = \frac{P}{A}$$

MODULUS OF ELASTICITY | Stress divided by strain

$$\sigma = E\varepsilon$$

MODULUS OF ELASTICITY | Constant in graph's equation

| Specimen A2.3 | | |
|---|---|---|
| | Unit | Value |
| $\delta$ at $\sigma$ max | mm | 1.23436 |
| $\varepsilon$ at $\sigma$ max | - | 0.014522 |
| $\sigma$ max | MPa | 1.702985 |
| Yield Stress | MPa | 1.505706 |
| Young's Modulus | MPa | 204.83 |

**Specimen A2.3 | Stress - Strain**

y = 204.83x + 0.0112

## Specimen A2.4

| | Unit | Initial | Tested |
|---|---|---|---|
| Area | | | |
| Length - total | mm | 230 | 228 |
| Length - gauge | mm | 90 | 85 |
| Width - grip | mm | 24 | 24 |
| Width - gauge | mm | 12 | 12 |
| Thickness | mm | 6 | 6.5 |
| Cross Section Area | mm² | 72 | 78 |

STRAIN | Elongation divided by length

$$\varepsilon = \frac{\delta}{L}$$

STRESS | Axial force divided by cross section area

$$\sigma = \frac{P}{A}$$

MODULUS OF ELASTICITY | Stress divided by strain

$$\sigma = E\varepsilon$$

MODULUS OF ELASTICITY | Constant in graph's equation

## Specimen A2.4

| | Unit | Value |
|---|---|---|
| $\delta$ at $\sigma$ max | mm | 1.53639 |
| $\varepsilon$ at $\sigma$ max | - | 0.018075 |
| $\sigma$ max | MPa | 1.092912 |
| Yield Stress | MPa | 0.807859 |
| Young's Modulus | MPa | 126.89 |



Specimen A2.4 | Stress - Strain

y = 126.89x + 0.0187
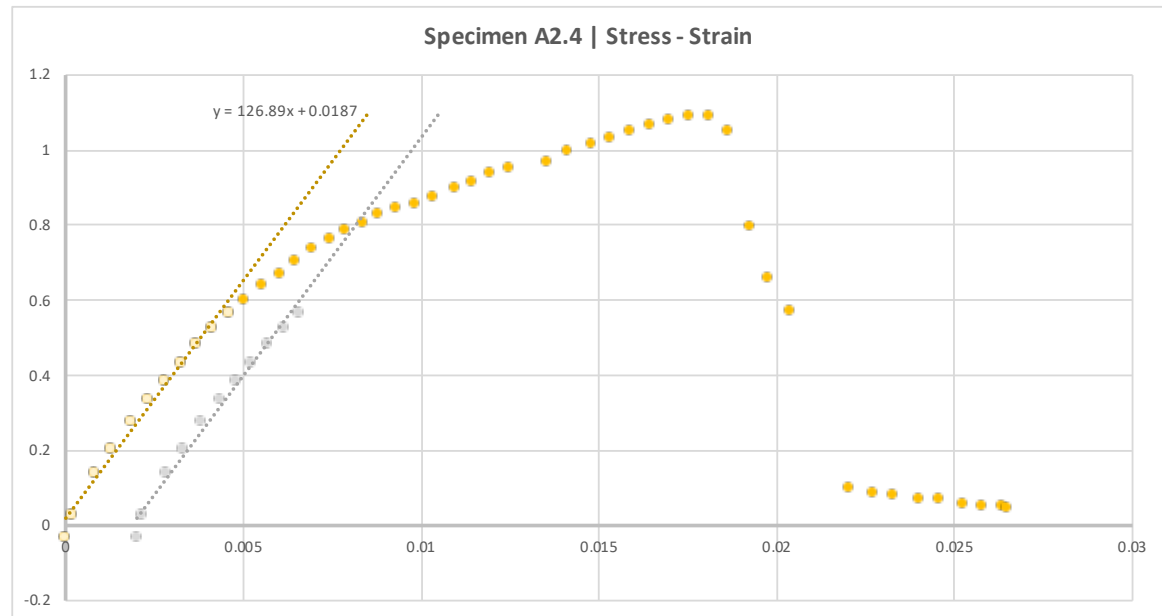
| Specimen A2.5 | | | |
|---|---|---|---|
| | Unit | Initial | Tested |
| Area | | | |
| Length - total | mm | 230 | 227 |
| Length - gauge | mm | 90 | 85 |
| Width - grip | mm | 24 | 24 |
| Width - gauge | mm | 12 | 12 |
| Thickness | mm | 6 | 6 |
| Cross Section Area | mm² | 72 | 72 |

STRAIN | Elongation divided by length

$$\varepsilon = \frac{\delta}{L}$$

STRESS | Axial force divided by cross section area

$$\sigma = \frac{P}{A}$$

MODULUS OF ELASTICITY | Stress divided by strain

$$\sigma = E\varepsilon$$

MODULUS OF ELASTICITY | Constant in graph's equation

| Specimen A2.5 | | |
|---|---|---|
| | Unit | Value |
| $\delta$ at $\sigma$ max | mm | 0.806204 |
| $\varepsilon$ at $\sigma$ max | - | 0.009485 |
| $\sigma$ max | MPa | 0.98186 |
| Yield Stress | MPa | 0.969313 |
| Young's Modulus | MPa | 134.18 |



Specimen A2.5 | Stress - Strain

y = 134.18x + 0.0089
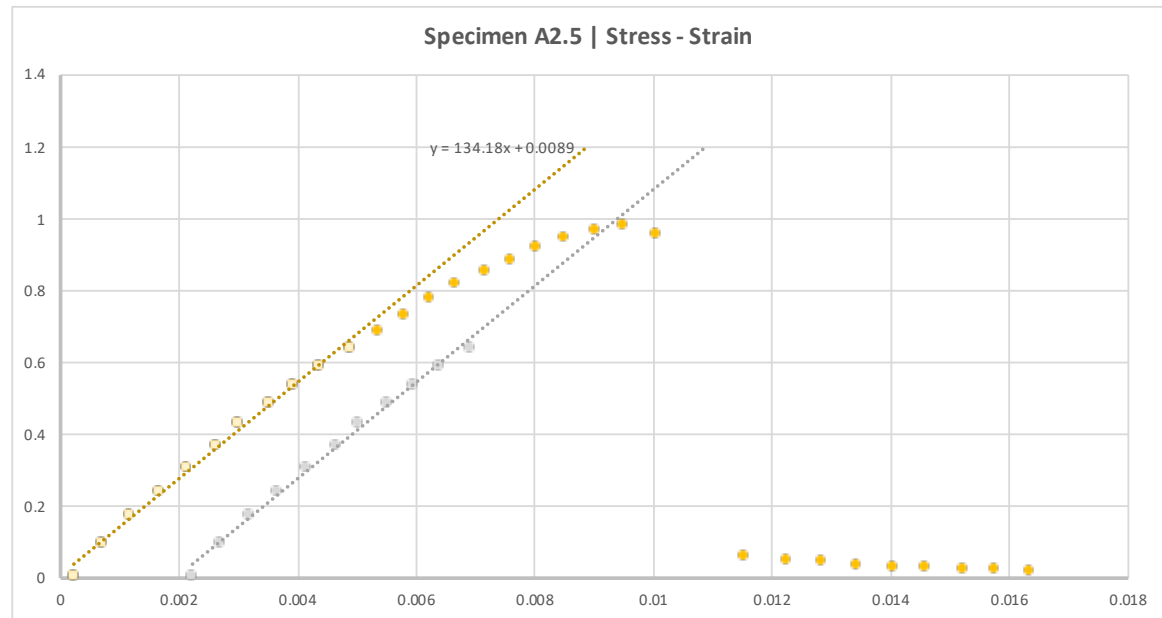
| Specimen A3.1 | | | |
|---|---|---|---|
| | Unit | Initial | Tested |
| Area | | | |
| Length - total | mm | 230 | 216 |
| Length - gauge | mm | 90 | 85 |
| Width - grip | mm | 24 | 20 |
| Width - gauge | mm | 12 | 10 |
| Thickness | mm | 6 | 7 |
| Cross Section Area | mm² | 72 | 70 |

STRAIN | Elongation divided by length

$$\varepsilon = \frac{\delta}{L}$$

STRESS | Axial force divided by cross section area

$$\sigma = \frac{P}{A}$$

MODULUS OF ELASTICITY | Stress divided by strain

$$\sigma = E\varepsilon$$

MODULUS OF ELASTICITY | Constant in graph's equation

| Specimen A3.1 | | |
|---|---|---|
| | Unit | Value |
| $\delta$ at $\sigma$ max | mm | 13.3126 |
| $\varepsilon$ at $\sigma$ max | - | 0.156619 |
| $\sigma$ max | MPa | 6.992 |
| Yield Stress | MPa | 4.814043 |
| Young's Modulus | MPa | 301.33 |

**Specimen A3.1 | Stress - Strain**

y = 301.33x + 1.2398
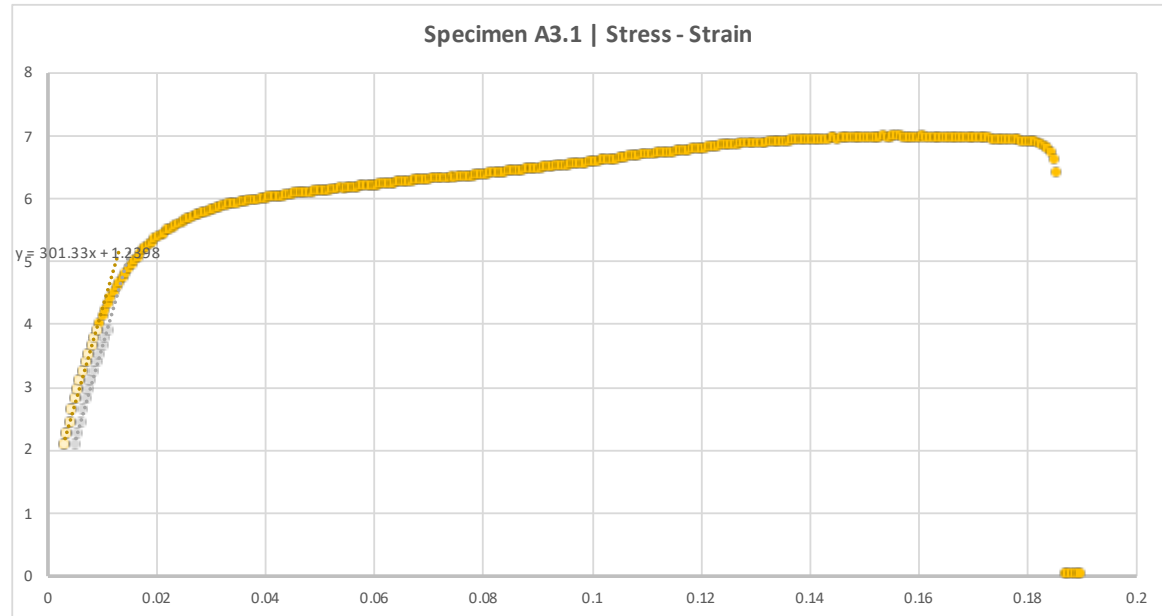
## Specimen A3.2

| | Unit | Initial | Tested |
|---|---|---|---|
| Area | | | |
| Length - total | mm | 230 | 214 |
| Length - gauge | mm | 90 | 85 |
| Width - grip | mm | 24 | 22 |
| Width - gauge | mm | 12 | 10.5 |
| Thickness | mm | 6 | 7 |
| Cross Section Area | mm² | 72 | 73.5 |

STRAIN | Elongation divided by length

$$\varepsilon = \frac{\delta}{L}$$

STRESS | Axial force divided by cross section area

$$\sigma = \frac{P}{A}$$

MODULUS OF ELASTICITY | Stress divided by strain

$$\sigma = E\varepsilon$$

MODULUS OF ELASTICITY | Constant in graph's equation

## Specimen A3.2

| | Unit | Value |
|---|---|---|
| $\delta$ at $\sigma$ max | mm | 12.4505 |
| $\varepsilon$ at $\sigma$ max | - | 0.146476 |
| $\sigma$ max | MPa | 6.688313 |
| Yield Stress | MPa | 3.582871 |
| Young's Modulus | MPa | 580.72 |

### Specimen A3.2 | Stress - Strain

y = 580.72x + 0.2657
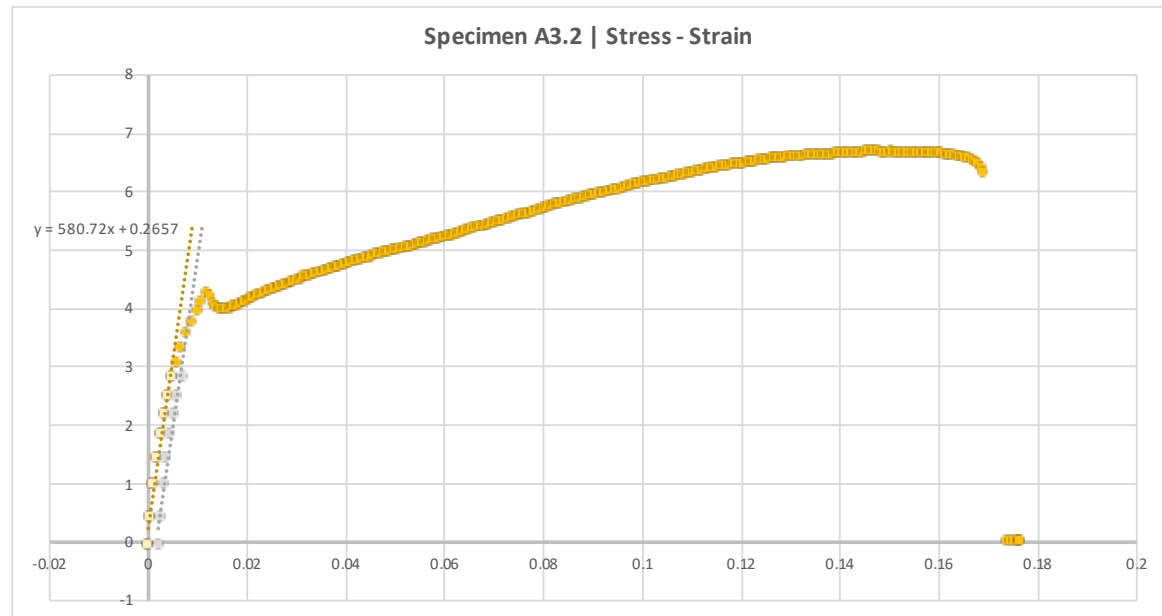
| Specimen A3.3 | | | |
|---|---|---|---|
| | Unit | Initial | Tested |
| Area | | | |
| Length - total | mm | 230 | 215 |
| Length - gauge | mm | 90 | 85 |
| Width - grip | mm | 24 | 20.5 |
| Width - gauge | mm | 12 | 10 |
| Thickness | mm | 6 | 7 |
| Cross Section Area | mm² | 72 | 70 |

STRAIN | Elongation divided by length

$$\varepsilon = \frac{\delta}{L}$$

STRESS | Axial force divided by cross section area

$$\sigma = \frac{P}{A}$$

MODULUS OF ELASTICITY | Stress divided by strain

$$\sigma = E\varepsilon$$

MODULUS OF ELASTICITY | Constant in graph's equation

| Specimen A3.3 | | |
|---|---|---|
| | Unit | Value |
| $\delta$ at $\sigma$ max | mm | 9.80828 |
| $\varepsilon$ at $\sigma$ max | - | 0.115392 |
| $\sigma$ max | MPa | 7.656429 |
| Yield Stress | MPa | 4.2617 |
| Young's Modulus | MPa | 407.69 |



Specimen A3.3 | Stress - Strain

y = 407.69x + 0.1399
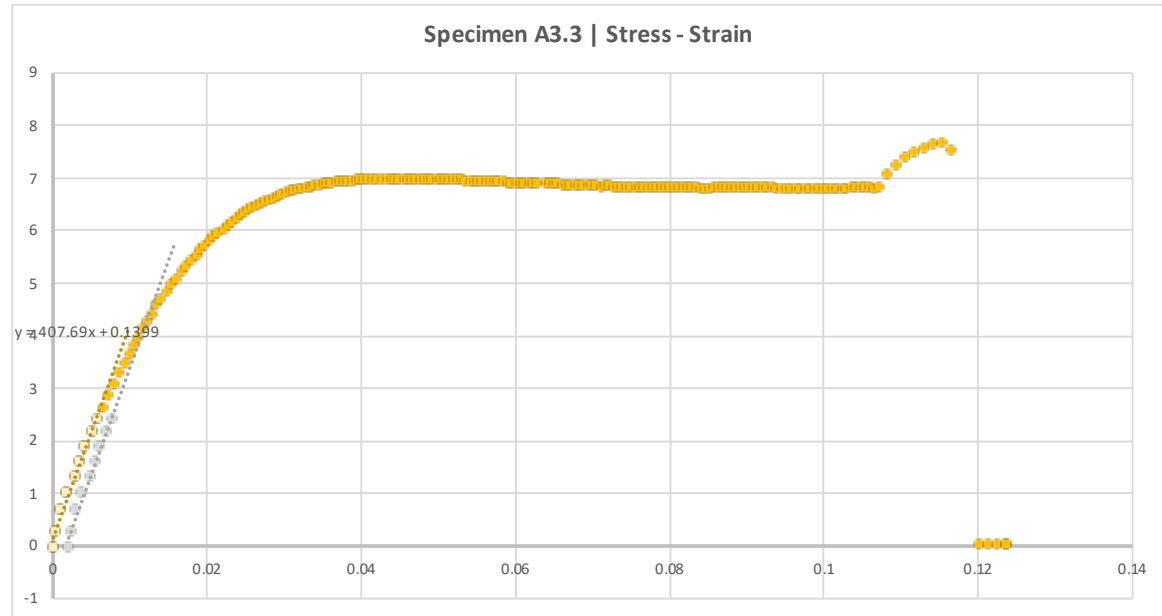
| Specimen A3.4 | | | |
|---|---|---|---|
| | Unit | Initial | Tested |
| Area | | | |
| Length - total | mm | 230 | 215 |
| Length - gauge | mm | 90 | 85 |
| Width - grip | mm | 24 | 20.5 |
| Width - gauge | mm | 12 | 10 |
| Thickness | mm | 6 | 7 |
| Cross Section Area | mm² | 72 | 70 |

STRAIN | Elongation divided by length

$$\varepsilon = \frac{\delta}{L}$$

STRESS | Axial force divided by cross section area

$$\sigma = \frac{P}{A}$$

MODULUS OF ELASTICITY | Stress divided by strain

$$\sigma = E\varepsilon$$

MODULUS OF ELASTICITY | Constant in graph's equation

| Specimen A3.4 | | |
|---|---|---|
| | Unit | Value |
| $\delta$ at $\sigma$ max | mm | 11.2411 |
| $\varepsilon$ at $\sigma$ max | - | 0.132248 |
| $\sigma$ max | MPa | 7.038486 |
| Yield Stress | MPa | 3.576957 |
| Young's Modulus | MPa | 642.54 |



Specimen A3.4 | Stress - Strain

y = 642.54x - 0.0039
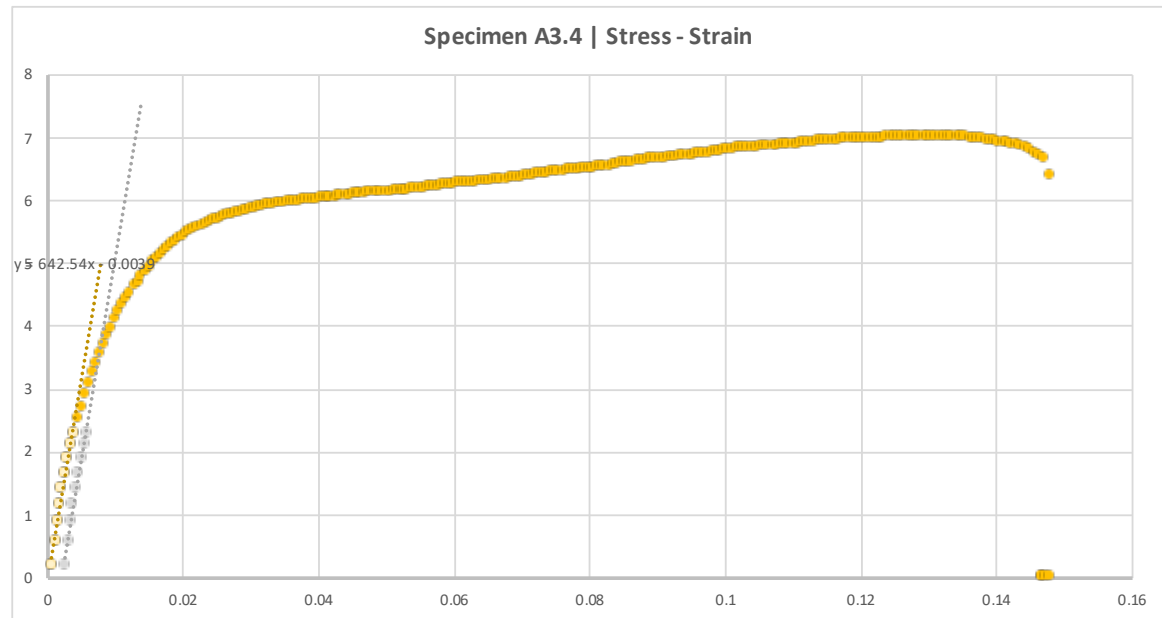
## Specimen A3.5

| | Unit | Initial | Tested |
|---|---|---|---|
| Area | | | |
| Length - total | mm | 230 | 216 |
| Length - gauge | mm | 90 | 85 |
| Width - grip | mm | 24 | 21 |
| Width - gauge | mm | 12 | 10 |
| Thickness | mm | 6 | 7 |
| Cross Section Area | mm² | 72 | 70 |

STRAIN | Elongation divided by length

$$\varepsilon = \frac{\delta}{L}$$

STRESS | Axial force divided by cross section area

$$\sigma = \frac{P}{A}$$

MODULUS OF ELASTICITY | Stress divided by strain

$$\sigma = E\varepsilon$$

MODULUS OF ELASTICITY | Constant in graph's equation

## Specimen A3.5

| | Unit | Value |
|---|---|---|
| $\delta$ at $\sigma$ max | mm | 9.50996 |
| $\varepsilon$ at $\sigma$ max | - | 0.111882 |
| $\sigma$ max | MPa | 6.662757 |
| Yield Stress | MPa | 3.735671 |
| Young's Modulus | MPa | 768.38 |

### Specimen A3.5 | Stress - Strain

$y = 768.38x + 0.142$
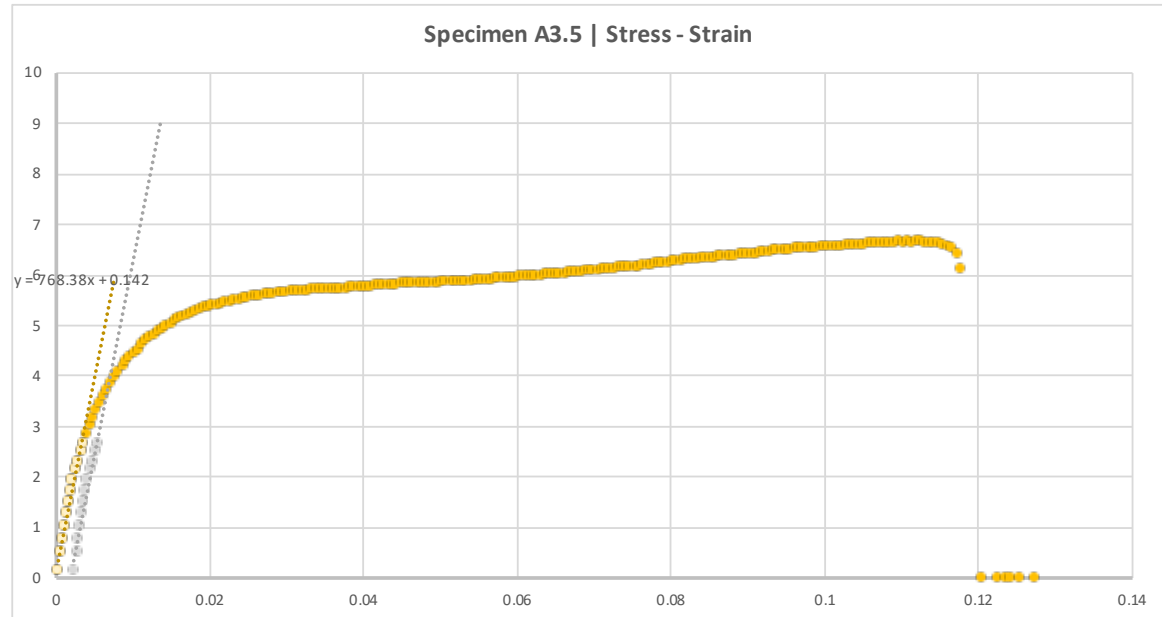
| Specimen A5.1 | | | |
|---|---|---|---|
| | Unit | Initial | Tested |
| Area | | | |
| Length - total | mm | 230 | 221 |
| Length - gauge | mm | 90 | 80 |
| Width - grip | mm | 24 | 23 |
| Width - gauge | mm | 12 | 12 |
| Thickness | mm | 6 | 7 |
| Cross Section Area | mm² | 72 | 84 |

STRAIN | Elongation divided by length

$$\varepsilon = \frac{\delta}{L}$$

STRESS | Axial force divided by cross section area

$$\sigma = \frac{P}{A}$$

MODULUS OF ELASTICITY | Stress divided by strain

$$\sigma = E\varepsilon$$

MODULUS OF ELASTICITY | Constant in graph's equation

| Specimen A5.1 | | |
|---|---|---|
| | Unit | Value |
| $\delta$ at $\sigma$ max | mm | 1.11025 |
| $\varepsilon$ at $\sigma$ max | - | 0.013878 |
| $\sigma$ max | MPa | 3.139845 |
| Yield Stress | MPa | 2.577226 |
| Young's Modulus | MPa | 418.48 |



Specimen A5.1 | Stress - Strain

y = 418.48x + 0.1314
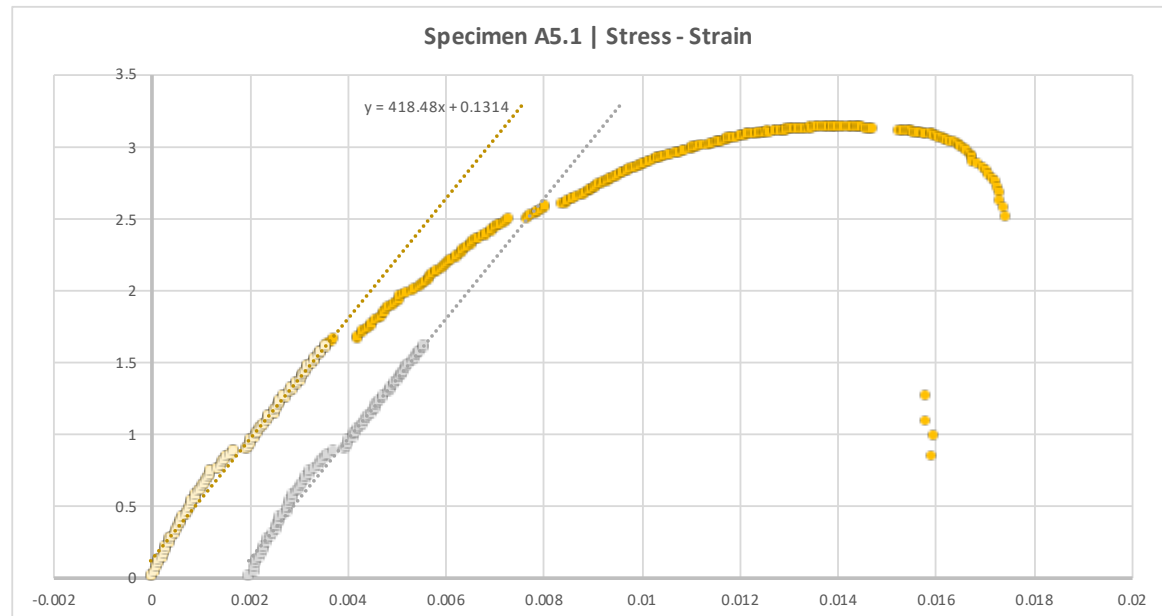
| Specimen A5.2 | | | |
|---|---|---|---|
| | Unit | Initial | Tested |
| Area | | | |
| Length - total | mm | 230 | 222 |
| Length - gauge | mm | 90 | 80 |
| Width - grip | mm | 24 | 24 |
| Width - gauge | mm | 12 | 12 |
| Thickness | mm | 6 | 7 |
| Cross Section Area | mm² | 72 | 84 |

STRAIN | Elongation divided by length

$$\varepsilon = \frac{\delta}{L}$$

STRESS | Axial force divided by cross section area

$$\sigma = \frac{P}{A}$$

MODULUS OF ELASTICITY | Stress divided by strain

$$\sigma = E\varepsilon$$

MODULUS OF ELASTICITY | Constant in graph's equation

| Specimen A5.2 | | |
|---|---|---|
| | Unit | Value |
| $\delta$ at $\sigma$ max | mm | 1.05913 |
| $\varepsilon$ at $\sigma$ max | - | 0.013239 |
| $\sigma$ max | MPa | 3.451929 |
| Yield Stress | MPa | 3.103845 |
| Young's Modulus | MPa | 457.03 |



Specimen A5.2 | Stress - Strain

y = 457.03x - 0.1672
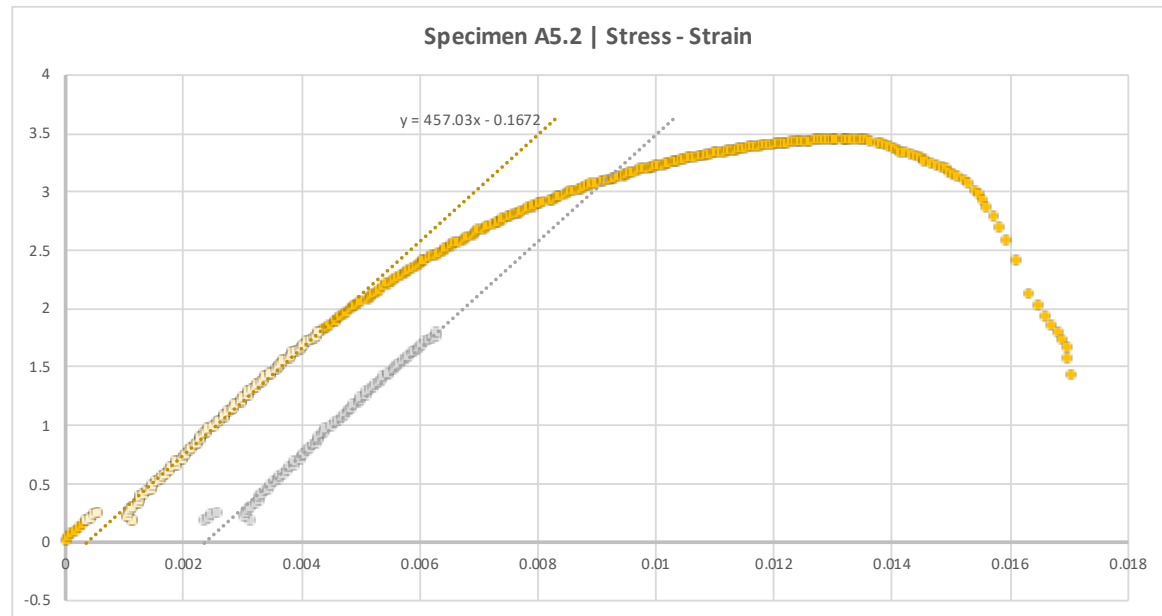
## Specimen A5.3

| | Unit | Initial | Tested |
|---|---|---|---|
| **Area** | | | |
| **Length - total** | mm | 230 | 221 |
| **Length - gauge** | mm | 90 | 80 |
| **Width - grip** | mm | 24 | 24 |
| **Width - gauge** | mm | 12 | 12 |
| **Thickness** | mm | 6 | 7 |
| **Cross Section Area** | mm² | 72 | 84 |

STRAIN | Elongation divided by length

$$\varepsilon = \frac{\delta}{L}$$

STRESS | Axial force divided by cross section area

$$\sigma = \frac{P}{A}$$

MODULUS OF ELASTICITY | Stress divided by strain

$$\sigma = E\varepsilon$$

MODULUS OF ELASTICITY | Constant in graph's equation

## Specimen A5.3

| | Unit | Value |
|---|---|---|
| $\delta$ at $\sigma$ max | mm | 0.750371 |
| $\varepsilon$ at $\sigma$ max | - | 0.00938 |
| $\sigma$ max | MPa | 3.23031 |
| Yield Stress | MPa | 2.982798 |
| Young's Modulus | MPa | 524.39 |



Specimen A5.3 | Stress - Strain

y = 524.39x + 0.0467
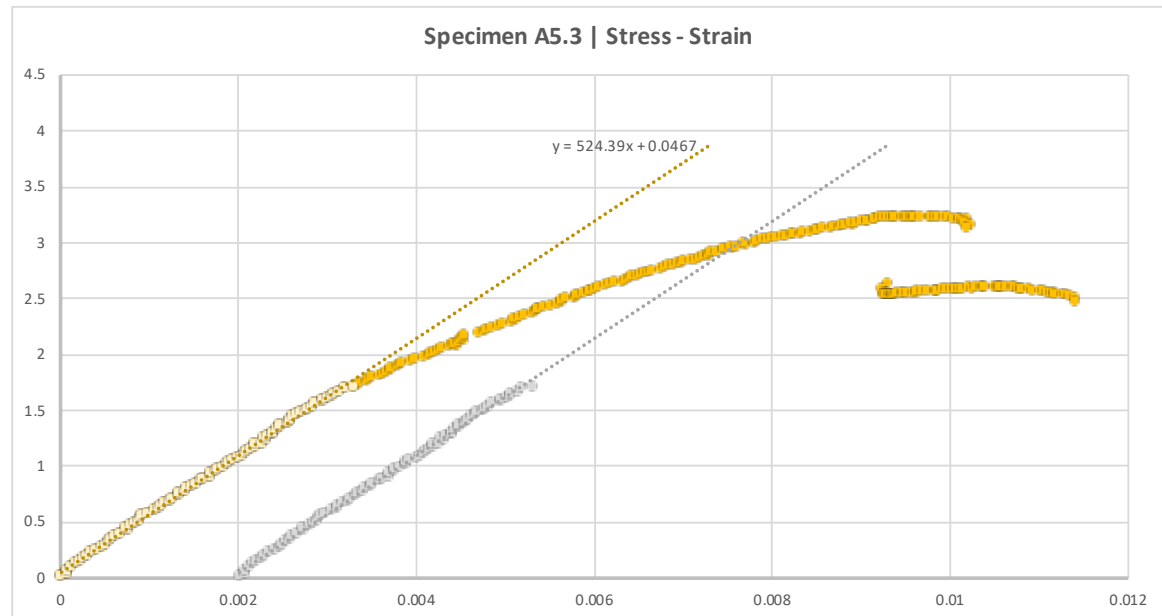
## Specimen A5.4

| | Unit | Initial | Tested |
|---|---|---|---|
| Area | | | |
| Length - total | mm | 230 | 224 |
| Length - gauge | mm | 90 | 80 |
| Width - grip | mm | 24 | 21 |
| Width - gauge | mm | 12 | 15 |
| Thickness | mm | 6 | 7 |
| Cross Section Area | mm² | 72 | 105 |

STRAIN | Elongation divided by length

$$\varepsilon = \frac{\delta}{L}$$

STRESS | Axial force divided by cross section area

$$\sigma = \frac{P}{A}$$

MODULUS OF ELASTICITY | Stress divided by strain

$$\sigma = E\varepsilon$$

MODULUS OF ELASTICITY | Constant in graph's equation

## Specimen A5.4

| | Unit | Value |
|---|---|---|
| $\delta$ at $\sigma$ max | mm | 0.674359 |
| $\varepsilon$ at $\sigma$ max | - | 0.008429 |
| $\sigma$ max | MPa | 2.427067 |
| Yield Stress | MPa | 2.376505 |
| Young's Modulus | MPa | 438.82 |

### Specimen A5.4 | Stress - Strain



y = 438.82x + 0.0477
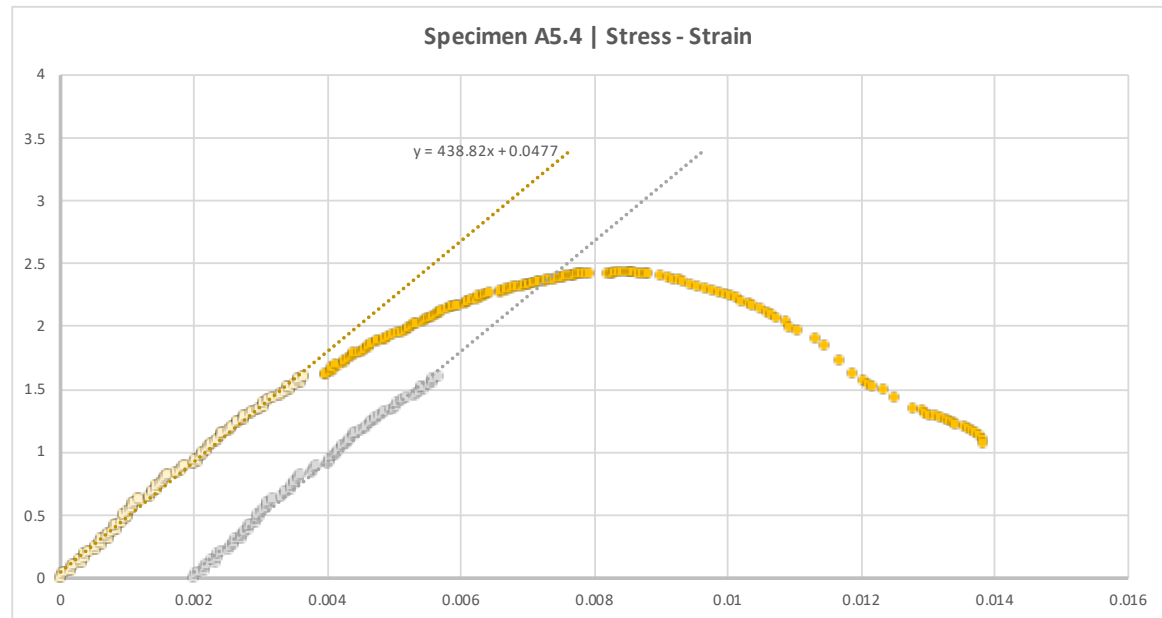
## Specimen A5.5

| | Unit | Initial | Tested |
|---|---|---|---|
| Area | | | |
| Length - total | mm | 230 | 220 |
| Length - gauge | mm | 90 | 80 |
| Width - grip | mm | 24 | 25 |
| Width - gauge | mm | 12 | 15 |
| Thickness | mm | 6 | 7 |
| Cross Section Area | mm² | 72 | 105 |

STRAIN | Elongation divided by length

$$\varepsilon = \frac{\delta}{L}$$

STRESS | Axial force divided by cross section area

$$\sigma = \frac{P}{A}$$

MODULUS OF ELASTICITY | Stress divided by strain

$$\sigma = E\varepsilon$$

MODULUS OF ELASTICITY | Constant in graph's equation

## Specimen A5.5

| | Unit | Value |
|---|---|---|
| $\delta$ at $\sigma$ max | mm | 0.8506 |
| $\varepsilon$ at $\sigma$ max | - | 0.010633 |
| $\sigma$ max | MPa | 2.641324 |
| Yield Stress | MPa | 2.514152 |
| Young's Modulus | MPa | 404.29 |

### Specimen A5.5 | Stress - Strain



y = 404.29x - 0.3901
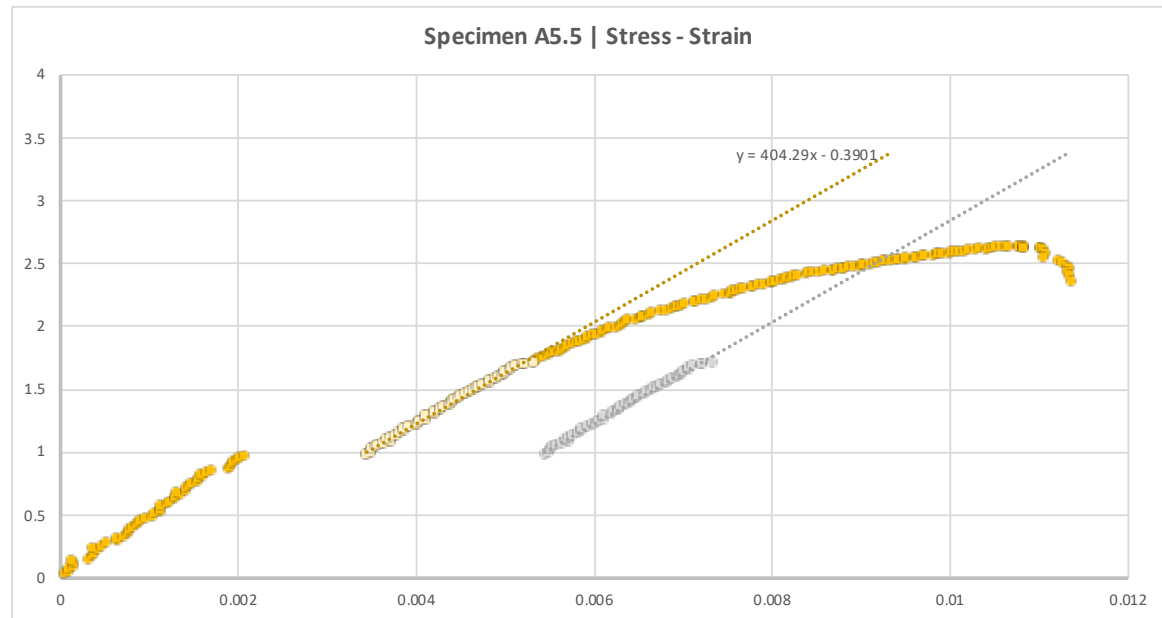
## Specimen B1.1

| | Unit | Initial | Tested |
|---|---|---|---|
| Area | mm² | | 3020 |
| Volume | mm³ | | 13288 |
| Length - total beam | mm | | 151 |
| Length between sup - L | mm | | 80 |
| Width - w | mm | | 20 |
| Thickness - d | mm | | 4.4 |
| Cross Section Area - w*d | mm² | | 88 |
| Moment of Inertia - I | mm⁴ | | 141.9733 |

MOMENT OF INERTIA

$$I = \frac{wd^3}{12}$$

FLEXURAL STRAIN

$$\varepsilon = \frac{6\delta d}{L^2}$$

FLEXURAL STRENGTH | Force multiplied by length divided by cs

$$\sigma = \frac{3FL}{2wd^2}$$

MODULUS OF ELASTICITY | Stress divided by strain

$$E = \frac{FL^3}{48I\delta} \qquad E = \frac{F}{\delta} \times \frac{L^3}{48I}$$

BENDING STIFFNESS | Constant in graph's equation



Specimen B1.1 | Force - Displacement

$y = 11.944x + 0.2515$

## Specimen B1.1

| | Unit | Value |
|---|---|---|
| Failure Load - F | N | 30.372 |
| Max Flexural Strength - σ | MPa | 9.41281 |
| Young's Modulus - E | GPa | 0.89737 |
| Bending Stiffness - k (F/δ) | - | 11.944 |

| Specimen B1.2 | | | |
|---|---|---|---|
| | Unit | Initial | Tested |
| Area | mm² | | 3171 |
| Volume | mm³ | | 12684 |
| Length - total beam | mm | | 151 |
| Length between sup - L | mm | | 80 |
| Width - w | mm | | 21 |
| Thickness - d | mm | | 4 |
| Cross Section Area - w*d | mm² | | 84 |
| Moment of Inertia - I | mm⁴ | | 112 |
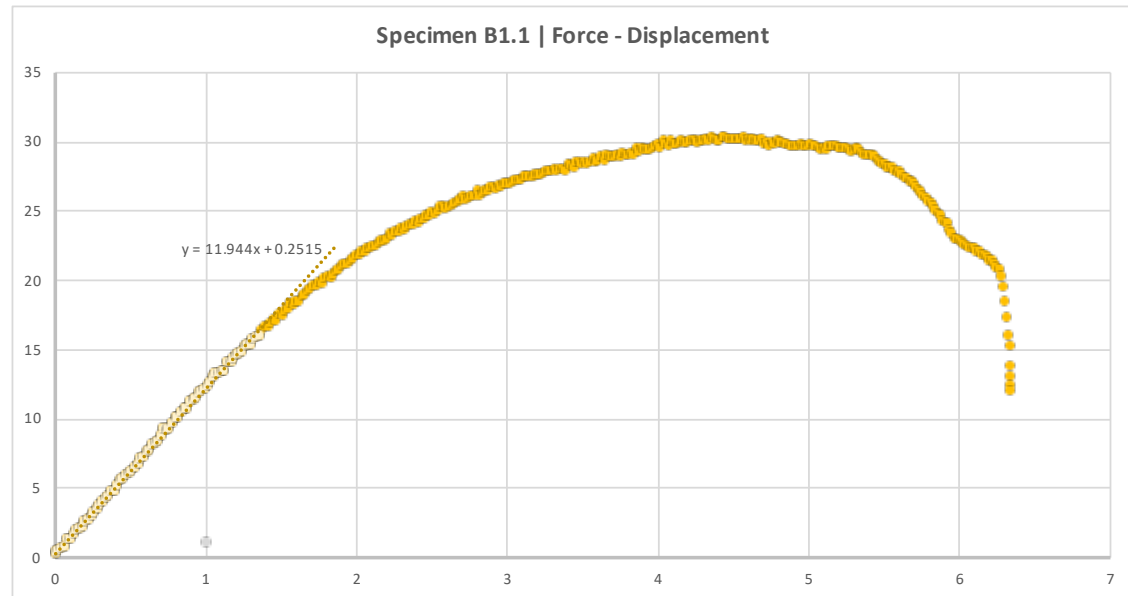
MOMENT OF INERTIA

$$I = \frac{wd^3}{12}$$

FLEXURAL STRAIN

$$\varepsilon = \frac{6\delta d}{L^2}$$

FLEXURAL STRENGTH | Force multiplied by length divided by cs

$$\sigma = \frac{3FL}{2wd^2}$$

MODULUS OF ELASTICITY | Stress divided by strain

$$E = \frac{FL^3}{48I\delta} \qquad E = \frac{F}{\delta} \times \frac{L^3}{48I}$$

BENDING STIFFNESS | Constant in graph's equation

**Specimen B1.2 | Force - Displacement**

y = 7.0155x - 0.0005

| Specimen B1.2 | | |
|---|---|---|
| | Unit | Value |
| Failure Load - F | N | 27.9921 |
| Max Flexural Strength - σ | MPa | 9.997179 |
| Young's Modulus - E | GPa | 0.668143 |
| Bending Stiffness - k (F/δ) | - | 7.0155 |

| Specimen B1.3 | | | |
|---|---|---|---|
| | Unit | Initial | Tested |
| Area | mm² | | 3000 |
| Volume | mm³ | | 12000 |
| Length - total beam | mm | | 150 |
| Length between sup - L | mm | | 80 |
| Width - w | mm | | 20 |
| Thickness - d | mm | | 4 |
| Cross Section Area - w*d | mm² | | 80 |
| Moment of Inertia - I | mm⁴ | | 106.6667 |
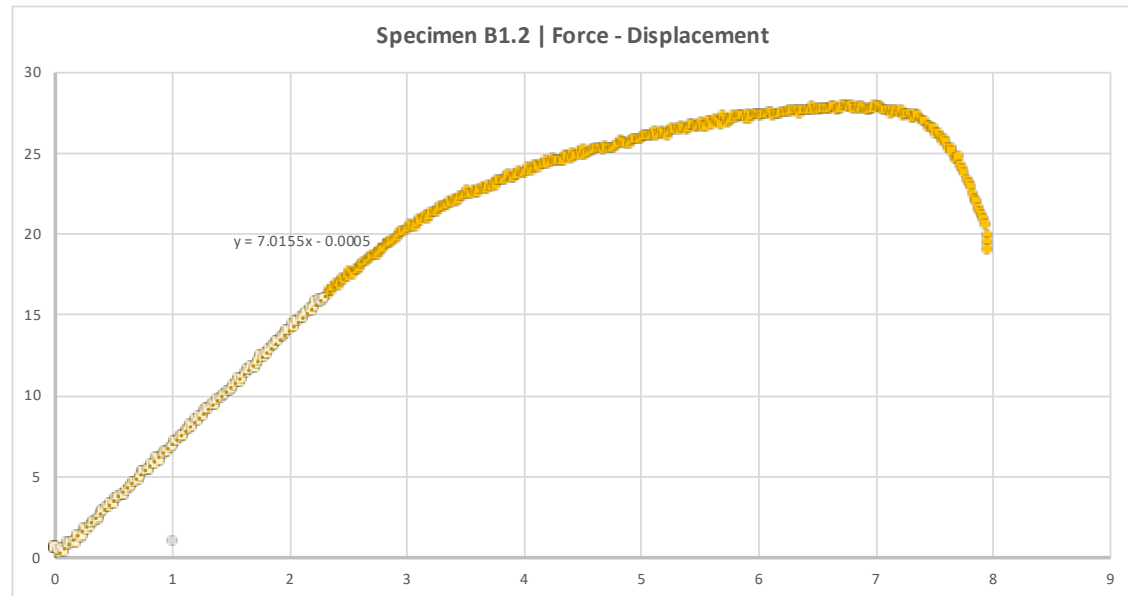
MOMENT OF INERTIA

$$I = \frac{wd^3}{12}$$

FLEXURAL STRAIN

$$\varepsilon = \frac{6\delta d}{L^2}$$

FLEXURAL STRENGTH | Force multiplied by length divided by cs

$$\sigma = \frac{3FL}{2wd^2}$$

MODULUS OF ELASTICITY | Stress divided by strain

$$E = \frac{FL^3}{48I\delta} \qquad E = \frac{F}{\delta} \times \frac{L^3}{48I}$$

BENDING STIFFNESS | Constant in graph's equation

| Specimen B1.3 | | |
|---|---|---|
| | Unit | Value |
| Failure Load - F | N | 22.9095 |
| Max Flexural Strength - $\sigma$ | MPa | 8.591063 |
| Young's Modulus - E | GPa | 0.81576 |
| Bending Stiffness - k (F/$\delta$) | - | 8.1576 |

**Specimen B1.3 | Force - Displacement**

y = 8.1576x - 0.7691

| Specimen B1.4 | | | |
|---|---|---|---|
| | Unit | Initial | Tested |
| Area | mm² | | 3020 |
| Volume | mm³ | | 12080 |
| Length - total beam | mm | | 151 |
| Length between sup - L | mm | | 80 |
| Width - w | mm | | 20 |
| Thickness - d | mm | | 4 |
| Cross Section Area - w*d | mm² | | 80 |
| Moment of Inertia - I | mm⁴ | | 106.6667 |

MOMENT OF INERTIA

$$I = \frac{wd^3}{12}$$

FLEXURAL STRAIN

$$\varepsilon = \frac{6\delta d}{l^2}$$

FLEXURAL STRENGTH | Force multiplied by length divided by cs

$$\sigma = \frac{3FL}{2wd^2}$$

MODULUS OF ELASTICITY | Stress divided by strain

$$E = \frac{FL^3}{48I\delta} \qquad E = \frac{F}{\delta} \times \frac{L^3}{48I}$$

BENDING STIFFNESS | Constant in graph's equation

| Specimen B1.4 | | |
|---|---|---|
| | Unit | Value |
| Failure Load - F | N | 28.2578 |
| Max Flexural Strength - $\sigma$ | MPa | 10.59668 |
| Young's Modulus - E | GPa | 1.0246 |
| Bending Stiffness - k (F/$\delta$) | - | 10.246 |

**Specimen B1.4 | Force - Displacement**



y = 10.246x + 1.1008
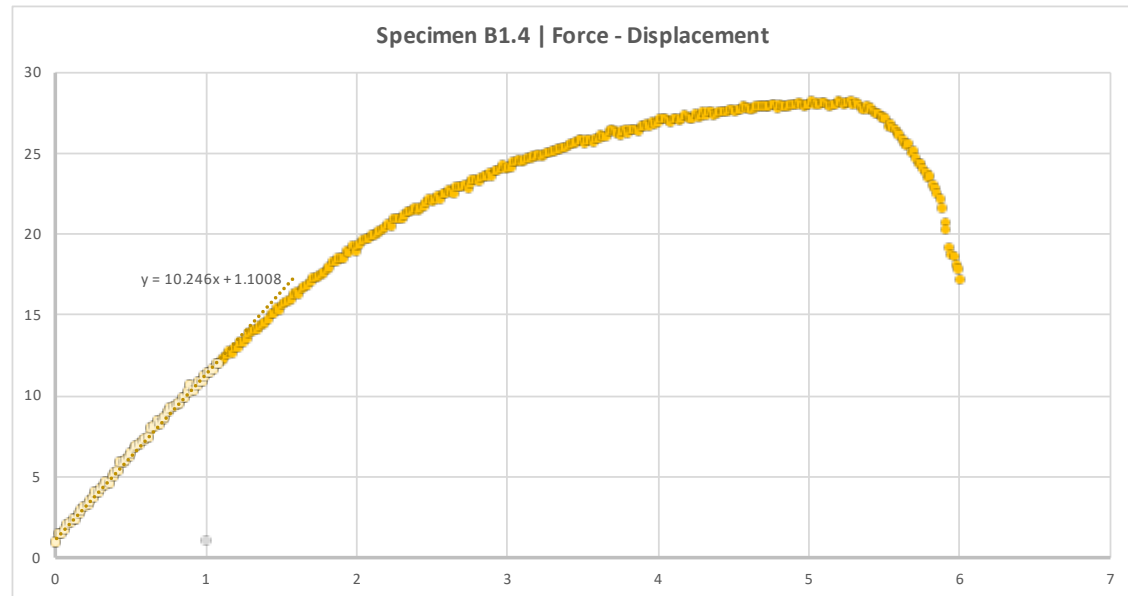
| Specimen B1.5 | | | |
|---|---|---|---|
| | Unit | Initial | Tested |
| Area | mm² | | 2838.8 |
| Volume | mm³ | | 11639.08 |
| Length - total beam | mm | | 151 |
| Length between sup - L | mm | | 80 |
| Width - w | mm | | 18.8 |
| Thickness - d | mm | | 4.1 |
| Cross Section Area - w*d | mm² | | 77.08 |
| Moment of Inertia - I | mm⁴ | | 107.9762 |

MOMENT OF INERTIA

$$I = \frac{wd^3}{12}$$

FLEXURAL STRAIN

$$\varepsilon = \frac{6\delta d}{l^2}$$

FLEXURAL STRENGTH | Force multiplied by length divided by cs

$$\sigma = \frac{3FL}{2wd^2}$$

MODULUS OF ELASTICITY | Stress divided by strain

$$E = \frac{FL^3}{48I\delta} \qquad E = \frac{F}{\delta} \times \frac{L^3}{48I}$$

BENDING STIFFNESS | Constant in graph's equation

| Specimen B1.5 | | |
|---|---|---|
| | Unit | Value |
| Failure Load - F | N | 28.5711 |
| Max Flexural Strength - σ | MPa | 10.84882 |
| Young's Modulus - E | GPa | 1.047342 |
| Bending Stiffness - k (F/δ) | - | 10.602 |



Specimen B1.5 | Force - Displacement

y = 10.602x - 0.9264
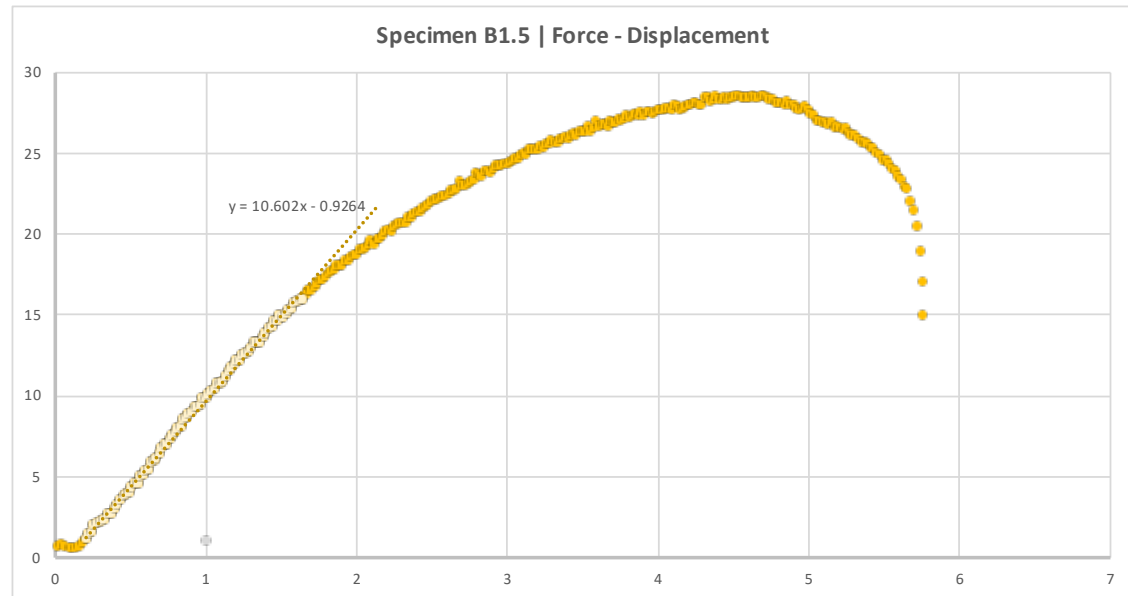
| Specimen B2.1 | | | |
|---|---|---|---|
| | Unit | Initial | Tested |
| Area | mm² | | 3520 |
| Volume | mm³ | | 21120 |
| Length - total beam | mm | | 160 |
| Length between sup - L | mm | | 80 |
| Width - w | mm | | 22 |
| Thickness - d | mm | | 6 |
| Cross Section Area - w*d | mm² | | 132 |
| Moment of Inertia - I | mm⁴ | | 396 |

MOMENT OF INERTIA

$$I = \frac{wd^3}{12}$$

FLEXURAL STRAIN

$$\varepsilon = \frac{6\delta d}{l^2}$$

FLEXURAL STRENGTH | Force multiplied by length divided by cs

$$\sigma = \frac{3FL}{2wd^2}$$

MODULUS OF ELASTICITY | Stress divided by strain

$$E = \frac{FL^3}{48I\delta} \qquad E = \frac{F}{\delta} \times \frac{L^3}{48I}$$

BENDING STIFFNESS | Constant in graph's equation

| Specimen B2.1 | | |
|---|---|---|
| | Unit | Value |
| Failure Load - F | N | 61.8749 |
| Max Flexural Strength - σ | MPa | 9.374985 |
| Young's Modulus - E | GPa | 0.148218 |
| Bending Stiffness - k (F/δ) | - | 5.5026 |

**Specimen B2.1 | Force - Displacement**



y = 5.5026x - 1.0105
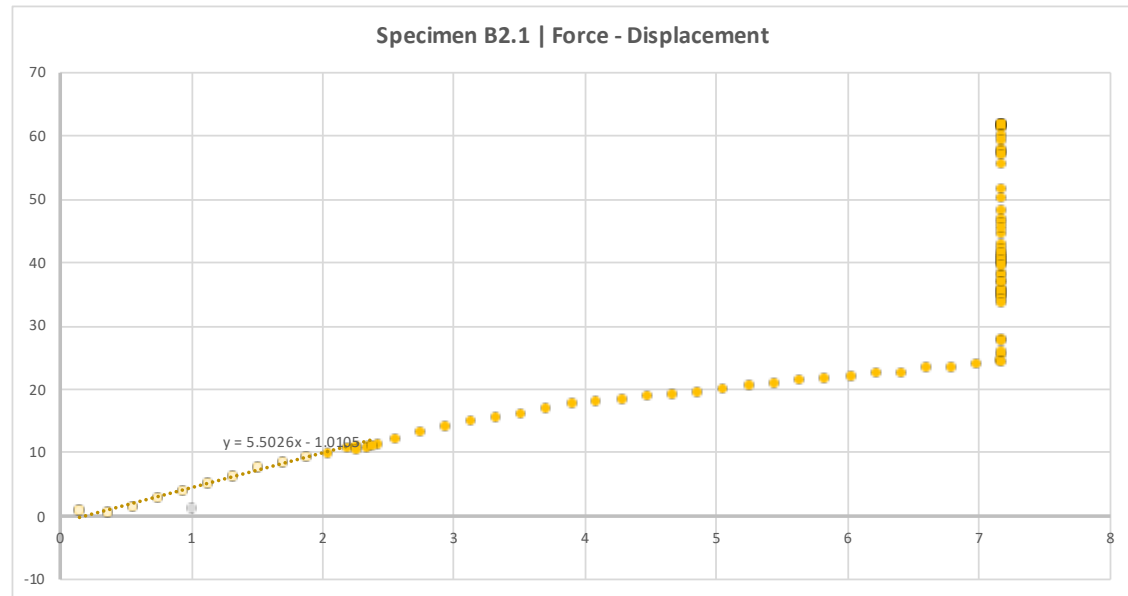
| Specimen B2.2 | | | |
|---|---|---|---|
| | Unit | Initial | Tested |
| Area | mm² | | 3407.75 |
| Volume | mm³ | | 18742.63 |
| Length - total beam | mm | | 158.5 |
| Length between sup - L | mm | | 80 |
| Width - w | mm | | 21.5 |
| Thickness - d | mm | | 5.5 |
| Cross Section Area - w*d | mm² | | 118.25 |
| Moment of Inertia - I | mm⁴ | | 298.0885 |

MOMENT OF INERTIA

$$I = \frac{wd^3}{12}$$

FLEXURAL STRAIN

$$\varepsilon = \frac{6\delta d}{l^2}$$

FLEXURAL STRENGTH | Force multiplied by length divided by cs

$$\sigma = \frac{3FL}{2wd^2}$$

MODULUS OF ELASTICITY | Stress divided by strain

$$E = \frac{FL^3}{48I\delta} \qquad E = \frac{F}{\delta} \times \frac{L^3}{48I}$$

BENDING STIFFNESS | Constant in graph's equation

| Specimen B2.2 | | |
|---|---|---|
| | Unit | Value |
| Failure Load - F | N | 37.1606 |
| Max Flexural Strength - $\sigma$ | MPa | 6.856463 |
| Young's Modulus - E | GPa | 0.215413 |
| Bending Stiffness - k (F/$\delta$) | - | 6.0199 |

Specimen B2.2 | Force - Displacement

y = 6.0199x + 0.52
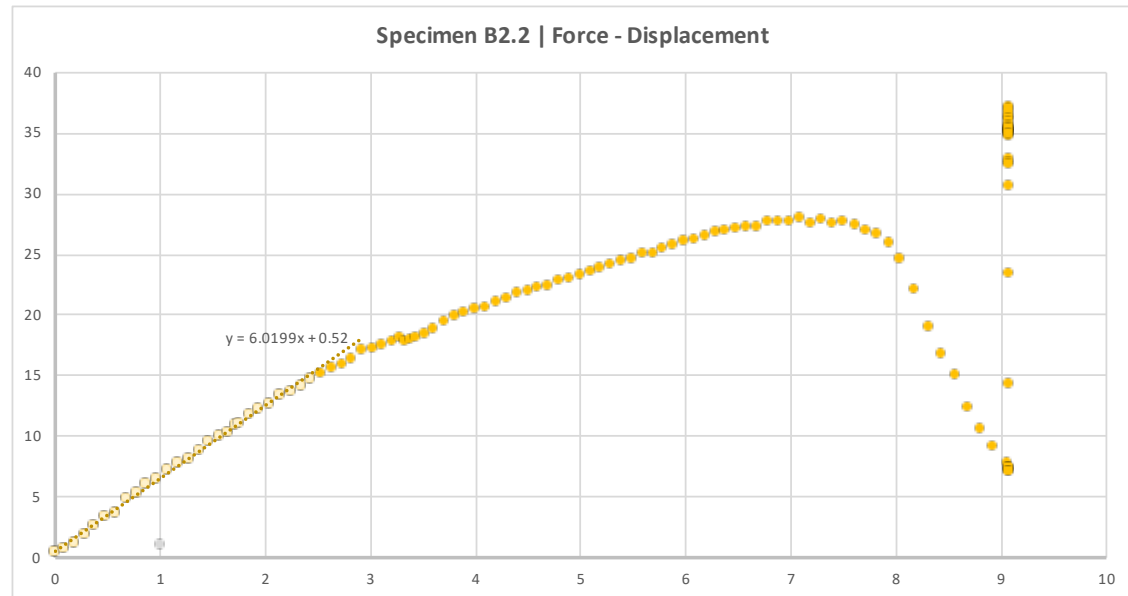
| Specimen B2.1 | | | |
| --- | --- | --- | --- |
| | Unit | Initial | Tested |
| Area | mm² | | 3297 |
| Volume | mm³ | | 19782 |
| Length - total beam | mm | | 157 |
| Length between sup - L | mm | | 80 |
| Width - w | mm | | 21 |
| Thickness - d | mm | | 6 |
| Cross Section Area - w*d | mm² | | 126 |
| Moment of Inertia - I | mm⁴ | | 378 |

MOMENT OF INERTIA

$$I = \frac{wd^3}{12}$$

FLEXURAL STRAIN

$$\varepsilon = \frac{6\delta d}{l^2}$$

FLEXURAL STRENGTH | Force multiplied by length divided by cs

$$\sigma = \frac{3FL}{2wd^2}$$

MODULUS OF ELASTICITY | Stress divided by strain

$$E = \frac{FL^3}{48I\delta} \qquad E = \frac{F}{\delta} \times \frac{L^3}{48I}$$

BENDING STIFFNESS | Constant in graph's equation

**Specimen B2.1 | Force - Displacement**

y = 7.2097x - 0.1513

| Specimen B2.1 | | |
| --- | --- | --- |
| | Unit | Value |
| Failure Load - F | N | 61.3673 |
| Max Flexural Strength - $\sigma$ | MPa | 9.740841 |
| Young's Modulus - E | GPa | 0.203448 |
| Bending Stiffness - k (F/$\delta$) | - | 7.2097 |

| Specimen B2.4 | | | |
|---|---|---|---|
| | Unit | Initial | Tested |
| Area | mm² | | 3555 |
| Volume | mm³ | | 21330 |
| Length - total beam | mm | | 158 |
| Length between sup - L | mm | | 80 |
| Width - w | mm | | 22.5 |
| Thickness - d | mm | | 6 |
| Cross Section Area - w*d | mm² | | 135 |
| Moment of Inertia - I | mm⁴ | | 405 |
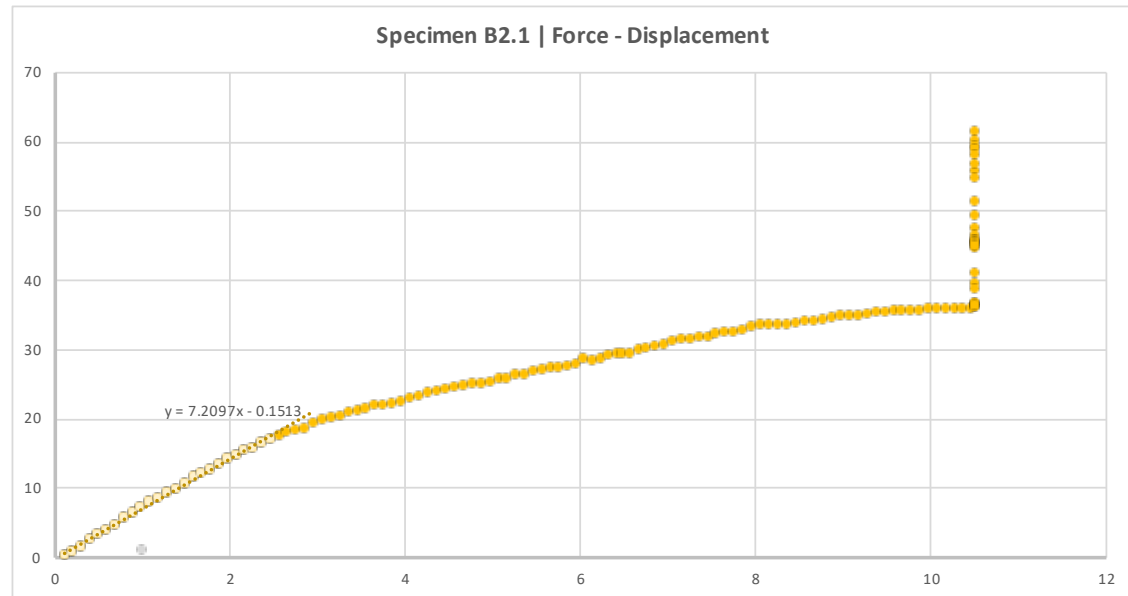
MOMENT OF INERTIA

$$I = \frac{wd^3}{12}$$

FLEXURAL STRAIN

$$\varepsilon = \frac{6\delta d}{l^2}$$

FLEXURAL STRENGTH | Force multiplied by length divided by cs

$$\sigma = \frac{3FL}{2wd^2}$$

MODULUS OF ELASTICITY | Stress divided by strain

$$E = \frac{FL^3}{48I\delta} \qquad E = \frac{F}{\delta} \times \frac{L^3}{48I}$$

BENDING STIFFNESS | Constant in graph's equation

**Specimen B2.4 | Force - Displacement**

y = 14.15x + 2.0313

| Specimen B2.4 | | |
|---|---|---|
| | Unit | Value |
| Failure Load - F | N | 38.4827 |
| Max Flexural Strength - $\sigma$ | MPa | 5.701141 |
| Young's Modulus - E | GPa | 0.372675 |
| Bending Stiffness - k (F/$\delta$) | - | 14.15 |

| Specimen B2.5 | | | |
|---|---|---|---|
| | Unit | Initial | Tested |
| Area | mm² | | 3360 |
| Volume | mm³ | | 20160 |
| Length - total beam | mm | | 160 |
| Length between sup - L | mm | | 80 |
| Width - w | mm | | 21 |
| Thickness - d | mm | | 6 |
| Cross Section Area - w*d | mm² | | 126 |
| Moment of Inertia - I | mm⁴ | | 378 |
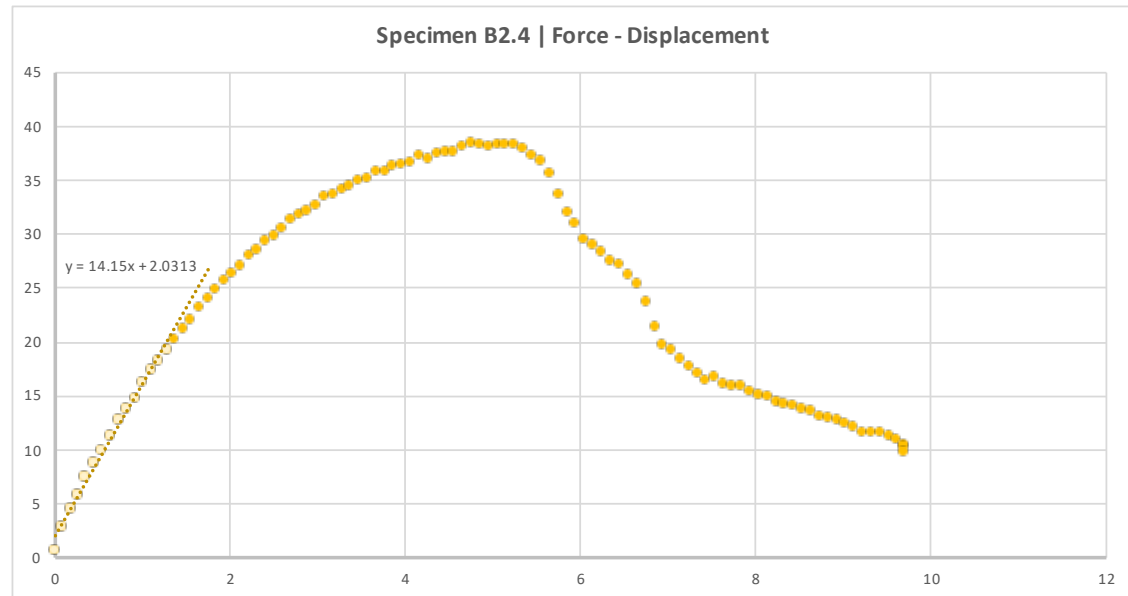
MOMENT OF INERTIA

$$I = \frac{wd^3}{12}$$

FLEXURAL STRAIN

$$\varepsilon = \frac{6\delta d}{l^2}$$

FLEXURAL STRENGTH | Force multiplied by length divided by cs

$$\sigma = \frac{3FL}{2wd^2}$$

MODULUS OF ELASTICITY | Stress divided by strain

$$E = \frac{FL^3}{48I\delta} \qquad E = \frac{F}{\delta} \times \frac{L^3}{48I}$$

BENDING STIFFNESS | Constant in graph's equation

**Specimen B2.5 | Force - Displacement**

$y = 11.695x - 1.3476$

| Specimen B2.5 | | |
|---|---|---|
| | Unit | Value |
| Failure Load - F | N | 30.0352 |
| Max Flexural Strength - σ | MPa | 4.767492 |
| Young's Modulus - E | GPa | 0.330018 |
| Bending Stiffness - k (F/δ) | - | 11.695 |

| Specimen B3.1 | | | |
|---|---|---|---|
| | Unit | Initial | Tested |
| Area | mm² | | 2950.2 |
| Volume | mm³ | | 17701.2 |
| Length - total beam | mm | | 149 |
| Length between sup - L | mm | | 80 |
| Width - w | mm | | 19.8 |
| Thickness - d | mm | | 6 |
| Cross Section Area - w*d | mm² | | 118.8 |
| Moment of Inertia - I | mm⁴ | | 356.4 |
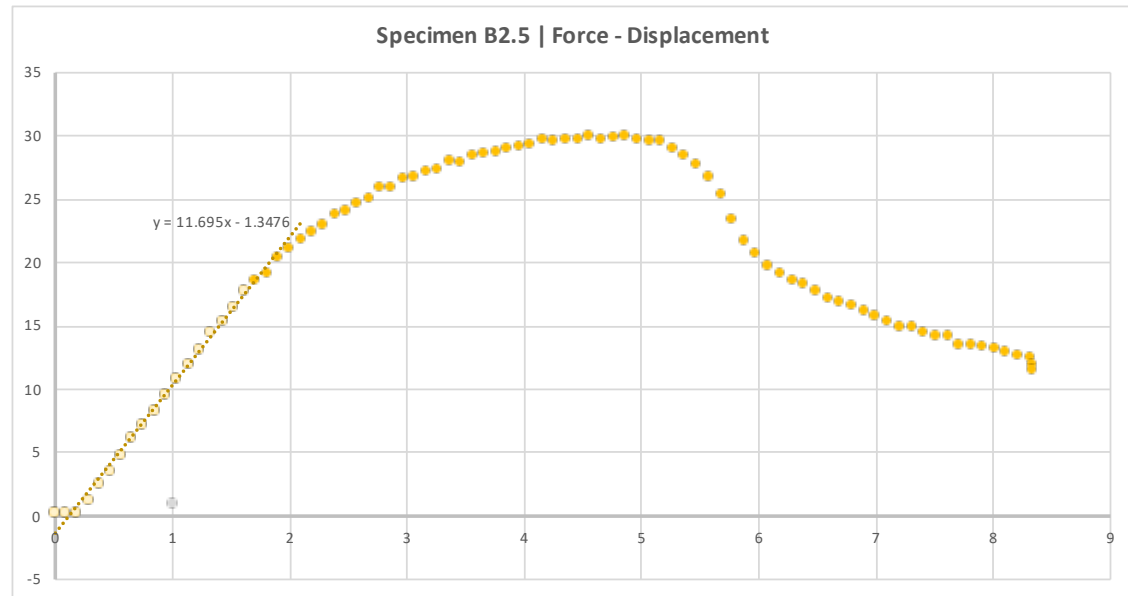
MOMENT OF INERTIA

$$I = \frac{wd^3}{12}$$

FLEXURAL STRAIN

$$\varepsilon = \frac{6\delta d}{L^2}$$

FLEXURAL STRENGTH | Force multiplied by length divided by cs

$$\sigma = \frac{3FL}{2wd^2}$$

MODULUS OF ELASTICITY | Stress divided by strain

$$E = \frac{FL^3}{48I\delta} \qquad E = \frac{F}{\delta} \times \frac{L^3}{48I}$$

BENDING STIFFNESS | Constant in graph's equation

| Specimen B3.1 | | |
|---|---|---|
| | Unit | Value |
| Failure Load - F | N | 122.782 |
| Max Flexural Strength - $\sigma$ | MPa | 20.67037 |
| Young's Modulus - E | GPa | 0.674867 |
| Bending Stiffness - k (F/$\delta$) | - | 22.549 |



Specimen B3.1 | Force - Displacement

y = 22.549x - 10.627
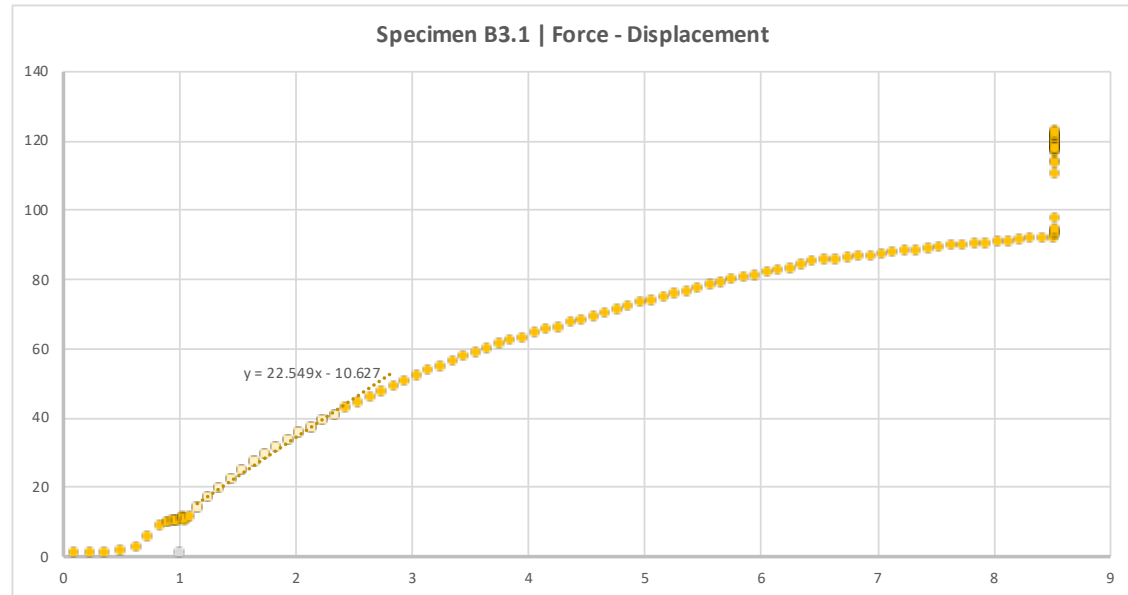
## Specimen B3.2

| | Unit | Initial | Tested |
|---|---|---|---|
| Area | mm² | | 3030 |
| Volume | mm³ | | 18180 |
| Length - total beam | mm | | 151.5 |
| Length between sup - L | mm | | 80 |
| Width - w | mm | | 20 |
| Thickness - d | mm | | 6 |
| Cross Section Area - w*d | mm² | | 120 |
| Moment of Inertia - I | mm⁴ | | 360 |

MOMENT OF INERTIA

$$I = \frac{wd^3}{12}$$

FLEXURAL STRAIN

$$\varepsilon = \frac{6\delta d}{l^2}$$

FLEXURAL STRENGTH | Force multiplied by length divided by cs

$$\sigma = \frac{3FL}{2wd^2}$$

MODULUS OF ELASTICITY | Stress divided by strain

$$E = \frac{FL^3}{48I\delta} \qquad E = \frac{F}{\delta} \times \frac{L^3}{48I}$$

BENDING STIFFNESS | Constant in graph's equation

## Specimen B3.2

| | Unit | Value |
|---|---|---|
| Failure Load - F | N | 143.364 |
| Max Flexural Strength - $\sigma$ | MPa | 23.894 |
| Young's Modulus - E | GPa | 0.641363 |
| Bending Stiffness - k (F/$\delta$) | - | 21.646 |

### Specimen B3.2 | Force - Displacement

y = 21.646x + 1.2888
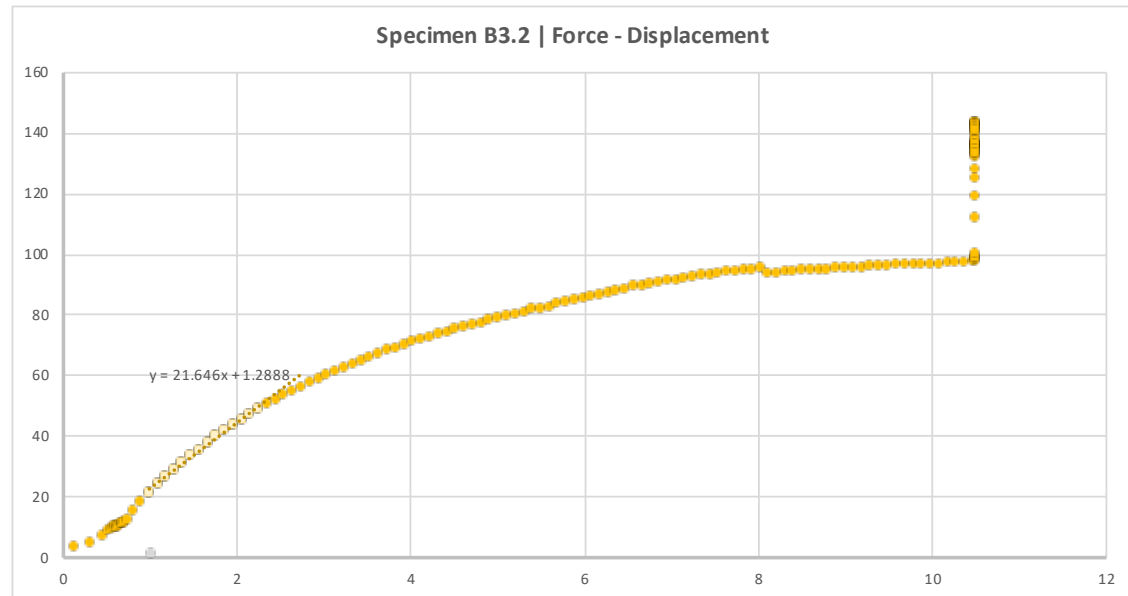
| Specimen B3.3 | | | |
|---|---|---|---|
| | Unit | Initial | Tested |
| Area | mm² | | 3030 |
| Volume | mm³ | | 18180 |
| Length - total beam | mm | | 151.5 |
| Length between sup - L | mm | | 80 |
| Width - w | mm | | 20 |
| Thickness - d | mm | | 6 |
| Cross Section Area - w*d | mm² | | 120 |
| Moment of Inertia - I | mm⁴ | | 360 |

MOMENT OF INERTIA

$$I = \frac{wd^3}{12}$$

FLEXURAL STRAIN

$$\varepsilon = \frac{6\delta d}{L^2}$$

FLEXURAL STRENGTH | Force multiplied by length divided by cs

$$\sigma = \frac{3FL}{2wd^2}$$

MODULUS OF ELASTICITY | Stress divided by strain

$$E = \frac{FL^3}{48I\delta} \qquad E = \frac{F}{\delta} \times \frac{L^3}{48I}$$

BENDING STIFFNESS | Constant in graph's equation

| Specimen B3.3 | | |
|---|---|---|
| | Unit | Value |
| Failure Load - F | N | 173.33 |
| Max Flexural Strength - σ | MPa | 28.88833 |
| Young's Modulus - E | GPa | 0.78723 |
| Bending Stiffness - k (F/δ) | - | 26.569 |



Specimen B3.3 | Force - Displacement

y = 26.569x - 12.405
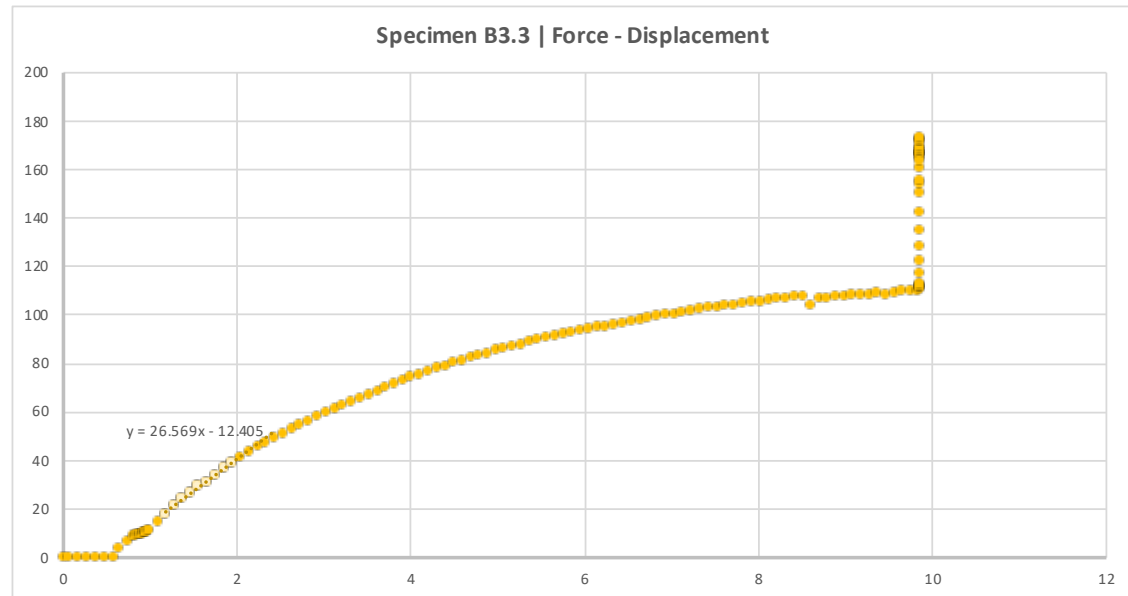
| Specimen B3.4 | | | |
|---|---|---|---|
| | Unit | Initial | Tested |
| Area | mm² | | 2869 |
| Volume | mm³ | | 17787.8 |
| Length - total beam | mm | | 151 |
| Length between sup - L | mm | | 80 |
| Width - w | mm | | 19 |
| Thickness - d | mm | | 6.2 |
| Cross Section Area - w*d | mm² | | 117.8 |
| Moment of Inertia - I | mm⁴ | | 377.3527 |

MOMENT OF INERTIA

$$I = \frac{wd^3}{12}$$

FLEXURAL STRAIN

$$\varepsilon = \frac{6\delta d}{l^2}$$

FLEXURAL STRENGTH | Force multiplied by length divided by cs

$$\sigma = \frac{3FL}{2wd^2}$$

MODULUS OF ELASTICITY | Stress divided by strain

$$E = \frac{FL^3}{48I\delta} \qquad E = \frac{F}{\delta} \times \frac{L^3}{48I}$$

BENDING STIFFNESS | Constant in graph's equation

**Specimen B3.4 | Force - Displacement**



y = 31.864x - 12.904

| Specimen B3.4 | | |
|---|---|---|
| | Unit | Value |
| Failure Load - F | N | 166.053 |
| Max Flexural Strength - σ | MPa | 27.28293 |
| Young's Modulus - E | GPa | 0.900703 |
| Bending Stiffness - k (F/δ) | - | 31.864 |
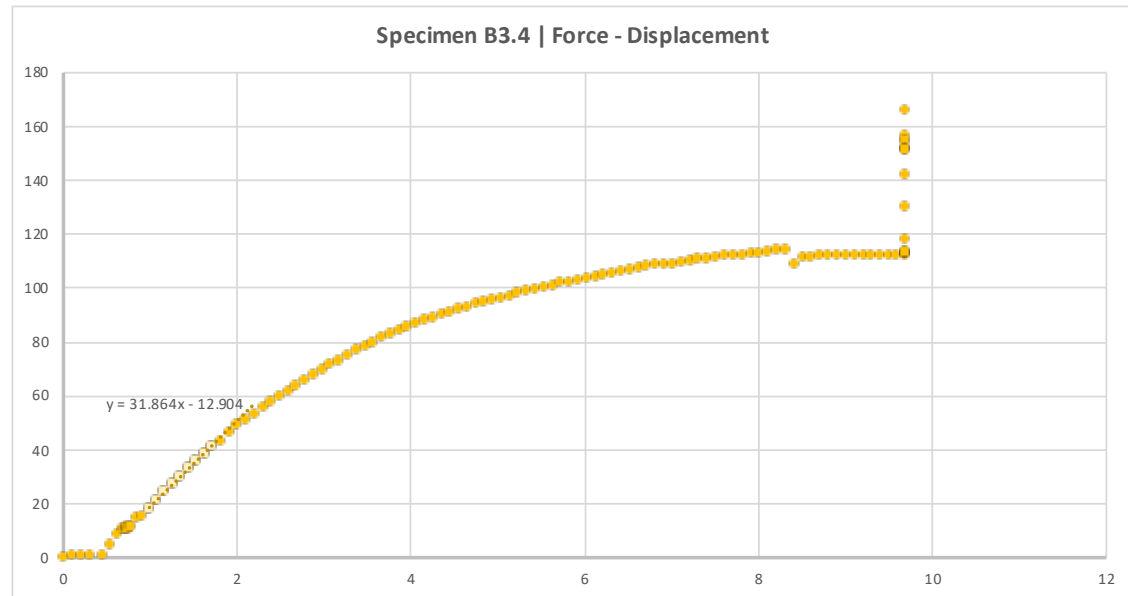
## Specimen B3.5

| | Unit | Initial | Tested |
|---|---|---|---|
| Area | mm² | | 2925 |
| Volume | mm³ | | 17550 |
| Length - total beam | mm | | 150 |
| Length between sup - L | mm | | 80 |
| Width - w | mm | | 19.5 |
| Thickness - d | mm | | 6 |
| Cross Section Area - w*d | mm² | | 117 |
| Moment of Inertia - I | mm⁴ | | 351 |

MOMENT OF INERTIA

$$I = \frac{wd^3}{12}$$

FLEXURAL STRAIN

$$\varepsilon = \frac{6\delta d}{L^2}$$

FLEXURAL STRENGTH | Force multiplied by length divided by cs

$$\sigma = \frac{3FL}{2wd^2}$$

MODULUS OF ELASTICITY | Stress divided by strain

$$E = \frac{FL^3}{48I\delta} \qquad E = \frac{F}{\delta} \times \frac{L^3}{48I}$$

BENDING STIFFNESS | Constant in graph's equation

## Specimen B3.5

| | Unit | Value |
|---|---|---|
| Failure Load - F | N | 158.292 |
| Max Flexural Strength - $\sigma$ | MPa | 27.05846 |
| Young's Modulus - E | GPa | 0.786963 |
| Bending Stiffness - k (F/$\delta$) | - | 25.896 |

**Specimen B3.5 | Force - Displacement**



y = 25.896x - 6.0634
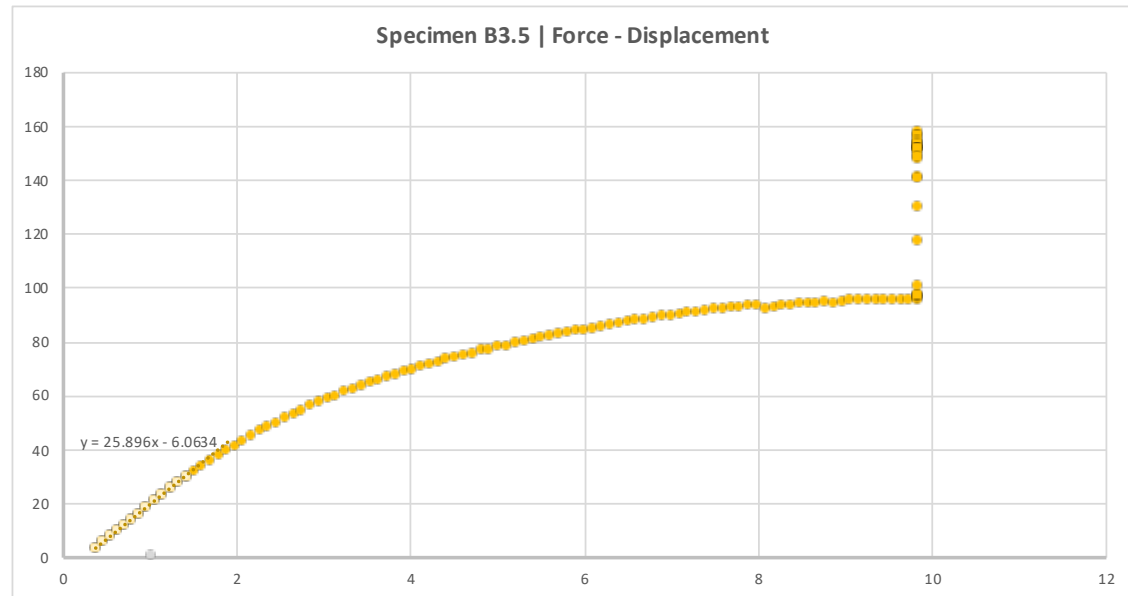
| Specimen B5.1 | | | |
|---|---|---|---|
| | Unit | Initial | Tested |
| Area | mm² | | 3504 |
| Volume | mm³ | | 21024 |
| Length - total beam | mm | | 146 |
| Length between sup - L | mm | | 80 |
| Width - w | mm | | 24 |
| Thickness - d | mm | | 6 |
| Cross Section Area - w*d | mm² | | 144 |
| Moment of Inertia - I | mm⁴ | | 432 |

MOMENT OF INERTIA

$$I = \frac{wd^3}{12}$$

FLEXURAL STRAIN

$$\varepsilon = \frac{6\delta d}{l^2}$$

FLEXURAL STRENGTH | Force multiplied by length divided by cs

$$\sigma = \frac{3FL}{2wd^2}$$

MODULUS OF ELASTICITY | Stress divided by strain

$$E = \frac{FL^3}{48I\delta} \qquad E = \frac{F}{\delta} \times \frac{L^3}{48I}$$

BENDING STIFFNESS | Constant in graph's equation

| Specimen B5.1 | | |
|---|---|---|
| | Unit | Value |
| Failure Load - F | N | 68.7709 |
| Max Flexural Strength - σ | MPa | 9.551514 |
| Young's Modulus - E | GPa | 0.598691 |
| Bending Stiffness - k (F/δ) | - | 24.247 |

**Specimen B5.1 | Force - Displacement**

y = 24.247x - 1.8421
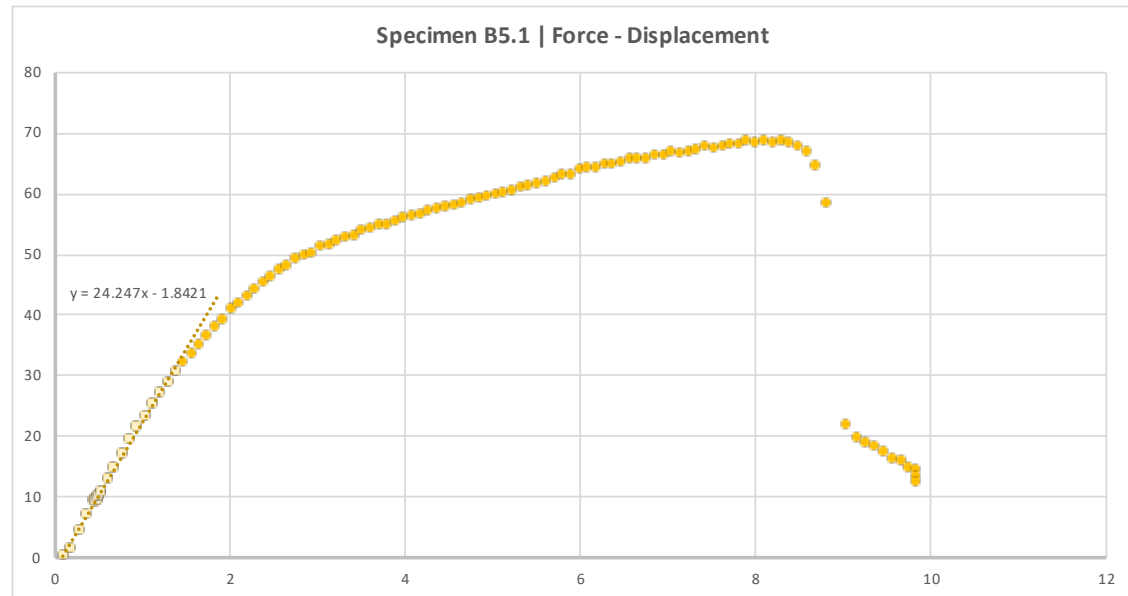
| Specimen B5.2 | | | |
|---|---|---|---|
| | Unit | Initial | Tested |
| Area | mm² | | 3601.5 |
| Volume | mm³ | | 21609 |
| Length - total beam | mm | | 147 |
| Length between sup - L | mm | | 80 |
| Width - w | mm | | 24.5 |
| Thickness - d | mm | | 6 |
| Cross Section Area - w*d | mm² | | 147 |
| Moment of Inertia - I | mm⁴ | | 441 |

MOMENT OF INERTIA

$$I = \frac{wd^3}{12}$$

FLEXURAL STRAIN

$$\varepsilon = \frac{6\delta d}{L^2}$$

FLEXURAL STRENGTH | Force multiplied by length divided by cs

$$\sigma = \frac{3FL}{2wd^2}$$

MODULUS OF ELASTICITY | Stress divided by strain

$$E = \frac{FL^3}{48I\delta} \qquad E = \frac{F}{\delta} \times \frac{L^3}{48I}$$

BENDING STIFFNESS | Constant in graph's equation

| Specimen B5.2 | | |
|---|---|---|
| | Unit | Value |
| Failure Load - F | N | 62.3502 |
| Max Flexural Strength - $\sigma$ | MPa | 8.48302 |
| Young's Modulus - E | GPa | 0.643701 |
| Bending Stiffness - k (F/$\delta$) | - | 26.613 |

**Specimen B5.2 | Force - Displacement**

y = 26.613x + 13.252
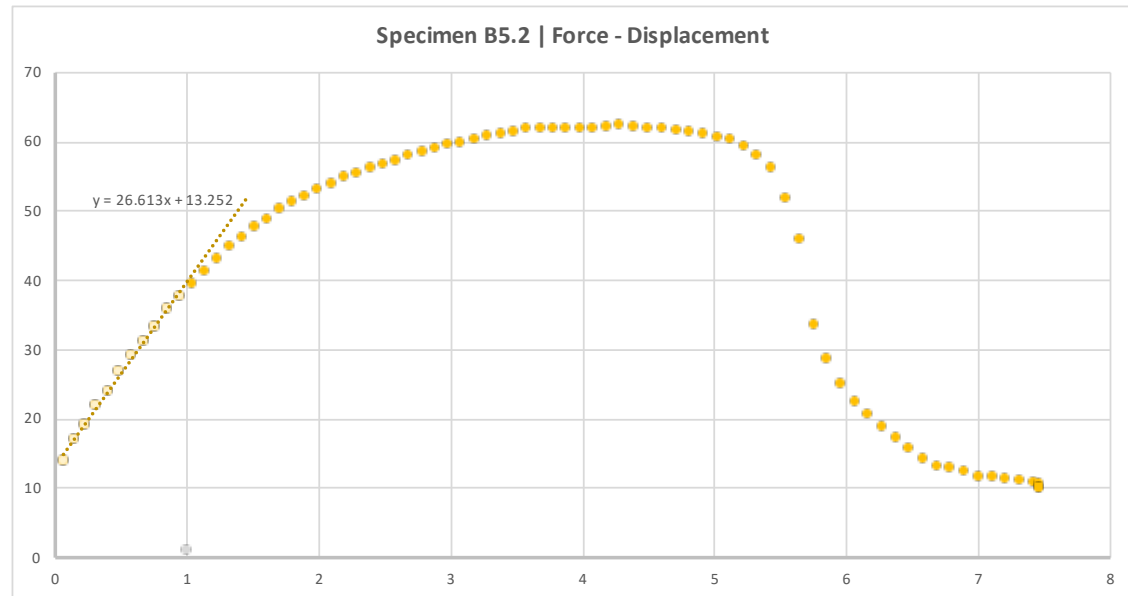
| Specimen B5.3 | | | |
| --- | --- | --- | --- |
| | Unit | Initial | Tested |
| Area | mm² | | 3504 |
| Volume | mm³ | | 21024 |
| Length - total beam | mm | | 146 |
| Length between sup - L | mm | | 80 |
| Width - w | mm | | 24 |
| Thickness - d | mm | | 6 |
| Cross Section Area - w*d | mm² | | 144 |
| Moment of Inertia - I | mm⁴ | | 432 |

MOMENT OF INERTIA

$$I = \frac{wd^3}{12}$$

FLEXURAL STRAIN

$$\varepsilon = \frac{6\delta d}{l^2}$$

FLEXURAL STRENGTH | Force multiplied by length divided by cs

$$\sigma = \frac{3FL}{2wd^2}$$

MODULUS OF ELASTICITY | Stress divided by strain

$$E = \frac{FL^3}{48I\delta} \qquad E = \frac{F}{\delta} \times \frac{L^3}{48I}$$

BENDING STIFFNESS | Constant in graph's equation



Specimen B5.3 | Force - Displacement

y = 24.869x - 23.136

| Specimen B5.3 | | |
| --- | --- | --- |
| | Unit | Value |
| Failure Load - F | N | 68.5089 |
| Max Flexural Strength - $\sigma$ | MPa | 9.515125 |
| Young's Modulus - E | GPa | 0.614049 |
| Bending Stiffness - k (F/$\delta$) | - | 24.869 |